IOWA STATE UNIVERSITY
Digital Repository

Retrospective Theses and Dissertations

Iowa State University Capstones, Theses and Dissertations

1995

Performance assessment modeling of alternative high level nuclear wasteforms

William Mark Nutt
Iowa State University

Follow this and additional works at: https://lib.dr.iastate.edu/rtd

 Part of the Environmental Sciences Commons, and the Nuclear Engineering Commons

Recommended Citation
Nutt, William Mark, "Performance assessment modeling of alternative high level nuclear wasteforms " (1995). *Retrospective Theses and Dissertations*. 10969.
https://lib.dr.iastate.edu/rtd/10969

This Dissertation is brought to you for free and open access by the Iowa State University Capstones, Theses and Dissertations at Iowa State University Digital Repository. It has been accepted for inclusion in Retrospective Theses and Dissertations by an authorized administrator of Iowa State University Digital Repository. For more information, please contact digirep@iastate.edu.

INFORMATION TO USERS

This manuscript has been reproduced from the microfilm master. UMI films the text directly from the original or copy submitted. Thus, some thesis and dissertation copies are in typewriter face, while others may be from any type of computer printer.

The quality of this reproduction is dependent upon the quality of the copy submitted. Broken or indistinct print, colored or poor quality illustrations and photographs, print bleedthrough, substandard margins, and improper alignment can adversely affect reproduction.

In the unlikely event that the author did not send UMI a complete manuscript and there are missing pages, these will be noted. Also, if unauthorized copyright material had to be removed, a note will indicate the deletion.

Oversize materials (e.g., maps, drawings, charts) are reproduced by sectioning the original, beginning at the upper left-hand corner and continuing from left to right in equal sections with small overlaps. Each original is also photographed in one exposure and is included in reduced form at the back of the book.

Photographs included in the original manuscript have been reproduced xerographically in this copy. Higher quality 6" x 9" black and white photographic prints are available for any photographs or illustrations appearing in this copy for an additional charge. Contact UMI directly to order.

UMI

A Bell & Howell Information Company
300 North Zeeb Road, Ann Arbor, MI 48106-1346 USA
313/761-4700 800/521-0600

Performance assessment modeling of alternative high level nuclear wasteforms

by

William Mark Nutt

A Dissertation Submitted to the

Graduate Faculty in Partial Fulfillment of

Requirements for the Degree of

DOCTOR OF PHILOSOPHY

Department: Mechanical Engineering
Major: Nuclear Engineering

Approved:

Signature was redacted for privacy.

In Charge of Major Work

Signature was redacted for privacy.

For the Major Department

Signature was redacted for privacy.

For the Graduate College

Members of Committee:

Signature was redacted for privacy.

Signature was redacted for privacy.

Signature was redacted for privacy.

Signature was redacted for privacy.

Signature was redacted for privacy.

Iowa State University
Ames, Iowa

1995

Copyright © William Mark Nutt, 1995. All rights reserved.

UMI Number: 9540929

Copyright 1995 by
Nutt, William Mark
All rights reserved.

UMI Microform 9540929
Copyright 1995, by UMI Company. All rights reserved.

This microform edition is protected against unauthorized
copying under Title 17, United States Code.

UMI

300 North Zeeb Road
Ann Arbor, MI 48103

TABLE OF CONTENTS

LIST OF FIGURES

LIST OF TABLES

ACKNOWLEDGEMENTS

First the formality. I would like to thank Argonne National Laboratory and Iowa State University for providing me the opportunity to further my eductation and complete this project. This work was partially supported by United States Government Contract W-31-109-ENG-38.

I would like to express my sincere gratitude to Dr. Daniel B. Bullen, my Major Professor, for both his formal and informal support in completing this project. The several discussions that we had, either related to this specific work or not, helped me tremendously in gaining knowledge related to high level waste disposal. I would like to thank J.D.B. Lambert of Argonne National Laboratory for initially providing me the opportunity to continue my eductation. I would like to express my appreciation to Dr. Robert N. Hill of Argonne National Laboratory who saw the importance of my work and had me transferred to the Reactor Analysis division, where efforts such as this more belong. Bob and the RA division provided the stability needed to complete this project and was extremely instrumental in my being at Argonne to finish.

I would also like to thank my committee members for thier support and input regarding this research effort: Dr. G.I. Maldonado, Dr. T.J. Rudolphi, Dr. M. Edelson, and Dr. C. Schilling. I would also like to express my sincere thanks to Becky Staedtler for her unfailing help. My office mate in Ames, John Hawkinson also deserves my thanks. His efforts in installing the IMARC code on the Project Vincent workstations and in the development of post-processing software made my life an awful lot easier. I also enjoyed the many conversations that we had regarding politics, life, the nuclear industry, running, the list goes on.

As far as diversions go, I would like to thank the Ames Jaycees for providing me the opportunity to give some of my free time back to the community and at the same time gain some wonderful friends. Although they will never know it, I would like to thank the many road race directors for providing me the opportunity to develop goals and habits outside of work and studies. As far as unhealthy habits, I want to express my thanks to the Ames Hash House Harriers for their once a month chances to "play" in the woods, creeks, swamps, snow, and shiggy. ARE YOU? ON and ON, Flood Queen.

I cannot in writing express my appreciation to my parents, Patricia and Edward Nutt. Their unfailing support, yet again, made returning home to complete my education a truly rewarding experience. I also want to thank Mike and Katy Carlin for teaching me how to play euchre. I very much enjoyed the Saturday nights spent at "Bower School." It may seem strange, but I want to thank my computer buddy Sebastian. She won't be around to enjoy all the fruits of this effort, but she sure was a great companion during the days hacking on the computer in a quest to finish this and other work. She never turned down the opportunity for me to unload some of my frustrations on her with a good romp.

Last but definitely not least, I want to give my sincere thanks to my loving wife Kathy. You have stood behind me every inch of the way through this little adventure. Some times were tough: first adjusting, qualifier, funding, preliminary, moving, final, job search. I believe that these times were few (and not too bad) and are far over-shadowed by the wonderful times we had in Ames and Chicago (weekends, Bo Deans, Melissa, Crowes, REM, Okoboji, Washington DC, Atlanta, Las Vegas, Cubs, road

racing, triathlons, dinners out, the list goes on). I cannot even begin to express my gratitude for the unfailing support you have given me. Deciding to return home was, I believe, the best choice we made. We have been able to again get close with something that really matters to the both of us, family. Now, what's next? The adventure has just begun!

ABSTRACT

Performance assessment (PA) analyses have been completed for high level nuclear waste forms derived from once through Light Water Reactor (LWR) spent fuel (SF), defense high level waste (DHLW), the closed advanced liquid metal reactor (ALMR) pyroprocess fuel cycle, and the front end processing of LWR spent fuel for possible recycling of the actinides in the closed ALMR fuel cycle. The IMARC (Integrated Multiple Assumptions and Release Calculations) and RIP (Repository Integration Program) PA tools were utilized to predict the performance of these wasteforms for emplacement in the proposed Yucca Mountain Repository.

A model was developed to predict the time dependent failure distribution of the engineered barrier system. This model utilized the Weibull distribution as the tool to estimate the failure properties of each barrier of the multi-barrier waste containers. The sequential failure of each barrier was included in the model. The results were used in the subsequent PA analyses.

The overall conclusion drawn from the use of two PA tools is that the total actinide release to the accessible environment is substantially lower for the closed ALMR fuel cycle and LWR actinide recycle wasteforms relative to directly disposed LWR SF. The release of fission products is similar. This is due to the significantly lower actinide inventory within these wasteforms.

The maximum releases were found to occur for fracture dominated flow for all wasteforms considered. Under matrix dominated flow, sorption of the actinides is greatly enhanced. The dominant actinide under fracture flow conditions is ^{239}Pu while under matrix flow conditions ^{237}Np dominates as the Pu is effectively sorbed onto the

tuff. The release of fission products is independent of the flow mode since they do not strongly sorb to tuff and will dominate the total release in a matrix flow situation.

The benefits of incorporating LWR actinides into the closed ALMR fuel cycle are apparent at Yucca Mountain regardless of the flow mode. If fracture flow dominates, the reduction in the plutonium inventory through recycling leads to reductions in the total actinide release relative to that from LWR SF. If matrix flow dominates, the reduction in the neptunium and plutonium inventory (particularly ^{241}Pu) through recycling again leads to reductions in the total actinide release relative to that from LWR SF. The degree of reduction is largest when matrix flow dominates.

1 INTRODUCTION

1.1 Statement of the Problem

The back end of the nuclear fuel cycle begins with the discharge of spent nuclear fuel (SF) from nuclear reactor cores. SF consists of fissile and fertile isotopes, radioactive fission products, radioactive actinides derived from the transmutation of charged actinides, and low activation level structural materials. The highly radioactive fission products and actinides are hazardous and must be properly isolated from the environment. The United States is currently considering isolating these materials through burial in a deep underground repository.

The nuclear industry in the United States consists primarily of light water reactors (LWR). The disposal of LWR nuclear waste currently being considered in the U.S. is the direct burial of intact fuel assemblies. Defense operations have resulted in the reprocessing of SF generated in defense reactors to recover weapons-grade materials. This has resulted in the generation of liquid high level nuclear waste. This waste is called defense high level waste (DHLW). It is currently being planned to vitrify this waste in borosilicate glass and bury it in the repository.

Many geologic formations have been investigated as potential sites for nuclear waste repositories. In 1987, the U.S. Department of Energy (DOE) selected the beds located at Yucca Mountain, Nevada as the probable site for the nation's first nuclear

waste repository. Characterization studies are being carried out to determine if this site can isolate nuclear waste within the criteria required for the site to be licensed by the U.S. Nuclear Regulatory Commission (NRC).

The design of a repository is based on the premise of isolating the waste from the environment for a sufficient amount of time to allow the waste to decay to acceptable levels. After a relatively short period of time (~300 years), the vast majority of the fission products will have decayed to negligible levels. The radioactivity of the waste is then dominated by long-life fission products and actinides, which continue to be hazardous to human health for hundreds of thousands of years. Current NRC requirements state that the waste must be contained for a period of 1,000 years and at no time after shall the release rate exceed 1 part in 100,000 per year of the 1,000 year inventory of each radionuclide. These requirements may be changed in the near future.

The primary means for nuclear waste migration back to the environment at the Yucca Mountain site is by ground water flow. Isolation can be assured if little or no waste dissolves into the ground water. If the waste is in solution, isolation can also be assured if the waste decays to permissible levels prior to release to the accessible environment. A repository can be designed to incorporate a multiplicity of isolation barriers against waste migration. These barriers will limit both the rate at which ground water contacts the waste and the rate at which the waste in solution flows towards the accessible environment.

The migration barriers include both engineered and natural barriers. The engineered barriers include the waste form, the waste container, and backfill and seal

materials. The natural barriers include long flow paths, low ground water flow rates, and retardation properties of the host rock.

Several performance assessment (PA) analyses have been completed to estimate the release of radionuclides to the accessible environment. These PAs utilize a probabilistic approach given the long time scales involved and uncertainties in models and relevant data. In the United States, these PAs have exclusively analyzed intact SF from LWRs and DHLW disposed at the proposed Yucca Mountain site.

Research is currently underway to develop advanced nuclear reactor concepts. In particular, Argonne National Laboratory (ANL) and General Electric Corporation (GE) are developing the advanced liquid metal reactor (ALMR). The ALMR design utilizes a closed fuel cycle that effectively separates actinides from the remainder of the waste. The actinides are subsequently recycled for use as fuel in the ALMR.

Additional research has been conducted at ANL to develop a process that is capable of separating the actinides from the remainder of the waste materials from LWR spent fuel. The recovered actinides can be used as fuel in the ALMR and the waste disposed in the repository or emplaced in a wasteform that may prove superior to LWR SF. Using the actinides as fuel in an ALMR is expected to reduce the long term repository isolation requirements due to the destruction of these long-lived radionuclides in addition to providing an energy benefit from their re-use.

Preliminary investigations have been undertaken to determine the performance properties of the ALMR waste forms. No PAs have been completed to estimate the performance of a repository containing waste from the ALMR or from an LWR actinide recycle campaign. As such, it cannot be concluded that the wastes generated from an

ALMR and an actinide recycle campaign will perform better than directly disposed LWR SF.

The ending of the cold war in conjunction with nuclear arms reduction treaties will result in large stockpiles of weapons materials, namely highly enriched ^{235}U (greater than 95%) and weapons-grade (high purity) ^{239}Pu. In order to reduce the risk of proliferation, these materials must be properly disposed. The ^{235}U can be easily processed for use as fuel in LWRs that are either currently operating or will be constructed in the future. The disposition of the ^{239}Pu is more difficult. Several options are being considered including 1) using as fuel in an LWR to effectively "spike" the ^{239}Pu and disposal as intact SF, 2) using as fuel in an ALMR to either "spike" the ^{239}Pu or completely fission the entire stockpile and, 3) mixing the ^{239}Pu with DHLW and vitrification into borosilicate glass for ultimate disposal into a repository. Studies have been completed to determine which disposition alternative can alter the ^{239}Pu into a form not suitable for use as a nuclear weapon. None of these studies analyzed the performance of the disposed waste in the repository.

The primary objective of this study is to perform PAs of the waste forms discussed above that have not been investigated. This effort will be directed at the use of the ALMR as 1) a source of electricity, 2) a means of utilizing the actinides from LWR SF, 3) a means of destroying the weapons grade ^{239}Pu. The performance of the waste from the ALMR with and without LWR actinide recycle is compared to the performance of directly disposed LWR SF. The various options for the disposition of weapons grade ^{239}Pu in an ALMR are compared to "spiking" the fuel in an LWR followed by direct disposal and co-mixing with DHLW. The results of this study will

identify whether the ALMR waste forms are superior to those generated from the other processes.

The secondary objective of this study is to demonstrate the use of PA to analyze alternative nuclear waste forms. This methodology may prove beneficial in the analysis of the performance of waste forms not currently being considered, such as research and test reactor waste and naval reactor waste.

1.2 Description of the Problem

Two PA tools will be utilized to perform the study. The first tool utilized is the Integrated Multiple Assumptions and Release Calculations (IMARC) computer software developed by the Electric Power Research Institute (EPRI) and Risk Engineering Incorporated (REI). IMARC is a probabilistic based PA tool that utilizes a logic tree approach to account for model and parameter uncertainty. The second tool utilized is the Repository Integration Program (RIP) developed by Golder and Associates, Incorporated (GAI). RIP is another probabilistic based PA tool that utilizes a Monte Carlo approach to sample probability distributions of relevant parameters or models.

Several PAs have been completed for the disposal of LWR SF in Yucca Mountain. These PAs contain the most up to date models and parameters relevant to Yucca Mountain. In general, the models and parameters presented in these PAs are used to model the repository in this evaluation of alternative wasteforms. However, certain models had to be modified to account for the differing wasteforms and their effects on the near field repository conditions. The models that were modified include the engineered barrier system performance model and the source term model.

The engineered barrier system performance model is detailed in Chapter 3. This model utilizes Weibull distributions to predict the time dependent failure rates of the waste containers. Sequential failure of each of the barriers is explicitly modeled. The design of the waste packages for SF and DHLW are presented along with a proposed design for the ALMR wasteforms. The model is based on the corrosion properties of the materials being considered in the fabrication of the waste packages. The corrosion properties depend on the near field repository conditions, primarily temperature and the ground water chemistry. These are addressed for each waste-form considered.

The source term model is modified to account for the differing properties of each wasteform, in particular the dissolution rate. These models are presented in Chapter 4. Models are presented that predict the alteration rate of the wasteform when contacting ground water and the migration of waste radionuclides away from the waste package. Several of these models depend on the near field conditions as well, again namely the ground water temperature and chemistry. These are also addressed for each wasteform considered. The initial inventory of waste radionuclides and the build-in of actinide daughter products for each wasteform are also presented in Chapter 4.

Chapter 5 presents results of the PA analyses utilizing the IMARC PA tool. First a description of the IMARC PA tool is presented followed by changes required to model the various wasteforms being considered. The performance of the LWR SF and DHLW wasteforms are then presented as baselines for future comparisons. The performance of the ALMR wasteform with and with out actinide recycle are presented

and compared with the baseline LWR SF wasteform performance. The performance of the various alternatives (LWR, ALMR, DHLW) for disposition of weapons grade ^{239}Pu was also investigated using IMARC and the results presented in Chapter 5. A sensitivity study was also conducted using IMARC to determine the dependency of total repository system behavior on several key wasteform (ALMR) and environmental parameters. These results are also presented in Chapter 5

In order to obtain a "second opinion", the above analyses were repeated using the RIP PA software. The results of this study are presented in Chapter 6. First a description of the RIP PA tool is presented followed by details regarding the RIP model developed for this study. As with the IMARC study, the performance of the LWR SF and DHLW wasteforms are then presented as baselines for future comparisons. The performance of the ALMR wasteform with and with out actinide recycle are presented and compared with the baseline LWR SF wasteform performance. The performance of the various alternatives (LWR, ALMR, DHLW) for disposition of weapons grade ^{239}Pu was also investigated using RIP and the results presented in Chapter 6. A sensitivity study was also conducted using RIP to determine the dependency of total repository system behavior on several key wasteform (ALMR) and environmental parameters. These results are also presented in Chapter 6

Chapter 7 presents the overall conclusions drawn from each of the analyses conducted. The repository performance for each wasteform is summarized, followed by a comparison of repository performance between wasteforms. The results obtained using the two PA tools are compared and conclusions are drawn. Finally, a discussion of future work is presented.

2 LITERATURE REVIEW

The management of radioactive waste has been an issue since the inception of nuclear energy. Radioactive waste can be classified into five categories [1]. These are:

1) High Level Waste (HLW) -- Results from the reprocessing of spent fuel from a defense or commercial nuclear reactor.
2) Spent Nuclear Fuel (SF) -- Fuel that has been discharged from a nuclear reactor and not reprocessed.
3) Transuranic (TRU) Waste -- Material that is contaminated with alpha-emitting radionuclides of sufficiently long life (greater than 20 years) of elements with atomic number greater than 92 and concentrations greater than 100 nanocuries per gram.
4) Low-Level Waste (LLW) -- Waste with little radioactivity and no TRU elements.
5) Mill Tailings -- Discharge from uranium ore processing mills with low radioactivity levels.

The source of SF is commercial nuclear reactors, namely light water reactors (LWR). The vast majority of SF is currently stored at the reactor sites in either pools or dry storage casks. The number of SF assemblies discharged and expected to be discharged from commercial LWRs is provided in the Characteristic Data Base (CDB)

[2]. A small amount of SF has been reprocessed during the late 1960s and early 1970s and only a small amount of HLW was generated. The majority of HLW has been generated at defense reprocessing facilities (DHLW). This HLW inventory is also provided in the CDB [2].

The activities involving HLW and SF management are regulated by the Federal Government. In 1982 the United States Congress passed the Nuclear Waste Policy Act (NWPA) [3]. The NWPA established the Office of Civilian Radioactive Waste Management (OCRWM) within the U.S. Department of Energy (DOE) and gave it the task of locating a suitable site for the nations first nuclear waste repository. The NWPA detailed schedule milestones related to Federal storage of nuclear waste, set up extensive procedures for state and public involvement, and established the Nuclear Waste Fund.

The OCRWM began investigating the feasibility of three sites: Deaf Smith County, Texas (bedded salt), the Hanford Reservation, near Richland Washington (basalt flows), and Yucca Mountain on the Nevada Test Site (bedded Tuff) [4,5,6]. In 1987, the NWPA was amended by the Nuclear Waste Policy Amendment Act [7] which redirected initial studies to the Yucca Mountain site.

The OCRWM subsequently developed the Yucca Mountain Site Characterization Plan (SCP) [8]. The SCP is a compilation of all the data that had been collected regarding Yucca Mountain and provided a frame work through which studies are to be carried out to quantify the feasibility of the site to isolate nuclear waste. The SCP provides descriptions of the reference designs of the repository, including the container and wasteform designs.

The Nuclear Regulatory Commission (NRC) is responsible for licensing the Yucca Mountain repository. The NRC regulations concerning the repository are provided in 10 CFR Part 60 [9]. The objective of these regulations is to provide reasonable assurance that the waste will be isolated for 10000 years without undue risk to the public [1]. The technical requirements include [9]:

1) The waste package shall contain the waste for a period of 300 to 1000 years.
2) The rate of radionuclide release from the engineered system shall not exceed one part in 100000 per year after the containment period for each significant radionuclide
3) The pre-emplacement ground water travel times from the repository to the accessible environment are to exceed 1000 years.

The NRC requirements are based on the Environmental Protection Agency (EPA) requirements provided in 40 CFR Part 191 [10]. These requirements limit the cumulative release of radionuclides over a 10000 year period to the accessible environment (five kilometers from the repository). The Energy Policy Act of 1992 [11] requires that new standards be developed for the Yucca Mountain site. These standards are to prescribe the maximum annual effective dose equivalent to individual members of the public from releases to the accessible environment. The NRC is then required to make its regulations consistent with these standards. These requirements are being developed by the National Academy of Science and have not yet been set.

Several total repository system performance assessment (PA) analyses have been completed for the proposed Yucca Mountain Repository [12,13,14,17,18]. Based

on the complexity of the repository, the long time scales involved, and uncertainty in the relevant data, lack of data, probabilistic methods were utilized.

The Electric Power Research Institute (EPRI) and Risk Engineering Incorporated (REI) developed the computer code IMARC (Integrated Multiple Assumptions and Release Calculations) for use as a probabilistic PA tool [12,13]. IMARC utilizes the logic tree as the basic representation of uncertain models and parameters. The computer code RIP (Repository Integration Program), developed by Golder Associates, Incorporated (GAI) [15,16], was utilized by Intera in their PA of Yucca Mountain [14]. RIP employs a simulation approach utilizing the Monte Carlo method to sample the probability distributions for uncertain parameters. RIP simulates a large number of system realizations to determine probabilistic distributions of site performance. The PAs performed by Sandia National Laboratories (SNL) utilize a series of computer codes that also use a Monte Carlo simulation method [17,18].

It should be noted that all of these codes use simple models to predict the behavior of complex systems. The complexity of the various models used will be increased if it is demonstrated that improved accuracy is essential in predicting overall repository performance. The PAs completed to date only consider SF and DHLW wasteforms. No alternative wasteforms that would be produced from advanced nuclear reactor concepts have been analyzed.

Several advanced reactor designs are being investigated including advanced LWRs, advanced liquid metal reactors (ALMR), and high temperature gas reactors (HTGR) [19]. The design characteristics of the LMR will be detailed. The proposed ALMR is a merging of the Integral Fast Reactor (IFR) concept, being developed at

Argonne National Laboratory (ANL), with General Electric's (GE) Power Reactor Innovative Small Module (PRISM) design.

The concept consists of liquid sodium cooling, a pool-type reactor configuration, metallic fuel, and an integral fuel cycle based on the pyrometallurgical processing of the fuel. Key features of the design include compact reactor modules to facilitate factory fabrication, passive reactivity reductions during undercooling and over power transients with failure to scram, passive decay heat removal from loss-of-heat sink accidents, simple and passive safety features to protect against severe accidents, and breeding capability [19].

The design and operating characteristics of a commercial ALMR are based on the GE PRISM design [19,20,21]. A commercial ALMR site produces 1395 Megawatts electric (MWe) and consists of three power blocks producing 465 MWe each. Smaller sites of 465 MWe and 930 MWe can be built. The reactor module is a pool type design with primary coolant circulated within the reactor vessel by four electromagnetic pumps through two intermediate heat exchanger (IHTS). The nuclear steam supply system (NSSS) includes the reactor module and the IHTS. All equipment within the reactor module is classified as nuclear safety related while the rest of the NSSS (beginning with the IHTS piping) is non-nuclear safety related. If the normal external heat sink is lost, alternative means of cooling are provided by the auxiliary cooling system (ACS) and the reactor vessel auxiliary cooling system (RVACS). The ACS provides direct cooling of the steam generator shell by forced or natural circulation of atmospheric air. The RVACS cools the reactor vessel through natural circulation of air around the vessel.

The fuel design and fuel cycle are based on ANL's IFR design [22-30]. The reference fuel for the ALMR is metallic uranium-plutonium-zirconium alloy with the ferritic alloy HT9 used as cladding and assembly ducts [22]. Metallic fuels were the original type used in liquid metal reactors, however in the late 1960s, interest turned towards ceramic fuels based on their superior performance realized at that time. Metallic fuel development continued at ANL's Experimental Breeder Reactor Number 2 (EBR-II) through the 1970s. During this time, the performance related problems of metallic fuel were resolved and additional attributes were identified. A ternary alloy with typical composition of 10% Zr and 20% Pu was chosen to increase the solidus temperature and preclude inter-diffusion of fuel and clad constituents. The fuel rod design was changed to allow the fuel to swell prior to contacting the clad, permitting fission gas bubbles to interconnect, thus releasing the fission gas to the plenum. This effectively removes the driving force for continued swelling of the fuel [27].

A metallic fuel performance demonstration program was initiated to establish the burnup potential of the fuel and to quantify the optimum design. This program consists of irradiations in EBR-II, development of transient and steady state fuel modelling codes, and fuel/clad compatibility testing [27]. As of 1992, U-Pu-Zr fuel had attained burnups in excess of twenty atom percent in EBR-11 [29].

The ALMR is designed to improve the high level of plant safety already achieved in the nuclear industry. Active and passive safety systems are included in the design. Normal operating conditions provide substantial margins to sodium boiling (400 °C), fuel centerline melt (140 °C), and fuel-clad eutectic formation (150 °C). Reactivity shutdown is accomplished through three mechanisms. In the event of a

transient, the reactor protection system (RPS) will insert nine control rods by gravity drop or forced run-in. Any one of the nine control rods can shut the reactor down. The probability of the RPS failing to shut the reactor down is estimated to be less than 10^{-6} per demand. A second (back-up) active system is the operator actuated ultimate shutdown system. When this system is activated, boron balls are dropped into the central core location leading to shutdown independent of the control rods. Finally, three gas expansion modules (GEM) are included along the core periphery as a passive shutdown system. The GEMs are hollow assembly ducts closed at the top, open at the bottom and filled with gas. When the pumps are operating, the pressure compresses the gas and fills the ducts with sodium. When the pumps stop running, the gas expands and expels the sodium, causing increased neutron leakage from the core. This results in a significant reactivity reduction in loss of flow accidents [21].

The use of metallic fuel in sodium pool cores provides a substantial safety feature in beyond design basis anticipated transient without scram (ATWS) events [22]. Loss of flow without scram (LOFWS) and loss of heat sink without scram (LOHSWS) events result in rapidly increasing coolant and fuel temperatures. Thermal expansion of the core components results in negative reactivity insertion causing a power reduction. As the power is reduced, stored Doppler reactivity within the fuel will contribute a positive reactivity insertion, tending to cancel any negative reactivity feedback. The high thermal conductivity of metallic fuel and the low operating temperatures in an ALMR result in a small degree of stored Doppler reactivity [30]. Analyses of LOFWS and LOHSWS events in the ALMR demonstrated that a significant margin exists to the sodium boiling and fuel melting temperatures. The fuel-clad

eutectic temperature is exceeded for a limited period of time and no clad failures are expected [30]. Safety analyses demonstrated that under transient overpower without scram (TOPWS) events, significant margin exists to the sodium boiling, fuel melting, and fuel-clad eutectic formation temperatures [30].

Usage of metal fuel also enhances internal conversion allowing low reactivity loss rates. This reduces the excess reactivity requirements and corresponding control rod worths.

Two landmark tests were conducted in 1986 at EBR-II to demonstrate the safety features of sodium pool, metallic fueled fast reactors. These tests were LOFWS and a LOHSWS events. The results of these tests provide concrete evidence of the passive features of these systems [29].

The goal of the ALMR design team (ANL and GE) is to reduce the cost and scheduling requirements realized in previous LWR construction. This is accomplished by 1) constraining the nuclear safety related envelope so that the balance of plant can be constructed with conventional high quality practices, 2) sizing the nuclear safety related components so they can be fabricated in a factory and shipped to the plant site, 3) reduce the demonstration cost [20]. The closed IFR fuel cycle provides a drastic reduction in complexity over the Purex based oxide closed fuel cycle. There are few steps involved and the steps are compact, as such large capital costs are not expected [22,28]. Calculations have estimated that the IFR fuel cycle costs are less than those realized by LWRs currently operating [22].

The use of metallic fuel in the ALMR allows for an integral based fuel cycle based on pyrometallurgical processing of the fuel. This process uses high temperature

molten salts and metals to separate the actinides from the fission products. Essentially all of the actinides are re-cast into the fuel while the fission products are treated as waste. A summary of the process follows [31-40].

The key step in the process is electrorefining, where the fuel material (plutonium) is partially separated from the uranium and fission products. The electro-refiner (ER) is a one meter diameter steel crucible containing a 1000 kilogram pool of molten Cd overlain with a 500 kg mixture of liquid chloride salts (LiCl - 50 wt% KCl - 6 wt% actinide chlorides) [36]. A diagram of the ER process is shown in Figure 2.1.

The core fuel is chopped, placed into an basket and immersed into the salt and made anodic with respect to the Cd pool. The alkali, alkaline earth, and rare earth fission product metals are oxidized into the salt. The noble metal fission products and

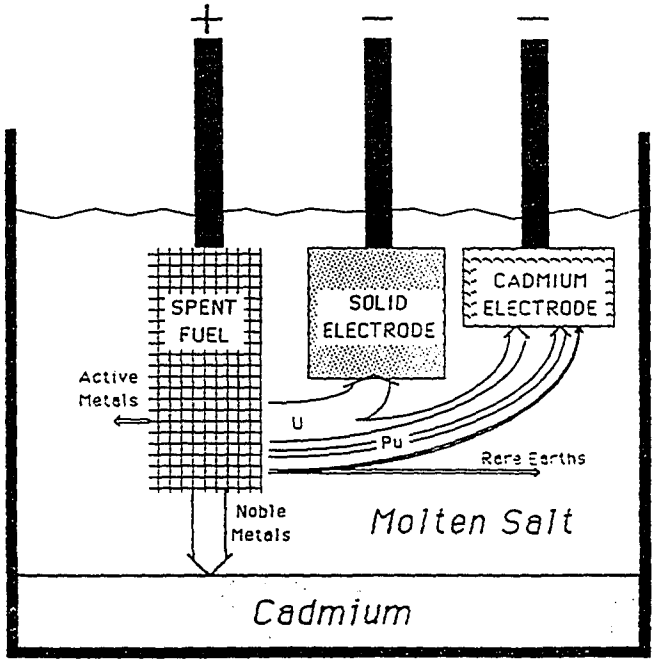

Figure 2.1 Pyrprocess Electrorefiner Schematic [31,32]

clad hulls are not oxidized and remain in the anode basket. Some fine particles fall into the Cd pool at the bottom of the ER [31].

Following dissolution, a portion of the uranium from the fuel is electro-transported onto a solid cathode. This step recovers pure uranium for the fabrication of blanket fuel and controls the ratio of $PuCl_3$ to UCl_3 in the salt, which is critical in determining the composition of the recovered uranium-transuranium product [32].

Next, a smaller Cd pool is introduced as a cathode into the salt. The remaining uranium, actinides and a small amount of rare earth fission products are electro-transported to the liquid cadmium cathode. The mixture of TRU elements and uranium is recovered from the Cd cathode through distillation of the Cd. This is used to fabricate core fuel.

The process is similar for blanket fuel, in that the uranium is electrotransported to a solid steel cathode. TRU elements accumulate in the salt through the processing of several batches of blanket fuel. The remaining TRU elements are then recovered in a Cd cathode as described above.

Unlike PUREX processing techniques, at no time during the process is Pu totally separated from the rest of the actinides and a portion of the rare earth fission products. This does not affect the performance of the fuel or operation of the reactor, but it does provide a high degree of proliferation resistance.

The principal wastes of the pyroprocess fuel cycle are the gases released during fuel chopping/dissolution, and the metals and salts discharged from the ER [34]. The fission products, except for tritium, Kr, and Xe, accumulate in the ER during processing. The alkali metal, alkaline earth, rare earth and halide fission products

collect in the salt. The clad hulls, noble fission products and Zr are in either the anode basket, filters or in the cadmium pool. After several batches of core and blanket fuel are processed, the salt and cadmium are treated to recover residual TRU elements and concentrate the fission products for incorporation into a wasteform [34].

Processes have been proposed and investigated for treating the HLW discharged from the ER and cover gas and incorporating the waste into forms suitable for burial [34-41]. The current process being developed at ANL is summarized.

The Kr and Xe fission gases are to be collected by a cryogenic process and loaded into pressurized bottles. The tritium fission gas is collected in a purification system that converts it to water and traps it on molecular sieves [37].

The salt purification process is shown in Figure 2.2 [41]. The salt is first contacted with a Li-Cd solution to reduce the actinide chlorides and a small amount of rare earth fission products. A small concentration of the TRU chlorides remains and is recovered in an extraction step. In this step, the remaining actinide chlorides are removed by contacting the salt with depleted uranium in cadmium. The salt at this point contains the rare earth elements and nearly all of the alkali metal, alkaline earth, and halide fission products with only trace amounts of the actinides.

The salt from the extraction step is then passed through a zeolite bed that removes Cs, Sr and Ba by ion exchange. Excess salt is purged, but the bed retains a considerable amount of salt occluded in the zeolite cavities and adhering to the zeolite surface. The zeolite is then mixed with an organic matrix material and hot pressed. Ninety percent of the salt, with its fission product content reduced by 10-20%, is returned to the ER [34,36]. This is the mineral wasteform.

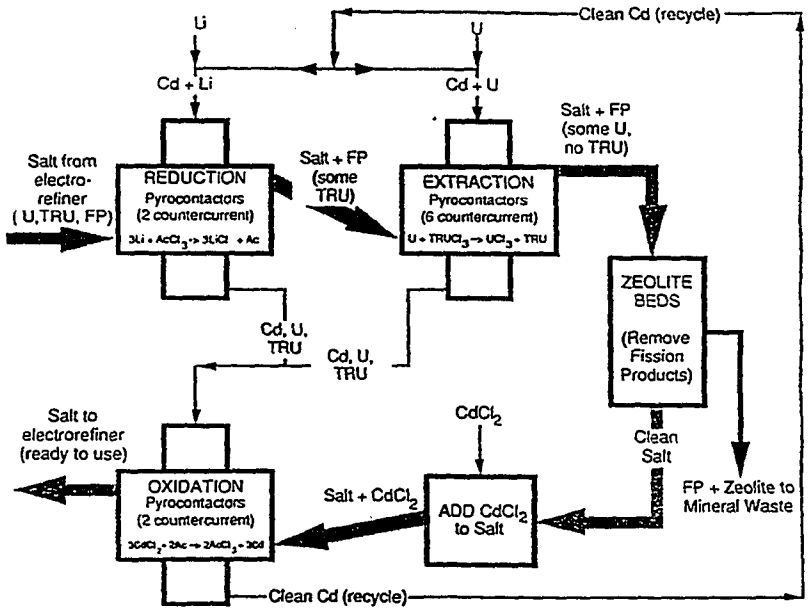

Figure 2.2 Electrorefiner Salt Purification Process [41]

Prior to re-introducing this salt into the ER, $CdCl_2$ is added. Next the salt is combined with the Cd, U and TRU from the reduction and extraction steps in an oxidation step. Clean Cd is obtained for re-use and the U and TRU are oxidized into the salt for introduction into the ER [41].

The unoxidized noble metal fission products, clad hulls and a residual portion of the TRU remains in either the anode basket or in filters. The basket and filters are melted together under a calcium chloride flux, see Figure 2.3. The flux removes essentially all of the remaining rare earth and transuranics which are re-introduced into the ER. The metallic waste stream at this point contains only the noble metal fission products, stainless steel, zirconium, and a very low amount of TRU. A stainless steel - zirconium metal ingot is formed whose composition depends upon the fuel clad material [41]. This is the metallic wasteform.

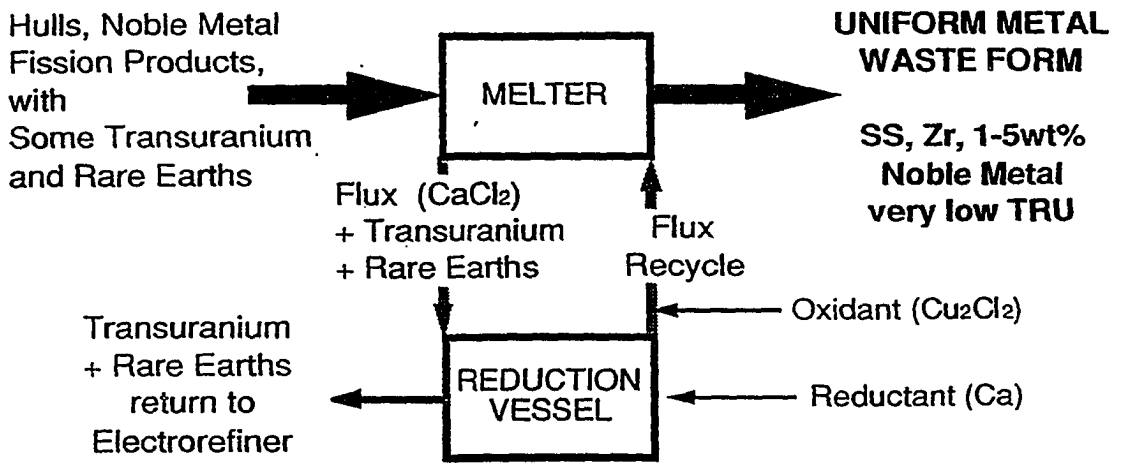

Figure 2.3 Metallic Waste Stream Process [41]

The expected inventories for each wasteform discharged from a pyroprocess fuel cycle have been calculated for both low and high actinide decontamination [35,37,40]. These calculations assume that the salt waste stream is processed to transport the rare earth fission products to the metal waste stream. As described above, the current process has the rare earth fission products remaining with the salt stream.

The radioactivity of SF from a once through LWR fuel cycle is larger than that of the original U ore for a period of several tens of thousands of years. After approximately one thousand years this activity is dominated by the TRU elements. The removal of the TRU from the waste leaves only the fission products and may reduce the risk of geologic isolation of HLW [42], although the benefits of TRU

separation have been questioned [43]. In the hard neutron spectrum of an ALMR, TRU elements are suitable for use as fuel. In the thermal neutron spectrum of a LWR, even numbered TRU elements build up and act as poisons in the reactor [36].

Investigations are underway at ANL to develop a process for separating the actinides from the remaining fission products of LWR SF. The actinides are to be incorporated in the ALMR fuel cycle while the fission products will enter the ALMR waste streams [36-41]. The process being considered is a head-end process that is added to the entire pyrometallurgical process.

The LWR oxide fuel would first be reduced to a metallic form for insertion into the ER [41]. The current process is shown in Figure 2.4. First the oxide fuel is mechanically chopped and fragmented. The fuel is then placed in molten lithium chloride. The actinide and noble metal fission product oxides are reduced. The metal product is separated from adherent salt and fed to the ER. This process produces lithium oxide which is reduced to lithium for re-use. Particulate and salt soluble fission products and any un-reduced actinides are then passed through a zeolite bed and processed as discussed previously.

After processing the metallic product through the ER, waste streams (metallic and mineral) identical to those discussed above are produced. The recovered uranium and TRU elements are stored for use as fuel in ALMRs. Once the uranium and TRU elements enter the ALMR closed fuel cycle, they essentially remain there until they are fissioned.

This front-end process produces four additional wasteforms in addition to those of the baseline ALMR. Fission gases would be produced through fuel disassembly and

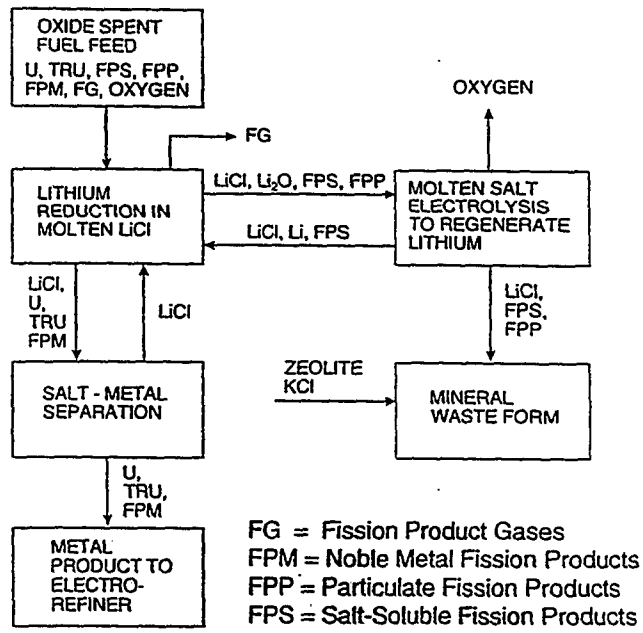

Figure 2.4 Oxide Fuel Reduction Process [41]

dissolution. Conversion of the LWR SF from oxide to metal will produce a salt waste stream. A salt and metal waste stream will be produced through subsequent ER processing. These waste streams are processed as discussed earlier. The amount of waste generated in each of these processes has been estimated [37,40], but it should be noted that these estimates are based on past process developments.

The accumulating stockpile of nuclear weapons grade material has given rise to an issue that was not contemplated even a few years ago. At issue is what to do with this the material. The disposition of highly enriched uranium (HEU) is relatively simple while the disposition of weapons grade plutonium poses a more complex problem.

Recovered HEU can be de-enriched with depleted U (depleted in U-235) produced through enriching uranium ore to three to five weight percent and used as

fuel in currently operating LWRs [44]. A portion of the HEU stockpile could be maintained to fuel naval and research reactors. A 600 metric ton stockpile could fuel the world's 600 gigawatts of nuclear generated electric capacity for approximately three years [44].

In July of 1992, two U.S. companies (Nuclear Fuel Services and Allied-Signal) signed a preliminary agreement with the Russian Ministry of Atomic Energy (MINATOM) to convert HEU to LEU. In addition, President Bush announced that a twenty year agreement with Russia had been signed regarding Russian HEU. The U.S. is to purchase Russian HEU for subsequent conversion to LEU or purchase Russian LEU derived from HEU [45].

Weapons grade Pu disposition cannot be handled in the same manner as HEU. Several disposition options have been proposed including: storage, co-mixing with DHLW and isolating in a geologic repository, fissioning in a nuclear reactor, transmutation in an accelerator, using in deep underground explosions to vitrify the Pu in the glass produced by the molten rock, and rocketing it to the sun [44]. Only the first four options have been seriously considered.

The storage of Pu will be required on an interim basis until one of the other disposition options is chosen. A storage facility will have to be highly safeguarded to prevent theft or diversion. The cost of operating such a facility has been estimated at $100 million per year per 100 metric tons stored [44]. The form of stored Pu has been investigated and it is believed that the best storage form is an intact component, or pit [46]. A pit is a sturdy metal container that isolates the metallic Pu from the environment in a criticality safe geometry. A pit has certified seals, known material

properties, a defined Pu inventory, and a trouble free history for over forty years of storage. Storage of intact pits represents a finite, but small, diversion potential. In addition, as long as the Pu remains in a form that could easily be re-fabricated into a weapon, a nation could rapidly increase its weapons stockpiles [47]. The U.S. DOE is proposing to construct and operate a new Pu storage facility, called Complex-21 [48]. Whether this facility is used as a long term solution to the Pu storage question remains to be seen.

The mixing of Pu with HLW and incorporation into borosilicate glass for geologic disposal is believed by some to represent a quick and cost effective solution [45,46]. The Savannah River Site (SRS) has the facilities to support a HLW/Pu vitrification process. SRS could vitrify 50 metric tons of HLW/Pu by 2013 when the existing HLW stores would be depleted. Other "spiking" materials would then be required [49]. The disposing of HLW/Pu will pose problems identical to those being considered for the direct disposal of LWR SF, namely the isolation of long lived actinides from the accessible environment. The disposal of HLW/Pu would also effectively destroy a potential energy source.

Another option considered is the fissioning of the weapons grade Pu in already operating LWR cores. This is accomplished by substituting the Pu for U-235 in the oxide fuel, which is termed as mixed oxide fuel (MOX). The neutronic properties of Pu limit the MOX loading to one-third of the core for current operating LWRs [46]. It is unlikely, given regulatory and safeguards requirements, that U.S. utilities will consider using MOX [46]. Western European nations and Japan are not likely to be willing to irradiate U.S. and former U.S.S.R. Pu as MOX, even if the political and safeguards

issues are surmounted. These nations have a large and increasing civil Pu stockpiles. Due to the economics involved in storing civil Pu ($1-$4 per gram per year at the Sellafield and La Hague facilities) [50], these nations are not likely to want to irradiate U.S. and former U.S.S.R. Pu in place of their civil stockpile.

To further evaluate the disposition of weapons grade Pu in fission reactors, the U.S. DOE released the Plutonium Disposition Study Requirements Document [51]. This document requested information on the capability of advanced fission reactor designs to transform the Pu into a form not readily suitable for weapons use.

Advanced reactor designs evaluated include the ALWR [52-54], the ALMR [55,56], molten salt reactors [57], and the modular high temperature gas cooled reactor [58]. In addition, accelerators [59] and a reactor utilizing a non uranium fuel form [60] have been considered.

An evaluation by the Idaho National Engineering Laboratory (INEL) of all reactor/accelerator designs considered indicated that the ALMR is the best option [61]. Four technical areas were evaluated: fuel status, reactor/accelerator system status, waste processing status, and waste disposal status. It was deemed that annihilation is preferred over denaturing as it is still possible to construct a weapon from denatured Pu. The time period required to annihilate the stockpile was also considered in the evaluation.

The isolation of wasteforms other than commercial SF or DHLW will alter the characteristics of the repository system from those currently being investigated. Namely, the container design, waste inventory, near field hydrothermal environment, and radionuclide source term will be impacted.

The reference container design for commercial SF and DHLW is detailed in the Yucca Mountain SCP [8]. This design is a small single barrier container that is to be placed in boreholes drilled either horizontally in the tunnel floors or vertically into the walls. The container is to be fabricated from a corrosion resistant material. The container will hold either six intact pressurized water reactor (PWR) or eighteen intact boiling water reactor (BWR) fuel assemblies. An alternative fuel loading strategy considered in the SCP is the placing of three intact PWR and four intact BWR fuel assemblies in the container. Excess BWR fuel assemblies will be buried in a ten assembly container. The reference SCP container can hold one DHLW pour canister.

Several advanced conceptual container designs are being considered [62]. These designs include large and small metallic multi-purpose/multi-barrier containers, self shielded containers, and non-metallic containers. Both corrosion allowance and corrosion resistant materials are being considered for fabrication of the metallic containers. These containers can hold various numbers of intact fuel assemblies or DHLW pour containers, depending on the design. The largest can hold 21 intact PWR fuel assemblies or four DHLW pour containers.

The preliminary design of containers for ALMR wastes and wastes generated from an actinide recycle campaign are based on the SCP design [37,41]. These designs may be modified if one of the advanced conceptual designs is ultimately utilized.

Six candidate materials are considered for container fabrication in the Yucca Mountain SCP [8]. These materials fall into two alloy families, austenitic materials and copper based materials. The austenitic alloys are AISI 304L, AISI 316L, and Alloy

825. The copper based materials are defined by the Copper Development Association (CDA) as oxygen-free copper (CDA 102), 8% aluminum-bronze (CDA 613), and 70-30 Cu-Ni (CDA 715). The degradation of these materials under repository relevant conditions has been investigated [63]. Similar studies have been completed for plain carbon steels [64] and for four Ni-Cr-Mo alloys [65]. The performance of SF cladding materials under repository relevant conditions has been investigated [66].

Models have been developed to predict the performance of waste containers in the repository [12,13,14,17,18,67,68,69]. These models utilize statistical techniques to predict the number of containers that fail as a function of time. The form of these models and their results depend heavily on the near field hydrothermal condition of the repository. These models are based primarily on the corrosion behavior of the container materials.

Several studies have been completed that predict the hydrothermal response of the repository due to the emplacement of SF and DHLW [12,13,14,17,18,62,70,71]. The primary purpose of these studies is to predict the time dependent temperature and water saturation distributions within Yucca Mountain due to the heat generated by the waste. These parameters are important in evaluation the performance of both the wasteform and the containers.

The dissolution of SF in ground water [8,12,13,72,73,74] and air/inert atmospheres [75] has been evaluated. Releases from spent fuel will arise from three sources: The fuel-clad gap, dissolution of the uranium-dioxide matrix, and the zircaloy clad. The release of radionuclides is dependent on the temperature, ground water composition, ground water pH, solubility of the radioactive elements, and the velocity of

the ground water moving past the wasteform. Dissolution may be limited by the reaction rate of the wasteform or the solubility of the radioactive elements. Models for the dissolution of SF have been developed [12,13,14,17,18].

The dissolution of DHLW borosilicate glass in groundwater has also been investigated [8,76]. The dissolution rate was found to be dependent on the exposed surface area, the ground water chemistry, the ground water pH, and the temperature. A model for DHLW dissolution has been developed [14].

Preliminary studies have been completed regarding the dissolution of ALMR wasteforms at 96 °C in water representative of Yucca Mountain ground water. These studies indicate that the performance of both the ALMR metal and zeolitic wasteforms is superior to that of DHLW borosilicate glass [39].

3 WASTE PACKAGE PERFORMANCE ANALYSIS

3.1 Introduction

In order to complete performance assessment analyses of a high level nuclear waste repository, it is necessary to predict the behavior of waste containers (or packages) in the repository environment. This chapter presents the model developed to predict the time dependent cumulative failure distribution (CFD) of the containers that are to be used to isolate high level nuclear waste. A summary of the current waste package designs proposed for spent light water reactor (LWR) fuel (SF) and defense high level waste (DHLW) will first be presented. Next a discussion of container design options for alternative wasteforms, in particular those of the Advanced Liquid Metal Reactor (ALMR) will be presented. A discussion of the materials being considered for container fabrication is next presented. Near field repository conditions that are expected to impact waste container performance will then be discussed. The model developed to predict the time dependent CFD of the waste containers will be presented. A discussion of model parameter selection will be presented. Finally, the time dependent failure distributions for each waste package container design and their associated uncertainties will be presented. The effect of waste container performance uncertainty on overall repository system performance is presented in Chapters 5 and 6.

3.2 Container Designs

Several waste container designs have been proposed for SF and DHLW. The reference SF and DHLW container designs are given in the Yucca Mountain Site Characterization Plan (SCP) [8]. The reference design is a right circular metallic cylinder having a diameter of 66 cm and nominal wall thickness of one centimeter. This container (with a height of 4.7 meters) will hold three intact pressurized water reactor (PWR) fuel assemblies or 6 intact boiling water reactor (BWR) fuel assemblies. If the fuel assemblies are consolidated, this package will hold the equivalent of 6 PWR or 18 BWR fuel assemblies. The reference package will also hold one 61 cm outer diameter DHLW pour container. This package is to be emplaced in boreholes drilled in the floor of the repository tunnel, which are called drifts. A diagram of the reference SCP waste package is shown in Figure 3.1.

As of September 1993, several alternative waste package designs have been proposed for SF and DHLW and are being evaluated [62]. The proposed design for SF holds 21 intact PWR fuel assemblies and is shown in Figure 3.2. It is composed of a 3.5 cm thick inner liner and a 11.5 cm thick outer case. The inner liner is fabricated from Alloy 825 and the outer barrier is fabricated from plain carbon steel. The fuel assembly basket structure is fabricated from either borated stainless steel or borated aluminum. Type 316 stainless steel is used to provide support to the basket structure.

Several alternative designs have been proposed for DHLW that utilize either drift or borehole emplacement. For borehole emplacement, a single pour canister is placed in a multi-barrier container, similar to the reference SCP design. For drift

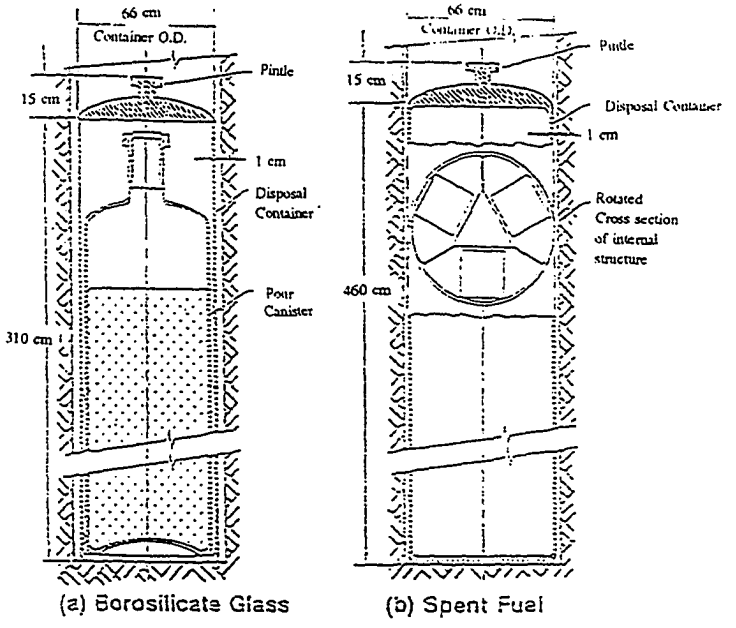

Figure 3.1: Reference SCP Single-Barrier Waste Package [8]

emplacement, either three or four pour containers are to be placed in a multi-barrier container similar in design to the spent fuel metallic multi-barrier concept shown in Figure 3.2.

Conceptual waste container designs for ALMR wasteforms have been proposed [37]. An ALMR being used in a LWR actinide recycle program will produce several high level waste streams. The primary high level waste streams are 1) a salt waste-form, 2) a metallic wasteform, and 3) gaseous waste. The reference ALMR waste container designs is similar to the reference DHLW container design. The waste is placed in an inner canister (or pressure bottle for gases), similar to the DHLW pour container. The inner container is placed inside an outer container. The dimensions of the containers by waste type are given in Table 3.1 [37]. It is estimated that the containers are one centimeter thick consistent with the container thickness of

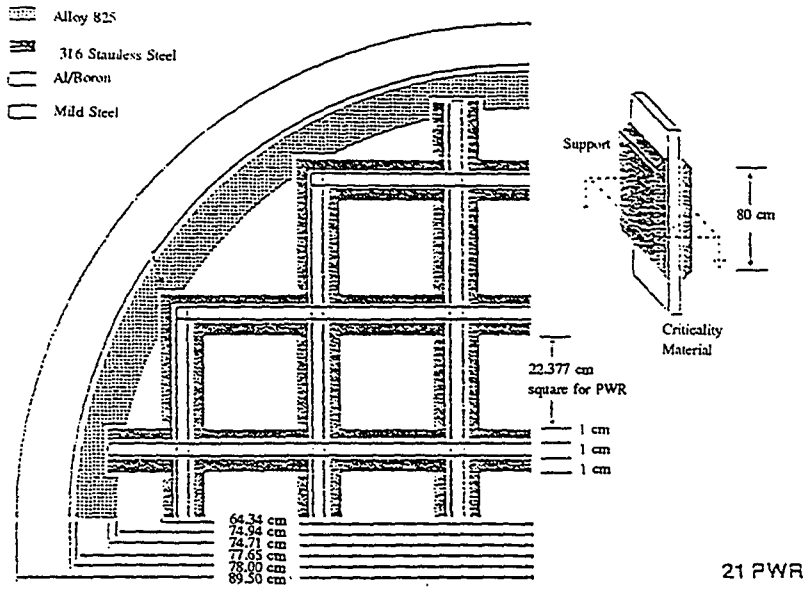

Figure 3.2: Metallic Multi-Barrier Waste Package [62]

the reference DHLW containers.

The ALMR containers were sized to allow borehole emplacement. Alternatives similar to those being investigated for drift emplacing DHLW (3 or 4 pour canisters per container) may prove useful for ALMR waste. Current studies are focused on the containers shown in Figures 3.1 and 3.2.

3.3 Materials Being Considered For High Level Waste Containers

Several austenitic and copper based materials are being considered for waste package design [8]. The austenitic materials being considered include AISI 304L, AISI 316L, and Alloy 825. Copper based materials being considered include oxygen-free copper (CDA 102), 8% aluminum bronze (CDA 613) and 70Cu-30Ni (CDA 715).

Recently the use of mild steels, low alloy steels and irons has been investigated

Table 3.1: Container Design for ALMR Wastes

	Inner Container			Outer Container		
Waste Type	Mtl.	Ht. (cm)	Dia. (cm)	Mtl.	Ht. (cm)	Dia. (cm)
Mineral	Stainless Steel	298	59	Stainless Steel	320	66
Metal	Stainless Steel	290	50	Stainless Steel	320	66
Gas	Carbon Steel	47	16	Stainless Steel	320	66

primarily for use in multi-barrier designs or designs with thick barriers. Lead may be used in totally self-shielded container designs. The expected behavior of carbon and low alloy steels and austenitic alloys is summarized as these materials will most likely be utilized in the fabrication of metallic multi-barrier type containers.

Carbon and Low Alloys Steels The lifetime of container barriers fabricated out of mild steel, alloy steels, and irons is expected to be limited by the corrosion behavior of the metal. The aqueous corrosion of irons and steels depends primarily on the concentration of dissolved oxygen and is independent of pH in the range of 4-10. All mild steels, low alloy steels, and cast irons are essentially identical in terms of aqueous corrosion performance. Heat treatment or metallurgical factors do not appear to greatly influence the aqueous corrosion rate. Only when Cr is added to the levels commensurate with a stainless steel is the corrosion rate appreciably impacted. The corrosion rate of irons and steels approximately doubles for every 30°C rise in temperature until about 80°C, where it begins to decrease. This reduction is due to the decrease in the oxygen solubility in water [77]. The concentration levels of species in

the Yucca Mountain ground water are not expected to result in accelerated corrosion of irons and steels. The drying out of the repository may concentrate certain species, specifically Na^+ and Cl^-, to levels where increased corrosion may occur. Under atmospheric conditions, the corrosion rate depends on the humidity. Essentially no corrosion occurs until the humidity reaches about 60% and then increases by approximately two orders of magnitude at 100% humidity. Sulfates and dissolved salts accelerate atmospheric corrosion of irons and steels [77].

Localized and galvanic corrosion will most likely limit the life of carbon steel barriers. A study performed recently at Iowa State University indicates that carbon steels are susceptible to radiation enhanced corrosion under atmospheric exposure conditions [78]. Recent work completed at Iowa State University indicates that carbon steels may be susceptible to accelerated dry oxidation under the high repository temperatures that may occur with some loading scenarios [69]. These enhanced corrosion modes will not be directly included in this investigation, but will be evaluated as part of the total repository system performance assessment.

Austenitic Alloys A survey of the degradation modes of austenitic alloys has been conducted [63]. The results are summarized. Equilibrium thermodynamic studies indicate that Alloys 304L and 316L are metastable and body-centered cubic phases may precipitate out of the face-centered cubic matrix. Martensitic transformations may also occur in these alloys. These phase transformations have not been observed, but may occur under the conditions required for long term isolation of nuclear waste. An intermetallic phase has also been observed in alloy 316L. During the long time periods required for isolation, these reactions may limit the life of the

containers. Again, these enhanced failure modes will not be directly included in this investigation, but overall container performance uncertainty is evaluated as part of the total repository system performance assessment (see section 5.4.6).

Uniform corrosion is not expected to limit the life of austenitic containers. Sensitization, a process where chromium rich carbides precipitate at grain boundaries, can lead to intergranular stress corrosion cracking (IGSCC) and typically occurs in the heat affected zones near welds. Controlling the carbon content to less than 0.035% in alloys 304L and 316L minimizes the potential for sensitization. Titanium additions to Alloy 825 eliminates the potential for sensitization. All three austenitic alloys demonstrate susceptibility to pitting in chloride-containing environments. Of the three, Alloy 825 is most resistant and alloy 304L the most susceptible. Stressed austenitic specimens in an environment containing sufficient dissolved chloride can undergo trans-granular stress corrosion cracking (SCC). The drying out of the repository may concentrate Cl^- to levels that could lead to pitting or SCC. Alloy 304L may be susceptible to radiation enhanced corrosion and microbiologically induced corrosion, but Alloy 825 appears to not be affected. Hydrogen attack is not expected to limit the life of austenitic containers [63].

3.4 Summary of Near Field Repository Conditions

The repository horizon at Yucca Mountain lies in an unsaturated zone (65±19%) of rock approximately 200-400 meters above the water table [8]. The composition of the ground water at the repository horizon is expected to be similar to that of well J-13 water [8] and is shown in Table 3.2. This water is of neutral pH and in

Table 3.2: Element Concentration (mg/L) of Well J-13 Water pH = 6.9

Elements		Anions	
Ca	11.5	F^-	2.1
Mg	1.76	Cl^-	6.4
Na	45.0	SO_3^{2-}	18.1
K	5.3	HCO_3^-	143.0
Li	0.06	NO_3^-	10.1
Fe	0.04	O_2	5.7
Mn	0.001		
Al	0.03		
Si	30.0		

its un-altered state contains no ionic species expected to lead to accelerated corrosion of the waste packages.

The near field repository environment will be altered due to the emplacement of the waste packages. Nuclear waste generates heat due to radioactive decay which will result in near field alteration primarily due to hydro-thermal effects. The rock temperature, wasteform temperature, and dry-out time depend on several factors, most importantly the waste thermal output and the waste package spacing. For SF, these two parameters dictate the Areal Power Density (APD - Kw/acre) and Areal Mass Loading (AML -- MTU/acre). The AML and APD are connected through the thermal output from the waste. The thermal output of the waste is dictated by the burnup of the fuel and the cooling time prior to being emplaced in the repository. For example, if a repository has a constant APD, more 30 year cooled SF will need to be loaded per acre than 10 year cooled SF (provided the burnup on each is similar). For

a given APD and SF age, fuel having a higher burnup will result in lower AMLs.

The SF that will be loaded into the repository will have varying ages and burnup. As such, it is impossible to predict the actual repository temperature behavior until the repository design and waste loading patterns are determined. Analyses of repository thermal effects consider loadings that result in either a hot, nominal, or cool repository. Comprehensive studies of the heat driven hydro-thermal ground water flow at Yucca Mountain have been completed for the SF wasteform [70,71].

The emplacement of SF in a repository will increase the rock temperature. The temperature will rise to a peak and then begin to decrease as the heat output from the waste decays. If the repository temperature increases above the boiling point of water, a dry-out front will occur. The dry-out front will move outward from the waste packages as the repository continues to heat up. When the thermal output of the waste begins to decay, the repository temperature will begin to decrease and the dry-out front will shrink towards the waste packages. Once the temperature of the waste container surface drops below the boiling point, liquid water will then be able to contact the material surface. The degree of saturation during the rewetting period will be less than the initial saturation of the rock for a long time span (up to 100000 years).

The heat output of either DHLW or ALMR waste packages is small when compared to that of SF due to the low actinide inventories. If these waste packages are co-located with SF, the repository hydro-thermal behavior will be affected only by the SF loading strategy. If the DHLW or the ALMR waste are emplaced in the repository such that no effects of the SF are realized, the hydro-thermal behavior is not expected to be altered significantly.

3.5 Models Used To Predict Container Failures

A waste package failure model was developed as part of Yucca Mountain total repository system performance studies [12,13]. Due to the complexity of the waste package container failure modes and the uncertainty in the repository environment, it was decided that statistical techniques should be used as the basis for waste package failure models [12]. The statistical technique utilized was the Weibull Distribution which is employed in many fields of engineering for component life prediction (Equation 3.1).

$$P(t)=1-\exp\left[-\left(\frac{t-t_f}{t_m}\right)^b\right] \tag{3.1}$$

Where:
- P(t)= Fraction of Containers Failed at time t
- t_f = Threshold time to failure (lower limit of container lifetime).
- t_m = Mean time to failure (mean container lifetime)
- b = Weibull slope (failure rate at mean lifetime)

During the first phase of the study [12], the three Weibull parameters were chosen based on qualitative estimates of the container lifetimes. During the second phase of the study [13], the model was expanded to account for early failures and multiple barriers. This model is given in equation 3.2.

$$P(t)=C_e\times\left(1-\exp\left[-\left(\frac{t}{t_e}\right)^b\right]\right)+(1-C_e)\times\left(1-\exp\left[-\left(\frac{t-t_{f1}}{t_{m1}}\right)^{b1}\right]\right)$$
$$\times\left(1-\exp\left[-\left(\frac{t-t_{f2}}{t_{m2}}\right)^{b2}\right]\right)\times\left(1-\exp\left[-\left(\frac{t-t_{f3}}{t_{m3}}\right)^{b3}\right]\right) \tag{3.2}$$

Where: P = Fraction of containers failed at time t

C_e = Fraction of containers susceptible to early failure

t_e = Mean time for early container failure

t_f = Lower limit of barrier lifetime, (barriers 1-3)

t_m = Mean lifetime, (barriers 1-3)

b = Weibull slope, (barriers 1-3)

The Weibull parameters for the outer barriers were based on uniform corrosion and pitting models. The Weibull parameters for the clad were based on estimates of clad lifetimes (creep rupture and radial re-orientation of zirconium-hydride platelets). Sequential failure of the multiple barriers was modelled in the following fashion.

1. The threshold time to failure of the second barrier is calculated as the threshold time of the first barrier plus the threshold time of the second barrier as if it were the only barrier.
2. The mean time to failure of the second barrier is calculated as the mean time of the first barrier plus the mean time of the second barrier as if it were the only barrier.
3. The threshold time to failure of the clad is calculated as the threshold time of the second barrier plus the threshold time of the clad as if it were the only barrier.
4. The mean time to failure of the clad is calculated as the mean time of the second barrier plus the mean time of the clad as if it were the only barrier.

The container failure model was subsequently modified to account for the varying repository near field conditions [67]. The revised model considered the effects of the thermal pulse, the time delay until re-wetting occurs and the near field geochemistry. The model (equation 3.2) was expanded to include four time dependent

temperature profiles, three hydrothermal modes, and dry versus wet water contact modes.

The model was again modified to further refine the water contact modes [68]. The two water contact modes were expanded to four; wet-drip, moist-continuous, episodic, and dry. Under wet-drip conditions local differences in the rock characteristics allow water to drip onto the waste container. If the waste package is contacting the surrounding rock or the repository is saturated, a moist-continuous condition results and the package surface is always wet. Under episodic conditions, the package experiences periods of wetting and drying. The four temperature regimes and three hydrothermal modes continued to be included in the model. The modified model is shown in equation 3.3.

$$P(t) = C_e\left(1-\exp\left(-\frac{t}{t_1}\right)\right) + \sum_i \sum_j \sum_k C_{ijk} \times \left(1-\exp\left[-\left(\frac{t-t_{f1_{ijk}}-dt_{ijk}}{t_{m1_{ijk}}}\right)^{b1_{ijk}}\right]\right) \times \left(1-\exp\left[-\left(\frac{t-t_{f2_{ijk}}-dt_{ijk}}{t_{m2_{ijk}}}\right)^{b2_{ijk}}\right]\right) \times \left(1-\exp\left[-\left(\frac{t-t_{f3_{ijk}}-dt_{ijk}}{t_{m3_{ijk}}}\right)^{b3_{ijk}}\right]\right) \quad (3.3)$$

Where:

- P= Fraction of containers failed at time t
- C_e = Fraction of containers susceptible to early failure
- C_{ijk}= Fraction of containers in thermal mode i, water contact mode j, and temperature regime k
- dt= Dryout time
- t_1 = Mean time for early container failure
- t_f = Lower limit of barrier lifetime (barriers 1-3)
- t_m= Mean barrier lifetime, (barriers 1-3)
- b = Weibull slope, (barriers 1-3)

It can be seen from Equation 3.3 that in this model each barrier begins to experience a non-zero probability of failure once the threshold time to failure (plus any dryout period) is exceeded and does not account for sequential failure of the barriers. Under actual repository conditions, the inner barrier may not begin to experience any probability of failure until the outer barrier has failed and the cladding will also not begin to experience any probability of failure until the inner barrier has failed. In addition, the dry out period is added to all three barriers. The inner barriers will not experience any dryout period when they begin to contact the repository environment. Figure 3.3 demonstrates how the failure distribution may be modeled. Figure 3.3 shows the probability that an entire container has failed (complete penetration) at time t given the probability of inner barrier failure at time t2 given outer barrier failure at time t1.

For the curve shown in Figure 3.3, the probability of complete failure of the waste container (penetration of all three barriers) with outer barrier failure at time t1 and inner barrier failure at time t2 is given by equation 3.4.

$$P(t) = \left(1 - \exp\left[-\left(\frac{t1 - t_{f1}}{t_{m1}}\right)^{b1}\right]\right) \times \left(1 - \exp\left[-\left(\frac{t2 - t1 - t_{f2}}{t_{m2}}\right)^{b2}\right]\right) \times \left(1 - \exp\left[-\left(\frac{t - t2 - t_{f3}}{t_{m3}}\right)^{b3}\right]\right) \tag{3.4}$$

Where: P(t)= Probability that a container has completely failed at time t give failures of outer barrier at time t1 and inner barrier at time t2

t_f = Lower limit of barrier lifetime, (barriers 1-3)

t_m = Mean lifetime, (barriers 1-3)

b = Weibull slope, (barriers 1-3)

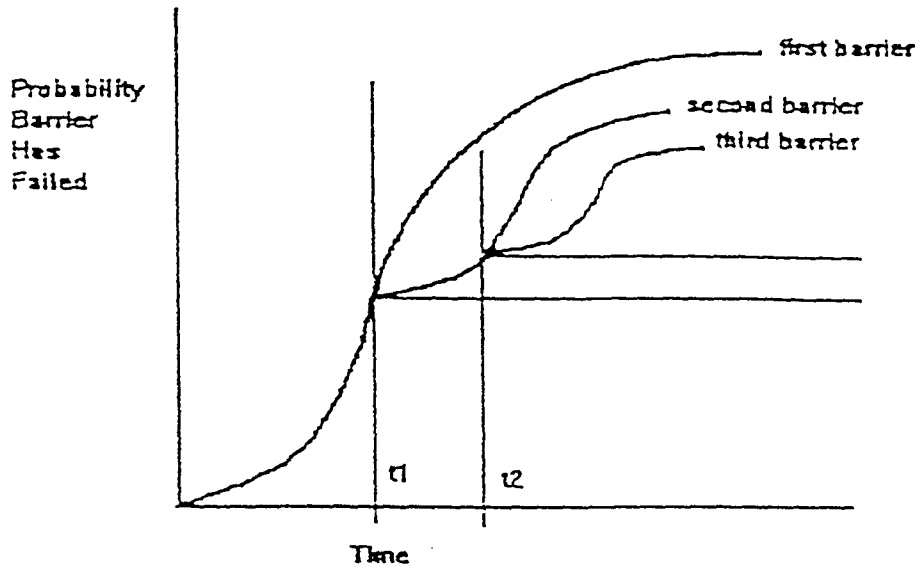

Figure 3.3: Failure Probability Distribution of a Multi-Barrier Waste Container

The cumulative failure distribution of the barrier system within the repository system will be an integration of an infinite series of the curves shown in Figure 3.3. This distribution is derived through equations 3.5 and 3.6.

$$dP = dP_1 \times dP_2 \times P_3 \tag{3.5}$$

$$P = \int_0^t \int_0^t dP_1 \times dP_2 \times P_3 \tag{3.6}$$

Where: dP_1= The fraction of containers with outer barrier failed at t1 about dt1.

dP_2= The fraction of containers with inner barrier failed at t2 about dt2 given the probability of failure of the outer barrier at t1.

P_3 = The Fraction of containers with the clad failed at t given the probability of outer barrier failure at t1 and inner barrier failure at t2.

The differential probability for one barrier is given in equation 3.7. The final equation, when integrated is given as equation 3.8. This model was implemented in a FORTRAN computer program provided in Appendix A.

$$\frac{dP}{dt} = \frac{b}{t_m} \times \left(\frac{t-t_f}{t_m}\right)^{b-1} \times \exp\left(-\frac{t-t_f}{t_m}\right)^{b} \tag{3.7}$$

$$P(t) = \sum_i \sum_j \sum_k C_{ijk} \int_0^t \int_{t1}^t \frac{b1_{ijk}}{t_{m1_{ijk}}} \left(\frac{t1-(t_{f1_{ijk}}+dt_{ijk})}{t_{m1_{ijk}}}\right)^{b1_{ijk}-1}$$

$$\exp\left(-\frac{t1-(t_{f1_{ijk}}+dt_{ijk})}{t_{m1_{ijk}}}\right)^{b1_{ijk}} \frac{b2_{ijk}}{t_{m2_{ijk}}} \left(\frac{t2-t1-t_{f2_{ijk}}}{t_{m2_{ijk}}}\right)^{b2_{ijk}-1} \tag{3.8}$$

$$\exp\left(-\frac{t2-t1-t_{f2_{ijk}}}{t_{m2_{ijk}}}\right)^{b2_{ijk}} \exp\left(-\frac{t-t2-t_{f3_{ijk}}}{t_{m3_{ijk}}}\right)^{b3_{ijk}} dt2 \cdot dt1$$

Where:

- $P(t)$= The fraction of containers failed at time t
- c_{ijk}= The fraction of containers in hydrothermal mode i water contact mode j and temperature regime k
- dt_{ijk}= The dryout time
- tf_{ijk}= Lower limit of barrier lifetime, (barriers 1-3)
- tm_{ijk}= Mean barrier lifetime, (barriers 1-3)
- b_{ijk} = Weibull slope, (barriers 1-3)
- t1 = dummy variable of integration -- failure time of first barrier
- t2 = dummy variable of integration -- failure time of second barrier

3.6 Determination of Container Performance Parameters

For this study, the complexity of the model is going to be reduced to a single hydrothermal environment (undefined), and only wet or dry water contact. This reduces the number of calculations required at each time step.

A study of the repository near field thermohydrologic behavior was completed in support of the 1993 Total System Performance Analysis using the V-TOUGH code [14]. V-TOUGH simulates the coupled multi-dimensional transport of water, vapor, air, and heat in porous and fractured media. The repository waste panels (sub-areas within the repository that hold the waste) were divided into eight rings of equal area. The inner six rings contain spent fuel. The seventh ring is assumed to contain DHLW and the outer ring represented the access drifts. An r-z model was utilized assuming that a panel does not interact with other panels or the surrounding rock. No flow of heat or fluid was allowed at the panel interfaces as a result of symmetry in the interface conditions. This assumption has been shown to result in only a mild impact on the temperature and saturation distributions within a panel. The vertical discretization consisted of 42 layers, from the ground surface to approximately one kilometer of the saturated zone. The current measured properties for each stratigraphic unit were utilized.

A "youngest fuel first" SF loading strategy was assumed. The characteristics of the SF assumed in calculation of the hydro-thermal response is shown in Table 3.3. The thermal decay of this blended fuel is shown in Figure 3.4. The repository temperature was determined for each ring for a cool repository (loading = 28.5 Kw/acre), a nominal repository (loading = 57 Kw/acre), and a hot repository

Table 3.3: Characteristics of SF Assumed in Thermohydrologic Analysis

Attribute	BWR	PWR
Amount (10^3 MTU)	22.25	40.75
Average Age (yr)	23.5	22.5
Burnup (GWd/MTU)	32.2	42.2

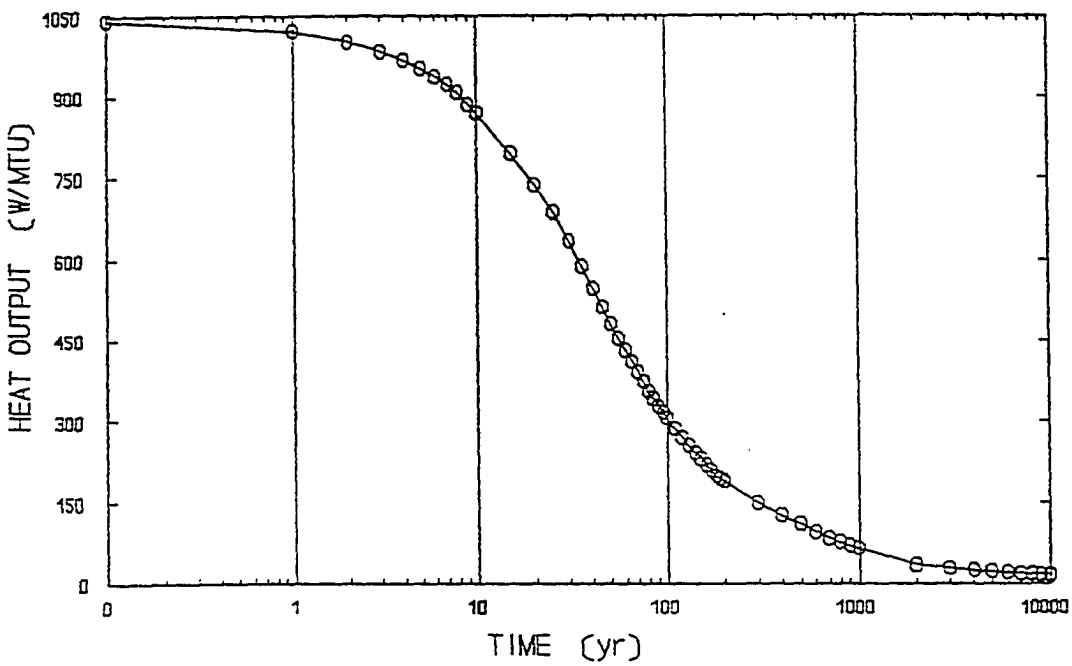

Figure 3.4: Thermal Decay of Blended Spent Fuel [14]

(loading = 114 kw/acre). The resultant time dependent temperature distributions for the inner six rings are shown in Figures 3.5 - 3.7 for a cool, nominal, and hot repository, respectively. The time period for which the waste package temperature is above 100°C, hence dry, is shown in Table 3.4.

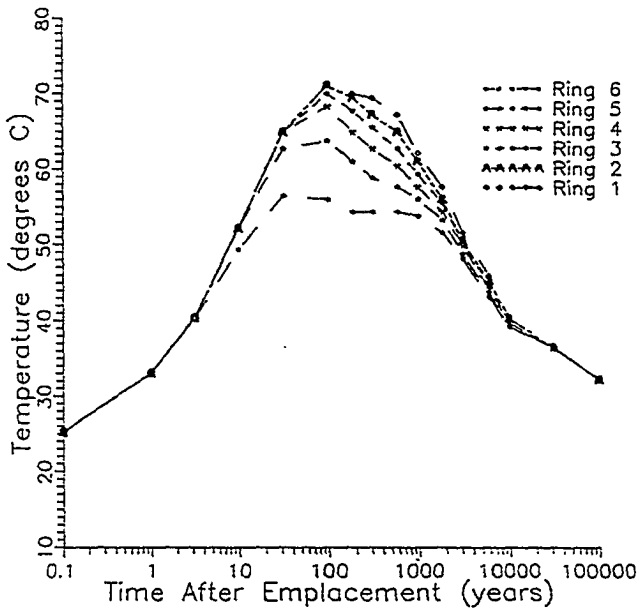

Figure 3.5: Temperature History of Six Inner Panel Rings (APD = 28.5 Kw/Acre) [14]

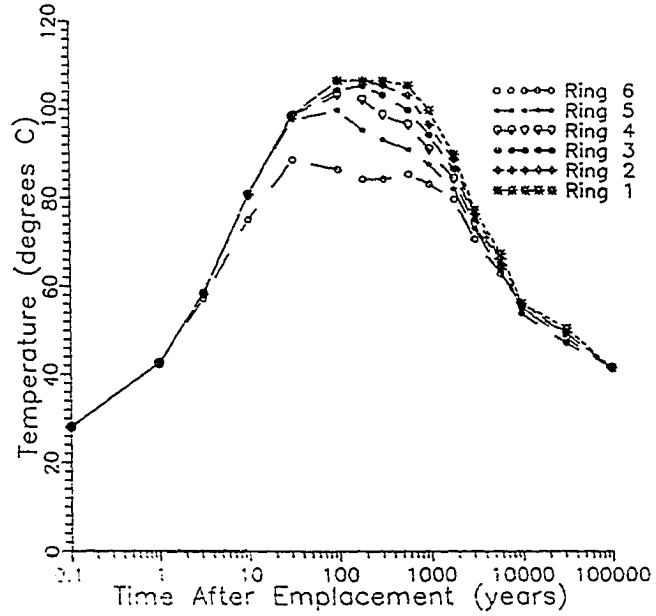

Figure 3.6: Temperature History of Six Inner Panel Rings (APD = 57.0 Kw/Acre) [14]

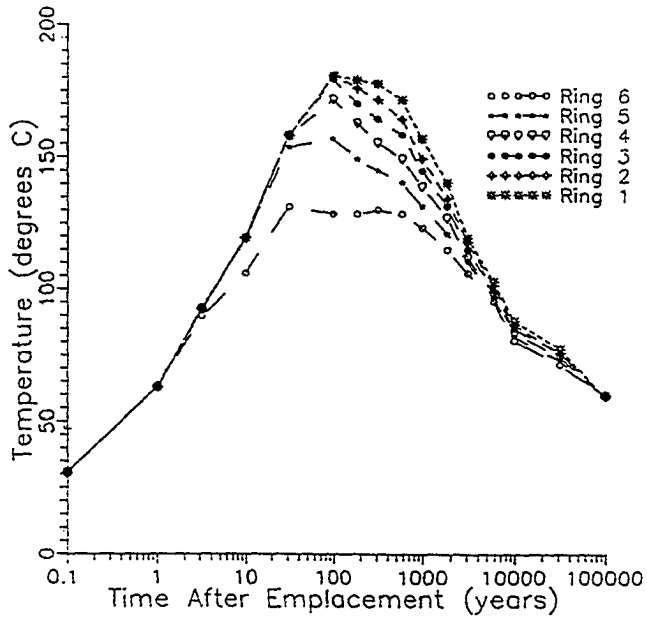

Figure 3.7: Temperature History of Six Inner Panel Rings (APD = 114.0 Kw/Acre) [14]

Table 3.4: Time Period That the Waste Package is Dry (years)

APD (Kw/Acre)	Ring 1	Ring 2	Ring 3	Ring 4	Ring 5	Ring 6	Ring 7
28.5	0	0	0	0	0	0	0
57.0	973	774	562	259	0	0	0
114.0	6774	6337	5930	5622	5314	4743	3600

As was discussed previously, DHLW and ALMR wasteforms generate a negligible amount of heat as compared to the SF. If either DHLW or ALMR waste is loaded alone, the temperature will not increase significantly and can be assumed to be the ambient temperature of the rock (assumed to be 30 °C).

The Weibull parameters are determined assuming that the barriers failed by corrosion processes, specifically uniform and localized corrosion. Corrosion is

assumed to follow either a non-passivating behavior (equation 3.9) or passivating behavior (equation 3.10).

$$d = g \cdot t \tag{3.9}$$

$$d = k \cdot t^{n} \tag{3.10}$$

Where:
- d = the penetration (cm)
- g = the non-passivating penetration rate (cm/yr)
- k = the passivating penetration "rate" (cm/yr^{n})
- n = the passivation coefficient (< 1.0)
- t = time (years)

The corrosion equations can be used to determine the Weibull parameters. The threshold time to failure of a given barrier is defined as the time required for penetration of 50% of the thickness. The mean time to failure of a given barrier is defined as the time required for complete penetration. The Weibull slope is determined through a least squares method [79]. The following equations are used to determine the Weibull slopes. F(t) is the fraction of the container thickness that has corroded.

$$X = \ln(t - t_i) \qquad Y = \ln \ln \left(\frac{1}{1 - F(t)} \right)$$

$$b = \frac{\sum_i (X_i - \bar{X}) \cdot (Y_i - \bar{Y})}{\sum_i (X_i - \bar{X})^2} \tag{3.11}$$

As part of the Intera 1993 Total System Performance Analysis, a model has been developed to predict the corrosion behavior of carbon steel [14]. This model assumes that pitting will occur and is passivated and includes a temperature dependence. The carbon steel corrosion model utilized is given in equation 3.12.

$$d = 1010 \times t^{0.47} \times e^{-\frac{2850}{T}} \quad (3.12)$$

Where: d = Penetration (cm)

T = Temperature (Kelvin)

t = Time (years)

Models have been developed models for corrosion resistant barriers (Alloy 825 and 304L). The model for the corrosion of Alloy 825 (penetration depth versus time) is shown in Figure 3.8 and is developed from data provided in Reference 63. No temperature dependence is assumed. 304L may corrode quite rapidly due to increased corrosion (pitting and SCC) in the sensitized region near the welds resulting from the concentrating of Cl^- in the ground water. The data indicates that Alloy 825 will corrode by localized corrosion at rates much less than 304L. Based on this, only Alloy 825 will be considered for the inner barrier.

The final set of parameters to determine are those that describe clad life for SF. An investigation calculated that if the clad peak temperature is maintained below 350°C, the clad will not fail by creep rupture within a period of 10000 years [66]. No data exists regarding the corrosion of zircaloy in low temperature aqueous environments. High temperature aqueous corrosion data was used to estimate the corrosion rate of the clad. In 600° F water, the corrosion rate of Zircaloy-4 was measured to be 3.71E-4 cm/yr [80]. A typical clad thickness (PWR) of 0.06 cm [81] results in a time to complete penetration of 1615 years.

The carbon steel barrier performance parameters were calculated using equation 3.14 in conjunction with the temperature histories shown in Figures 3.5-3.7. The Alloy 825 parameters were calculated using the curve shown in Figure 3.8. The

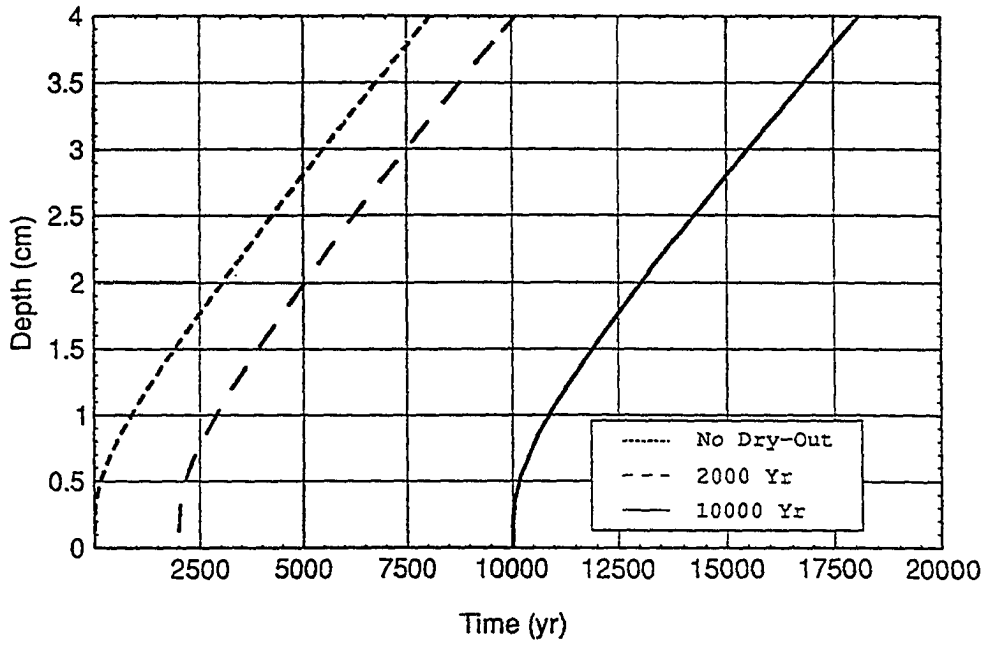

Figure 3.8: Corrosion of Alloy 825

clad performance parameters were calculated using the relation presented above. The parameters for the carbon steel barrier are shown in Table 3.5. The parameters for the Alloy 825 inner barrier, the clad, and an Alloy 825 pour container are shown in Table 3.6. These values apply to all rings.

3.7 Analysis of Container Performance

The time dependent failure distribution of metallic multi-barrier type containers have been analyzed under cool (28.5 Kw/acre), nominal (57.0 Kw/acre), and hot (114.0 Kw/acre) repository loadings for SF and DHLW/ALMR wasteforms and under ambient conditions for the DHLW/ALMR wasteforms. It was assumed that the containers did

Table 3.5: Performance Parameters for Carbon Steel Barrier

	Ring 1	Ring 2	Ring 3	Ring 4	Ring 5	Ring 6	Ring 7
Cool Repository (28.5 KW/acre)							
Threshold (yrs)	1060	1110	1150	1240	1470	1520	1750
Mean Time (yrs)	4950	5250	5450	6010	7360	7670	9100
Weibull Slope	1.22	1.22	1.22	1.22	1.21	1.21	1.20
Nominal Repository (57 KW/acre)							
Threshold (yrs)	160	240	240	320	360	480	890
Mean Time (yrs)	504	830	830	1190	1360	1960	4180
Weibull Slope	1.29	1.27	1.27	1.26	1.26	1.25	1.22
Hot Repository (114 KW/acre)							
Threshold (yrs)	210	700	1150	414	542	362	340
Mean Time (yrs)	970	2670	3840	1710	3000	1560	1450
Weibull Slope	1.22	1.26	1.28	1.24	1.24	1.24	1.24

not start corroding until they were contacted with water (after the dryout period was exceeded, Table 3.3). The results for the reference SCP container are presented in Figures 3.9 through 3.11. The results for the metallic multi-barrier container are shown in Figures 3.12 through 3.14. Figures 3.15 and 3.16 provide the results for DHLW/ALMR bearing containers. The FORTRAN program in Appendix A was used

Table 3.6: Performance Parameters for Inner Barrier, Cladding, and Pour Container

	Inner Barrier (Alloy 825)	Cladding (Zircaloy)	SCP Single Barrier and Pour Container (Alloy 825)
Threshold Time to Failure (years)	2190	0	270
Mean Time to Failure (years)	7025	1615	860
Weibull Slope	1.29	2.00	1.30

It can be seen for the SF cases that the MMB containers fail more rapidly once the dry-out period is exceeded as the APD increases due to the increased waste package temperature resulting in more rapid failure of the carbon steel barrier. This is not seen with the SCP design as the Alloy 825 corrosion model does not have a temperature dependence.

The majority of the SCP containers fail within approximately 10000 years following emplacement regardless of the thermal load. The MMB containers fail within a 50000 year following emplacement. The most rapid failure occurs for an APD of 57.0 kW/acre while the least rapid occurs for an APD of 114.0 kW/acre. The failure of the MMB containers depends on both the dry-out time and the post dry-out time repository temperature. An APD of 28.5 kW/acre results in no dry-out time and relatively low corrosion rates. An APD of 114.0 kW/acre results in a long dry-out time (10000 years) and high corrosion rates. An APD of 57.0 kW/acre results in shorter dry-out times and lower corrosion rates than those from an APD of 114.0 kW/acre. The shorter dry-out time results in more rapid failure in spite of lower corrosion for an

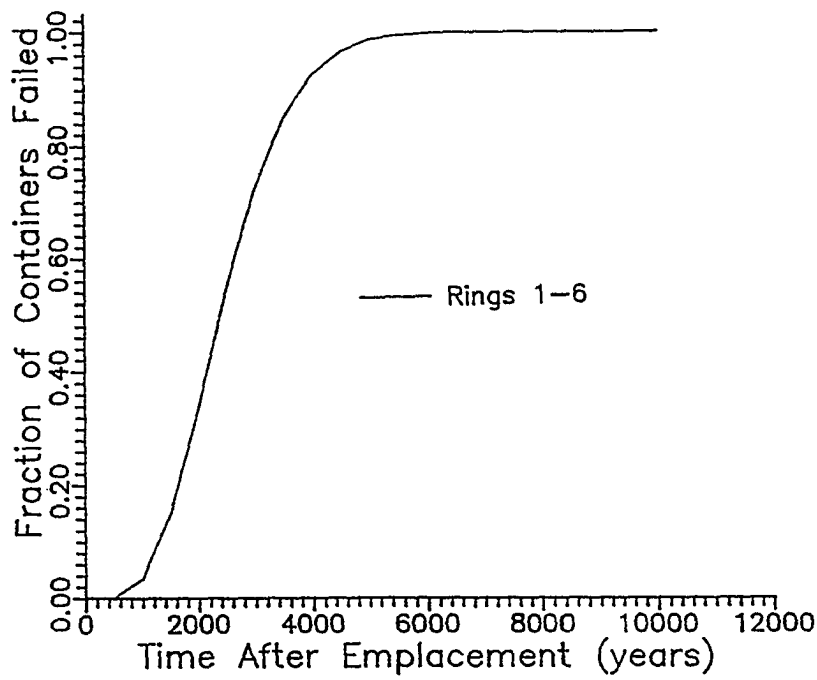

Figure 3.9: Reference SCP Container Performance (28.5 Kw/acre)

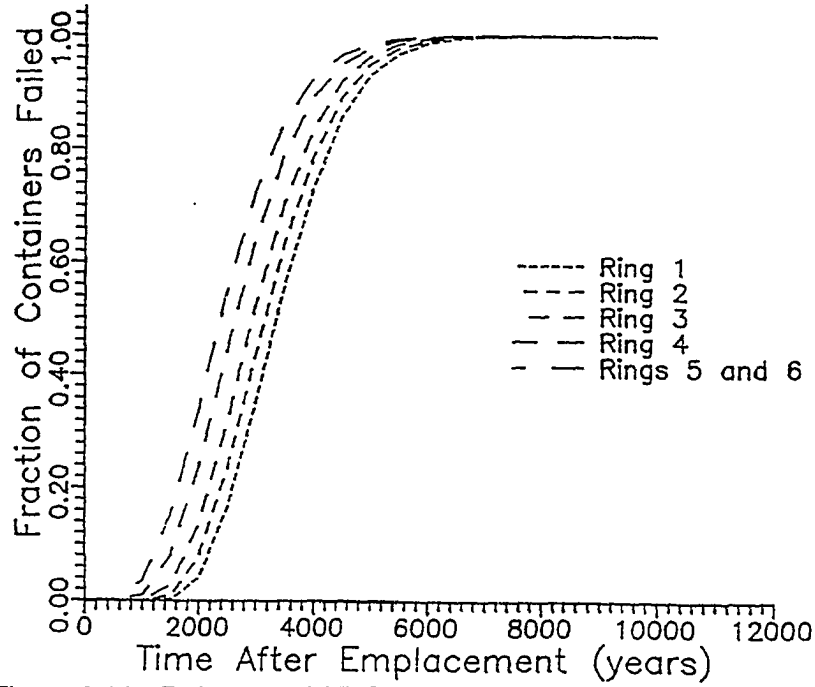

Figure 3.10: Reference SCP Container Performance (57.0 Kw/acre)

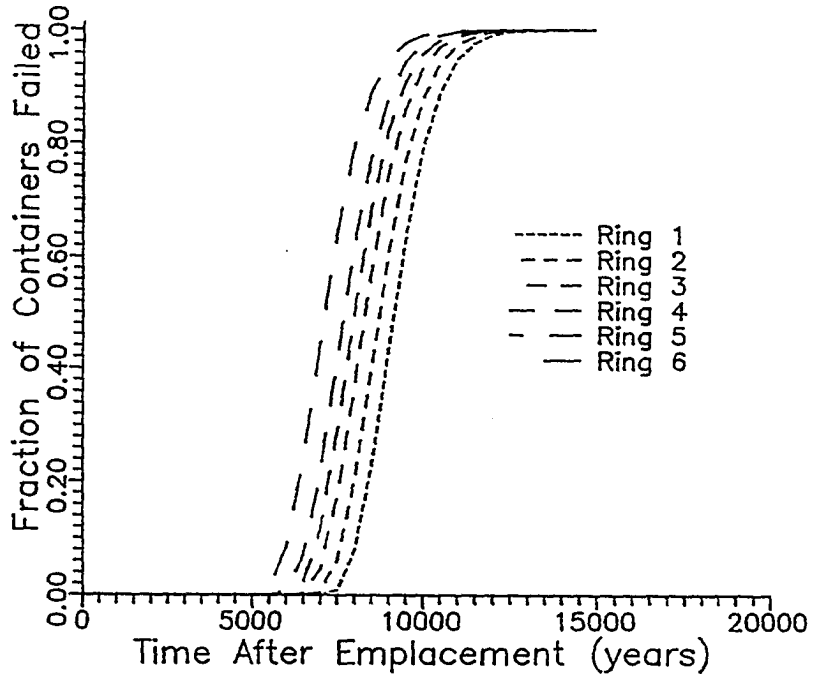

Figure 3.11: Reference SCP Container Performance (114.0 Kw/acre)

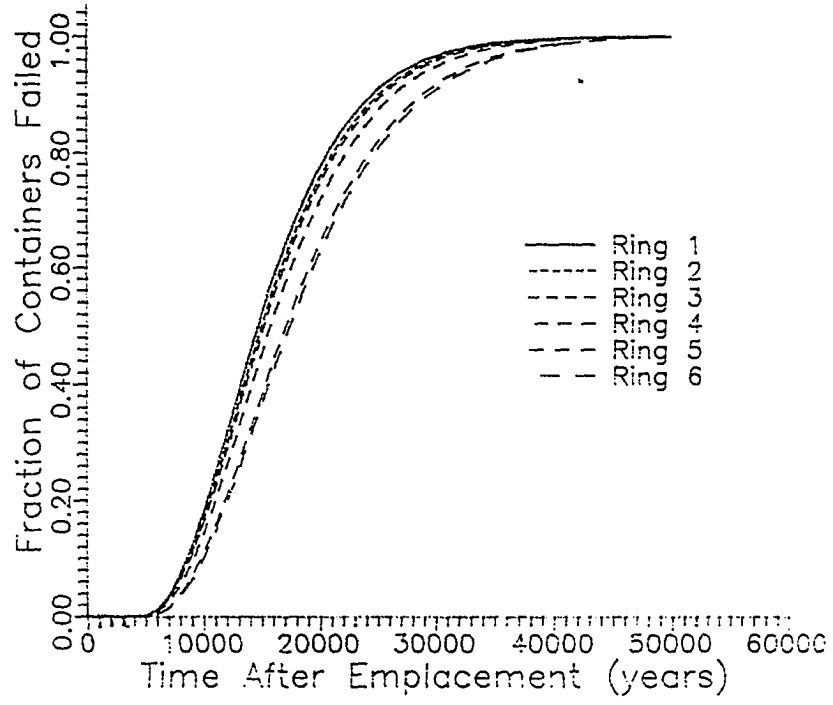

Figure 3.12: Metallic Multi-Barrier Container Performance (28.5 Kw/acre)

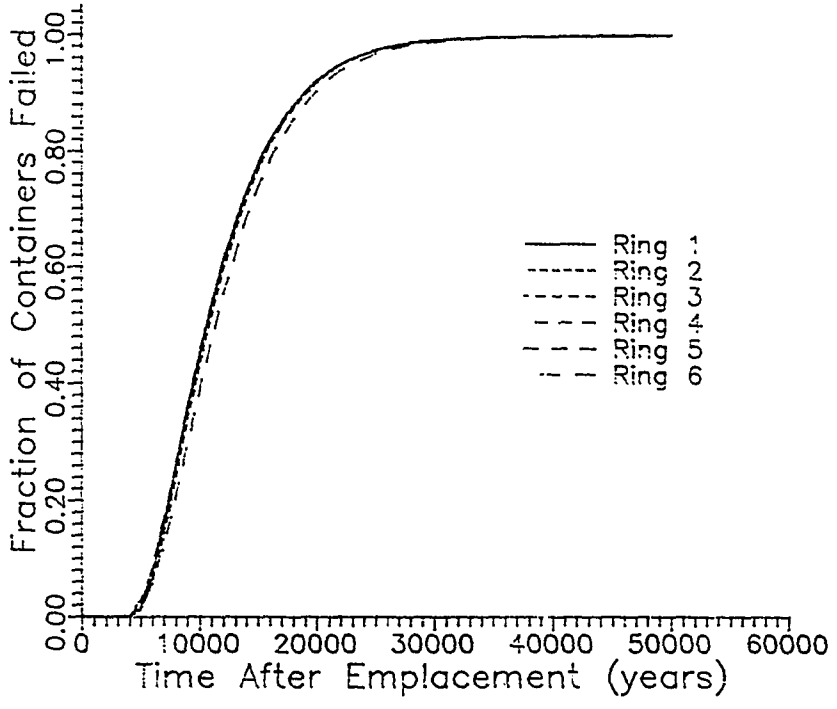

Figure 3.13: Metallic Multi-Barrier Container Performance (57.0 Kw/acre)

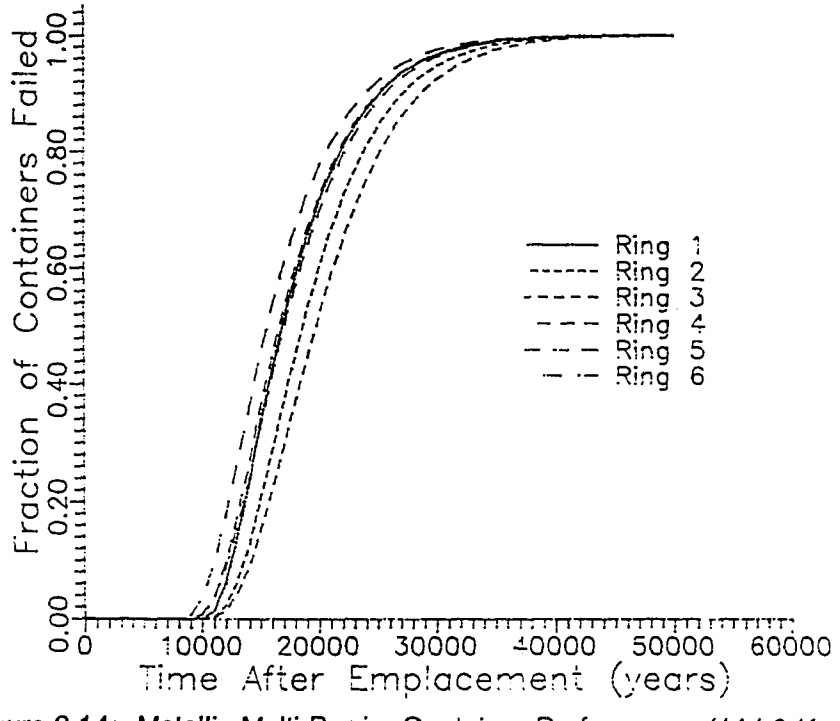

Figure 3.14: Metallic Multi-Barrier Container Performance (114.0 Kw/acre)

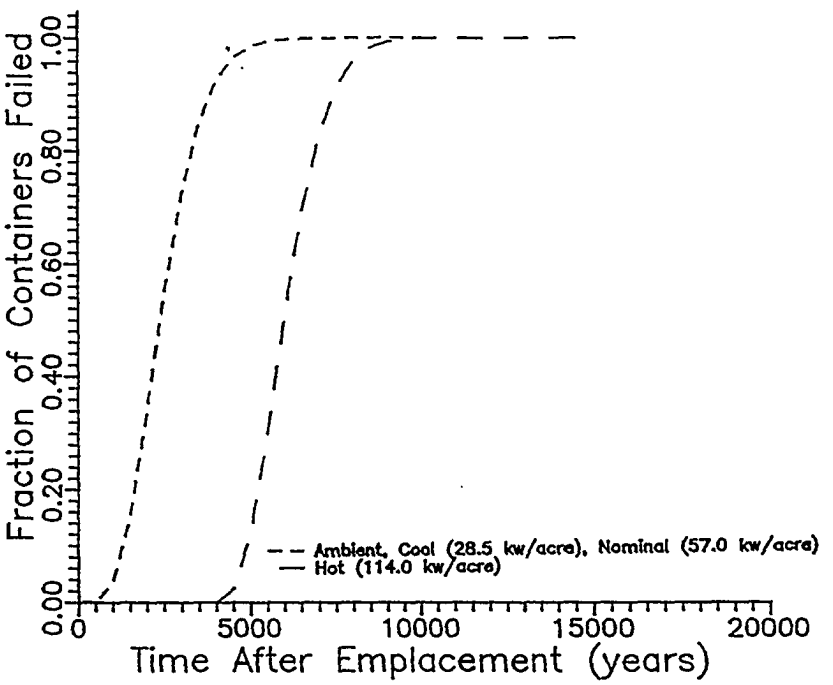

Figure 3.15: Reference SCP Container Performance for DHLW/ALMR Wastes

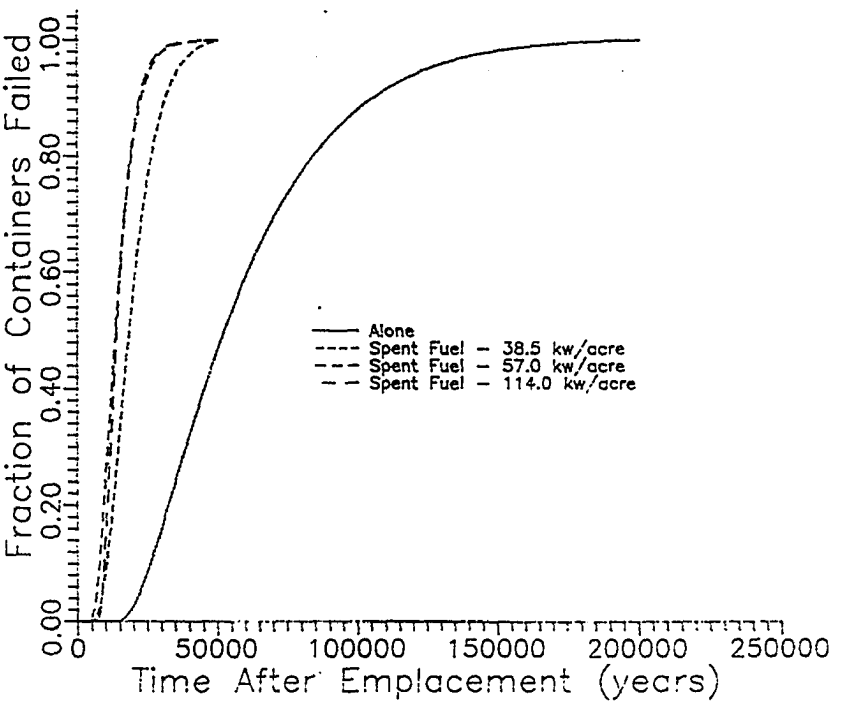

Figure 3.16: Metallic Multi-Barrier Container Performance for DHLW/ALMR Wastes

APD of 57.0 kW/acre relative to an APD of 114.0 kw/acre. The more rapid corrosion at 57.0 kW/acre following the dry-out results in more rapid failure relative to an APD of 28.5 kW/acre.

Figure 3.15 shows that when DHLW/ALMR wastes are emplaced in an SCP container the least rapid failure occurs when the containers are co-located with SF at an APD of 114.0 kW/acre. Since the Alloy 825 corrosion model has no temperature dependence, only the effect of the dry-out time impacts the failure distribution for this container design. When the DHLW/ALMR wastes are co-located with SF at an APD of 114.0 kW/acre, failure of the containers occurs within approximately a 10000 year period. For the other loading scenarios (co-location at APDs of 28.5/57.0 kW/acre and alone), failure of the containers occurs within a 5000 year period.

Figure 3.16 shows that when DHLW/ALMR wastes are emplaced in an MMB container the least rapid failure occurs when the containers are emplaced alone (200000 years). Co-location with SF results in failure of the majority of the containers within a 20000 year period. Emplacing these containers in the repository alone results in low temperatures leading to slow corrosion of the carbon steel outer barrier.

The data for each case was fit to Weibull distributions for subsequent use in the overall repository system performance analysis codes. The parameters are shown in Table 3.7 for SF and DHLW/ALMR co-located with SF. For DHLW/ALMR loaded into the repository alone, the following parameters were calculated for the metallic multi-barrier package: Threshold time to failure = 17000 years; Mean time to failure = 45000 years; Weibull slope = 1.3. For the Reference SCP container, the cool repository parameters are utilized.

Table 3.7: Performance Parameters for Reference SCP and Metallic Multi-Barrier Waste Containers (top parameters for SCP, bottom for MMB)

	Ring 1	Ring 2	Ring 3	Ring 4	Ring 5	Ring 6	Ring 7
Cool Repository (28.5 KW/acre)							
Threshold (yrs)	500 5000	500 5500	500 5500	500 5500	500 6000	500 6000	500 6000
Mean Time (yrs)	2250 12000	2250 12000	2250 12000	2250 13000	2250 13750	2250 14000	2250 15000
Weibull Slope	2.00 1.70	2.00 1.70	2.00 1.70	2.00 1.75	2.00 1.70	2.00 1.70	2.00 1.65
Nominal Repository (57 KW/acre)							
Threshold (yrs)	1500 5000	1500 5000	1250 5000	1000 5000	500 5000	500 5000	500 5500
Mean Time (yrs)	2250 7500	2000 7500	2000 7500	2000 7500	2250 7500	2250 8000	2250 10250
Weibull Slope	2.00 1.40	2.00 1.40	2.00 1.40	2.00 1.35	2.00 1.35	2.00 1.35	2.00 1.55
Hot Repository (114 KW/acre)							
Threshold (yrs)	7500 10000	7000 11500	6500 11500	6000 10000	6000 10000	5500 9000	4250 7000
Mean Time (yrs)	2000 9000	2000 9250	2250 10000	2300 8500	2150 9000	2100 8500	2100 9000
Weibull Slope	2.10 1.60	2.00 1.60	2.10 1.60	2.10 1.55	2.10 1.55	2.10 1.55	2.10 1.60

4 SOURCE TERM MODELING

4.1 Introduction

This chapter describes the models used to estimate the release of aqueous radionuclides from failed waste containers. First a description of the various waste-forms being analyzed is presented. Details of several models used to predict the release of radionuclides will next be presented. The assumptions utilized in the development of each model and their limitations will be discussed. The treatment of radionuclide build-in over time will be presented. Finally, the radionuclide inventory of each wasteform that is used in subsequent analyses will be provided.

4.2 Wasteform Characteristics

4.2.1 Spent Fuel Wasteform

Spent fuel (SF) consists of UO_2 pellets clad in zircaloy tubing, forming fuel rods. A fuel assembly is a number of these rods held together by the fuel assembly hardware. A diagram of an intact fuel assembly is shown in Figure 4.1. During reactor operation, the fissioning of uranium causes the pellets to undergo physical changes. The pellets expand and crack due to both the radiation and thermal environment. Many of the fission products are insoluble in UO_2 and form secondary phases in the matrix or on the grain boundaries. Several radionuclides migrate to the fuel-clad gap.

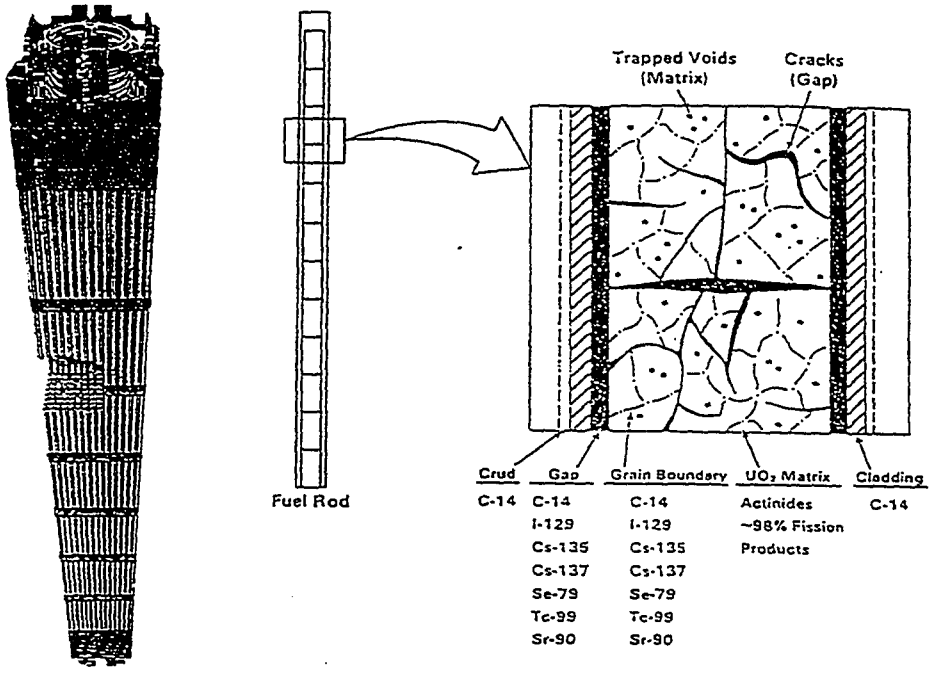

Figure 4.1: Schematic of Intact PWR Fuel Assembly [72]

Gaseous fission products escape to the fuel-clad gap and the plenum at the top of the fuel rod. Figure 4.1 also shows a cross section of a fuel rod after irradiation and identifies where several of the fission products are located. Intact spent fuel assemblies are loaded into the waste container. The container is then filled with an inert gas to preclude clad and fuel oxidation and welded shut [72].

The characteristics of the SF wasteform relevant to source term modelling are provided in Table 4.1. The parameters for the reference SCP container assume the hybrid container design (3 PWR/4 BWR) is used. The MMB parameters are determined assuming the container contains 21 intact PWR assemblies. PWR fuel assembly parameters were calculated assuming a Westinghouse 17x17 fuel assembly.

Table 4.1: Source Term Parameters for LWR Spent Fuel

	Reference SCP Container	Metallic Mult-Barrier Container
Waste Package Height	4.76 m [8]	4.6 m [62]
Waste Package Outer Diameter	0.66 m [8]	1.79 m [62]
Waste Package Overall Volume	1.62 m^3 [8]	5.5 m^3 [62]
Waste Package Internal Void Volume	1.22 m^3 [13]	5.5 m^3 [62,81]
Waste Package Loading	2.1 MTHM [14]	9.74 MTHM [14]
Surface Area of Intact Fuel	140 m^2 [78]	522 m^2 [81]
Air Gap Between Waste Container and Emplacement Hole	0.03 m [13]	0.0 m [62]

BWR fuel assembly parameters were calculated assuming a General Electric 8x8 fuel assembly [81].

4.2.2 DHLW Wasteform

The high level waste from reprocessing facilities is to be immobilized in borosilicate glass [8]. In this section the process used to solidify waste in borosilicate glass and the glass properties are summarized [42]. Liquid HLW is calcined to form a solid form, combined with a glass frit, melted, placed into containers and allowed to solidify. The melted glass-HLW mixture is either put in the pour containers and allowed to solidify or melted within the pour container and then allowed to solidify. The pour container is not considered a primary barrier due to residual stresses resulting from the melting/solidifying process. For this analysis, however, the pour container is ascribed containment capability in the multi-barrier isolation system.

Chemical properties of the glass limit the fission product loading to 20 to 25 weight percent [42]. The surface of the glass may be rough or cracked, which increases the area of the glass that may be exposed to ground water. During dissolution, an alteration "rind" may form on the surface of the glass, affecting the subsequent dissolution rate of the glass. Additional concerns regarding the performance of borosilicate glass are thermal and radiation stability of the glass matrix [8]. Parameters of borosilicate glass relevant to source term modeling are provided in Table 4.2.

4.2.3 ALMR Wasteform

The ALMR pyroprocess fuel cycle produces primarily two HLW waste streams, a metallic stream and a salt stream. The salt waste stream is treated to recover residual TRU and separate out insoluble impurities. The salt stream is then passed through a zeolite bed that removes Cs, Sr, and Ba by ion exchange. Excess salt is purged from the bed, but a considerable amount is occluded in the zeolite cavities and adhered to the zeolite surface. The salt-laden zeolite is mixed with an organic matrix and then hot pressed to form a dense ceramic monolith [34].

Two matrix materials are currently being considered, glass bonded zeolites (Zeolite A) and sodalite [39]. These materials form an aluminum-silicon matrix. The unit cell of Zeolite A is $Na_{12}[(AlO_2)_{12}(SiO_2)_{12}]$ and the unit cell of sodalite is $Na_6[(AlO_2)_6(SiO_2)_6] \cdot 2NaCl$ [82]. The crystal framework contains cages or cavities that are several Angstroms in size. Molecules or ions enter the cages through openings, or apertures, with sizes ranging from two to eight Angstroms. Molecules with sizes

Table 4.2: DHLW Wasteform Parameters

	Reference SCP	Metallic Multi-Barrier
Pour Container Outer Diameter	61 cm [8]	
Pour Container Height	300 cm [8]	
Pour Container Thickness	1.0 cm [8]	
Waste Package Outer Diameter	0.66 m [8]	1.79 m [62]
Waste Package Height	3.28 m [8]	3.28 m [8]
Waste Package Overall Volume	1.12 m^3	8.25 m^3
Waste Package Free Volume	0.178 m^3	2.142 m^3
Borosilicate Glass Surface Area	5.5 m^2 [8]	22 m^2 [8]
Borosilicate Glass Cracking Factor	10 - 30	10 - 30

smaller than the aperture are sorbed, while those larger are excluded. The sodium ions in the crystal are those that are exchanged with waste radionuclide ions.

The metallic waste stream is mixed with a matrix alloy. Previous studies indicated that a suitable matrix alloy is Cu-Al [34]. Current studies have shown that a stainless steel - zirconium alloy is superior to the Cu-Al alloy [39]. The molten alloy system is allowed to cool, solidify and hence, immobilize the fission products and residual actinides in a homogeneous metal ingot [39].

The size of the ALMR wasteform has not been determined, however calculations have been performed assuming it is of the same size as the DHLW waste-forms [37,40]. In subsequent analyses of the ALMR wasteform, the DHLW parameters listed in Table 4.2, except for the cracking factor, are used.

4.3 Source Term Models

4.3.1 Source Term Models for Spent Fuel

Several models have been developed to predict the release of radionuclides from spent fuel. The SF dissolution rate used by Intera in their PA is given by equation 4.1 and depends on the ground water pH, total carbonate concentration, and the temperature of the SF. This relation was developed through fitting a curve to experimental UO_2 dissolution data [14,74]. In the Intera PA, the pH is assumed to be the pH of ground water and was sampled from a uniform distribution from 6.0 to 9.0. The carbonate concentration was sampled over a uniform distribution from 0.002 to 0.02 [14].

$$R_{dis} = 0.602 + 0.515(\log[C]) + 0.01245\,pH + 0.0584\,T \tag{4.1}$$

Where: R_{dis} = UO_2 matrix dissolution rate (g/m^2y)
C = Total carbonate concentration in ground water (molarity)
pH = Nominal pH of water contacting the matrix
T = Temperature of SF (centrigrade)

A key input to this model is the surface area of the SF contacting the water. The Intera PA [14] assumed the entire SF surface is contacting water upon failure of the cladding. This assumption is conservative as the clad will initially fail through a local breach or pin-hole failure. Oxidation of the UO_2 matrix to U_3O_8 will result in fuel expansion leading to a longitudinal crack along the entire length of the fuel rod. Only a limited area of the fuel near the crack will be exposed to water.

The SF dissolution rate used by SNL in their PA is give by equation 4.2 [18,74].

$$R_{dis} = 0.414 \cdot 10^{[7.45 + 0.258(\log[C]) - 0.142 pH - 1550/T]} \quad (4.2)$$

Where: R_{dis} = UO_2 matrix dissolution rate (g/m^2y)
C = Total carbonate concentration in ground water (molarity)
pH = Nominal pH of water contacting the matrix
T = Temperature of SF (Kelvin)

The EPRI PA utilizes three discrete matrix alteration rates in their logic tree approach. These represent low, moderate, and high alteration rates and are independent of temperature and ground water chemistry [13,86]. These alteration rates are assigned a probability of occurrence. The discrete alteration rates and the associated probabilities used by EPRI are shown in Table 4.3. These alteration rates tend to be lower than those given by equations 4.1 and 4.2.

The alteration of the UO_2 matrix releases the radionuclides to either the water film surrounding the waste or to the environment as a gas. The release of aqueous radionuclides is a function of the mode of transport (advection/diffusion) and the concentration of the radionuclides in the water. This concentration may be limited by the solubility of the element. In the PA analyses conducted to date (and this study), the elemental solubility is the limiting release mechanism. Colloid formation, ionic complexing and speciation may impact the wasteform release characteristics. The governing mode of transport depends on the hydraulic saturation and the ground water flow properties.

The aqueous release model incorporated into RIP [14,15] considers both advective and diffusive releases of radionuclides. The amount of exposed (available) mass of radio-nuclide n at the waste package at time t, M(t), is given by equation 4.3.

Table 4.3: EPRI Spent Fuel Alteration Rates

Condition	Alteration Rate (g/m^2yr)	Probability
Low	0.11	0.05
Moderate	0.55	0.90
High	2.80	0.05

$$M(n,t) = \int_0^t [e(n,\tau) - r(n,\tau)]\, d\tau \tag{4.3}$$

Where: $e(n,\tau)$ = The rate at which radionuclide n is being exposed to the near field environment at time t. (R_{dis} • Surface area)

$r(n\tau)$ = Release rate of radionuclide n from the waste package at time t

The release rate, r(n,t), is determined as follows.

1. If M(n,t) = 0, then r(n,t) = MIN [$k_t(n,t)$, e(n,t)]
2. If M(n,t) > 0 and M(n,t) > $k_t(n,t)\bullet\Delta t$, then r(n,t) = $k_t(n,t)$
3. If M(n,t) > 0 and M(n,t) ≤ $k_t(n,t)\bullet\Delta t$,
   then r(n,t) = MIN [$k_t(n,t)$, e(n,t) + M(n,t)/Δt]

Where $k_t(n,t)$ is the maximum possible mass transfer rate of radionuclide n out and away from the waste package at time t. Case 1 represents the condition of no excess exposed mass. Case 2 represents the condition of excess exposed mass. Case 3 is used to handle discretization errors.

The maximum release rate, $k_t(n,t)$, consists of advective, $k_{t/a}(n,t)$, and diffusive, $k_{t/d}(n,t)$, terms. These are given in equation 4.4.

$$\begin{aligned} k_{t/a} &= F \cdot C \cdot C(n) \\ k_{t/d} &= D_{eff} \cdot \omega \cdot C(n) \\ C(n) &= MIN\left[\frac{M}{V},\ C_s(n)\right] \end{aligned} \tag{4.4}$$

Where: F = Flow rate of groundwater through repository (m^3/yr)

C = Effective catchment area (m^2)

D_{eff}= Effective diffusion coefficient

ω = Geometric factor for diffusion

The effective diffusion coefficient used by Intera for crushed tuff is given as equation 4.5.

$$D_{eff} = -5.9135\times10^{-5} + 7.9154\times10^{-4}S + 2.1034\times10^{-3}S^2 \quad (4.5)$$

Where: D_{eff} = Effective Diffusion Coefficient (m^2/y)

S = Saturation

Intera [14] assumed that the wasteform is approximated as a bare sphere, and that the geometric factor for diffusion is given by equation 4.6.

$$\omega = 4 \cdot \pi \cdot R_s \cdot \eta \quad (4.6)$$

Where: R_s = Equivalent spherical radius of wasteform

η = Porosity of the backfill material

The SNL aqueous release model considers that the release from the container is the minimum of either the amount of a given radionuclide released from the altered UO_2 or the solubility limit of the radionuclide times the volume of water within the failed waste package [18]. No considerations are made for advective/diffusive modes of transport.

The EPRI PA considers the release of insoluble and soluble radionuclides from two water contact modes, wet-drip and moist-continuous [13]. Under wet-drip conditions, local variations in the rock permeability and fractures may divert water to the container. Dripping water may enter and fill the breached container. Once the

container is filled, the release of radionuclides will occur at a rate equal to the drip rate. If the waste container is contacting the rock or the repository is saturated, a moist-continuous water contact mode results. Under this condition, the release is controlled by diffusion and/or advection.

The wet-drip release models utilized by EPRI are given in equation 4.7 for insoluble radionuclides and equations 4.8 and 4.9 for soluble radionuclides. For the case when the fill time is less than the waste alteration time, Equation 4.5 is used. When the fill time is longer than the waste alteration time, Equation 4.6 is used [13].

$$\begin{aligned} M_i &= 0.0 && t<t_f \\ M_i &= F \cdot A \cdot \Phi_i \cdot C_s && t \geq t_f \end{aligned} \tag{4.7}$$

Where : F = infiltration rate (m/yr)

A = cross-sectional area normal to infiltrating water that diverts flow into waste package (m^2)

Φ = mass fraction of isotope i among all isotopes of the same element

C_s = solubility of the species within the container (g/m^3)

t_f = time required to fill container = V/(F· A)

V = free volume

$$M_i = \alpha \exp[\lambda_{it} - \alpha t] f_a m_i^o \left[\left(\frac{1}{\alpha} + t_1 + \frac{1}{f_a} \right) \left(\exp[\alpha t] - \exp[\alpha t_2] \right) - \frac{\exp[\alpha t](\alpha t - 1)}{\alpha} - \frac{\exp[\alpha t_2](\alpha t_2 - 1)}{\alpha^2} \right] + \frac{\alpha \exp[-\lambda_i t_2] M_i^o}{(t_2 - t_1)} \cdot \left(t_2 - t_1 - \frac{1}{2 f_a} \right) \exp[-(\lambda_i - \alpha)(t - t_2)] \tag{4.8}$$

$$M_i = f_a M_i^o \left[(\exp[\alpha(t_2 + \frac{1}{f_a})] - \exp[\alpha t_2]) + \frac{1}{2}\alpha(t_2 - t_1)\exp[\lambda t_2] \right] \exp[-(\alpha + \lambda_i)t] \quad (4.9)$$

Where : α = FA/V = $1/t_f$

λ_i = decay constant (yr^{-1})

t = time after emplacement (yr)

f_a = fractional alteration of waste matrix = $j_o A/M_m^o$ (gm/yr)

j_o= forward reaction of waste matrix container (g/m^2yr) = R_{dis}

M_m^o = initial mass inventory of matrix (gm)

M_i^o = initial mass inventory of nuclide i (gm)

t_1 = time after emplacement when waste container is penetrated (yr)

t_2 = time after emplacement when waste package is full (yr)

The moist-continuous release models utilized by EPRI for soluble and insoluble radionuclides are given in equations 4.10 and 4.11, respectively.

$$M_i = \frac{\Psi\, j_o\, A\, M_i^o \exp[-\lambda_i t]}{M_m^o \exp[-\lambda_m t]} \quad (4.10)$$

$$M_i = \frac{4\,\Pi\,\epsilon\,\Psi\, D_b\, r_o\, C_s [Sh\, r_1\sqrt{k}]}{[(Sh - 1)\sinh d + r_1\sqrt{k}\cosh d} \quad (4.11)$$

Where : ϵ = porosity of backfill

Ψ = degree of hydraulic saturation

D_b = effective diffusion coefficient (m^2/yr)

r_o= wasteform radius (m)

r_1 = radius of backfill/rock interface (m)

Sh = Sherwood number = (1+0.5 Pe) / (1+0.63 $Pe^{1/2}$)

Pe = Peclet number = $r_1 U / D_b$

U = groundwater pore velocity (m/yr)

$k = \lambda R / D_a$

R = retardation coefficient = $1 + \rho [(1-\epsilon)/\epsilon \Psi] k_d$

ρ = bulk density of tuff (kg/m^3)

$d = (r_1 - r_0) k^{1/2}$

Certain simplifications and assumptions were used in the development of the EPRI models, a few of which are summarized. The geometry of the waste package was generalized to a sphere in some cases. Steady state, rather than transient, release models were utilized. A limited amount of certain nuclides (Cs^{137}, Se^{79}, I^{129}) are assumed to be released from the fuel-clad gap immediately upon clad breach. No temperature dependence is assumed [13].

4.3.2 Source Term Models for DHLW

The DHLW dissolution rate used by Intera is given as equation 4.12 [14,76]. Intera assumed that the radionuclides are released as rapidly as the borosilicate glass dissolves. The Intera model does not consider the solubility of the elements or the mode of transport away from the package (advection/diffusion). The formation of the alteration layer on the surface of the glass is not considered nor are thermal/radiation effects on the glass matrix. This model can be used to calculate the alteration rate. It should be noted that Intera assumed that the surface area is increased by a factor between 10 and 30 due to cracking. These alteration rates could be utilized in refined models that 1) consider the solubility of the radionuclides, as is done by SNL, 2) consider the solubility and mode of transport away from the package, as is done by Intera, and 3) consider the solubility and the mode of water contact, as is done by EPRI.

$$R_{dis} = A \cdot k\,(1 - Q/K)$$

$$k = 10^{[-0.00172 - 0.0231T + 0.00149T^2 - 1.136\times10^{-5}T^3 - 1.155pH + 0.0813pH^2 + 0.000138pH^3]} \qquad (4.12)$$

$$Q/K = 0.145 + 0.001878T$$

Where: R_{dis} = Dissolution rate of glass (g/d)

A = Surface area of exposed glass (m^2)

Q = Concentration of dissolved silica in water

K = Equilibrium constant for amorphous silica

pH = Nominal pH of water contacting the glass

T = Temperature of SF (centegrade)

4.3.3 Source Term Models for ALMR Wasteforms

Preliminary studies have been conducted at ANL to determine the dissolution characteristics of the proposed ALMR metallic and mineral wasteforms [39]. Corrosion tests were conducted on the metallic wasteform in simulated Yucca Mountain J-13 ground water at 363°K. Several alloys consisting of ferritic alloy HT9 and zirconium were tested. The results obtained are shown in Table 4.4. Static leach testing of the proposed mineral wasteforms were conducted in deionized water and brine for glass bonded zeolite and in deionized water for sodalite. The glass bonded zeolite was subjected to 28 and 56 day exposures while the sodalite was tested for four seven day periods. All tests were conducted at 363°K. The results for the mineral wasteform are reported as normalized release rates (NRR) given as equation 4.13.

Table 4.4: Corrosion of Proposed ALMR Metallic Wasteform

Alloy	Corrosion Rate (mg/cm^2 yr)
HT9 - 5 w/o Zr	0.3
HT9 - 10 w/o Zr	2.8
HT9 - 15 w/o Zr	4.0
HT9 - 20 w/o Zr	0.6

$$NRR = \frac{C_i V}{F_i A d} \tag{4.13}$$

Where: NRR = Normalized release rate (g/m^{2}d)

C_i = Concentration of element i in leachate

V = Volume of leachant

F_i = Fraction of element i in solid

A = Surface area of solid

d = duration of test

V/A = 10 cm for test

The results for the glass bonded zeolite are shown in Table 4.5. The NRR was found to be less than 1 g/m^{2}d when the zeolite fraction in the monolith was less than 67%. The NRR was also found to decrease as the test duration increased from 28 to 56 days, indicating an initial pulse of non-occluded materials followed possibly by stabilization at a lower NRR. Iodine was not detectably leached, although the concentration in the test samples was low (0.01 - 0.03 w/o), implying an NRR less than one. Rare earth elements were also not detectably leached, but again the loadings were low (0.2 - 0.2 w/o), implying an NRR less than 0.5.

Table 4.5: Normalized Release Rate of Glass Bonded Zeolite (g/m^2d)

Element	28 Day Test	56 Day Test
Al	0.30	0.13
Ba	0.20	0.07
B	0.31	0.19
Ca	0.18	0.14
Cs	0.60	0.32
K	0.73	0.38
Li	0.60	0.35
Na	0.67	0.37
Si	0.25	0.11
Sr	0.23	0.11

The NRR for the sodalite was also found to decrease with time over a 28 day testing period. The NRR at 28 days is shown in Table 4.6.

The corrosion rate and NRR data are utilized in conjunction with the wasteform surface area to estimate the alteration rates of the ALMR wasteforms. A simple and conservative release model is to assume that the radionuclides are available for transport immediately upon alteration of the wasteform. Further refinements to the model could 1) consider the solubility of the radionuclides, as is done by SNL, 2) consider the solubility and mode of transport away form the package, as is done by Intera, and 3) consider the solubility and the mode of water contact, as is done by EPRI.

Table 4.6: Normalized Release Rate of Sodalite (g/m^2d) for 28 Day Test

Element	NRR
Cs	1.00
Ba	0.15
Na	1.00
K	0.60
Sr	0.10
Li	0.30
Al	0.40
Si	0.50

4.4 Radionuclide Inventories

4.4.1 Radionuclide Ingrowth and Daughter Product Buildup

Neither the EPRI or Intera PA models account for the buildup of daughter products [13,14]. In addition, the EPRI PA model does not account for the buildup of certain actinides [13]. This is a serious shortcoming when trying to estimate the long term behavior of the repository. The importance of ingrowth and buildup becomes even more important when considering the feasibility of actinide recycling.

Radionuclides that will build in to significant quantities are ^{237}Np, ^{240}Pu, and ^{234}U. The decay chains of ^{237}Np, ^{240}Pu, and ^{234}U will result in a transient equilibrium condition between the parents and daughters, with significant activity resulting from the daughters. The decay chains for these radionuclides is shown in Figure 4.2 [83].

$$^{241}Pu \rightarrow {}^{241}Am \rightarrow {}^{237}Np \rightarrow {}^{233}Pa \rightarrow {}^{233}U \rightarrow {}^{229}Th \rightarrow {}^{225}Ra \rightarrow$$

$$^{225}Ac \rightarrow {}^{221}Fr \rightarrow {}^{217}At \rightarrow {}^{213}Bi \rightarrow {}^{213}Po \rightarrow {}^{209}Pb \rightarrow {}^{209}Bi$$

$$^{209}Tl \rightarrow {}^{209}Pb \rightarrow {}^{209}Bi$$

$$^{238}Pu \rightarrow {}^{234}U \rightarrow {}^{230}Th \rightarrow {}^{226}Ra \rightarrow {}^{222}Rn \rightarrow {}^{218}Po \rightarrow {}^{214}Pb \rightarrow$$

$$^{214}Bi \rightarrow {}^{214}Po \rightarrow {}^{210}Pb \rightarrow {}^{210}Bi \rightarrow {}^{210}Po \rightarrow {}^{206}Pb$$

Figure 4.2: Decay Chains of ^{237}Np and ^{234}U

It is assumed that both ^{241}Pu and ^{241}Am decay immediately to ^{237}Np, ^{244}Cm decays immediately to ^{240}Pu, and ^{238}Pu decays immediately to ^{234}U. This assumption is valid considering the relatively short half-lives of these radionuclides when compared to the time scales used in repository performance calculations (i.e. ^{241}Am = 432 years) . The initial inventory of ^{237}Np, ^{240}Pu, and ^{234}U is increased by an amount given in equation 4.14.

$$A^{*} = A_i \frac{\lambda^{*}}{\lambda_i} \tag{4.14}$$

Where: A^{*} = Amount of increase (Ci) of ^{237}Np, ^{240}Pu, and ^{234}U from build-in
A_i = Initial inventory (Ci) of ^{241}Pu, ^{241}Am, ^{238}Pu, and ^{244}Cm
λ^{*} = Decay Constant of ^{237}Np, ^{240}Pu, and ^{234}U
λ_i = Decay Constant ^{241}Pu, ^{241}Am, ^{238}Pu, and ^{244}Cm

The build-in of the daughter products of ^{237}Np and ^{234}U was analyzed using the computer software RADDECAY [83]. It is extremely complicated to incorporate the build-in of the daughter radionuclides in simple source term and transport models used in PA tools. A simple approach is utilized to account for build-in of daughters. This

parent radionuclide increases over time as the daughter products build in. This approach will result in conservative estimates of received dose as the dose conversion factor of the parents is typically higher [14]. The cumulative radioactivity release may not be accurate as actual modeling of daughter product dissolution and transport is not modelled.

The increases in the activity due to daughter product build-in were found to obey the relation given as equation 4.15 for ^{237}Np and equation 4.16 for ^{234}U. It should be noted that the initial inventory of these radionuclides does decrease, however the overall inventory is assumed to increase due to build-in.

$$A^{*}_{Np\text{-}237} = \left[0.876 + 3.033\times10^{-5}t\right] A^{init}_{Np\text{-}237} \tag{4.15}$$

$$A^{*}_{U\text{-}234} = \left[-0.0902 + 8.289\times10^{-5}t - 3.213\times10^{-10}t^{2}\right] A^{init}_{U\text{-}234} \tag{4.16}$$

Where: A^{*}_{i} = Increase in ^{237}Np or ^{234}U activity due to daughter product build-in
A^{init}_{i} = Initial activity of ^{237}Np or ^{234}U
t = Time (years)

4.4.2 Initial Inventory Commercial Spent Fuel

The radionuclide inventory for spent fuel used in this study was obtained from the Intera PA [14] which utilized the CDB [2] in their calculations and is shown in Table 4.7. An average spent fuel burnup of 36,437 MWD/MTHM was used. This average burnup was based on a repository loading of 64.7% PWR fuel with a burnup of 42,300 Mwd/MTHM, and 35.32% BWR fuel with a burnup of 32250 Mwd/MTHM. It was assumed that the fuel had been cooled 30 years prior to emplacement in the

Table 4.7: Initial Inventory of Spent LWR Fuel

Isotope	Ci/MTHM	Isotope	Ci/MTHM
^{79}Se	4.80×10^{-1}	^{240}Pu	5.71×10^{2}
^{99}Tc	1.51×10^{1}	^{242}Pu	2.18×10^{0}
^{129}I	3.72×10^{-2}	^{241}Am	3.92×10^{3}
^{135}Cs	5.67×10^{-1}	^{241}Pu	3.56×10^{4}
^{226}Ra	2.64×10^{-6}	^{238}Pu	3.57×10^{3}
^{234}U	1.43×10^{0}	^{244}Cm	1.40×10^{3}
^{235}U	1.68×10^{-2}	Build-In Isotopes	
^{238}U	3.14×10^{-1}	$^{237}Np^{*}$	2.74×10^{0}
^{237}Np	4.86×10^{-1}	$^{234}U^{*}$	2.71×10^{0}
^{239}Pu	3.75×10^{2}	$^{240}Pu^{*}$	5.75×10^{2}

repository. The isotopes chosen for analysis are identical to those chosen by EPRI for their PA. These radioisotopes were chosen based on their long half-lives and their large inventory. These isotopes will be utilized in all subsequent analyses.

4.4.3 Initial Inventory DHLW

The initial inventory of DHLW was obtained from the Intera PA [14]. The inventory calculation assumes 7000 MTHM of vitrified borosilicate glass is buried in 14,000 containers. It has been estimated that 50 metric tons of weapons grade plutonium (^{239}Pu) could be spiked with the current supply of HLW and subsequently vitrified [49]. It is therefore assumed that the 50 metric ton inventory of surplus weapons grade plutonium is emplaced in the 14,000 containers. The initial inventory of DHLW and DHLW/weapons grade plutonium is shown in Table 4.8.

Table 4.8: Initial Inventory of DHLW and DHLW/Weapons Grade Pu

Isotope	Ci/MTHM	Isotope	Ci/MTHM
^{79}Se	4.59×10^{-2}	^{240}Pu	1.65×10^{0}
^{99}Tc	1.65×10^{0}	^{242}Pu	2.51×10^{-3}
^{129}I	9.50×10^{-7}	^{241}Am	4.33×10^{1}
^{135}Cs	5.75×10^{-2}	^{241}Pu	7.41×10^{1}
^{226}Ra	4.69×10^{-8}	^{238}Pu	2.00×10^{2}
^{234}U	2.50×10^{-2}	^{244}Cm	5.70×10^{0}
^{235}U	3.97×10^{-5}	^{237}Np (Build-in)	1.18×10^{-2}
^{238}U	1.89×10^{-3}	^{234}U (Build-in)	7.20×10^{-2}
^{237}Np	1.42×10^{-2}	^{240}Pu (Build-in)	1.57×10^{-2}
^{239}Pu	2.37×10^{0}	^{239}Pu (Weapons)	4.40×10^{2}

4.4.4 Initial Inventory ALMR and Actinide Recycle Waste

An estimate of the waste radionuclide inventory from the ALMR pyroprocess has been calculated [37,40]. This calculation analyzed the waste inventory from the closed ALMR fuel cycle and from a LWR actinide recovery process. The calculations assumed burnups of 158,000 MWd/MTU for the ALMR fuel and 33,000 MWd/MTU for the processed LWR fuel. A ten year cooling time was assumed . Calculations were performed for low and high electrorefiner actinide decontamination factors.

The GE calculations [37] were based on a LWR actinide recovery process that is no longer being considered. The current process is detailed in chapter 2. The inventory calculations performed by GE can still be utilized with appropriate modifications to account for the current process. For example, the process utilized by

GE had a salt transport step between salt reduction and electrorefining that recovered the uranium. This process produced mineral and metallic wasteforms with ^{99}Tc being partitioned into the metallic wasteform. In the current process, a metallic stream from the oxide reduction process is fed to the ER, where uranium and TRU are recovered. ^{99}Tc and other noble metal fission products are also fed to the ER and after processing reside in the metallic wasteform.

For spent ALMR fuel, the low and high pyroprocess actinide decontamination factors (inverse of loss fraction) used in this study were 1×10^4 and 5×10^4, respectively. For the case of processing spent LWR fuel, the low and high actinide decontamination factors used in this study were 1×10^3 and 1×10^4, respectively [84]. These values differ from those used in the GE calculations [37] and are based on current calculations performed at ANL regarding actinide recovery pyroprocessing. In addition, it is assumed that in the LWR oxide fuel reduction process, 0.01% of the actinide inventory is lost to the waste stream as un-reduced oxides [41].

The calculated inventories are shown in Table 4.9. The values for the actinide inventories are for low actinide decontamination factors. Use of a high actinide decontamination factor results in a reduction in the actinide inventory by a factor of five. Note that the actinides are assumed to be lost to both of the electrorefiner wastestreams. The fuel hardware wastes are assumed to be combined with the electrorefiner - metallic waste stream. During the head-end processing of LWR SF, iodine is released as a gas and will be collected as silver iodide on silver impregnated zeolite [37]. For this study it is assumed that iodine is combined with the salt reduction mineral wasteform.

Table 4.9: Initial Inventory of ALMR Wasteforms (Ci/MTHM)

Nuclide	Actinide Recovery Oxide Reduction Mineral	Actinide Recovery Electro - Refiner Mineral	Actinide Recovery Electro-Refiner Metal	ALMR Electro - Refiner Mineral	ALMR Electro-Refiner Metal
^{79}Se			$4.09x10^{-1}$		$2.38x10^{0}$
^{99}Tc			$1.30x10^{1}$		$8.17x10^{1}$
^{129}I	$3.16x10^{-2}$			$2.75x10^{-1}$	
^{135}Cs	$3.42x10^{-1}$	$3.45x10^{-3}$		$9.99x10^{-1}$	
^{93}Zr			$1.94x10^{0}$		$1.06x10^{1}$
^{107}Pd			$1.12x10^{-1}$		$1.26x10^{0}$
^{126}Sn			$7.77x10^{-1}$		$9.87x10^{0}$
^{234}U	$1.15x10^{-4}$	$1.15x10^{-3}$	$1.15x10^{-3}$	$9.97x10^{-4}$	$9.97x10^{-4}$
^{235}U	$1.97x10^{-6}$	$1.97x10^{-5}$	$1.97x10^{-5}$	$4.98x10^{-7}$	$4.98x10^{-7}$
^{238}U	$3.12x10^{-5}$	$3.12x10^{-4}$	$3.12x10^{-4}$	$6.19x10^{-5}$	$6.19x10^{-5}$
Np^{237}	$3.12x10^{-5}$	$3.12x10^{-4}$	$3.12x10^{-4}$	$2.28x10^{-4}$	$2.28x10^{-4}$
^{239}Pu	$3.14x10^{-2}$	$3.14x10^{-1}$	$3.14x10^{-1}$	$1.35x10^{0}$	$1.35x10^{0}$
^{240}Pu	$5.25x10^{-2}$	$5.25x10^{-1}$	$5.25x10^{-1}$	$1.78x10^{0}$	$1.78x10^{0}$
^{242}Pu	$1.72x10^{-4}$	$1.72x10^{-3}$	$1.72x10^{-3}$	$3.42x10^{-3}$	$3.42x10^{-3}$
^{241}Am	$1.81x10^{-1}$	$1.81x10^{0}$	$1.81x10^{0}$	$3.13x10^{0}$	$3.13x10^{0}$
^{241}Pu	$7.55x10^{0}$	$7.55x10^{1}$	$7.55x10^{1}$	4.84x10	$4.84x10^{1}$
^{238}Pu	$2.22x10^{-1}$	$2.22x10^{0}$	$2.22x10^{0}$	$9.97x10^{0}$	$9.97x10^{0}$
^{244}Cm	$1.33x10^{-1}$	$1.33x10^{0}$	$1.33x10^{0}$	$1.33x10^{0}$	$1.33x10^{0}$
^{237}Np (Build -in)	$3.46x10^{-4}$	$3.46x10^{-3}$	$3.46x10^{-3}$	$2.62x10^{-3}$	$2.62x10^{-3}$
^{234}U (Build-in)	$7.99x10^{-5}$	$7.99x10^{-4}$	$7.99x10^{-4}$	$3.60x10^{-3}$	$3.60x10^{-3}$
^{240}Pu (Build-in)	$3.67x10^{-4}$	$3.67x10^{-3}$	$3.67x10^{-3}$	$1.39x10^{-2}$	$1.39x10^{-2}$

4.4.5 Initial Inventories From Weapons Grade Plutonium Disposition Options

Several options have been considered for the disposition of weapons grade plutonium. These include spiking (short term irradiations) in either an LWR or an ALMR, irradiating to burnup levels commensurate with spent fuel in either an LWR or an ALMR, complete destruction in an ALMR through recycling, and mixing with DHLW and incorporating into borosilicate glass. The expected inventories for each of these options is discussed.

The ORIGEN-2 isotope generation and depletion computer code [85] was used to estimate the initial radionuclide inventories for the weapons grade plutonium disposition options in an LWR, particularly a PWR. The Westinghouse 17x17 PWR design was utilized [81]. This reactor contains 193 fuel assemblies, a fuel loading of 90.2 metric tons uranium, and has a power level of 3411 MWth. This gives a specific power of 37.8 MWth/MTU. It was assumed that the entire PWR core was comprised of mixed-oxide fuel. The mixed-oxide fuel was assumed to derive from the blending of ^{239}Pu with depleted uranium stockpiles (0.0055 wt.% ^{234}U, 0.2 wt. % ^{235}U, and 99.745 wt. % ^{238}U) [41] with a further assumption that the fissile ^{235}U is replaced one-to-one with ^{239}Pu (number density).

The basis of the calculation was a uranium-fueled PWR with an enrichment of 3.2 w/o ^{235}U. The uranium fueled PWR fuel loading isotopic inventories are provided in Table 4.9 per metric ton of heavy metal. The isotopics of the mixed-oxide fuel were obtained by maintaining the number of fissile atoms and the fuel mass (one metric ton heavy metal) constant between the uranium and mixed-oxide fuel reactors. The mixed-oxide fuel isotopic inventories are also provided in Table 4.10.

Table 4.10: Isotopic Inventories of LWR Fuel (grams/metric ton heavy metal)

Isotope	Uranium Fueled LWR	Mixed-Oxide Fueled LWR
^{234}U	$2.90x10^{2}$	$5.33x10^{1}$
^{235}U	$3.20x10^{4}$	$1.94x10^{2}$
^{238}U	$9.68x10^{5}$	$9.67x10^{5}$
^{239}Pu		$3.06x10^{4}$

It was assumed that the spiking option consisted of an irradiation to a burnup of 10,000 MWd/MTHM (264.4 days) and the spent fuel option consisted of an irradiation to a burnup of 30,000 Mwd/MTHM (793.2 days). The ten year post cooling inventory of the mixed-oxide spent fuel calculated using ORIGEN-2 is shown in Table 4.11. ORIGEN-2 was also used to calculate the ten year inventory of a uranium-fueled LWR. The results were compared with the inventory provided in Table 4.7. The results are similar, verifying that the version of ORIGEN-2 being used was providing accurate information. The build-in isotopic inventory was obtained using the equations presented in section 4.4.1.

Three ALMR weapons grade plutonium disposition options are considered [56]. The first is the spiking option, the second is the spent fuel option, and the third is continued plutonium destruction following either of the two previously stated options in a recycle phase. A fourth option has been considered, termed the maximum destruction option. This option requires a new fuel design and the reactor physics (large positive void coefficient) associated with this option make it undesirable

The spiking option consists of loading three metric tons of weapons grade

Table 4.11: Initial Inventory of Mixed-Oxide Spent LWR Fuel Used For Weapons Grade Plutonium Disposition (Ci/MTHM)

Isotope	Spike	Spent Fuel	Isotope	Spike	Spent Fuel
^{79}Se	1.16×10^{-1}	3.18×10^{-1}	^{240}Pu	8.88×10^{2}	1.08×10^{3}
^{99}Tc	4.26×10^{0}	1.20×10^{1}	^{242}Pu	2.36×10^{-1}	4.41×10^{0}
^{129}I	1.41×10^{-2}	3.86×10^{-2}	^{241}Am	1.61×10^{3}	4.40×10^{3}
^{135}Cs	1.81×10^{-1}	4.26×10^{-1}	^{241}Pu	7.65×10^{4}	2.00×10^{5}
^{226}Ra	--	--	^{238}Pu	3.52×10^{1}	1.29×10^{3}
^{234}U	3.13×10^{-1}	2.82×10^{-1}	^{244}Cm	3.55×10^{0}	2.15×10^{3}
^{235}U	3.49×10^{-3}	1.74×10^{-3}	Build-In Isotopes		
^{238}U	3.24×10^{-1}	3.20×10^{-1}	$^{237}Np^{*}$	3.46×10^{0}	9.09×10^{0}
^{237}Np	1.55×10^{-2}	6.18×10^{-2}	$^{234}U^{*}$	1.27×10^{-2}	4.65×10^{-1}
^{239}Pu	1.17×10^{3}	4.21×10^{2}	$^{240}Pu^{*}$	9.80×10^{-3}	5.93×10^{0}

plutonium in each ALMR module and irradiating for forty-five days to a burnup level of 2,500 MWd/MTHM. At this point the spent fuel is either disposed or stored. If the fuel is stored, and the spiking phase is complete, the fuel is reloaded and irradiated to an average burnup of 90,100 MWd/MTHM and it is again stored or disposed. Following this phase, a recycling phase can be entered where the fuel is subjected to pyrometallurgical processing and continued irradiation.

The spent fuel option consists of irradiating the fuel to a burnup of 106,000 MWd/MTHM. At this point the spent fuel is either stored or disposed. Again, following this phase, a recycling phase can be entered where the fuel is subjected to pyrometallurgical processing and continued irradiation.

If the spent fuel is to be disposed after either the spiking or spent fuel option is

complete, a pyroprocessing operation will be undertaken. The actinides are assumed to be incorporated into the metal waste stream while the fission products will be incorporated into both the salt and metal waste streams. The actinides may actually be partitioned between both the salt and metallic waste streams. The isotopic inventory of the fuel actinides in the metal wasteform is provided in Table 4.12 for the ALMR spiking and spent fuel options.

It is assumed that continued irradiation to a burnup of 90100 MWd/MTHM following the spiking phase will result in an actinide isotopic inventory that is similar to those obtained from the spent fuel option. The recycling phase will result in waste stream inventories identical to those of the ALMR presented in Table 4.9.

Table 4.12: Initial Actinide Inventory of ALMR Wasteforms (Ci/MTHM) from the Spiking and Spent Fuel Weapons Grade Plutonium Disposition Options

Isotope	Spiking Option	Spent Fuel Option
^{235}U	3.32×10^{-3}	1.72×10^{-3}
^{238}U	2.64×10^{-1}	2.69×10^{-1}
^{237}Np	9.87×10^{-3}	1.97×10^{-1}
^{238}Pu		1.46×10^{3}
^{239}Pu	1.16×10^{4}	6.06×10^{3}
^{240}Pu	2.71×10^{3}	2.83×10^{3}
^{241}Pu	6.51×10^{4}	1.07×10^{5}
^{242}Pu		1.99×10^{1}
^{241}Am	2.10×10^{3}	1.09×10^{3}
Build-in Isotopes		
$^{237}Np^{*}$	3.09×10^{0}	4.61×10^{0}
$^{234}U^{*}$		5.26×10^{-1}

5 IMARC PERFORMANCE ASSESSMENT ANALYSES

5.1 Introduction

This chapter presents the results obtained for PA investigations of the spent fuel, DHLW (weapons grade Pu), baseline ALMR, and actinide recycle wasteforms. Section 5.2 provides a summary of the theory behind the IMARC PA tool. Section 5.3 presents details of changes to IMARC required to model the various wasteforms being analyzed. Section 5.4 provides the results obtained from the PA analyses.

5.2 Summary Description of the IMARC Theory

This section describes the IMARC (Integrated Multiple Assumptions and Release Calculations) PA tool [12,13,86]. IMARC is a probability- based PA model that investigates the possible release of radionuclides to the environment. IMARC was developed for the Electric Power Research Institute by Risk Engineering, Incorporated of Boulder, Colorado. A logic tree approach is used as the basic representation of uncertain models and parameters. The logic tree is ordered so independent processes are on the left side (up stream) and dependent processes are on the right side (down stream). Each branch is assigned a probability that represents a conditional probability of that branch correctly representing future occurrences or the state of nature. The path leading to each end branch represents a complete collection of assumptions

(models and variables) used for a performance assessment analysis. The total of all branches must sum to one.

Three separate computer codes are utilized. The first is a hydrologic transport model that calculates the amount of a given radionuclide released per cubic meter for one gram/cubic meter input. The second is a source term model that calculates the waste radionuclides available for transport once a container has failed (gram/cubic meter). The third is a routine that integrates the results from the transport and source term models using the master logic tree. Output is in the form of a complementary cumulative distribution function (CCDF) of total curies released over a given period of time.

Radionuclide releases are considered from aqueous/gaseous pathways and volcanic action. Experts in various fields have developed the models implemented in IMARC and quantified the probability, or uncertainty, associated with the input assumptions. The models incorporated into IMARC include: climate and rainfall; net infiltration; climate induced water table changes; earthquake and tectonics - container rupture and water table change; volcanism - transport to ground surface and water table change; hydrothermal effects; engineered barrier system failure; source term; ground water flow and mass transport; and gas phase transport.

The volcanism and earthquake models are not utilized in this investigation and as such, will not be discussed. In addition, only aqueous releases are considered. The temperature changes caused by waste emplacement and the engineered barrier system failure model are described in detail in Chapter 3. The source term model utilized by IMARC is described in Chapter 4.

The probabilistic climate and rainfall model utilized past climate changes to predict future changes at Yucca Mountain. Periods of glaciation lead to pluvial conditions at the mountain. The effect of greenhouse gases is assumed to lead to increased rainfall. Small periods of micro-pluvial conditions are also considered. The precipitation model simulated individual precipitation events in time. The duration of each rainfall event was assumed to be an exponential distribution. The intensity of each rainfall event was assumed to be constant through its duration. The intensity of the rainfall events were assumed to follow an exponential distribution. The distribution of rainfall events in time was assumed to follow a Poisson distribution.

Simulations of rainfall events select values of precipitation duration, intensity and time between events according to the designated distributions. Latin Hypercube sampling was used. Variable parameters included: 1) average rate of winter and summer precipitation (mm/yr); 2) average time between precipitation events, winter and summer; 3) the average duration of precipitation events, winter and summer. These parameters were modified to account for greenhouse and pluvial conditions. Estimates of the probability of future climatic conditions based on past glaciation history and predictions of greenhouse effects were made.

The net infiltration model utilized a probabilistic approach using climatological analysis, surface hydrology and numerical simulation of the infiltration process. The objectives were to 1) develop a defensible and realistic conceptual model for calculating infiltration, 2) address climatic variability, spatial variability, and physical/biologic processes and uncertainty.

The basic components of the model are physical and biologic processes that affect soil water flow, the variability of the climate, and spatial variability. Numerical models were used to simulate unsaturated zone water flow through the soil profile, plant water uptake, surface water runoff, plant growth dynamics, and daily climate conditions. Effects on infiltration were addressed by likely climates in the future. The variability of the climate was characterized by annual precipitation, the amount falling between 12/1 - 4/30, and the average annual air temperature. Spatial variability was addressed by identifying the soil/hydrologic land units in the repository area. The soil water flow model incorporated surface hydrology, soil water flow, and evapotranspiration. A one dimensional isothermal water flow model was utilized that accounted for the water budget, defined as drainage (net infiltration) = precipitation - evapotranspiration - runoff - soil storage.

Spatial variability accounted for factors that affect net infiltration, such as soil depth, soil structure, bedrock properties, and rainfall distribution (assumed equal, given small area of Yucca Mountain). Three soil/hydrologic units were considered.

1) shallow, ridge top: 0-0.5 meters in depth, loamy texture, rocky soil

2) slopes: moderately deep soils on side slopes, 0.5 - 2.0 meters deep, fairly well vegetated but susceptible to storm runoff and erosion, loamy with less permeable caliche layer at 0.2 to 0.5 meters deep

3) basins: deep soils of hydrologic accumulation occur in small basins at lower elevations, fine texture -- primary areas for net infiltration

The calculations included five climate scenarios and three soil/hydrologic units. 134 year numerical simulations were performed. The annual infiltration for each year

was calculated. The effects of year to year variability, storm patterns, sequences of wet and dry years, and other climate pattern variations were incorporated in the calculations. The results, shown in Table 5.1 for three soil/hydrologic units combined for each climate using a simple weighted average based on acreage fractions. The results shown in Table 5.1 were combined with climate scenario probabilities to develop overall probability of given infiltration.

The water table position is a key variable because engineered and geologic barriers are most effective when the rock is unsaturated. Changes in the climate may alter water table position. The results of the climate based water table change model are based on existing investigations into mineralogy to identify the level of the water table during past pluvial conditions. The actual values assigned to the probabilities are very uncertain as sufficient data do not exist to define probabilities with more confidence.

Table 5.1 Net Infiltration (mm/yr) [13]

Climate	Mean	Standard Deviation
current	0.93	0.52
Greenhouse	1.02	0.48
10% Full Glacial Maximum	1.23	0.70
50% Full Glacial Maximum	1.65	0.88
100% Full Glacial Maximum	2.35	1.36

The strategy for storing waste in a mined repository relies in part on geologic and hydrogeologic barriers. Yucca Mountain lies in an arid region, and consists of a thick unsaturated zone of rock. Ground water flow and mass transport is difficult toanalyze due to a complex pattern of geologic layering, differing hydraulic and transport properties for each layer, and the presence of faults and fractures.

The stratigraphy of Yucca Mountain consists of several layers of bedded tuff. The Tiva Canyon unit consists of partially saturated, densely fractured, welded tuff. This unit has a hydraulic conductivity of 9.7 E-12 m/s, a porosity of 8% and contains approximately 20 fractures/m^3 with a fracture hydraulic conductivity many orders of magnitude higher than that of the matrix. The Paintbrush tuff unit consists of non-welded ash-fall tuff with a low fracture density (1/m^3), a porosity of 40% and a matrix conductivity = 3.9 E-7 m/s. The Topopah Spring unit is to be the repository horizon and has a matrix conductivity of 1.9 E-11 m/s, and a porosity of 11%. The upper portion has a fracture density of 40/m^3 with a fracture conductivity of 2.2 E-5 m/s. The lower portion has a fracture density of 8/m^3 with a fracture conductivity of 1.7 E-5 m/s. The Calico Hills unit consists of vitric and zeolitic tuff. Below the Calico Hills unit lie older tuff beds that are fractured and have modest permeability. The water table is flat under Yucca Mountain, and lies approximately 500-600 m below ground surface. The water table has differing water table gradients, low to the northeast and southeast of repository and high to the north of repository. Discharge of water is in the Amaragosa Desert.

Flow in a fractured, porous medium is described mathematically by separate non-linear flow equations for the fracture and matrix. Terms are applied to account for

the fracture - matrix coupling, although it is possible to solve both simultaneously, but modeling becomes easier if the mathematics is simplified. The approach used in IMARC is to assume that the difference in the pressure head is instantaneously redistributed between the fractures and matrix. Single flow equations are used with the parameters averaged over the fractures and matrix to give composite values. The dissolved mass is also coupled. For strong coupling, the mass is redistributed instantaneously between the fractures and the matrix. For weak coupling, mineral precipitates along fractures reduce the rate of diffusive transport between the fractures and the matrix.

In order to capture the essence of complex flow, a transient, multi-dimensional model that reflects the complex pattern of layering and disruptions due to fault development is required. A simpler model, however, is needed for performance analyses to reduce the required computational resources. Three key features of hydrologic setting need to be included in a simpler model. These features are:

1) Changing hydraulic conductivities with depth and major faults may produce two dimensional flow. For example, down-dip faults and differences between the Paintbrush and Topopah Spring members will divert water down-dip and shield the repository. Open faults can also provide preferred vertical pathways.

2) The storage of water in the Paintbrush tuff member. A change in the flux at the surface may not be seen at repository horizon until a later time.

3) The lateral flow of water and radionuclide transport below water table.

Flow and transport modeling consists of one dimensional unsaturated flow from the repository to the water table and a connected saturated pathway that transports

radionuclides laterally 5 km to the accessible environment. Equation 5.1 describes the flow of ground water in an unsaturated medium.

$$\frac{\delta}{\delta z}[k_*(\psi)\frac{\delta(\psi+z)}{\delta z}]=\frac{\delta\theta}{\delta t}$$

$$k_*(\psi)=k_s \exp[\alpha\psi] \qquad (5.1)$$

$$\theta = \theta_r + (\theta_s - \theta_r) \exp[\alpha\psi]$$

Where: z = vertical component

Ψ = pressure head

k_* = unsaturated hydraulic conductivity (function of pressure head)

k_s = saturated hydraulic conductivity

θ = moisture content

θ_r = residual moisture content

θ_s = saturated moisture content

α = soil pore size distribution parameter

t = time

These simple relations are not able to represent composite conductivity curves, however they do approximate individual conductivity curves well. The approach utilized in IMARC is to use the flux at the repository horizon to determine which conductivity curve predominates. For cases where both are operating, the fracture curve is utilized.

The transport of mass in a one-dimensional unsaturated medium is given as equation 5.2.

$$D_z\frac{\delta^2}{\delta z^2} - V\frac{\delta C}{\delta z} - R_f\lambda C = R_f\frac{\delta C}{\delta t} \qquad (5.2)$$

Where: C = concentration

D_z = dispersion coefficient in z-direction

V = unsaturated flow velocity

λ = decay constant

R_f = retardation factor

The flow and mass transport equations are coupled by the velocity term. The boundary conditions and initial conditions are 1) the flux at repository is less than or equal to the net infiltration (water diverted laterally does not interact), 2) at the repository, the flux is specified in terms of an initial flux and a flux at time greater than zero. This implies a time lag between a change in the net infiltration and a change in the flux, given by equation 5.3.

$$t_{rep} = t_{surf} + t_{adj} \qquad t_{adj} = 25 \exp[\frac{-I_{sz}}{0.22}] \tag{5.3}$$

Where: t_{rep} = time when flux change occurs at repository (millennia)

t_{surf} = time when flux change occurs at surface (millennia)

t_{adj} = time lag (millennia)

I_{sz} = new net infiltration rate

3) at the water table the pressure head equals zero, its position is fixed, and the saturated zone velocity is constant, 4) the initial mass concentration equals zero, and 5) the mass reaching the boundary with accessible environment exits the system.

The modeling methodology utilizes a semi-analytical approach. The modeling of ground water flow is done analytically while the mass transport of radionuclides is done numerically. To calculate the water flow, $k_r(\psi)$, θ, and the elevation are used in the Darcy equation to determine the groundwater velocity or velocity of advective mass transport in the unsaturated zone. Again, velocity is assumed to be constant in the

saturated zone. Mass transport utilizes a moving particle approach subject to advection, retardation, decay, and dispersion (neglected). The transport of daughter product radionuclides is ignored in the original IMARC code. Mass transport adds a reference particle to the flow field at the repository at the beginning of a time step. During a given time step, a particle is moved according to equation 5.4.

$$\Delta z = V_c \, \Delta t \qquad V_c = \frac{V}{R_f}$$

$$R_f = 1 + \frac{\rho k_d}{\theta_m} \tag{5.4}$$

Where: ρ = bulk density of medium

k_d = distribution coefficient

θ_m = matrix moisture content

R_f = Retardation (R_f = 1 in saturated zone)

Each particle carries a certain amount of mass of a given radionuclide, determined by the leaching and container models. This model demonstrated good agreement with a higher order model.

The probability of lateral redistribution modes cannot be assigned with any certainty. It is assumed that the degree of diversion is dependent on the flux, given as equation 5.5. The probabilities assigned to fracture/matrix coupling indicate that strong fracture-matrix coupling is most likely, but weak coupling is a reasonable possibility. For strong coupling, mass is assumed to diffuse instantaneously from fractures to the matrix. For weak coupling, mass in fractures outruns mass moving through the matrix

$$
\begin{array}{ll}
\textit{NO DIVERSION} & \\
I_r = I_s & \textit{for all flux} \\
\textit{MODERATE DIVERSION} & \\
I_r = I_s & I_s \leq 0.2\ \textit{mm/yr} \\
I_r = 3I_s/(1+10I_s) & I_s > 0.2\ \textit{mm/yr} \\
\textit{EXTENSIVE DIVERSION} & \\
I_r = I_s & I_s \leq 0.7\ \textit{mm/yr} \\
I_r = 0.7 & I_s > 0.7\ \textit{mm/yr}
\end{array}
\qquad (5.5)
$$

I_s = *Flux at surface* I_r = *Flux at repository*

for a flux greater than 1 mm/yr. In order to model matrix sorption, solubilities from the Yucca Mountain Environmental Assessment [6] are utilized. High values are assumed to be five times larger than the base values. Low values are assumed to be five times smaller than the base values. Two values of saturated groundwater flow (1 mm/yr and 10 mm/yr) are assumed, with equal probability.

5.3 Changes to IMARC Required to Model Various Waste Forms

The models described above, their input parameters, and the associated logic tree probabilities do not require modification to perform PA analyses of any of the wasteforms considered in this study. The only areas that require modification are the source term model, the engineered barrier system failure model, and the handling of daughter product ingrowth. The tectonic and volcanic models are not utilized.

The source term models utilized by EPRI in the development of IMARC are described in detail in Chapter 4. These models, namely equations 4.4 through 4.8,

have not been modified and are assumed to be applicable for both the DHLW and ALMR wasteforms. Parameters relevant to each wasteform are incorporated into IMARC either as input variables or coded constants. Tables 4.1 and 4.2 provide several parameters for the SF and DHLW/ALMR wasteforms, respectively. One parameter not listed in Tables 4.1 and 4.2 is the effective catchment area, or the effective area where flux is diverted to drip on the waste package. EPRI [85] assumes a one meter diameter circle as the effective catchment area for the borehole emplaced SCP package. Intera [14] assumes an effective catchment area of 8.5 square meters for the drift emplaced MMB container.

The matrix alteration rates utilized by EPRI for SF are unchanged and shown in Table 4.3. The nominal matrix alteration rate is assigned a 50% occurrence probability while the high and low matrix alteration rates are assigned occurrence probabilities of 25%. This differs from those of the EPRI IMARC analyses where the low, nominal and high matrix alteration rates were assigned occurrence probabilities of 5%, 90%, and 5%, respectively. It is believed that that the uncertainty in the matrix alteration rate (and the elemental solubility limits) is larger than that assumed by EPRI.

For DHLW, the relation for glass alteration developed by Intera is utilized. This relation is given as equation 4.9. The nominal alteration rate utilized for the IMARC PAs is based on a temperature of 80 °C, a pH of 6.0, and a cracking factor of 20. The low alteration rate is based on a temperature of 80 °C, a pH of 7.0, and a cracking factor of 10. The low alteration rate is based on a temperature of 80 °C, a pH of 2.0, and a cracking factor of 30. These result in low, nominal and high alteration rates of 16.8, 40.6, 280.6 g/m^2 yr, respectively. It is assumed that high and low matrix

alteration rates are represented by an order of magnitude increase or decrease in the nominal alteration rate. The nominal DHLW matrix alteration rate is assigned an occurrence probability of 50% while the low and high values are each assigned an occurrence probability of 25%.

The nominal matrix alteration rate for the ALMR metallic wasteform is assumed to be 0.5 mg/cm^{2}yr (5 g/m^{2}yr). This value corresponds to the low corrosion rates provided in Table 4.4 for the stainless steel - zircaloy alloy. Local de-alloying, localized and galvanic corrosion, cracking and adverse repository conditions (compared to the test conditions) may increase the alteration rate. It is assumed that an increased alteration rate is represented by an order of magnitude increase in the nominal matrix alteration rate. After increased exposure times, a passivation layer may form on the surface of the metallic wasteform, lowering the matrix alteration rate. In addition, the repository near field environment may result in corrosion rates lower than those observed under test conditions. It is assumed that a decreased alteration rate is represented by an order of magnitude decrease in the nominal matrix alteration rate.

The nominal matrix alteration rate for the ALMR mineral wasteform is assumed to be 0.5 g/m^{2}d (182.5 g/m^{2}yr). This alteration rate is based on the NRR of the glass bonded zeolite that was exposed to 90 °C deionized water for 56 days. It can be seen in Table 4.5 that all elements measured had an NRR less than 0.5 g/m^{2}d. The NRR for sodalite tested under the same conditions is similar to that of glass bonded zeolite after 28 day exposures. It is assumed that the matrix alteration rate above is representative of both proposed mineral wasteforms.

Increased matrix alteration may result from repository near field conditions

differing from the test conditions. An increased alteration rate is assumed to be an order of magnitude larger than the nominal value. It can be seen in Table 4.5 that the NRR decreases with increased exposure time, indicating that the steady state release rate may be lower than that measured in the short-term tests. In addition, the development of the mineral wasteform is just beginning and improvements in the dissolution properties are expected as research continues. It is assumed that a decreased matrix alteration rate is an order of magnitude lower than the nominal value.

The nominal matrix alteration rate of each ALMR wasteform is given an occurrence probability of 50%. The low and high matrix alteration rates are each assigned an occurrence probability of 25%. This is consistent with those applied to LWR SF and DHLW. The matrix alteration rate occurrence probabilities can be modified in the future as additional data becomes available.

In the analysis of all wasteforms, it is assumed that 50% of the containers are experiencing a wet-drip water contact mode and 50% are experiencing a moist-continuous water contact mode. The containers and their associated performance parameters are assigned to temperature regimes that are detailed in Chapter 3. It should be noted that for SF the container performance parameters are provided for six temperature regimes. IMARC only considers four temperature regimes. In some cases, it was necessary to average the parameters from at most two of the six temperature regimes into a set of effective parameters for one temperature regime. This is not expected to impact the results as the parameters averaged do not differ significantly. This was not required for the DHLW or ALMR wasteforms as they will experience only one temperature history regardless of whether they are co-located with

SF or emplaced alone.

The initial radionuclide inventories provided in Chapter 4 for each wasteform were used as input to IMARC. The initial inventory of ^{237}Np, ^{234}U, and ^{240}Pu were adjusted to account for build-in according to equation 4.11. Daughter product build-up from ^{237}Np and ^{234}U was incorporated by implementing equations 4.12 and 4.13 into both the IMARC transport and source term models.

It should be noted that IMARC calculations are based on the amount of waste contained in each package while the inventory is provided in terms of Curies per MTHM. Table 5.2 provides the amount of waste contained in each package in terms of MTHM. The SCP container holds either 3 PWR and 4 BWR intact fuel assemblies or one pour container with DHLW/ALMR waste. The MMB container holds 21 intact fuel assemblies or four pour containers.

Table 5.2: Waste Contained in Each Waste Type Container (MTHM)

Wasteform	SPC Container	MMB Container
Spent Fuel	2.1 [8]	9.74 [14]
DHLW	0.5 [14]	2.0 [14]
Oxide Reduction Mineral	3.3 [37]	13.2 [37]
Actinide Recycle ER Mineral	22.1 [37]	88.6 [37]
Actinide Recycle ER Metallic	36.9 [37]	147.6 [37]
ALMR ER Mineral	0.3 [37]	1.2 [37]
ALMR ER Metallic	1.14 [37]	4.6 [37]

The output from IMARC for SF is total Curies released as a function of time per 1,000 MTHM of waste emplaced in the repository. The output for actinide recycle waste is also presented in terms of Ci released per 1,000 MTHM of waste emplaced. The output for DHLW is presented in terms of Curies released per 1,000 MTHM equivalent of waste emplaced. The output from the ALMR wasteform is normalized to the heavy metal loading required to produce the equivalent electric output as 1,000 MTHM of LWR fuel. It has been estimated that 421 MTHM of LWR fuel and 123 MTHM of ALMR fuel is required to produce 10^{11} kwh of electricity [37]. Based on these values, the output for the ALMR wasteforms is presented per 300 MTHM of waste emplaced.

The EPRI IMARC analyses assigned a probability of 0.90 to the nominal (as measured) element solubility and 0.05 to low and high estimates of the solubility. For this study, the assignment of probabilities is identical to that assumed for matrix alteration (since these parameters are coupled directly in the IMARC tool).

No other changes to the IMARC models are required to model the various wasteforms considered. The models summarized above and their associated parameters and occurrence probabilities [12,13,86] remain unchanged, except for the engineered barrier system (container) failure parameters (provided in Chapter 3).

5.4 Results of IMARC PA Analyses

The description of the input files required for the execution of IMARC are provided in the IMARC Users Manual [86]. All input files utilized in subsequent analyses are also provided in Appendix B.

5.4.1 Installation and Benchmarking of the IMARC Software

The IMARC software was installed on the Digital Electronics Corporation workstations at Iowa State University. The test case provided by Risk Engineering Incorporated was executed and the output compared to that provided in the IMARC users manual [86]. Identical results were obtained indicating that the software was properly installed and executed correctly.

5.4.2 IMARC Results for Commercial Spent Fuel

IMARC analyses have been completed for the SF wasteform emplaced in the SCP and MMB containers. The initial radionuclide inventory is provided in Table 4.7 and the container loading is provided in Table 5.2. The container performance parameters utilized are given in Table 3.7. As was discussed previously, in some cases it was necessary to average at most two of the six sets of container parameters in order to produce effective parameters for IMARC input. All input files utilized in IMARC are provided in Appendix B.

The complementary cumulative distribution functions (CCDF) of total actinide and total fission product cumulative Curie release per 10,000 MTHM for the SCP waste container is shown in Figures 5.1 through 5.3. Identical CCDFs for the MMB containers are provided in Figures 5.4 through 5.6. The CCDFs are presented at 10000, 50000, and 100000 years following emplacement for the three APDs considered (28.5, 57.0, 114.0 kw/acre). Table 5.3 provides the maximum release calculated from each container design for the three APDs considered at 10000, 50000, and 100000 years following emplacement.

Table 5.3: Maximum Possible Releases from LWR SF (Ci/1000 MTHM)

Time After Emplacement (years)	SCP		MMB	
	Actinides	Fission Products	Actinides	Fission Products
APD = 28.5 kW/acre				
10000	$1x10^4$	$1x10^4$	$2x10^2$	$3x10^2$
50000	$2x10^4$	$1x10^4$	$7x10^3$	$8x10^3$
100000	$3x10^4$	$2x10^4$	$1x10^4$	$8x10^3$
APD = 57.0 kW/acre				
10000	$1x10^4$	$1x10^4$	$1x10^3$	$1x10^3$
50000	$2x10^4$	$1x10^4$	$9x10^3$	$1x10^4$
100000	$3x10^4$	$2x10^4$	$1x10^4$	$1x10^4$
APD = 114.0 kW/acre				
10000	$3x10^3$	$2x10^3$	0	0
50000	$2x10^4$	$1x10^4$	$8x10^3$	$9x10^3$
100000	$3x10^4$	$2x10^4$	$1x10^4$	$9x10^3$

10000 years: Figures 5.1 and 5.4 demonstrate that the release of actinides and fission products at 10000 years is lowest for an APD of 114.0 kw/acre for both containers. For the SCP container, the release is slightly lower for an APD of 114.0 kW/acre due to the increased dry-out time. No release occurs within 10000 years for the MMB container at 114.0 kw/acre while the SCP container does release radionuclides within this time period. This is due to the increased time required to corrode the thicker MMB multiple barriers. The highest releases are observed for APDs of 57.0 kw/acre for the MMB container and 28.5 kW/acre (slightly larger than 57.0 kW/acre) for the SCP container. For the MMB container, the high releases for an

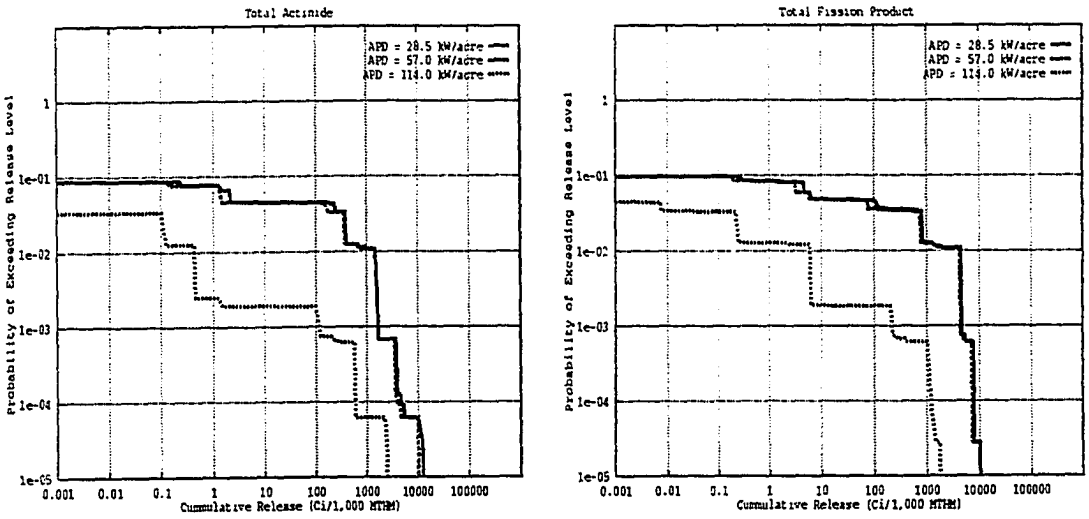

Figure 5.1 Total Actinide and Fission Product Release From SCP Container at 10,000 Years

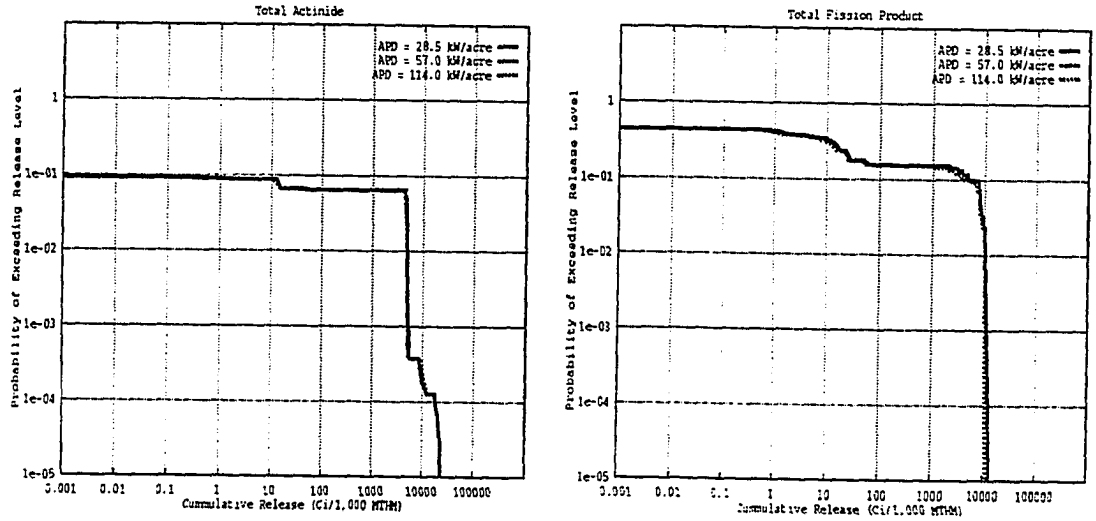

Figure 5.2 Total Actinide and Fission Product Release From SCP Container at 50,000 Years

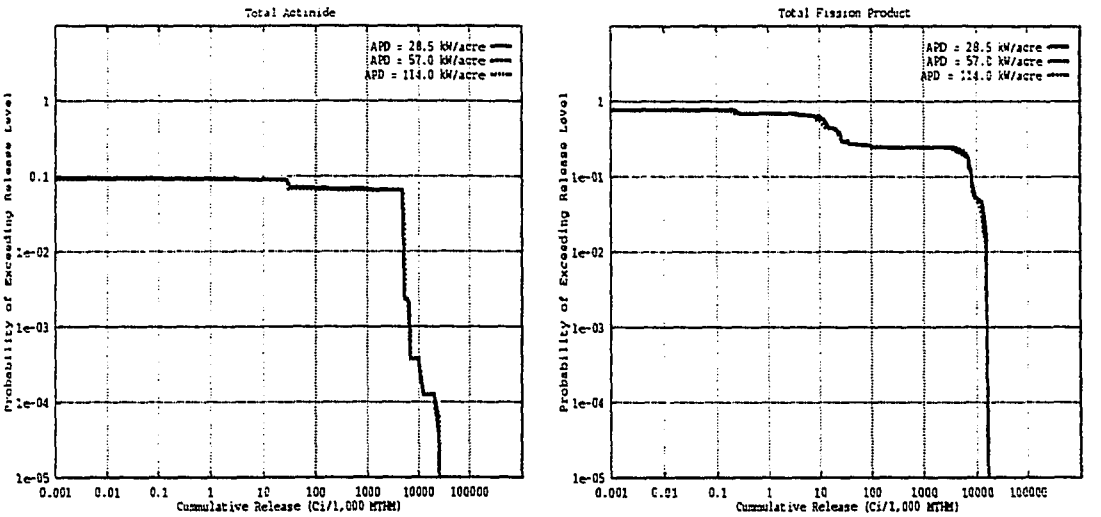

Figure 5.3 Total Actinide and Fission Product Release From SCP Container at 100,000 Years

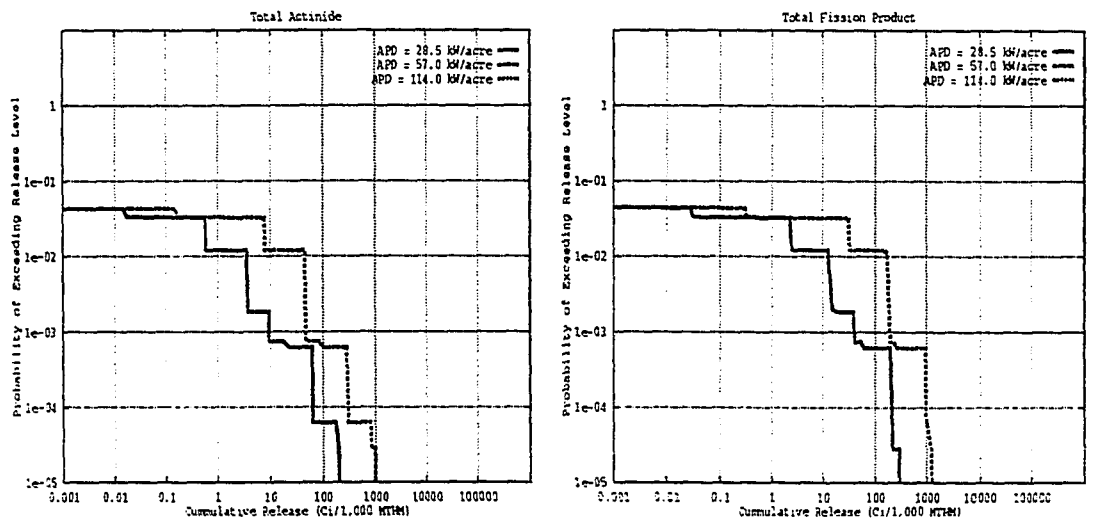

Figure 5.4 Total Actinide and Fission Product Release From MMB Container at 10,000 Years

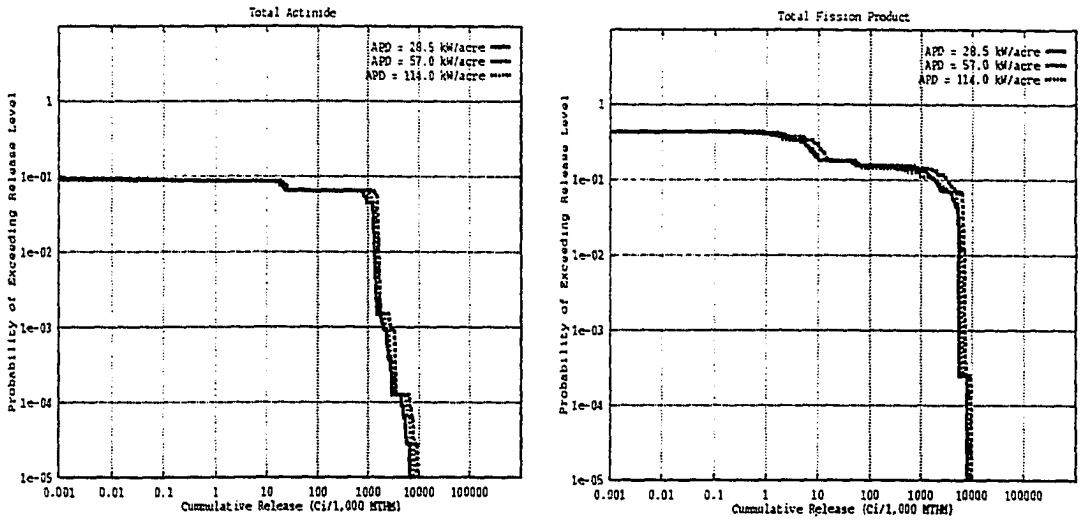

Figure 5.5 Total Actinide and Fission Product Release From MMB Container at 50,000 Years

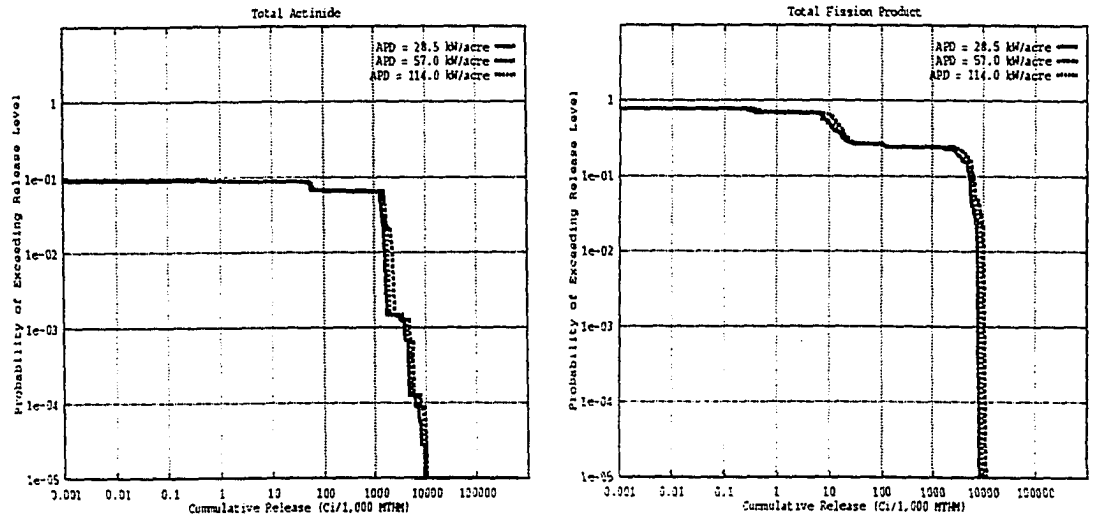

Figure 5.6 Total Actinide and Fission Product Release From MMB Container at 100,000 Years

APD of 57.0 kW/acre relative to an APD of 28.5 kW/acre are due to the higher post dry out repository temperature, resulting in more rapid corrosion failure of the barriers.

50000 and 100000 years: At 50000 and 100000 years, (Figures 5.2, 5.3, 5.5, 5.6) the cumulative release of both the actinides and fission products is essentially identical regardless of the thermal loading for both container designs. Slight differences are observed for the MMB container design. This indicates that for a given container design, releases in the long-term are independent of the repository thermal loading.

Radionuclide Contribution: Figure 5.7 provides the contribution of individual radionuclides to the total actinide and fission product CCDFs from the SCP container at 50000 years following emplacement for an APD of 57.0 kw/acre. Figure 5.8 provides similar plots for the MMB container. The total actinide release from both the SCP and MMB containers is primarily dominated by ^{237}Np and its daughters, ^{239}Pu, and ^{240}Pu. ^{234}U and its daughters and ^{242}Pu contribute slightly to the overall release. The release of the other actinides, ^{226}Ra, ^{235}U, and ^{238}U, are negligible when compared to the total. The total fission product release from the SCP and MMB containers is dominated by ^{99}Tc. The release of ^{135}Cs, ^{129}I, and ^{79}Se is at least one order of magnitude lower than ^{99}Tc.

Comparison of SCP vs. MMB: At 10000 years, the release from the MMB container is significantly lower (over an order of magnitude) than that from the SCP container at all APDs considered (no release from MMB at 114.0 kW/acre). The maximum possible cumulative release of fission products is also significantly lower for the MMB container relative to the SCP container at all APDs considered.

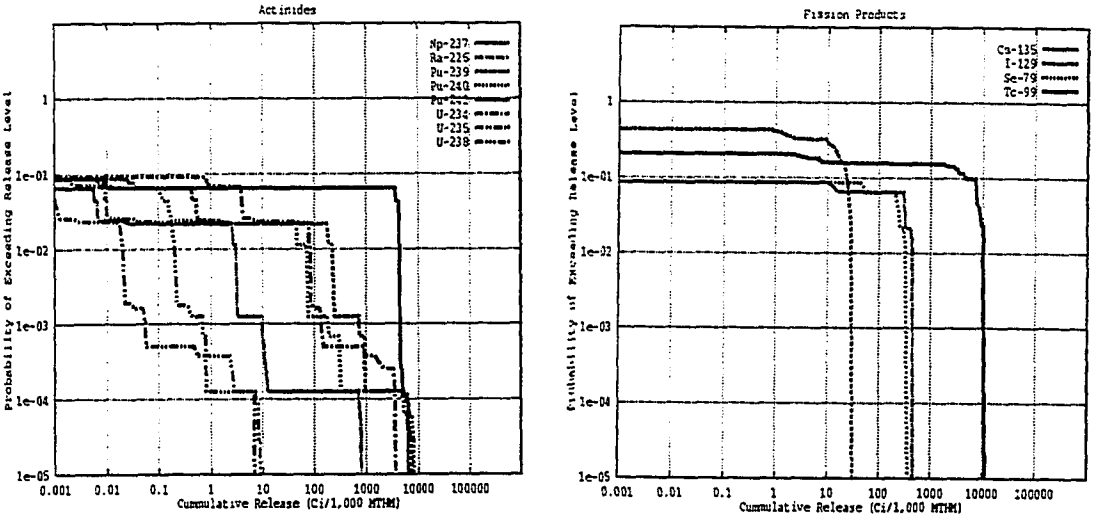

Figure 5.7 Radionuclides That Contribute to the Total Actinide and Fission Product Release From SCP Container at 50,000 Years, 57.0 kw/acre

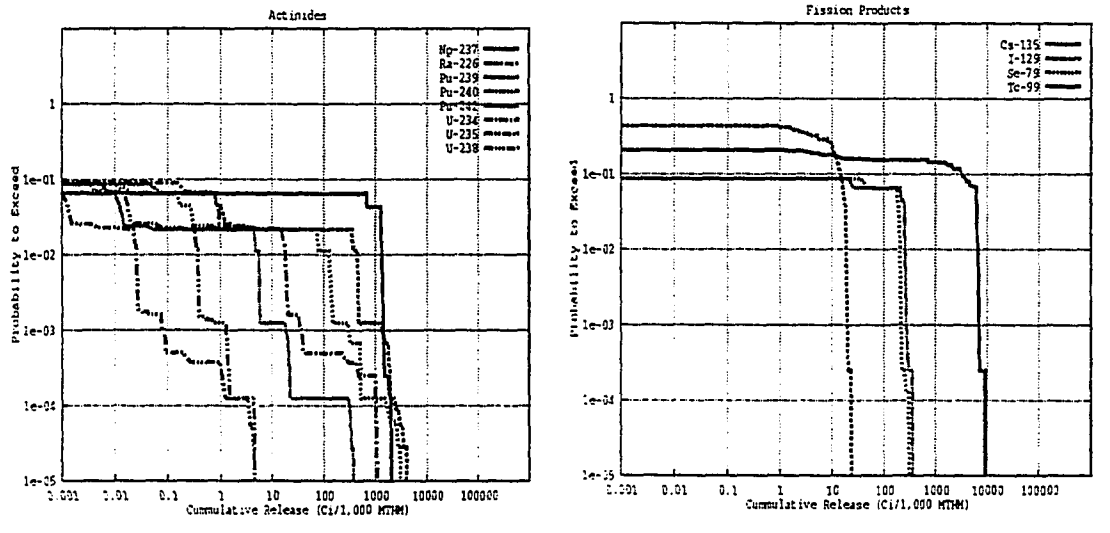

Figure 5.8 Radionuclides That Contribute to the Total Actinide and Fission Product Release From MMB Container at 50,000 Years, 57.0 kw/acre

A comparison of the cumulative release from the SCP and MMB containers 50000 years following emplacement (57.0 kw/acre) is shown in Figure 5.9. The performance of the MMB container is observed to be slightly better than the SCP container. The maximum cumulative release of actinides from the MMB container is lower than that from the SCP container by a factor of over two. The release of fission products is also observed to behave in a similar fashion. Similar results are observed at 100000 years for this APD and at 50000 years and 100000 years for APDs of 28.5 and 114.0 kw/acre.

These results indicate that in a 10000 year period, the release of radionuclides will be significantly lower when a large metallic multi-barrier container is utilized. Over the long-term, the release of radionuclides is reduced by less than an order of

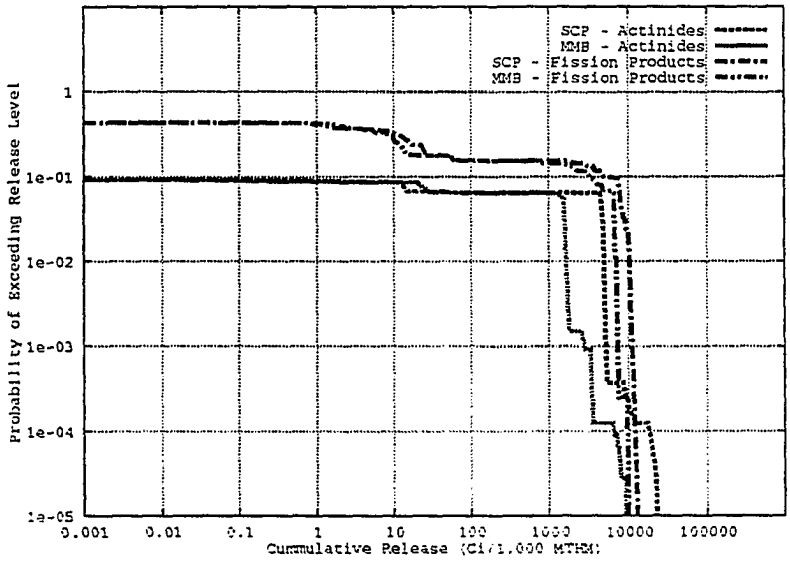

Figure 5.9 Release From SCP and MMB Containers, 50,000 Years, 57.0 kw/acre

magnitude when utilizing a large metallic multi-barrier container rather than a thin walled single barrier container.

5.4.3 IMARC Results for the ALMR Wasteforms

IMARC PAs have been completed for the ALMR closed pyroprocess fuel cycle wasteforms assuming that these wasteforms are 1) co-located with SF at an APD of 114.0 kw/acre, and 2) emplaced in the repository alone. Both low and high pyroprocess actinide decontamination factors were considered. The MMB container design was utilized based on the SF results. The initial inventory is provided in Table 4.9, the container loading (MTHM) is provided in Table 5.2, and the container performance parameters are provided in Chapter 4. All input files utilized in IMARC are provided in Appendix B.

CCDFs for the co-located ALMR metallic and mineral wasteforms are provided in Figures 5.10 through 5.12 at 10000, 50000 and 100000 years after emplacement, respectively. CCDFs for the ALMR wasteforms are provided in Figures 5.13 and 5.14 at 50000 and 100000 years after emplacement for the case when the ALMR waste is emplaced in the repository alone. No releases occur for this case at 10000 years after emplacement as none of the containers have failed. These CCDFs were obtained assuming a low pyroprocess actinide decontamination factor of $1x10^{4}$.

Comparison of Emplacement Strategies: The release of radionuclides to the accessible environment is observed to be significantly lower when the ALMR waste is not co-located with LWR SF. No release of either actinides or fission products occurs within the first 10000 years when the ALMR waste is emplaced alone.

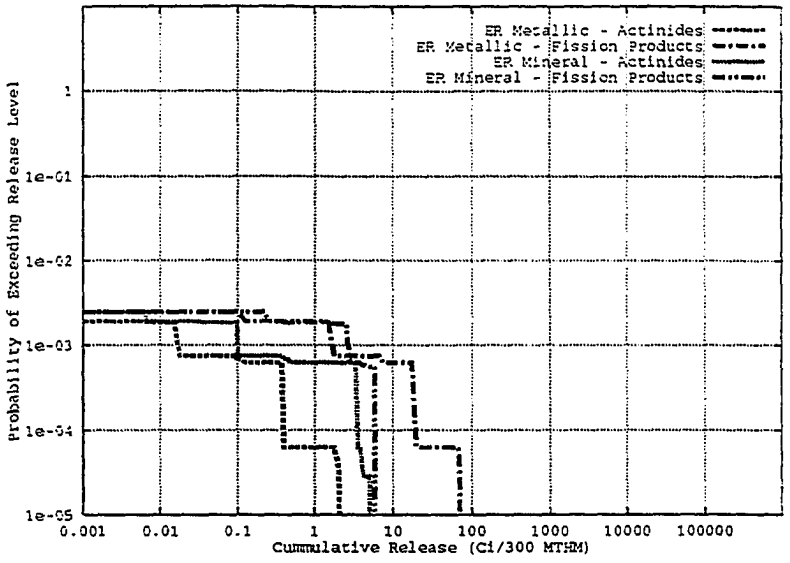

Figure 5.10 Release of Radionuclides From ALMR Wasteforms, MMB Container, Co-located, 114.0 kw/acre, 10,000 Years, Low Actinide Decontamination

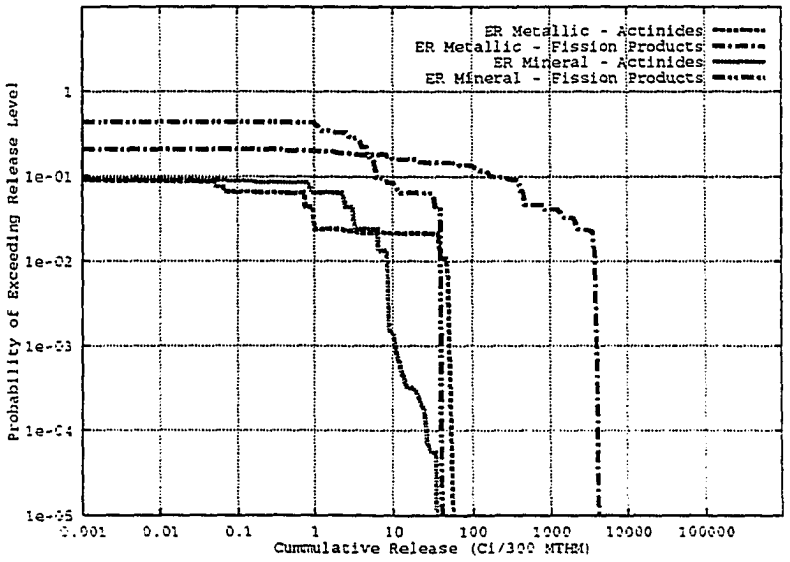

Figure 5.11 Release of Radionuclides From ALMR Wasteforms, MMB Container, Co-located, 114.0 kw/acre, 50,000 Years, Low Actinide Decontamination

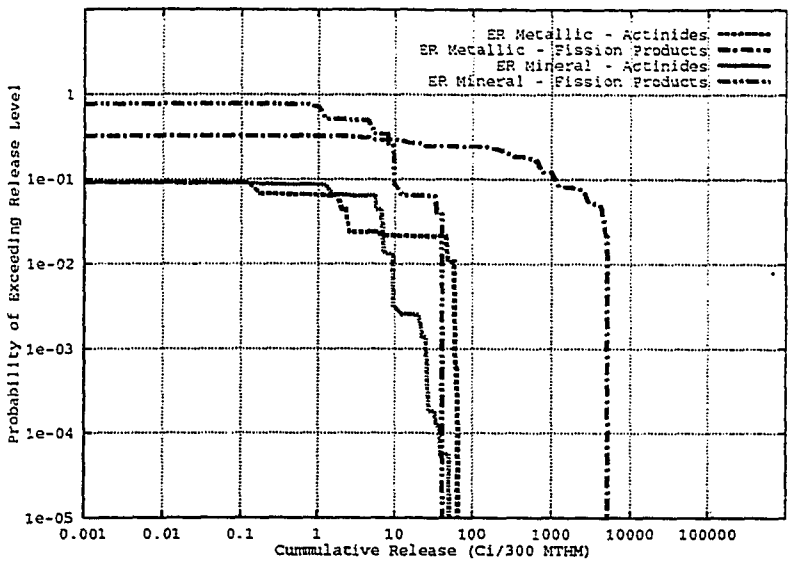

Figure 5.12 Release of Radionuclides From ALMR Wasteforms, MMB Container, Co-located, 114.0 kw/acre, 100,000 Years, Low Actinide Decontamination

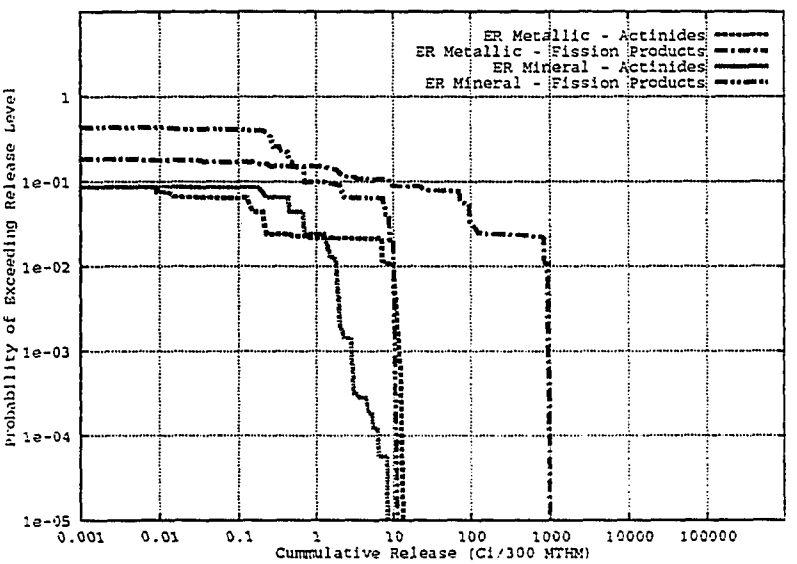

Figure 5.13 Release of Radionuclides From ALMR Wasteforms, MMB Container, Alone, 50,000 Years, Low Actinide Decontamination

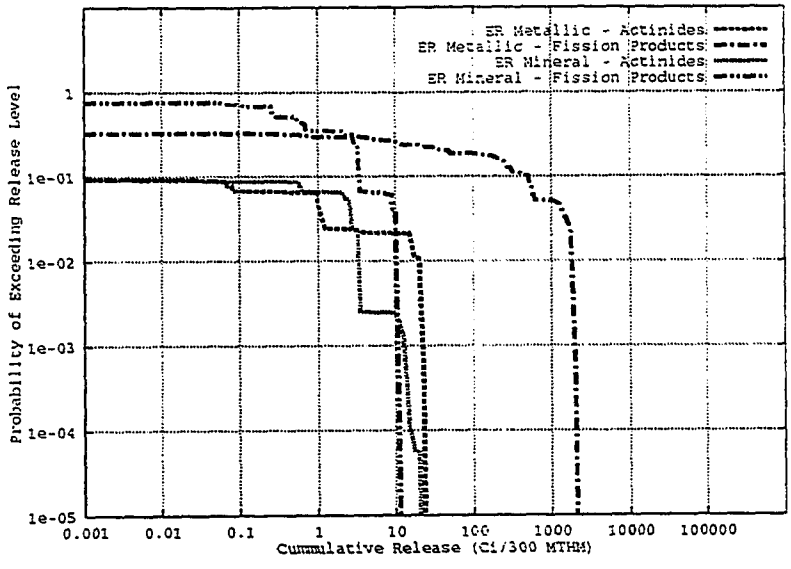

Figure 5.14 Release of Radionuclides From ALMR Wasteforms, MMB Container, Alone, 100,000 Years, Low Actinide Decontamination

At 50000 years, the release of both fission products and actinides is reduced by a factor of over four when the ALMR wasteforms are emplaced alone (low actinide recovery). The maximum possible cumulative release of actinides and fission products for the co-located ALMR waste is $6x10^{1}$ Ci and $4x10^{3}$ Ci, respectively. When the ALMR waste is emplaced alone, the maximum cumulative release of actinides and fission products is reduced to $1x10^{1}$ Ci and $1x10^{3}$ Ci, respectively.

At 100000 years, the release of both fission products and actinides is reduced by a factor of over two when the ALMR wasteforms are emplaced alone (low actinide recovery). The maximum possible cumulative release of actinides and fission products for the co-located ALMR waste is $7x10^{1}$ Ci and $5x10^{3}$ Ci, respectively. When the ALMR waste is emplaced alone, the maximum cumulative release of actinides and

fission products is reduced to 2 $x10^{1}$ Ci and $2x10^{3}$ Ci, respectively.

This reduction in the cumulative release is due to improved container performance resulting from lower barrier corrosion rates at the lower repository temperature. The results are summarized in Tables 5.4 and 5.5.

Contributions to Total Release: The total release is dominated by the total fission product release, primarily from the ER-metallic wasteform. The release of actinides is similar for each wasteform with the release from the mineral wasteform dominating slightly at 10000 years while that from the metallic wasteform dominate slightly at 50000 and 100000 years. Figures 5.15 and 5.16 show the contribution of individual radionuclides to the total actinide and fission product release at 50000 years for the metallic and mineral wasteforms, respectively. The total actinide release is dominated by ^{239}Pu and ^{240}Pu. This differs from the LWR SF results as it was observed that ^{237}Np contributed to the total actinide release. The total fission product release is dominated by ^{99}Tc for the metallic wasteform and ^{135}Cs for the mineral wasteform. The release of ^{99}Tc from the metallic wasteform is over two orders of magnitude larger than the release of ^{135}Cs from the mineral wasteform. This is similar to the results observed for LWR SF as ^{99}Tc also dominated the fission product release.

Comparison With LWR SF: Comparisons of Figures 5.5 and 5.6 (LWR SF - MMB 114.0 kW/acre, 50000 and 100000 years) with Figures 5.11 and 5.12 (LMR - MMB co-located at 114.0 kW/acre, 50000 and 100000 years) show that the release of actinides is significantly lower for the ALMR wasteforms. The maximum possible actinide release from the ALMR wasteforms are less than that from the LWR SF - MMB container (114.0 kW/acre) at 50000 and 100000 years after emplacement by

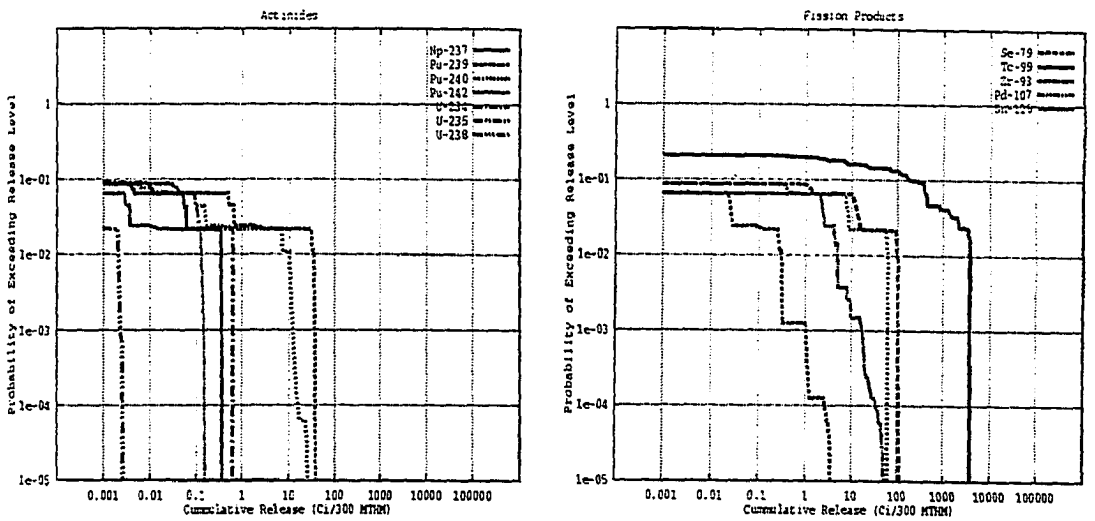

Figure 5.15 Radionuclides That Contribute to the Total Actinide and Fission Product Release From ALMR ER-Metallic Wasteform, MMB Container, Co-Located, 114.0 kW/acre, 50,000 Years, Low Actinide Decontamination

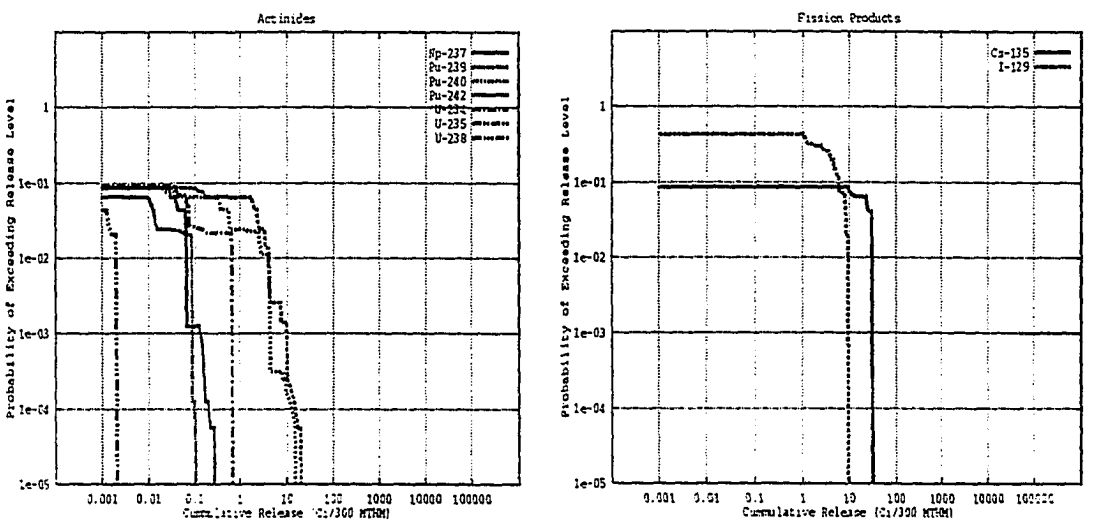

Figure 5.16 Radionuclides That Contribute to the Total Actinide and Fission Product Release From ALMR ER-Mineral Wasteform, MMB Container, Co-Located, 114.0 kW/acre, 50,000 Years, Low Actinide Decontamination

over two orders of magnitude. Figure 5.17 shows the comparison at 50000 years. At 50000 years, the maximum actinide possible release from LWR SF is $8x10^{3}$ Ci while from the ALMR wasteforms is $6x10^{1}$ Ci. At 100000 years, the maximum possible actinide releases are $1x10^{4}$ Ci for LWR SF and $7x10^{1}$.Ci for the ALMR wasteforms.

A greater reduction in the cumulative actinide release as compared to the SF-MMB container is observed at 50000 and 100000 years after emplacement when the ALMR waste is buried alone. The maximum possible releases are reduced by the following: LWR - $8x10^{4}$ Ci vs. ALMR - $1x10^{1}$ Ci at 50000 years, LWR - $1x10^{4}$ Ci vs. ALMR - $2x10^{1}$ Ci at 100000 years.

At 10000 years after emplacement no actinide release is observed for SF while the co-located ALMR metallic wasteform shows a release ($3x10^{0}$ Ci). Within this time period the SF containers are still dry, and hence not failed, while a fraction of the ALMR containers have already failed. Emplacing the ALMR wasteforms alone also results in no release at 10000 years.

It can be seen that the release of fission products is less than an order of magnitude lower for the co-located ALMR wasteforms (ER-metallic, ^{99}Tc) relative to LWR SF (^{99}Tc) at 50000 and 100000 years. The maximum cumulative release of fission products from the co-located ALMR metallic mineral wasteform - MMB container (^{99}Tc) is lower than that of SF - MMB container (^{99}Tc) by a factor of approximately two at 50000 and 100000 years (LWR - $9x10^{3}$ Ci vs. ALMR - $4x10^{3}$ Ci at 50000 years, LWR - $9x10^{3}$ Ci vs. ALMR - $5x10^{3}$ Ci at 100000 years). Again, Figure 5.17 shows the comparison at 50000 years. The general shape of the ALMR CCDFs at these time periods is similar to that observed for SF.

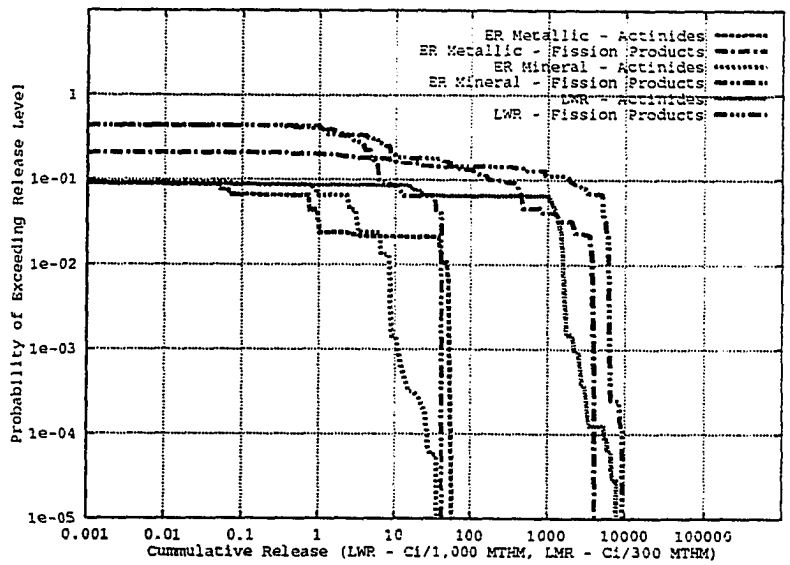

Figure 5.17: Comparison of the Release of Radionuclides From the LWR SF and ALMR Wasteforms, MMB Container, 114.0 kW/acre, 50000 Years.

Further reduction in the cumulative fission product release as compared to the SF-MMB container is again observed when the ALMR waste is emplaced alone. The maximum possible release of fission products are: LWR - $9x10^3$ Ci vs. ALMR -$1x10^3$ Ci at 50000 years, LWR - $9x10^3$ Ci vs. ALMR - $2x10^3$ Ci at 100000 years).

At 10000 years after emplacement, no fission product release is observed for SF while the co-located ALMR metallic wasteform shows a release ($7.0 x10^1$ Ci). Emplacing the ALMR wasteforms alone also results in no release at 10000 years.

It should be noted that the initial inventory of ^{99}Tc, in terms of Ci/MTHM, is larger in the ALMR waste. In order to produce the same electric output as an LWR, however, less fuel is required for the ALMR. In short, a similar amount of ^{99}Tc is

released to the environment for a given amount of electric generation regardless of the reactor type utilized.

Effect of Pyroprocess Actinide Decontamination Factor: Figure 5.18 shows the effects of the pyroprocess actinide decontamination factor on the cumulative total actinide release from the metallic wasteform at 50000 years. Increasing the actinide decontamination factor by half an order of magnitude results in a proportional reduction in the cumulative actinide release. It can be seen that the smallest release occurs when a high pyroprocess actinide decontamination factor is utilized and the waste is emplaced in the repository alone. The release of fission products is not changed as the actinide decontamination factor does not impact the fission product inventory.

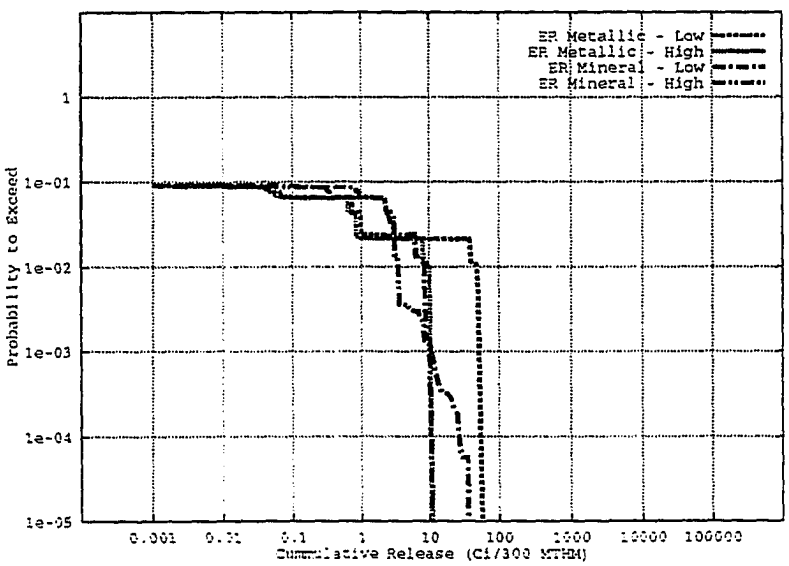

Figure 5.18 Effect of Actinide Decontamination Factor on the Release of Actinides From the ALMR Wasteforms, 50,000 Years

5.4.4 IMARC Results for the Actinide Recycle Wasteforms

CCDFs for the co-located actinide recycle metallic and mineral wasteforms are provided in Figures 5.19 through 5.21 at 10000, 50000 and 100000 years after emplacement, respectively. CCDFs for the actinide recycle wasteforms are provided in Figures 5.22 and 5.23 at 50000 and 100000 years after emplacement for the case when the waste is emplaced in the repository alone. Again, no releases occur for this case at 10000 years after emplacement as none of the containers have failed. These analyses have also assumed a low pyroprocess decontamination factor of $1x10^{3}$

Contributions to Total Release: It can be seen that the cumulative total actinide release is dominated by the ER mineral and metallic wasteform. The radionuclides that contribute to the total actinide release from each of these wasteforms are ^{239}Pu, ^{240}Pu, and ^{237}Np. The other wasteform containing actinides is the oxide reduction - mineral waste stream. The initial inventory of this wasteform is based on a 0.01% loss of actinides in the reduction process. This inventory, on a per MTHM basis, is equivalent to the high actinide decontamination ER wasteform inventories. As such, for the low actinide decontamination case, the ER wasteforms dominate the actinide release. The release of actinides from the oxide reduction - mineral wasteform will be comparable to that from the ER wasteforms if a high actinide decontamination factor is utilized. Again, ^{239}Pu, ^{240}Pu and ^{237}Np dominate the total actinide release from the oxide reduction - mineral wasteform.

The cumulative total fission product release is dominated by the ER-metallic wasteform. This form contains a large inventory of ^{99}Tc, (see Tables 4.10 and 5.2),

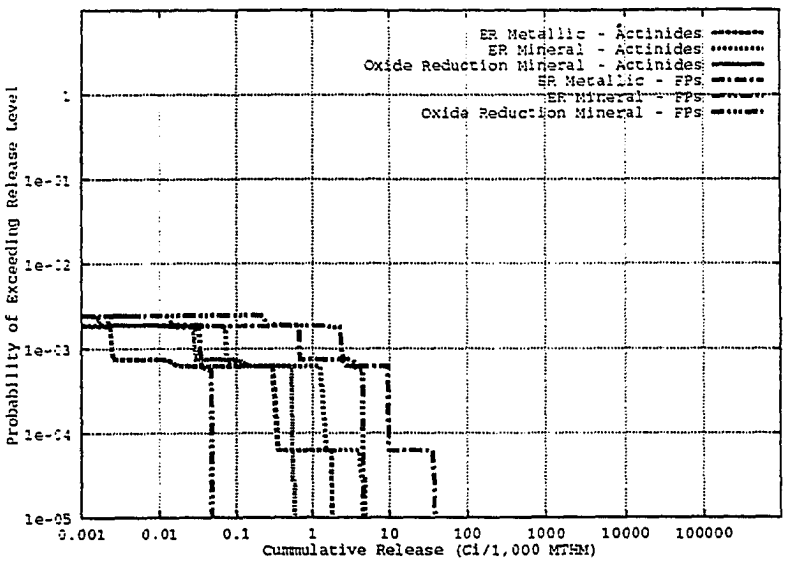

Figure 5.19 Release of Radionuclides From Actinide Recycle Wasteforms, MMB Container, Co-Located, 114.0 kw/acre, 10,000 Years, Low Actinide Decontamination

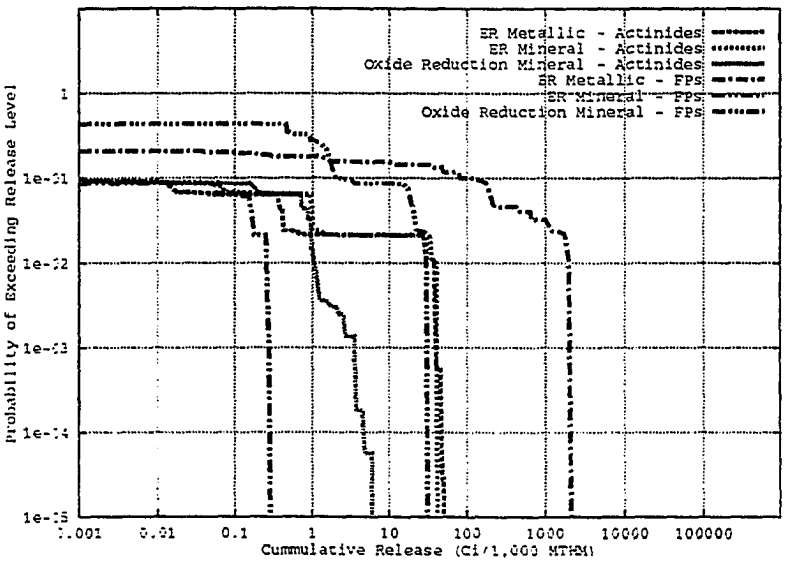

Figure 5.20 Release of Radionuclides From Actinide Recycle Wasteforms, MMB Container, Co-Located, 114.0 kw/acre, 50,000 Years, Low Actinide Decontamination

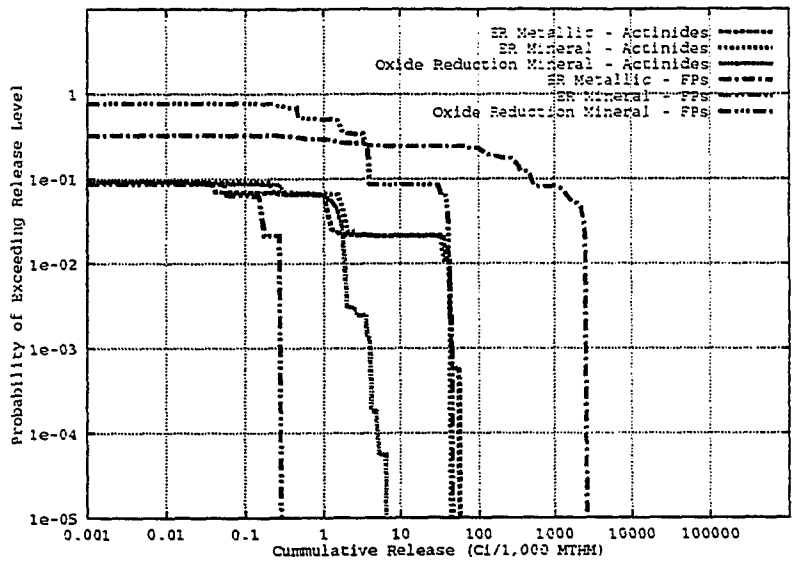

Figure 5.21 Release of Radionuclides From Actinide Recycle Wasteforms, MMB Container, Co-Located, 114.0 kw/acre, 100,000 Years, Low Actinide Decontamination

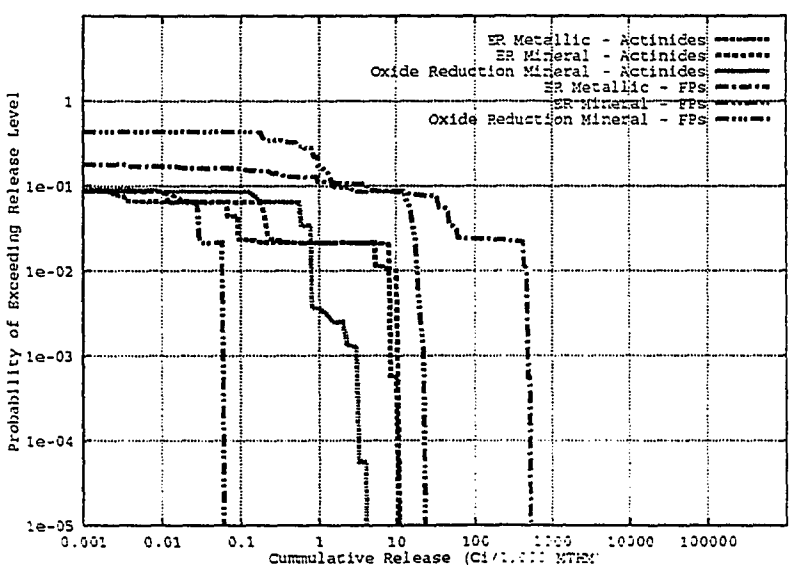

Figure 5.22 Release of Radionuclides From Actinide Recycle Wasteforms, MMB Container, Alone, 50,000 Years, Low Actinide Decontamination

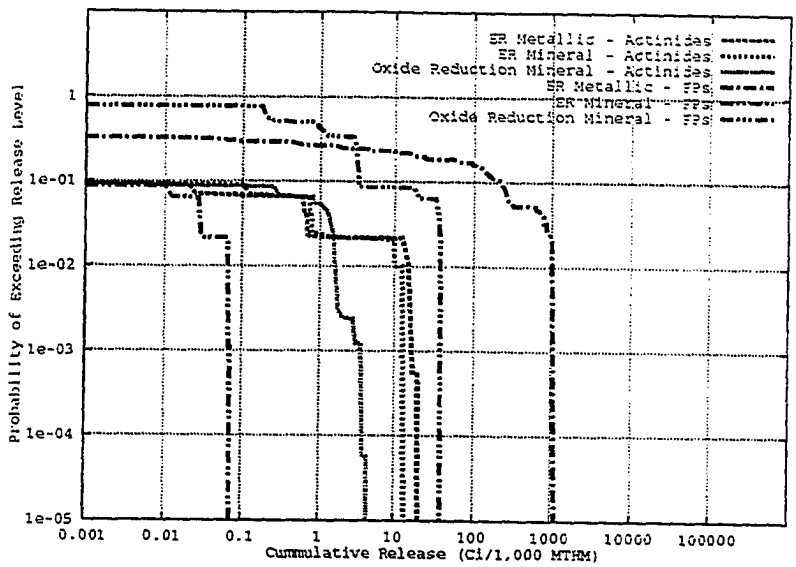

Figure 5.23 Release of Radionuclides From Actinide Recycle Wasteforms, MMB Container, Alone, 100,000 Years, Low Actinide Decontamination

which has been observed to be the only contributor to the total fission product release from SF. The release of fission products from the other wasteforms is at least an order of magnitude smaller. The primary fission products released from each wasteform are: Oxide Reduction Mineral - ^{135}Cs, and ER Mineral - ^{135}Cs (to a small extent).

Comparison with LWR SF: Comparisons of Figures 5.5 and 5.6 (LWR SF - MMB 114.0 kW/acre, 50000 and 100000 years) with Figures 5.20 and 5.21 (LMR - MMB co-located at 114.0 kW/acre, 50000 and 100000 years) shows that the release of actinides is significantly lower for the actinide recycle wasteforms The maximum

possible cumulative release of total actinides from the co-located actinide recycle, ER wasteforms are lower than that from the SF MMB container by over two orders of magnitude at 50000 and 100000 years (LWR - $8x10^3$ Ci vs. Actinide Recycle - $5x10^1$ Ci at 50000 years, LWR - $1x10^4$ Ci vs. Actinide Recycle $6x10^1$ Ci at 100000 years). Figure 5.24 provides the comparison at 50000 years.

A greater reduction in the actinide release is observed at 50000 and 100000 years after emplacement when the actinide recycle wasteforms are buried alone. The maximum possible releases are: LWR - $8x10^3$ Ci vs. Actinide Recycle - $1x10^1$ Ci at 50000 years, LWR - $1x10^4$ Ci vs. $2x10^1$ Ci at 100000 years).

At 10000 years after emplacement, no actinide release is observed for SF while the co-located actinide recycle wasteforms show releases (ER - metallic $5x10^0$ Ci). Again, within this time period, the SF containers are still dry, and hence not failed, while a fraction of the ALMR containers has failed. If the actinide recycle wasteforms are emplaced alone, no release occurs at 10000 years.

It can be seen that the release of fission products is slightly lower for the co-located ALMR wasteforms (ER-metallic,^{99}Tc) relative to LWR SF (^{99}Tc) at 50000 and 100000 years. The maximum cumulative release of total fission products (^{99}Tc) from the actinide recycle, ER-metallic wasteform is lower than the SF MMB in all cases except at 10000 years when the waste is co-located with SF at an APD of 114.0 kw/acre (LWR - $9x10^3$ Ci vs. Actinide Recycle - $2x10^3$ Ci at 50000 years, LWR - $9x10^3$ Ci vs. $3x10^3$ Ci at 100000 years). Again, Figure 5.24 provides the comparison at 50000 years.

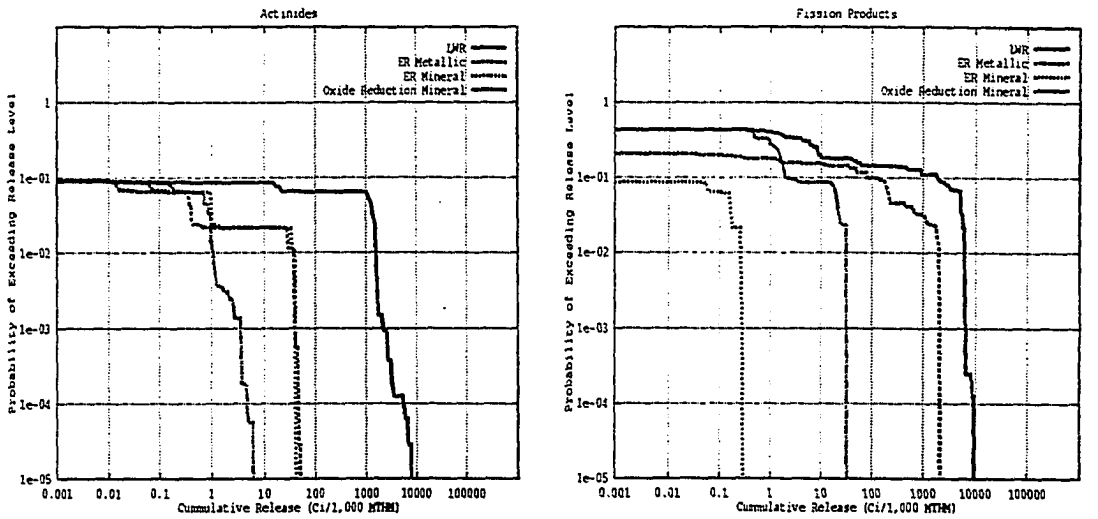

Figure 5.24: Comparison of the Release of Radionuclides From the LWR SF and Actinide Recycle Wasteforms, MMB Container, 114.0 kW/acre, 50000 Years.

The 10000 year results are again due to the dryout time experienced by the SF containers, which is discussed above.

Significant reductions in the total fission product cumulative release are observed when the actinide recycle waste is emplaced in the repository alone. No release of fission products occurs at 10000 years. The maximum possible releases are: LWR - $9x10^3$ Ci vs. Actinide Recycle - $5x10^2$ Ci at 50000 years, LWR - $9x10^3$ Ci vs. $1x10^3$ Ci at 100000 years.

Effect of Pyroprocess Actinide Decontamination Factor: Figure 5.25 shows the effects of the pyroprocess actinide decontamination factor on the cumulative total actinide release from the actinide recycle ER wasteforms at 50000 years. Increasing

the actinide decontamination factor by an order of magnitude results in a reduction in the cumulative total actinide release by approximately an order of magnitude. It can be seen that the smallest total actinide release occurs when a high pyroprocess actinide decontamination factor is utilized and the waste is emplaced in the repository alone. The release of fission products is not changed as the actinide decontamination factor does not impact the fission product inventory.

A summary of the comparisons between the ALMR/actinide recycle wasteforms and SF emplaced in MMB containers is provided in Table 5.4 for the actinides and in Table 5.5 for the fission products.

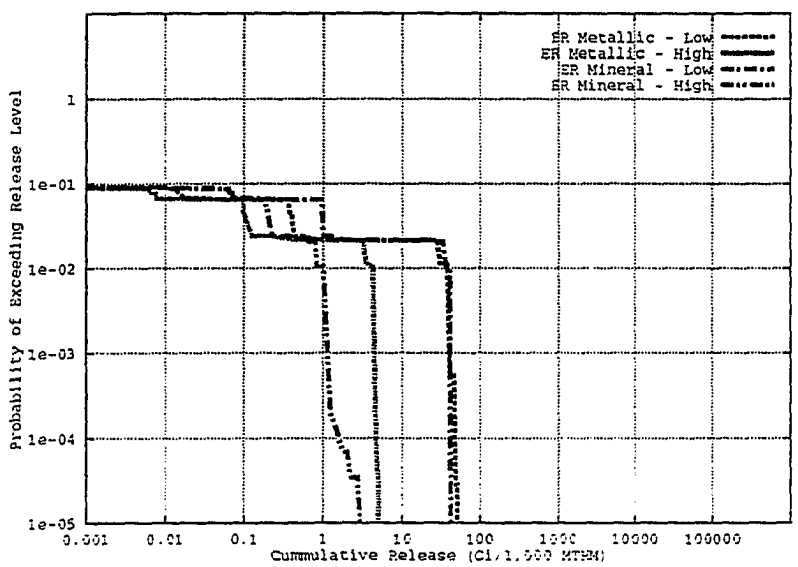

Figure 5.25 Effect of Actinide Decontamination Factor on the Release of Actinides From the Actinide Recycle, ER-Metallic Wasteform, 50,000 Years

Table 5.4 Maximum Cumulative Total Release of Actinides, from ALMR Wasteforms, (Ci/1000 MTHM equivalent)

Time After Emplacement (Years)	SF-MMB 114.0 kw/acre	ALMR Low/High Decontamination		Actinide Recycle Low/High Decontamination	
		Co-Located	Alone	Co-Located	Alone
10000	0	$3x10^{0}$ $2x10^{0}$	0 0	$5x10^{0}$ $5x10^{-1}$	0 0
50000	$8x10^{3}$	$6x10^{1}$ $1x10^{1}$	$1x10^{1}$ $3x10^{0}$	$5x10^{1}$ $5x10^{0}$	$1x10^{1}$ $1x10^{0}$
100000	$1x10^{4}$	$7x10^{1}$ $1x10^{1}$	$2x10^{1}$ $5x10^{0}$	$6x10^{1}$ $6x10^{0}$	$2x10^{1}$ $2x10^{0}$

Table 5.5 Maximum Cumulative Total Release of Fission Products from ALMR Wasteforms, (Ci/1000 MTHM equivalent)

Time After Emplacement (Years)	SF-MMB 114.0 kw/acre	ALMR		Actinide Recycle	
		Co-Located	Alone	Co-Located	Alone
10000	0	$7x10^{1}$	0	$4x10^{1}$	0
50000	$9x10^{3}$	$4x10^{3}$	$1x10^{3}$	$2x10^{3}$	$5x10^{2}$
100000	$9x10^{3}$	$5x10^{3}$	$2x10^{3}$	$3x10^{3}$	$1x10^{3}$

5.4.5 IMARC Results for Weapons Grade Plutonium Disposition Options

IMARC PAs have been completed for the wasteforms derived from the different options being considered for the disposition of weapons grade plutonium. The options evaluated are spiking (irradiating to low burnups) in both PWRs and ALMRs, irradiating to a burnup level commensurate with spent fuel in both PWRs and ALMRs, continued irradiation followed by recycling in an ALMR, and mixing with DHLW with vitrification

into borosilicate glass.

Details regarding the irradiation conditions and burnup levels are provided in Section 4.4.5 for the PWR and ALMR disposition options. The radionuclide inventories are provided in Table 4.11 for the PWR options, Table 4.12 for the ALMR options, and Table 4.8 for the DHLW option. The matrix alteration rates for each of the wasteforms are presented in section 5.3. In all cases, the MMB container design was utilized. All input files are provided in Appendix B.

The SF discharged from a PWR used to dispose of weapons grade plutonium was emplaced in the repository with commercial SF at an APD of 114.0 kW/acre. The spiked DHLW and the various ALMR plutonium disposition option wasteforms were assumed to be co-located with commercial SF at an APD of 114.0 kW/acre.

Figures 5.26 through 5.28 provide the CCDFs of cumulative total actinide release for each weapons grade plutonium disposition options at 10000, 50000, and 100000 years following emplacement. At 10000 years (Figure 5.26), the spiked DHLW gives the highest release (maximum possible of $1x10^{2}$ Ci). The ALMR spiking and spent fuel alternatives result in essentially identical releases that are slightly lower than that observed from DHLW (maximum of $6x10^{1}$ Ci). The ALMR recycling alternative with a low actinide decontamination factor ($1x10^{4}$) results in a significantly lower release (maximum of $2x10^{0}$ Ci). A high actinide decontamination factor ($5x10^{4}$) further reduces the release (maximum of $4x10^{-1}$ Ci). No release is observed from either LWR alternative as the containers have yet to fail.

At 50000 years, the DHLW option results in the largest releases. The DHLW option has the largest possible release ($2x10^{4}$ Ci), however, at lower release levels,

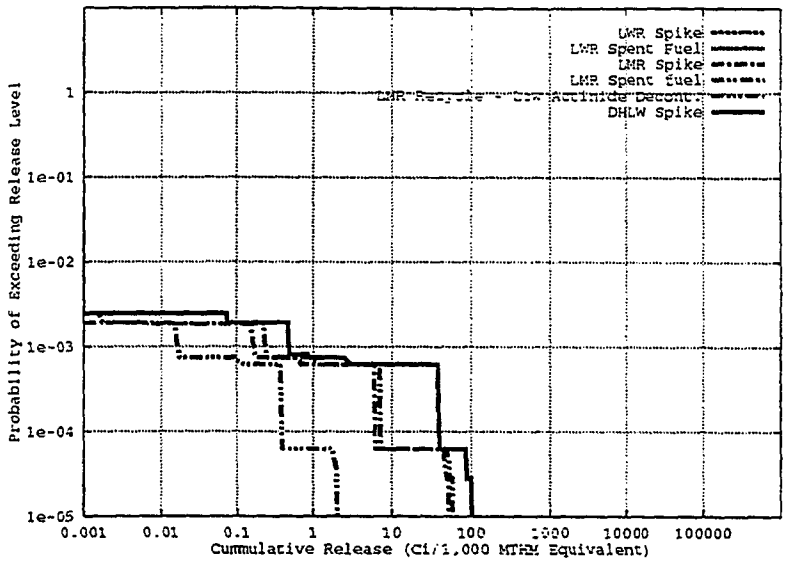

Figure 5.26 Total Actinide Release From Weapons Grade Plutonium Disposition Alternatives, MMB Container, ALMR Wastes Co-Located With SF, 10000 years

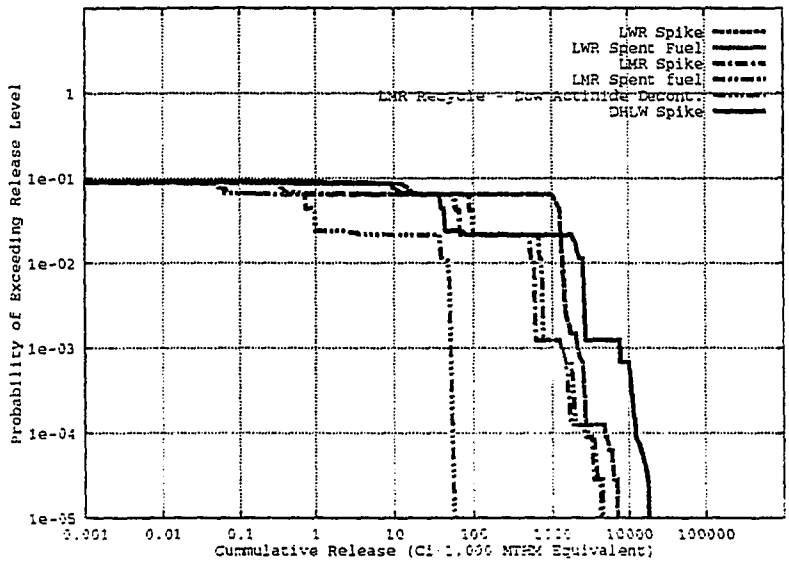

Figure 5.27 Total Actinide Release From Weapons Grade Plutonium Disposition Alternatives, MMB Container, ALMR Wastes Co-Located With SF, 50000 years

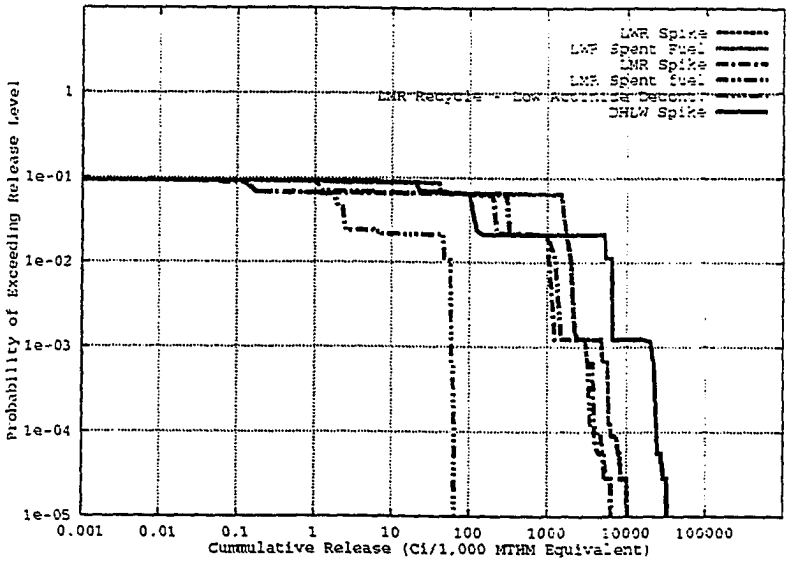

Figure 5.28 Total Actinide Release From Weapons Grade Plutonium Disposition Alternatives, MMB Container, ALMR Wastes Co-Located With SF, 100000 years

the probability of exceeding that release level is largest for the LWR options. The maximum release from the LWR options are $7x10^{3}$ Ci for both alternatives. Again, the ALMR spiking and spent fuel alternatives result in essentially identical releases (maximum of $5x10^{3}$ Ci) that are lower than those observed for the LWR options. The ALMR recycle alternative with a low actinide decontamination factor again results in a significantly lower release (maximum of $6x10^{1}$ Ci). The high actinide decontamination factor leads to a further reduction in the release (maximum of $1.00x10^{1}$ Ci).

The same trends are observed at 100000 years where the DHLW option results in the largest release while the ALMR recycle options results in the lowest releases. The maximum possible release from the DHLW is $3x10^{4}$ Ci, from the LWR spent fuel and spiking alternative is $1x10^{4}$ Ci, from the ALMR spiking and spent fuel alternatives

are $7x10^3$ Ci, from the ALMR recycle alternative with a low actinide decontamination factor is $7x10^1$ Ci, and with a high actinide decontamination factor is $1x10^1$ Ci.

A summary of the maximum total actinide release for each alternative is provided in Table 5.6.

5.4.6 IMARC Sensitivity Analysis, ALMR Electrorefiner Metallic Wasteform

Sensitivity analyses were conducted using IMARC for the ALMR ER metallic wasteform. The purpose of this analysis is to determine the factors that influence the release of radionuclides from this wasteform. This wasteform was chosen to be studied as it has actinide releases comparable to the mineral wasteform and results in the largest release of fission products, namely ^{99}Tc. The results obtained for the mineral wasteform will be similar. The scenario where the ALMR wastes are co-located with commercial LWR SF at an APD of 114.0 kW/acre was evaluated. The

Table 5.6: Maximum Cumulative Total Release of Actinides (Ci/1000 MTHM equivalent) from Weapons Grade Plutonium Disposition Alternatives

Alternative	10000 years	50000 years	100000 years
LWR Spike	0	$7x10^3$	$1x10^4$
LWR Spent Fuel	0	$7x10^3$	$1x10^4$
DHLW	$1x10^2$	$2x10^4$	$3x10^4$
ALMR Spike	$5x10^1$	$4x10^3$	$6x10^3$
ALMR Spent Fuel	$6x10^1$	$5x10^3$	$6x10^3$
ALMR Recycle Low / High Actinide Decont.	$2x10^0$ $4x10^{-1}$	$6x10^1$ $1x10^1$	$7x10^1$ $1x10^1$

radionuclide inventory resulting from the low actinide decontamination factor was utilized. It has been shown that a high actinide decontamination factor results in significantly lower releases. The MMB container design was utilized. All input files are in Appendix B.

The sensitivity analysis included the evaluation of various engineered barrier system parameters: container failure, wasteform alteration rate, water contact mode, backfill diffusion coefficient, backfill porosity, hydraulic saturation, backfill retardation, wasteform radius, wasteform free internal volume, and effective catchment area. In addition, a sensitivity analysis of fracture/matrix coupling was performed. Although fracture/matrix coupling is not important when considering the performance of the engineered barrier system, the release to the accessible environment depends strongly on the mode of fracture/matrix coupling. CCDFs of total cumulative actinide release 50000 years after emplacement are provided for each parameter investigated.

The sensitivity analysis of container failure was completed by doubling and halving the mean time to failure. Any changes in the threshold time to failure will only shift the release in time by a period equivalent to that change. The results are shown in Figure 5.29. It can be seen that changes in the maximum possible release is proportional to changes in the mean time to failure of the container. The longer mean time to failure results in lower maximum possible cumulative releases at 50000 years. The release is essentially pushed outward in time. It can be seen that at 50000 years after emplacement the release of radionuclides is not significantly dependent on the container failure parameters (50% uncertainty). A larger uncertainty in the container failure parameters will lead to a larger uncertainty in the release. At shorter time

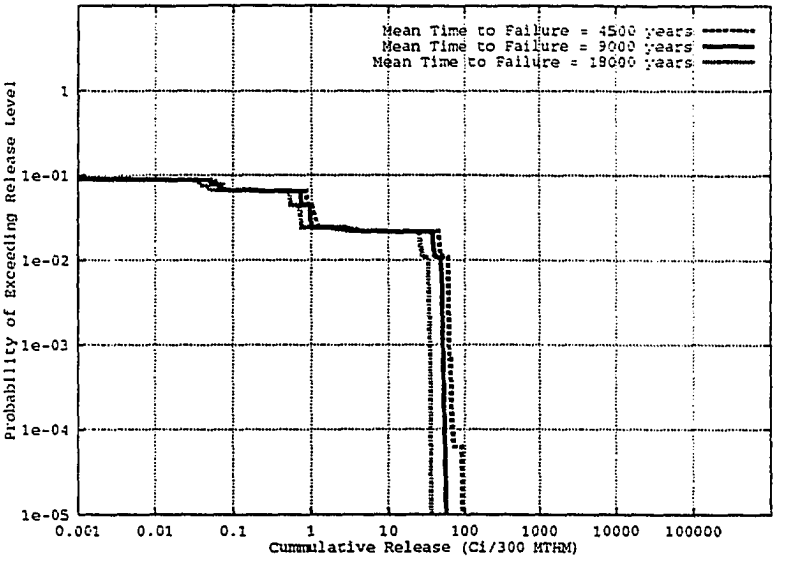

Figure 5.29 Sensitivity Analysis - Container Failure, MMB Container, ALMR ER Metallic Wasteform, Co-Located, 114.0 kW/acre, 50000 years

periods, the release becomes more dependent upon the uncertainty in the container failure parameters.

The sensitivity analysis of water contact mode was accomplished by executing IMARC with only one water contact mode active. The results are provided in Figure 5.30. It can be seen that the maximum possible release is fairly independent of the water contact mode. However, at lower release levels, the wet drip mode dominates. When both water contact modes are operating with the same occurrence probability, the wet drip mode dominates. Based on these results, it appears that water contact is

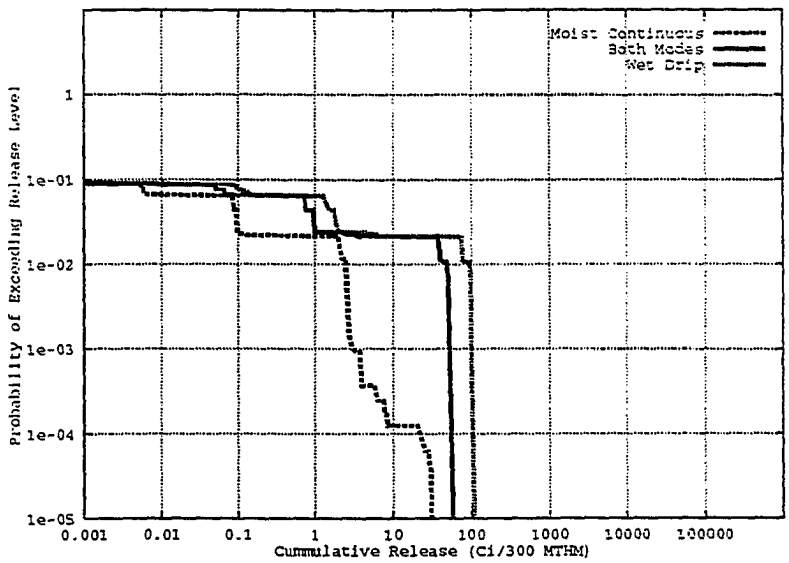

Figure 5.30 Sensitivity Analysis - Water Contact, MMB Container, ALMR ER Metallic Wasteform, Co-Located, 114.0 kW/acre, 50000 years

an important parameter in the determination of overall repository, and wasteform, performance.

The sensitivity analysis of matrix alteration rate was accomplished by executing IMARC with only one reaction rate (low, nominal, and high) active. The results are provided in Figure 5.31. It can be seen that the release of radionuclides is highlydependent on the alteration rate. Little difference in the maximum possible release is observed between the nominal and high alteration rates, indicating that the source term release is limited by the solubility of the radionuclides. The maximum possible release is reduced by an order of magnitude for the low relative to the nominal alteration rate. This indicates that the source term release is limited by matrix alteration. There are significant differences in the probability levels associated with the

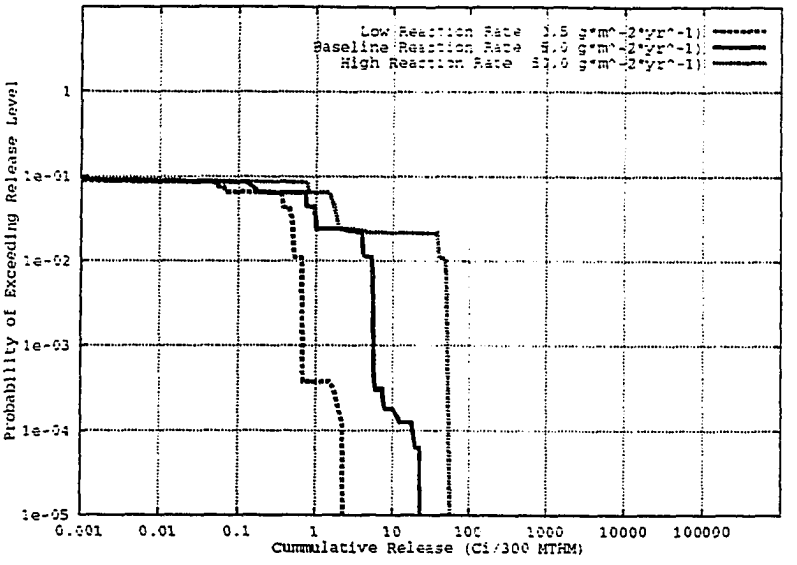

Figure 5.31 Sensitivity Analysis - Matrix Alteration Rate, MMB Container, ALMR Metallic Wasteform, Co-Located, 114.0 kW/acre, 50000 years

lower cumulative release levels with the high matrix alteration rate dominating. When all three alteration rates are included in an IMARC analysis, the release of radionuclides is dominated by the high alteration rate branches of the logic tree.

The sensitivity analyses for the backfill diffusion coefficient, backfill porosity, and hydraulic saturation were accomplished by executing IMARC with each of these parameters varied 50% about their nominal values. The nominal values are [87]: unsaturated diffusion coefficient = 1.0×10^{-7} cm^2/s, saturated diffusion coefficient = 7.0×10^{-6} cm^2/s, unsaturated porosity = 0.045, saturated porosity = 0.45, unsaturated degree of hydraulic saturation = 0.1. It should be noted that these parameters are coupled; for example, a change in the hydraulic saturation results in changes in the diffusion coefficient. In these analyses, however, each parameter is varied individually.

These parameters are used only in the calculation of the source term from the moist continuous water contact mode.

The dependencies of the total actinide release on the diffusion coefficient, porosity, and saturation, are provided in Figures 5.32 through 5.34. It can be seen that the shape of the CCDF at lower release levels is slightly dependent on these parameters. Changes in the diffusion coefficient, backfill porosity, and hydraulic saturation do not affect maximum possible cumulative release. It is concluded that the uncertainty in these parameters (within 50%) does not affect the overall repository, and wasteform, performance uncertainty.

The backfill retardation coefficient utilized by IMARC is used only in the source term calculation of insoluble radionuclides in a moist-continuous water contact mode

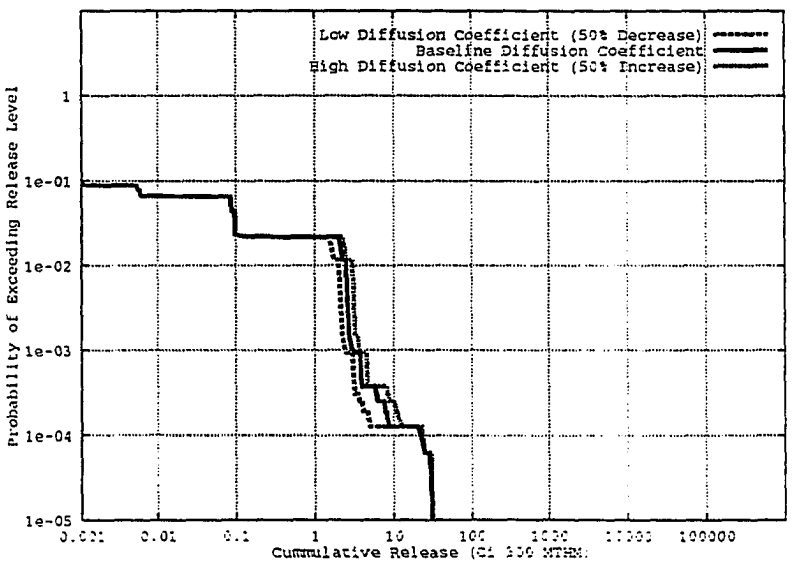

Figure 5.32 Sensitivity Analysis - Diffusion Coefficient, MMB Container, ALMR ER Metallic Wasteform, Co-Located, 114.0 kW/acre, 50000 years

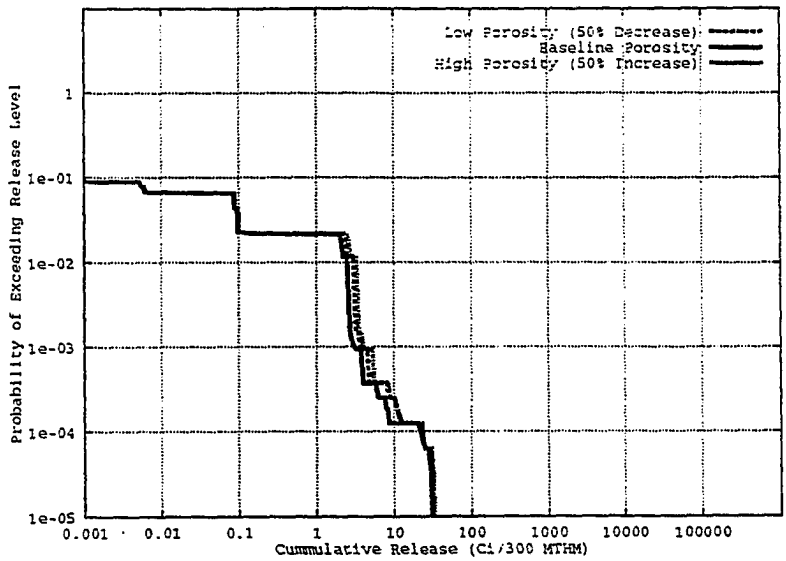

Figure 5.33 Sensitivity Analysis - Porosity, MMB Container, ALMR ER Metallic Wasteform, Co-Located, 114.0 kW/acre, 50000 years

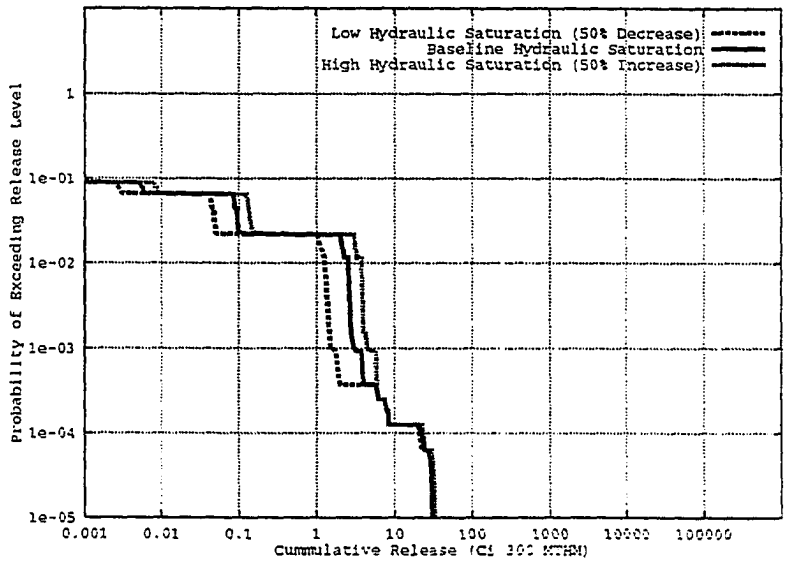

Figure 5.34 Sensitivity Analysis - Saturation, MMB Container, ALMR ER Metallic Wasteform, Co-Located, 114.0 kW/acre, 50000 years

(equation 4.11). The backfill retardation coefficient is given by equation 5.6 [13].

$$R = 1 + \rho K_d \left(\frac{1-\epsilon}{\epsilon \psi}\right) \qquad 5.6$$

The IMARC analyses previously conducted assume ρk_d is zero for the backfill, or R equal to 1, (no retardation), in source term calculations. Sensitivity analyses were conducted that varied the backfill retardation from one to 10000. The results indicated that the cumulative total actinide release is not dependent on the backfill retardation factor. A further study was conducted to determine the dependence of the ^{237}Np source term on backfill retardation. This study utilized equation 4.8 and varied ρk_d over several orders of magnitude. Unsaturated parameters were utilized. The results are shown in Figure 5.35. The source term is not reduced until ρk_d exceeds 10^4 (R exceeding approximately 10^6), where it then begins to decrease rapidly with increasing ρk_d. Retardation is notexpected to impact the release of radionuclides unless a backfill with high retardation properties is utilized.

A sensitivity study was also conducted on parameters used in the wet-drip water contact mode source term calculation. The parameters analyzed for the MMB container design were the waste package radius (0.895 meters), the waste package internal free volume (2.142 m^3), and the effective catchment area (8.5 m^2). The waste package radius was varied by five centimeters about its nominal value and the internal free volume was increased and decreased by a factor of two. Changes in only the effective catchment area were found to impact (minor) the release of radionuclides. Figure 5.36 shows the dependence of the release on the effective catchment area.

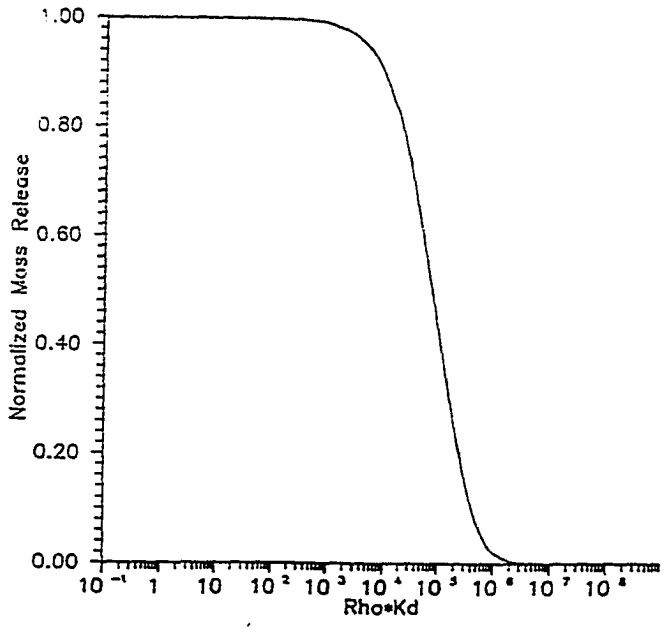

Figure 5.35 Sensitivity Analysis - Retardation ^{237}Np, MMB Container, ALMR ER Metallic Wasteform, Co-Located, 114.0 kW/acre, 50000 years

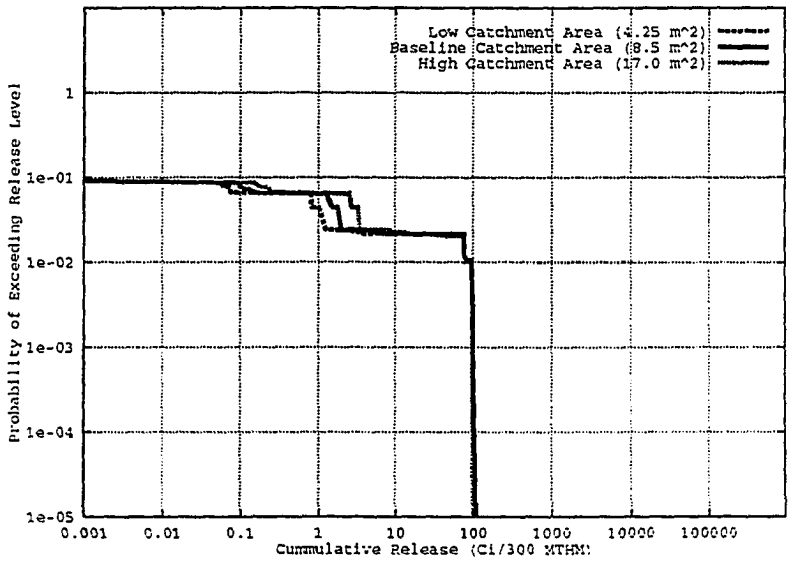

Figure 5.36 Sensitivity Analysis - Effective Catchment Area, MMB Container,ALMR ER Metallic Wasteform, Co-Located, 114.0 kW/acre, 50000 years

The dependence of the mode of fracture/matrix coupling on the total actinide release is shown in Figure 5.37. It can be seen that weak fracture/matrix coupling results in the largest total actinide release. The maximum possible releases are essentially identical, however the probability of obtaining that release level is three orders of magnitude lower when the fracture/matrix coupling is strong. For strong fracture/matrix coupling, mass transport occurs primarily through the rock matrix. Actinides with high retardation properties (namely plutonium) are strongly sorbed. Only instances of large fluctuations in the water table result in large releases. The probability of large water table fluctuations due only to climactic change is assumed to be very small in the IMARC PA analyses. For weak fracture/matrix coupling, a fast transport pathway exists where mass in the fractures essentially "outruns" the mass in the matrix with no retardation. This leads to large releases of actinides at all probability levels. It can be concluded that for strongly sorbing radionuclides the mode of fracture/matrix coupling is an extremely important process when attempting to predict the long term release characteristics of the repository.

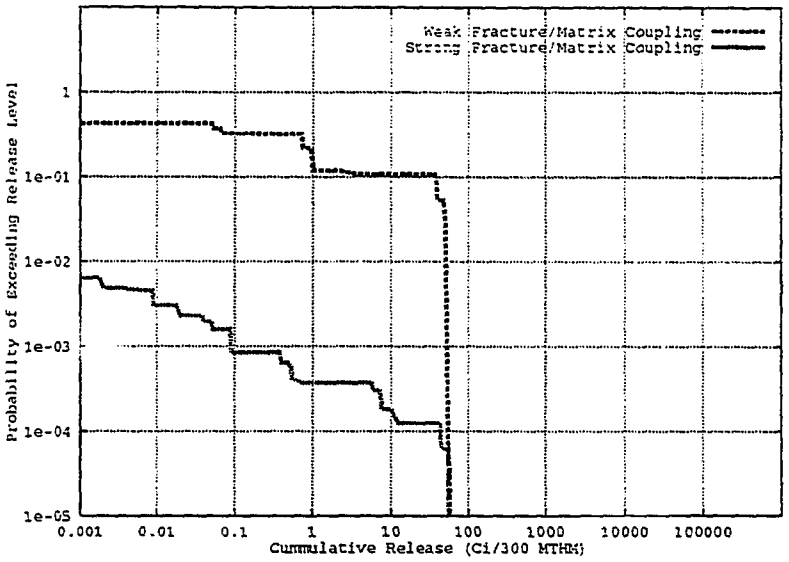

Figure 5.37 Sensitivity Analysis - Fracture/Matrix Coupling , MMB Container, ALMR ER Metallic Wasteform, Co-Located, 114.0 kW/acre, 50000 years

6 RIP PERFORMANCE ASSESSMENT ANALYSES

6.1 Introduction

This chapter presents the results obtained for PA investigations of the spent fuel, DHLW (weapons grade Pu) baseline ALMR, and actinide recycle wasteforms. Section 6.2 provides a summary of the theory behind the RIP PA tool. Section 6.3 presents details of the RIP model developed for this study. Section 6.4 provides the results obtained from the PA analyses.

6.2 Summary Description of the RIP Theory

This section describes the RIP (Repository Integration Program) PA tool [15,16]. RIP was developed by Golder Associates of Redmond Wa. RIP is similar to IMARC in that it is a probability-based PA tool that investigates the possible release of radionuclides to the accessible environment. That is the only similarity between the two tools.

IMARC was developed solely for Yucca Mountain. Each portion of the IMARC package (transport, source term, and integration) have Yucca Mountain specific scenarios, models, and parameters hardcoded within them. In short, IMARC was developed based on existing Yucca Mountain specific information. Significant modifications would be required to apply IMARC to any other potential repository site.

RIP was designed to be flexible and not limited to one specific site. RIP utilizes a "top down" approach to PA. A "bottom up" approach attempts to model the various processes in detail using complex models. Due to the complexity of repository systems, proper implementation, integration, and incorporation of uncertainty could be quite difficult.

A "top down" approach concentrates on the integration of all system components. Less detailed process models are utilized in "top-down" approaches. However, both model and parameter uncertainty must be included to account for the lack of detail in the simplified models.. The detail of the models can be increased when either more data becomes available or it is deemed that overall repository performance is sensitive to a certain process. Although detailed modeling is not directly implemented into RIP, it is still required in order to generate the input parameters for a top-level approach. These top-level parameters are generally analytical expressions, response surfaces, or statistical distributions based on detailed process modeling or experimental data.

RIP consists of four primary component models: waste package behavior and radionuclide release; fluid flow and radionuclide transport in the geosphere; disruptive events; and radionuclide fate and effect in the biosphere. Only the first two are utilized in this study (since only release to the accessible environment is being considered) and will be summarized. Detailed descriptions of the RIP models are provided in Reference 15 while the proper use of the tool is detailed in Reference 16.

Prior to describing the RIP models, it is first necessary to discuss the treatment and propagation of uncertainty. RIP uses a simulation approach utilizing the Monte

Carlo method to sample the probability distributions of uncertain parameters. RIP simulates a large number of system realizations to determine probability distributions of repository performance. In short, RIP samples all system parameters that are stochastically represented and performs calculations based on the realized values of each parameter (and other functions using those parameters). Figure 6.1 shows this approach. Enhanced sampling schemes using Importance Sampling and/or Latin Hypercube Sampling can be employed to resolve low probability, high consequence areas of the parameter distributions.

The waste package behavior and radionuclide release model simulates groups of waste packages, rather than individual packages. These groups are determined based on several factors, including: waste type, container design, and near field environment. The model parameters can be described as functions of environmental

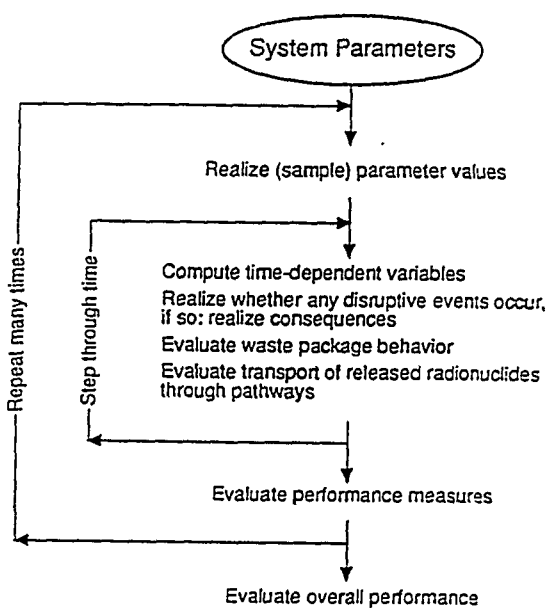

Figure 6.1 RIP Simulation Logic [15]

conditions, such as the near field temperature, the water contact mode, and ground water chemistry. Radioactive decay and daughter product build-up can be explicitly modeled. The sub-models are container failure, mass exposure, and mass transport.

Two levels of containment can be simulated with waste package failure described in terms of probability density functions of barrier failure frequency (Weibull, exponential, uniform). Waste package failure can be modeled by one or more independent failure modes that can again be functions of environmental conditions.

Mass exposure arises from container failure (Chapter 3) and wasteform matrix alteration/dissolution (Chapter 4). The radionuclide inventory can be assigned to be free inventory (immediately released upon primary container failure), gap inventory (immediately released upon secondary container failure, i.e. SF clad failure), and bound inventory (release controlled by matrix alteration/dissolution). Details regarding matrix alteration/dissolution are provided in Section 4.3.

Mass transfer of an aqueous radionuclide can be described by diffusive or advective processes. Several mass transfer processes can be defined that are dependent on the container failure modes. Details of the mass transfer models are also presented in Section 4.3.

The waste package model is coupled to the transport model such that the user defines the discharge pathways for each waste package group.

The near and far field transport model is based on a network of user defined pathways. These pathways are used to describe the major features of the system. The pathways represent homogeneous regions of a large heterogeneous system. For example, in a simple case, each rock formation between the repository and the water

table can be represented by a pathway. For a complex system (such as Yucca Mountain), the modeling of several pathways may be required to accurately represent the groundwater flow system.

To capture local heterogeneities, such as matrix and fracture flow, a pathway can consist of several flow modes. These flow modes are distinguished by their ground water velocities, sorptive properties, and fraction of mass in each.

The transport of radionuclides along a geosphere pathway is based on a break-through curve, or a cumulative probability distribution of radionuclide travel times. For a multiple flow mode pathway, the break-through curve combines all flow modes and is based on a Markov process algorithm, similar to a random walk process. If only one flow mode is used, the one-dimensional advection/dispersion equation is used to calculate the break-through curve.

For a multiple flow mode pathway, the random length traveled by a particle in a given pathway is based on the inverse of the exponential probability distribution and is given by equation 6.1.

$$l_i = -\frac{1}{\lambda_i} \ln[r(0,1)] \qquad (6.1)$$

Where: l_i = random length interval

λ_i = Poisson transition rate for flow mode i

r(0,1)= a random number between 0 and 1

In RIP, an approximation to the Markov algorithm is used. Particles are assumed to travel only their first random length in an individual flow mode. Anyremaining pathway length is traveled at the expected velocity over all flow modes. The travel time through a pathway is given as equation 6.2.

$$t_n = \left[\frac{l_i R_{ni}}{V_i} + (L_p - l_i) \sum_{j=1}^{N} \frac{f_{qj}}{V_j} R_{nj} \right] \quad (6.2)$$

Where:
- V_i = average linear fluid velocity for flow mode i
- R_{ni} = retardation factor for nuclide n in flow mode i
- N = number of flow modes
- f_{Qj} = proportion of total fluid flow in flow mode j
- V_i = average linear fluid velocity for flow mode j
- R_{nj} = retardation factor for nuclide n in flow mode j

By repeating this simulation a large number of times, the probability distribution for travel time in a given pathway can be numerically approximated.

6.3 RIP Model Development

As was discussed above, RIP is essentially a tool that is used to integrate the entire series of repository parameters using a "top-down" approach. The key factor in performing a PA analysis of a repository system is the development of the RIP model. This differs from IMARC where the Yucca Mountain model for LWR SF is essentially hardcoded into the tool. To model other wasteforms, it was necessary to change IMARC itself. This is not necessary with RIP as models can be developed to simulate each wasteform being considered. This section describes the RIP models that were developed for this study. It should be noted that each wasteform model is essentially identical. The only differences are in the areas of container design, wasteform characteristics and near field response.

The RIP model developed in this study was based on the model developed by Intera for use in their 1993 Total System Performance Assessment [14]. Several

modifications using information from the EPRI and SNL PA analyses [13,18] have been implemented and will be discussed.

Intera divided the repository drifts into seven rings for the performance of hydrothermal calculations. The inner six rings were assumed to contain LWR SF while the outer ring was assumed to hold DHLW. A six ring discretization has been maintained as the definition of LWR SF waste package groups. Only one waste package group was assumed for DHLW (ring 7), co-located ALMR wasteforms (assumed to be ring 7), and ALMR wasteforms emplaced alone.

The waste container failure parameters utilized are identical to those used in the IMARC PAs and are provided in Chapter 3 (Section 3.7). It should be noted that these failure parameters were calculated utilizing the near field temperature histories calculated by Intera for each of the six rings. Since the container failure parameters utilized were calculated from the multi-barrier failure model, only the primary barrier in the RIP model is ascribed containment capability. The secondary barrier is assumed to fail instantaneously.

The matrix alteration rate utilized for LWR SF is given by equation 4.1. This differs from that used by IMARC as a temperature dependence is assigned to the matrix alteration rate. Recall IMARC utilized three distinct matrix alteration rates representing low, medium and high alterating conditions. The matrix alteration rate for DHLW utilized is given by equation 4.9 and again has a temperature dependency. Again, recall that IMARC utilized three distinct alteration rates that were calculated from equation 4.9.

The matrix alteration rate for the ALMR metallic and mineral wasteforms utilized

in IMARC were used in a slightly different manner in the RIP analyses. Rather than utilizing discrete rates, as is done in IMARC, probability density distributions can be approximated with RIP using discrete points. The cumulative probability distribution was utilized where the low and high values were assigned 25% occurrence probabilities and the best estimate value was given a 50% occurrence value. It should be noted that RIP develops a probability distribution from these discrete points and samples from it. This differs from IMARC where only the discrete points are utilized in subsequent calculations. The actual values for the matrix alteration rates for each wasteform are provided in Section 5.3.

Parameters needed to convert matrix alteration to fractional alteration (as is needed by RIP) are provided in Table 4.1 for LWR SF and Table 4.2 for DHLW and the ALMR wasteforms. For DHLW, the cracking factor is assumed to be uniformly distributed between 10 and 30. No cracking factor is used for the ALMR wasteforms.

All inventory was designated as bound inventory. This differs slightly from the IMARC analyses where a fraction of some highly soluble radionuclided were assigned to the gap inventory. This is not expected to impact the results significantly as this assumption only impacts the timing of the release from the waste package. Over the time scales being considered significant releases occur from the waste package regardless of whether the inventory is bound or in the gap. The inventory for each wasteform is provided in Chapter 4.

Two water contact modes were also assumed in the RIP PA analyses. For the wet drip water contact mode, mass transfer was assumed to be only an advective process (equation 4.4). The effective catchment area for the SCP container was

assumed to be a circle with a radius uniformly distributed between 0.5 m and 1.5 m. For the MMB container, the effective catchment area is assumed to be uniformly distributed between 8.5 and 45 m^2, consistent with the Intera PA [14]. The volume of water contacting the matrix is the internal free volume given in Table 4.1 for LWR SF and Table 4.2 for the DHLW and ALMR wasteforms.

For the moist continuous water contact mode, mass transfer was assumed to be only a diffusive process (equation 4.4). The effective diffusion coefficient is given by equation 4.5. The geometric factor for diffusion is given by equation 4.6 with the equivalent spherical radius determined form the volume of each container. The volume of water contacting the matrix is the product of the water film thickness, 0.001 m [14], and the wasteform surface area. The surface areas are provided in Table 4.1 for LWR SF and Table 4.2 for the DHLW and ALMR wasteforms (including the cracking factor for DHLW).

Elemental solubility values are identical to those utilized by Intera [14] and are given in Tables 6.1 and 6.2. These elemental solubilities differ from those used by IMARC in that they are described by probability density functions rather than discrete points with assigned probability. In addition, the solubility of several elements is assigned temperature and pH dependence.

The pathway network utilized is identical to that used by Intera [14] and is similar to that used by SNL [18]. A nine column, six layer unsaturated zone pathway model was utilized. No cross-flow between columns was allowed. The unsaturated zone pathways release to a single five kilometer long saturated zone pathway. The release of radionuclides from each waste package group enters the top of the

Table 6.1: Elemental Solubilities [from 14 unless noted]

Element	Solubility Distribution Function (g/m^3)	Element	Solubility Distribution Function (g/m^3)
Am	See Table 6.2a	Se	LT 7.9e+2, 7.9e+3, 5.5E+5
Cm	T ≤ 55°C LT 1.2e-6, 1.2e-5, 1.2e-4 T > 55°C LT 1.5e-10, 1.5e-9, 1.5e-8	Pd	LB 5.9e-2, 5.9e-3, 105, 0.25 (Ni -- same periodicity)
Cs	LT 1.2e+0, 3.9e+2, 2.1e+3	Sn	U 1.3e-6, 1.3E-2
I	LT 0.025, 100, 9.9e+5 [13]	Tc	LT 3.5e-2, 1.0e+2, 9.9e+5
Np	See Table 6.2b	U	Same as Np
Ra	LB 2.3e-4, 2.3, 2.3e-2, 0.1	Zr	LU 9.18e-8, 9.1e-3
Pu	See Table 6.2c		

LT = log-triangular distribution: minimum, expected value, maximum
LB = log-beta distribution: minimum, maximum, expected value, coefficient of variation
U = uniform distribution: minimum, maximum
LU = log-uniform distribution: minimum, maximum

Table 6.2: Temperature and pH Dependent Solubility for Am, Np, and Pu (Normal distribution: mean, standard deviation g/m^3) [14]

a) Am

pH	T ≤ 42.5 °C	42.5 °C < T ≤ 75 °C	75 °C < T
pH ≤ 6.5	4.4e-4, 1.5e-4	6.1e-1, 1.7e-1	4.1e-4, 4.1e-4.
6.5 < pH ≤ 7.75	2.9e-4, 0.7e-4	2.4e-3, 2.2e-3	7.5e-5, 4.1e-5
7.75 < pH	5.8e-4, 4.6e-4	2.9e-3, 2.9e-3	8.3e-5, 5.1e-5

b) Np

pH	T ≤ 42.5 °C	42.5 °C < T ≤ 75 °C	75 °C < T
pH ≤ 6.5	1.3e+3, 0.07e+3	1.5e+3, 0.09e+3	2.8e+2, 0.2e+2
6.5 < pH ≤ 7.75	3.1e+1, 0.5e+1	2.3e+2, 0.2e+2	3.6e+1, 0.9e+1
7.75 < pH	1.0e+1, 0.2e+1	2.4e+1, 0.2e+1	2.1e+1, 0.09e+1

c) Pu

pH	T ≤ 42.5 °C	42.5 °C < T ≤ 75 °C	75 °C < T
pH ≤ 6.5	2.6e-1, 1.0e-1	6.5e-3, 2.6e-3	1.5e-3, 0.5e-3
6.5 < pH ≤ 7.75	5.5e-2, 3.4e-2	8.9e-3, 2.2e-3	2.1e-3, 0.2e-3
7.75 < pH	7.0e-2, 1.9e-2	2.9e-2, 0.2e-2	1.8e-3, 0.1e-3

unsaturated zone pathway model with mass distributed equally among the nine columns. Figure 6.2 shows a schematic of the pathway network. Figure 6.3 shows the location of each column within the repository. The thickness of each pathway is given in Table 6.3. The area of each column was calculated from Figure 6.3. Release to the accessible environment occurs at the end of the saturated zone pathway.

Intera chose to model aqueous transport using the one-dimensional advection/dispersion option within RIP [14]. This was maintained in this study. The effective ground water velocity for each pathway layer is given by equation 6.3.

$$V_j = \frac{u_j}{n_j S_j} \tag{6.3}$$

Where: V_j = effective ground water velocity for pathway j

u_j = percolation flux for pathway j

S_j = liquid saturation for pathway j

The unsaturated zone porosity distributions and liquid saturation for each layer are provided in Table 6.4. The porosity of the saturated zone was assumed to be 2% [14].

Table 6.5 provides the percolation flux for the unsaturated and saturated zones that were utilized by Intera [14]. To account for climactic change, Intera applied an unsaturated percolation flux multiplier that was distributed with a mean of 2.5, a minimum of 1.0 and a maximum of 5.0. This was based on a study that claimed the infiltration rate would increase by a factor of 2.5 under pluvial conditions. Intera assumed that the transition from present to pluvial conditions would occur linearly over 100,000 years. During the next 100,000 years, it was assumed that the percolation flux would return linearly to present day conditions. This 200,000 year cycle was

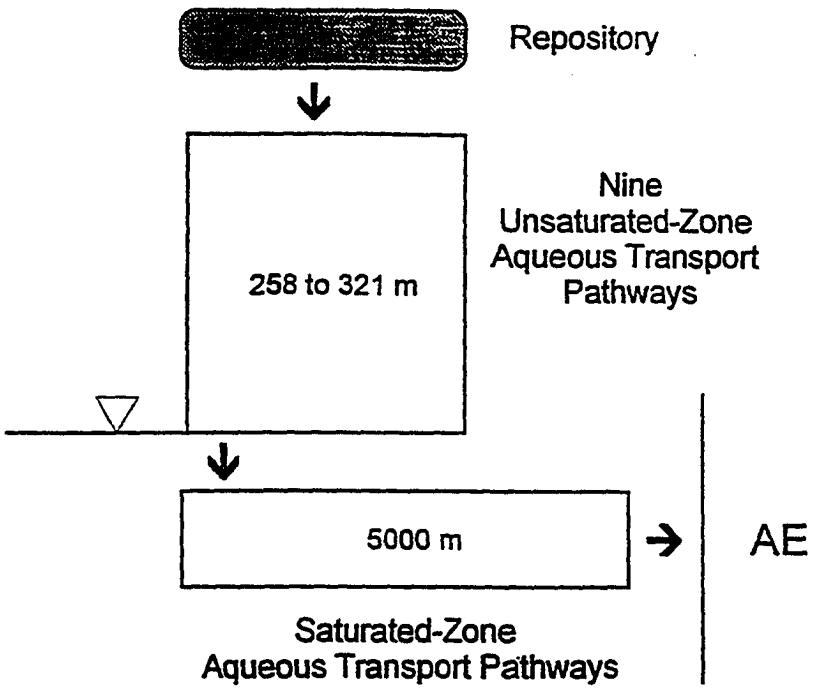

Figure 6.2 Aqueous Transport Pathway Schematic [14]

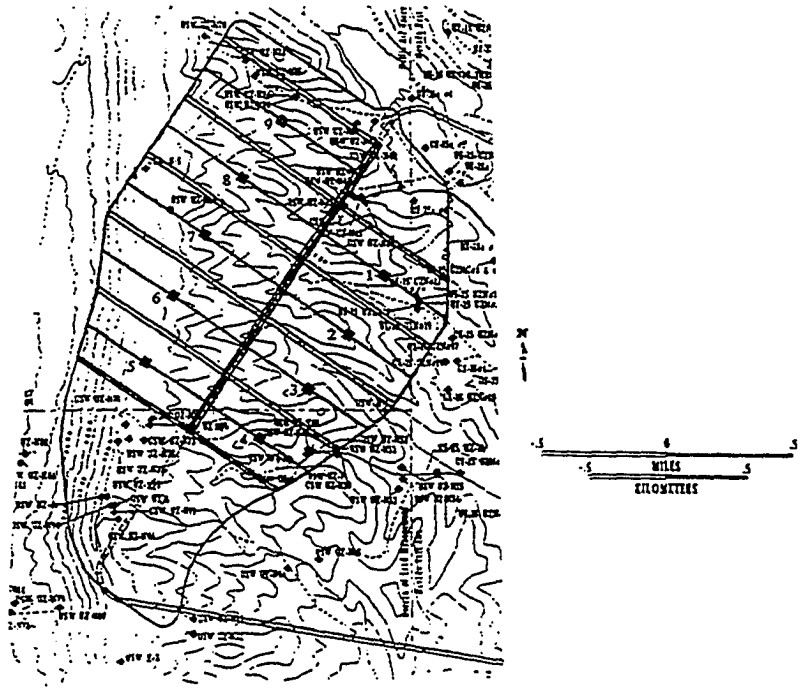

Figure 6.3 Conceptualization of Nine Column Unsaturated Zone Pathways [14]

Table 6.3: Thickness of Each Layer in Nine Unsaturated Zone Columns (m) [14]

Layer #	Layer	Col. 1	Col. 2	Col. 3	Col. 4	Col. 5	Col. 6	Col. 7	Col. 8	Col. 9
1	TSw2	131	143	109	75	45	68	100	89	78
2	TSw3	10	10	10	10	10	10	10	10	10
3	Chn1v	34	32	35	40	38	32	30	31	33
4	CHn1z	29	77	74	62	62	75	78	69	60
5	PPw	28	25	73	130	130	119	71	74	77
6	Bw	0	0	0	3	36	0	0	0	0

Table 6.4 Bulk Porosity Distributions (Beta) and Liquid Saturation [14]

Layer	Beta Bulk Porosity Distribution				Liquid Saturation
	Expected	Standard Deviation	Minimum	Maximum	
TSw2	0.11	0.022	0.044	0.197	0.681
TSw3	0.09	0.018	0.037	0.161	0.763
CHn1v	0.21	0.042	0.0	1.0	0.080
CHn1z	0.41	0.082	0.0	1.0	0.922
PPw	0.24	0.048	0.0	1.0	0.988
Bw	0.24	0.048	0.0	1.0	0.988

Table 6.5: Intera Unsaturated and Saturated Zone Aqueous Flux Distributions (m/yr) [14]

Zone	Distribution	Expected	Standard Deviation	Minimum	Maximum
Unsaturated	Beta	5.00e-4	4.8e-4	0.0e+0	1.25e-2
Saturated	Log-Normal	2.00e+0	3.16e+0		

assumed to continue indefinitely.

SNL used a different approach in calculating the unsaturated zone percolation flux [18]. It was assumed that the dry (present) and wet infiltration rates were exponentially distributed with means of 0.5 mm/yr and 10.0 mm/yr, respectively. The wet infiltration rate was based on an estimate of pluvial conditions causing a 40% increase in precipitation at Yucca Mountain. Next, SNL assumed there exists a 100,000 year period for climactic cycles, each cycle having a wet and dry period. It was assumed that the current dry period began 10,000 years ago. The start of the next wet period was assumed to begin at a time uniformly distributed between now and 90,000 years. At this point, the infiltration was assumed to change (step change) from dry to wet conditions.

SNL then calculates the unsaturated zone percolation flux based on the saturation conductivity of the Topopah Spring Welded matrix (TSw2). This is called the composite porosity model and is discussed in detail in Reference 18. The saturation conductivity, Ksm, was assumed to be distributed as shown in Figure 6.4. The percolation flux is then determined as described below.

If the infiltration < Ksm, percolation flux equals infiltration rate.
If the infiltration ≥ Ksm,
    percolation flux equals Ksm half the time
    percolation flux > Ksm distributed exponentially with Ksm as the e-folding length half the time.

In this study, the percolation flux is based on both the Intera and SNL models. The Intera approach is utilized to calculate the infiltration. The flux multiplier, however, is increased to a distribution with a mean of 20, a minimum of 1 and a maximum of 40.

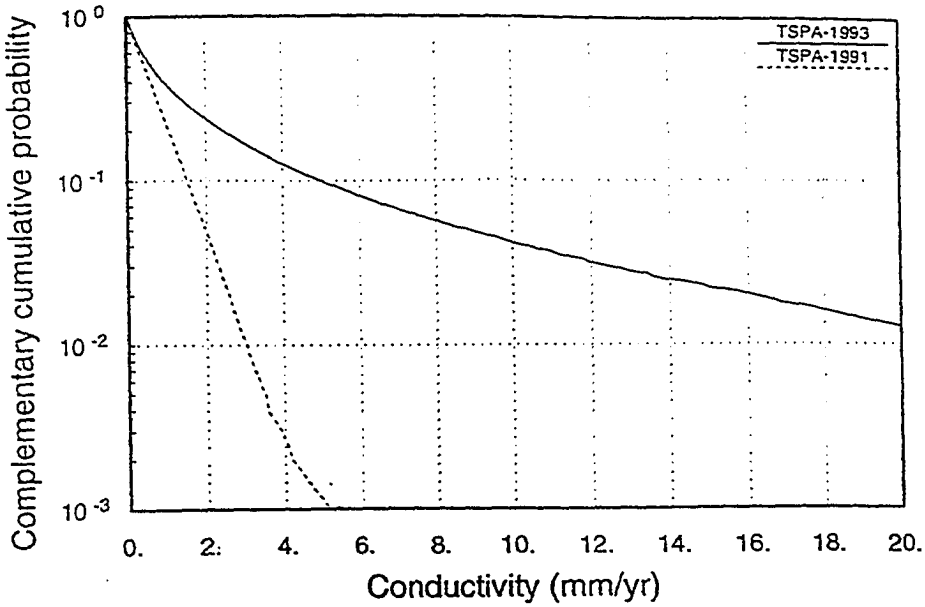

Figure 6.4 Probability Distribution of Saturation Conductivity for Topopah Spring Welded Matrix [18]

This gives the higher infiltration rates expected by SNL yet retains the linear change to the higher rates. The calculation of percolation flux is identical to the SNL composite porosity approach.

Both the Intera model and the SNL composite porosity approaches neglect fracture flow. This is believed to be a weakness in their modeling. As discussed in Chapter 5, the IMARC approach assumes that with weak fracture/matrix coupling mass within the fractures will outrun mass within the matrix. It was further assumed that retardation of aqueous radionuclides is negligible for fracture flow. The IMARC PA analyses assumed a 20% occurrence probability for weak fracture/matrix coupling.

Increases in the water table elevation due to climactic changes were modeled in a manner identical to that used in the IMARC analyses [13].

In this study, the one dimensional advection/dispersion approach utilized by Intera was maintained. No dispersion, however, was assumed to maintain consistency with the IMARC PA analyses. To simulate a fracture flow dominated scenario, the retardation of radionuclides is ignored within both the unsaturated and saturated zones. This scenario is assigned a 20% occurrence probability, consistent with IMARC. This is accomplished by sampling from a uniform distribution between 0 and 1 with realizations less than 0.2 being assigned to fracture flow. For the composite porosity approach (80% occurrence probability), matrix flow is assumed to dominate with retardation occurring. Retardation effectively slows the particle velocity according to equation 6.4.

$$V_e = \frac{V}{R_d} \tag{6.4}$$

Where: V_e = effective ground water velocity for a retarded radionuclide
V = ground water velocity
R_d = retardation coefficient

The retardation coefficient is given as equation 6.5.

$$R_{dnj} = 1 + \frac{\rho_j}{\epsilon_j} K_{dj} \tag{6.5}$$

Where: R_{dnj} = retardation coefficient for nuclide n in layer j
ρ_j = bulk density of layer j
ϵ_j = porosity of layer j
K_{dnj} = distribution coefficient for nuclide n in layer j

Table 6.6 provides bulk density distributions [14] and Table 6.7 provides the distribution coefficients utilized [14,18].

Table 6.6: Beta Bulk Density Distributions (g/mL)

Layer	Expected	Standard Deviation	Minimum	Maximum
TSw2	2.24	0.092	2.0	2.4
TSw3	2.15	0.191	1.7	2.5
CHn1v	1.68	0.220	1.3	2.1
CHn1z	1.68	0.220	1.3	2.1
PPw	2.00	0.181	1.7	2.4
Bw	2.00	0.181	1.7	2.4

6.4 Results of RIP PA Analyses

The model described above was implemented into RIP and is provided in Appendix C. The model differed slightly between each wasteform due to differences in each wasteform. Specific modeling details for each wasteform are discussed in the subsequent sections. The RIP User's Guide [16] provides detailed information regarding the proper development of a RIP model and execution of the RIP PA tool. A time step size of 1000 years was utilized and 100 realizations were sampled.

^{237}Np and ^{234}U daughter product build-up is not considered in order to reduce the computing time required; the simple empirical model described in Chapter 4 was not readily implemented into RIP. The IMARC results demonstrated that the actinide releases are dominated by ^{239}Pu, ^{240}Pu, and ^{237}Np. Of these radionuclides, only ^{237}Np experiences significant daughter product build-up. Since only a comparison of wasteform performance is being made, and the build-up of daughter product activity is directly proportional to the initial ^{237}Np inventory, the results of the comparison will not be impacted by neglecting to model ^{237}Np and ^{234}U daughter product build-up. The

Table 6.7: Distribution Coefficient Distributions (mL/g) [14]

Element	Rock Type	Distribution	Expected	Standard Deviation	Minimum	Maximum
Am	D	Uniform			100.0	2000.0
	V	Beta	380.0	76.0	100.0	1000.0
	Z	Uniform			100.0	1000.0
Cs	D	Uniform			100.0	1000.0
	V	Uniform			100.0	200.0
	Z	Uniform			500.0	3000.0
Np	D	Gamma	2.0	2.0	0.0	50.0
	V	Beta	0.5	0.5	0.0	12.5
	Z	Beta	4.0	4.0	0.0	100.0
Pu	D	Beta	100.0	25.0	50.0	200.0
	V	Beta	100.0	25.0	50.0	200.0
	Z	Beta	40.0	0.15	30.0	70.0
Ra	D	Uniform			100.0	500.0
	V	Uniform			100.0	500.0
	Z	Uniform			1000.0	5000.0
U	D	Uniform			0.0	5.0
	V	Uniform			0.0	4.0
	Z	Uniform			5.0	20.0
I, Pd, Se,	All	0.0				

D -- Devitrified Tuff, TSw2, TSw3, PPw, Bw, Saturated Zone
V -- Vitrified Tuff, CHn1v
Z -- Zeolitic Tuff, CHn1z

actual total actinide release will be slightly larger primarily due to ^{237}Np daughter product buildup.

6.4.1 Installation and Benchmarking of the RIP Software

The RIP software (version 3.21) was installed on a DOS based personal computer. No test case was provided with the software. As such, it was not possible to benchmark the tool to determine if it was properly installed and executing correctly. The results presented in subsequent sections will be compared with the IMARC results in order to determine if the results being output are consistent with the system model.

6.4.2 RIP Results for Commercial Spent Fuel

RIP analyses have been completed for the LWR-SF wasteform emplaced in the SCP and MMB containers. The initial radionuclide inventory is provided in Table 4.7 and the container loading is provided in Table 5.2. The container performance parameters utilized are given in Table 3.7.

The complementary cumulative distribution functions (CCDF) of total actinide and total fission product cumulative Curie release per 1,000 MTHM for the SCP waste container is shown in Figures 6.5 and 6.7. Identical CCDFs for the MMB containers are provided in Figures 6.8 through 6.10. The CCDFs are presented at 10000, 50000, and 100000 years following emplacement for the three APDs considered (28.5, 57.0, 114.0 kw/acre).

Table 6.8 provides the maximum possible release from each container for the three APDs considered at 10000, 50000, and 100000 years following emplacement.

10000 years: Within this time period no actinides are released from the MMB container while a small release is observed from the SCP container (less than $1x10^{-3}$ Ci). The IMARC PA analyses demonstrated that a larger amount of actinides are released within the first 10000 years for all container design/APD cases except for the MMB container at 114.0 Kw/acre. These releases result from higher unsaturated zone percolation flux values. IMARC considers three unsaturated percolation flux values, 0.5 mm/yr, 1.5 mm/yr and 5.4 mm/yr. The 5.4 mm/yr percolation flux assumed in IMARC is over ten times greater than the RIP expected percolation flux within the first 10000 years. This leads to faster travel times from the repository to the accessible

Table 6.8: Maximum Possible Releases from LWR SF (Ci/1000 MTHM)

Time After Emplacement (years)	SCP		MMB	
	Actinides	Fission Products	Actinides	Fission Products
APD = 28.5 kW/acre				
10000	0	$1x10^{3}$	0	0.0
50000	$8x10^{3}$	$1x10^{4}$	$4x10^{4}$	$1x10^{4}$
100000	$3x10^{4}$	$1x10^{4}$	$7x10^{4}$	$1x10^{4}$
APD = 57.0 kW/acre				
10000	0	$2x10^{3}$	0.0	0
50000	$5x10^{3}$	$1x10^{4}$	$6x10^{3}$	$1x10^{4}$
100000	$2x10^{4}$	$1x10^{4}$	$1x10^{4}$	$1x10^{4}$
APD = 114.0 kW/acre				
10000	0	0.0	0.0	0.0
50000	$2x10^{3}$	$2x10^{4}$	$4x10^{3}$	$1x10^{4}$
100000	$8x10^{3}$	$2x10^{4}$	$8x10^{3}$	$1x10^{4}$

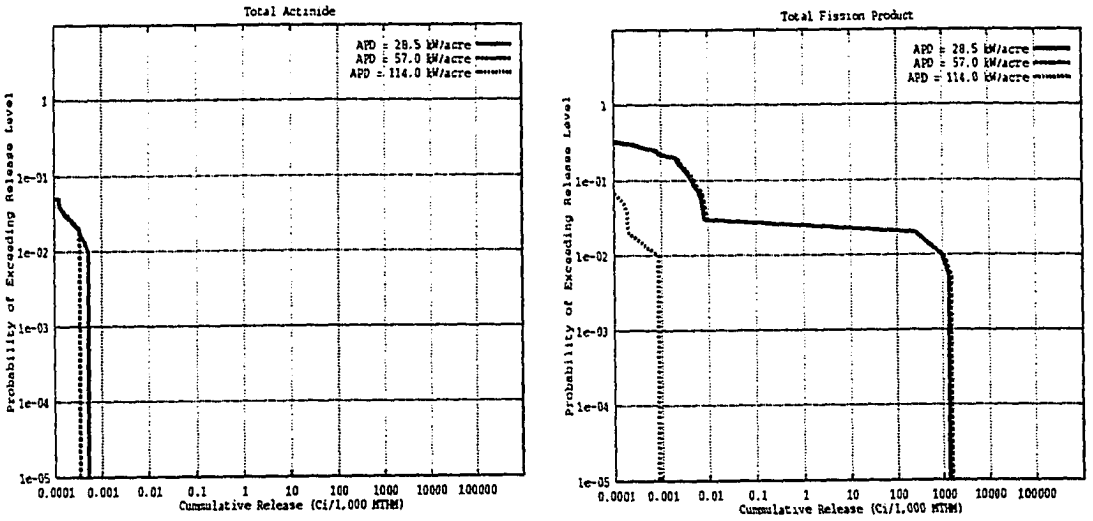

Figure 6.5 Total Actinide and Fission Product Release From SCP Container at 10,000 Years

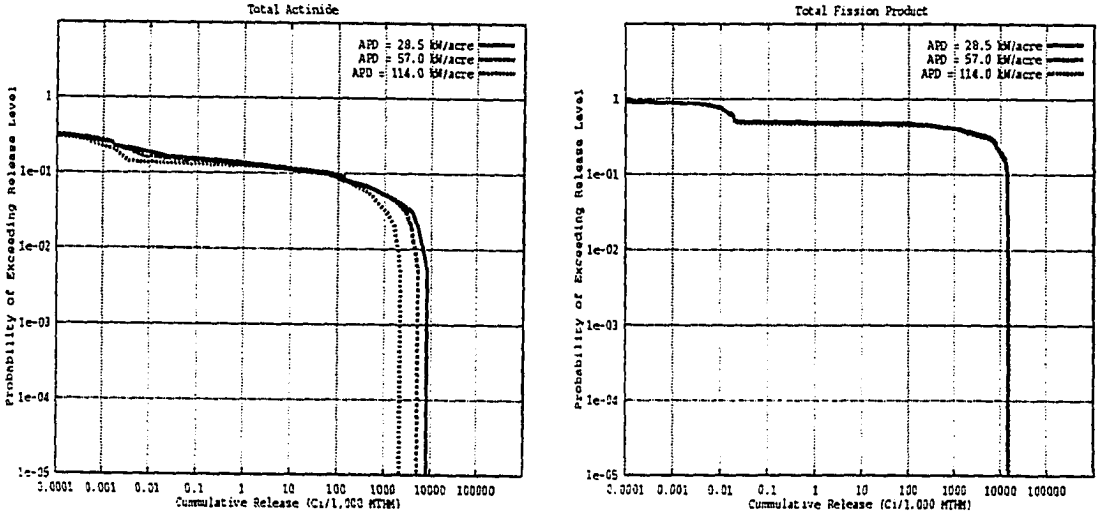

Figure 6.6 Total Actinide and Fission Product Release From SCP Container at 50,000 Years

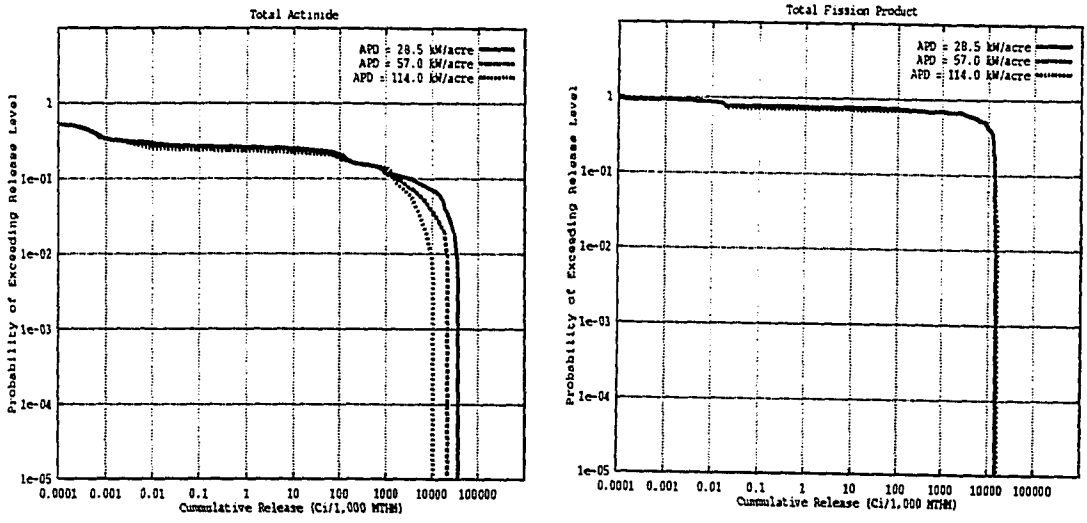

Figure 6.7 Total Actinide and Fission Product Release From SCP Container at 100,000 Years

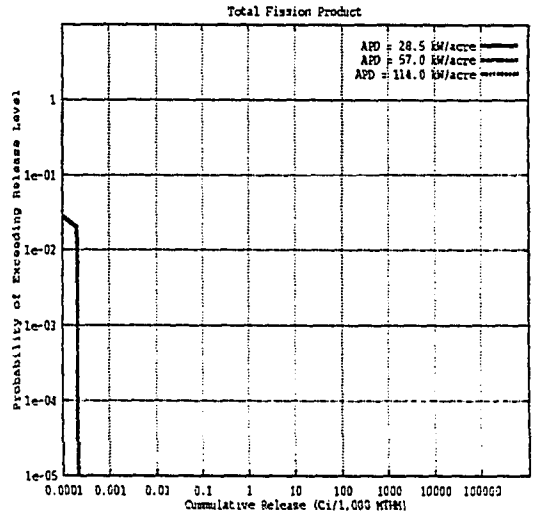

Figure 6.8 Total Fission Product Release From MMB Container at 10,000 Years

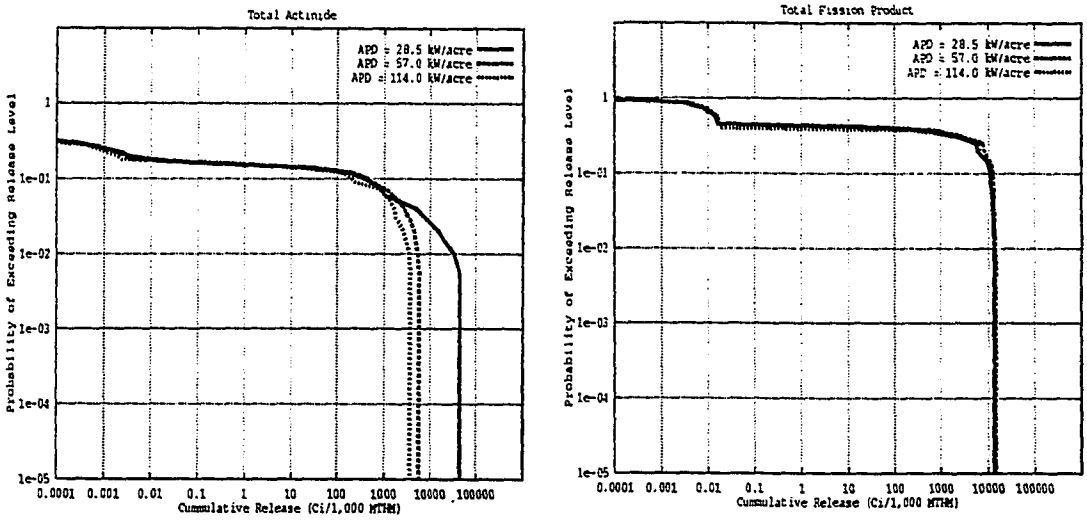

Figure 6.9 Total Actinide and Fission Product Release From MMB Container at 50,000 Years

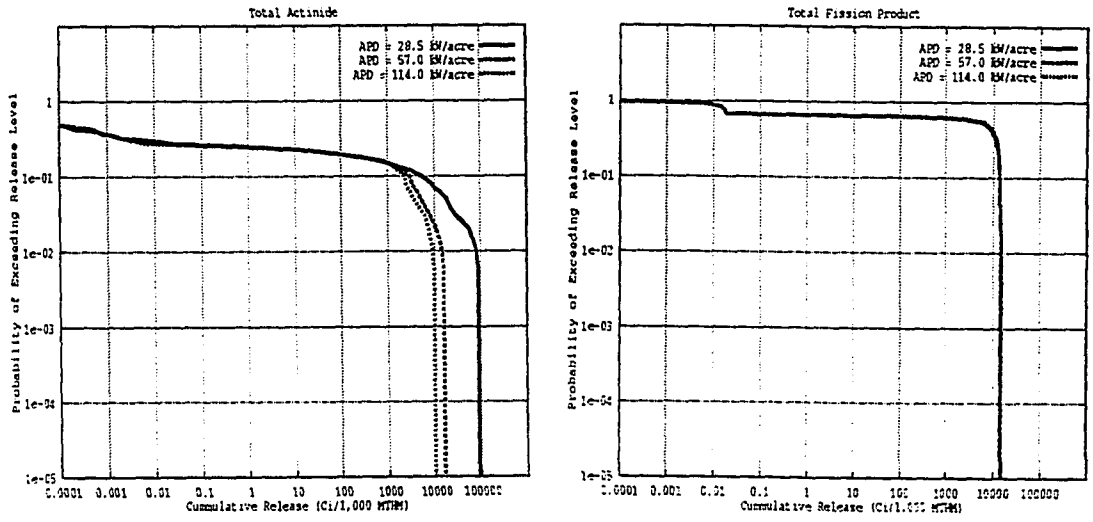

Figure 6.10 Total Actinide and Fission Product Release From MMB Container at 100,000 Years

environment in certain branches of the IMARC logic tree.

No release of fission products is observed from either container for an APD of 114.0 kW/acre while the release appears to be independent of the APD at 28.5 and 57.0 kW/acre. This is attributed to the longer dryout time associated with the 114.0 kW/acre thermal loading. IMARC results showed similar trends, however fission products were released to the accessible environment at an APD of 114.0 kW/acre. This is again attributed to the shorter travel times associated with certain logic tree branches in the IMARC model. The effect of the longer travel time can also be seen when comparing the releases for APDs of 28.5 and 57.0 kW/acre. The maximum possible fission product releases calculated with RIP are approximately one order of magnitude lower than those calculated with IMARC.

50000 and 100000 years: At 50000 and 100000 years, (Figures 6.6, 6.7, 6.9, and 6.10) the cumulative release of fission products is essentially identical regardless of the thermal loading for both container designs. This indicates that for a given container design, releases in the long-term are independent of the repository thermal loading. These trends were also observed from the IMARC results. The CCDFs resulting from each tool for cumulative fission product release are very similar at 50000 and 100000 years.

It can be seen that the actinide release at 50000 and 100000 years depends on the APD. This differs from the IMARC results. As will be demonstrated later, the total actinide release is dominated by Pu^{239}, U^{234}, and Np^{237} (with the plutonium isotopes being greater). The mass transport of actinides away from the waste package is solubility limited. Table 6.2c shows that the solubility of plutonium is strongly

dependent upon the temperature. Table 6.2b shows that the solubility of neptunium (and uranium) is not so strongly dependent upon temperature. As the APD, and hence repository temperature, is increased, the solubility of plutonium decreases. This results in a reduction in the amount of plutonium, hence total actinide, released. The most dramatic reduction is observed between the 28.5 kW/acre and 57.0 kW/acre loadings. For temperatures above 42.5° C, (as would occur in the 57.0 kW/acre case) the plutonium solubility drops by one to two orders of magnitude for a pH < 7.75 (58% probability). The reduction in solubility is not so large when the temperature is above 75° C (114.0 kW/acre case). IMARC does not model temperature dependent elemental solubility.

Radionuclide Contribution: Figure 6.11 provides the contribution of individual radionuclides to the total actinide and fission product CCDFs from the SCP container at 50000 years following emplacement for an APD of 57.0 kw/acre. Figure 6.12 provides similar plots for the MMB container. The total actinide release from both the SCP and MMB containers is primarily dominated by ^{239}Pu, ^{237}Np, and ^{234}U with ^{239}Pu contributing the greatest. The release of the other actinides, ^{240}Pu, ^{242}Pu, ^{226}Ra, ^{235}U, and ^{238}U, are negligible when compared to the total.

Similar results were observed with IMARC. The only differences noted were for probability levels above $1x10^{-4}$ where ^{237}Np tended to dominate the total release for the IMARC calculations. This difference is attributed primarily to the build-up of daughter products that is modeled in the IMARC PAs. If daughter product build-up were included in the RIP analyses, the contribution from ^{237}Np would increase. As discussed previously, the solubility, hence the release, of plutonium appears to be

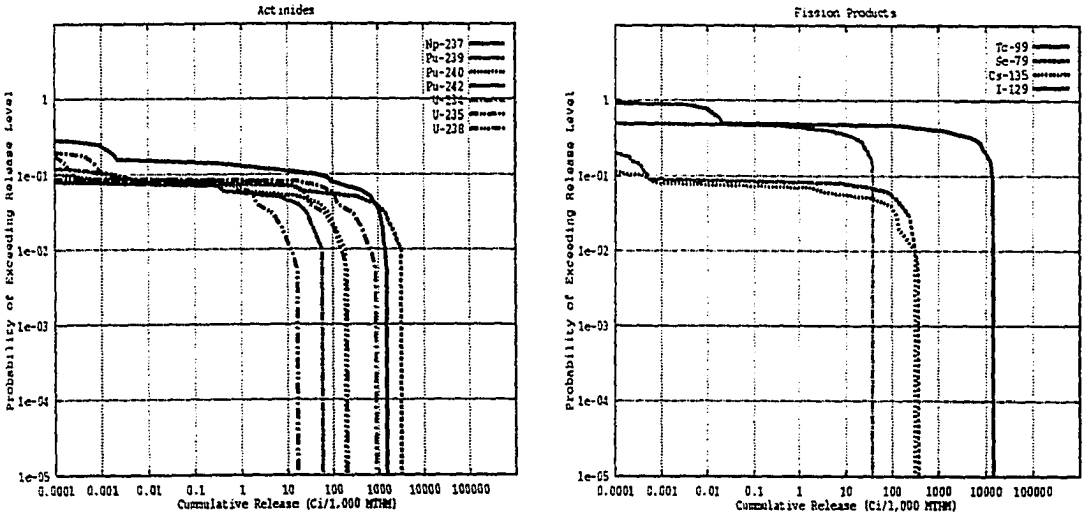

Figure 6.11 Radionuclides That Contribute to the Total Actinide and Fission Product Release From SCP Container at 50,000 Years, 57.0 kw/acre

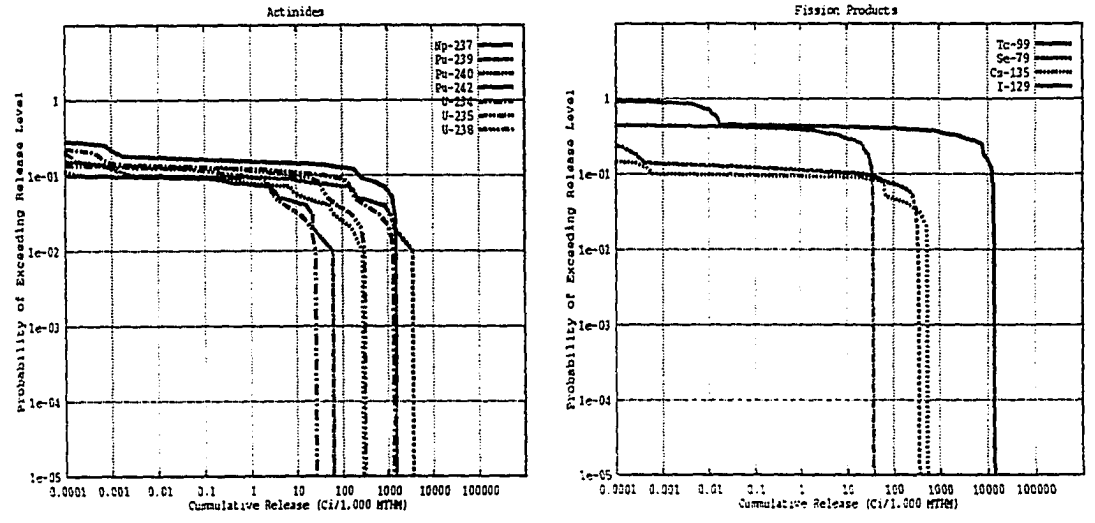

Figure 6.12 Radionuclides That Contribute to the Total Actinide and Fission Product Release From MMB Container at 50,000 Years, 57.0 kw/acre

strongly dependent on the repository temperature. Other loading scenarios result in differing temperatures (i.e., 28.5 kW/acre) leading to changes in the Pu solubility. A cooler repository will increase the plutonium release, and the total actinide release, while a warmer repository will decrease the plutonium release. Np release does not appear to be strongly impacted by temperature changes. These trends are shown in Figures 6.6 through 6.9.

The total fission product release from the SCP and MMB containers is dominated by ^{99}Tc. The release of ^{135}Cs, ^{129}I, and ^{79}Se is at least one order of magnitude lower than ^{99}Tc. These results are identical to what was observed using the IMARC tool.

Comparison of SCP vs. MMB: At 10000 years, no actinide release and a very small fission product release occurs from the MMB container. The SCP container does release a small amount of actinides and a significant amount of fission products within 10000 years.

A comparison of the cumulative release from the SCP and MMB containers 50000 years following emplacement (57.0 kw/acre) is shown in Figure 6.13. The performance of the two containers is observed to be essentially identical with the actinide release being slightly lower for the SCP container. This same trend is observed at 100000 years for this APD, but with the release from the MMB container slightly lower.

For an APD of 28.5 kW/acre, the actinide release from the SCP container is significantly lower than that from the MMB container at 50000 years and 100000 years. The fission product release from each container is identical. For APDs of 57.0 and

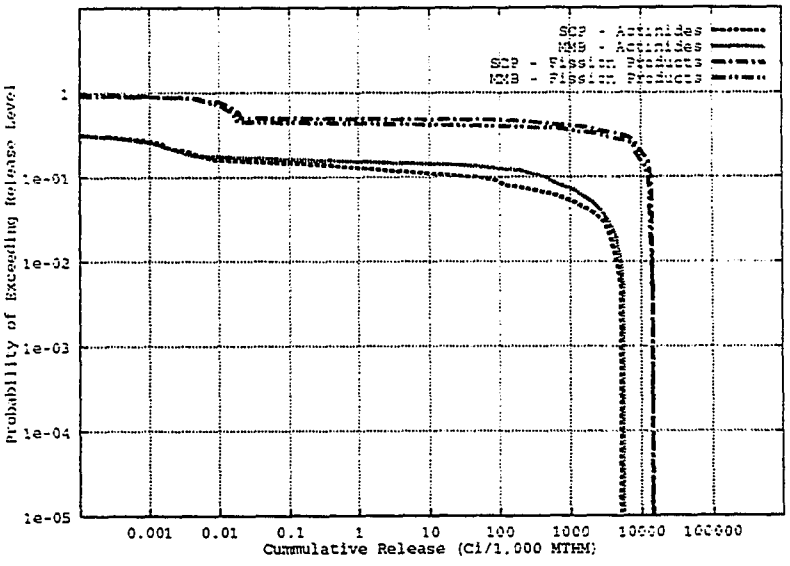

Figure 6.13 Release From SCP and MMB Containers, 50,000 Years, 57.0 kw/acre

114.0 kW/acre, the release of actinides from the SCP container, as compared to that from the MMB container, is slightly lower at 50000 years and essentially equivalent at 100000 years. Again, the fission product release from each container is identical. The actinide releases are impacted by the solubility limits. For an APD of 28.5 kW/acre, the large releases from the SCP containers are solubility limted (while those from the MMB container are not) given the smaller volume of water contacting the waste under the wet-drip water contact mode. As the APD increases and the plutonium solubility limit decreases, the releases from both containers tend to become solubility limited, leading the similarities in the releases observed for APDs of 57.0 and 114.0 kW/acre.

These results indicate that in a 10000 year period, the release of radionuclides will be minimal and limited to the fission products when a large metallic multi-barrier container is utilized. Over the long-term, the release of radionuclides does not appear to depend significantly on the container design

6.4.3 RIP Results for the ALMR Wasteforms

RIP PAs have been completed for the ALMR and LWR actinide recycle wasteforms assuming that these wasteforms are 1) co-located with SF at an APD of 114.0 kw/acre, and 2) emplaced in the repository alone. Both low and high pyroprocess actinide decontamination factors were considered. The MMB container design was utilized as it was used in the IMARC PA analyses. The initial inventory is provided in Table 4.9, the container loading (MTHM) is provided in Table 5.2, and the container performance parameters are provided in Chapter 4.

CCDFs for the co-located ALMR metallic and mineral wasteforms are provided in Figures 6.14 through 6.15 at 50000 and 100000 years after emplacement, respectively. No releases were observed at 10000 years. Minor releases were observed at 10000 years when utilizing IMARC. This difference is attributed to the RIP assumptions of lower unsaturated zone percolation flux as was discussed in Section 6.4.2. CCDFs for the ALMR wasteforms are provided in Figures 6.16 and 6.17 at 50000 and 100000 years after emplacement for the case when the ALMR waste is emplaced in the repository alone. No releases occur for this case at 10000 years after emplacement as none of the containers have failed. These CCDFs were obtained assuming a low pyroprocess actinide decontamination factor of $1x10^{-4}$.

Comparison of Emplacement Strategies: The release of radionuclides to the accessible environment is observed to be significantly lower when the ALMR waste is not co-located with LWR SF.

At 50000 years, the release of actinides is reduced by nearly an order of magnitude when the ALMR wasteforms are emplaced alone. The release of fission

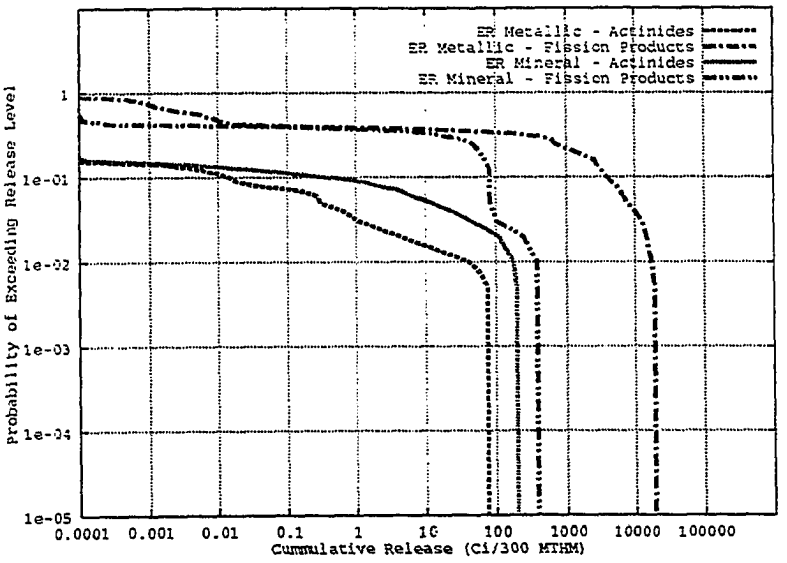

Figure 6.14 Release of Radionuclides From ALMR Wasteforms, MMB Container, Co-located, 114.0 kw/acre, 50,000 Years, Low Actinide Decontamination

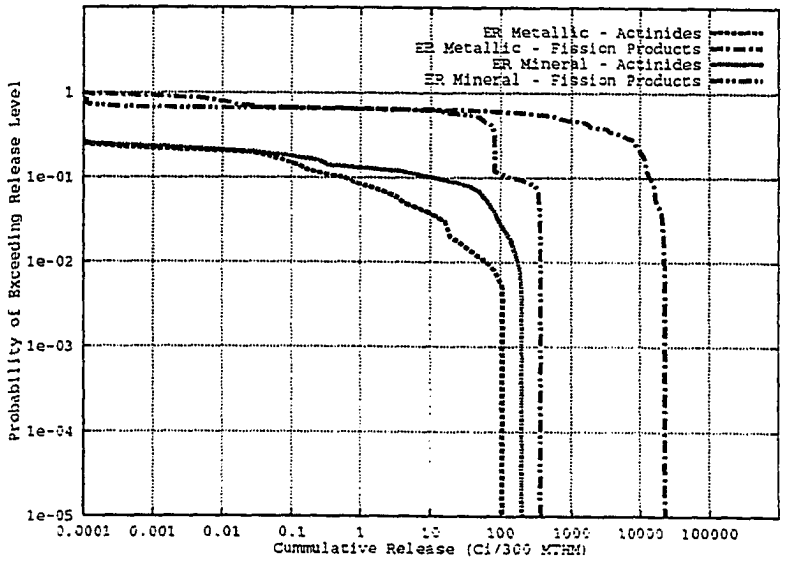

Figure 6.15 Release of Radionuclides From ALMR Wasteforms, MMB Container, Co-located, 114.0 kw/acre, 100,000 Years, Low Actinide Decontamination

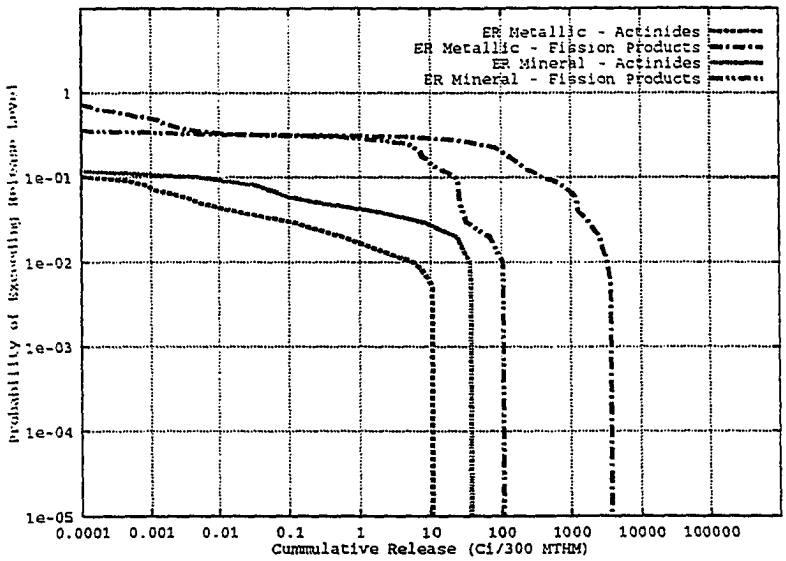

Figure 6.16 Release of Radionuclides From ALMR Wasteforms, MMB Container, Alone, 50,000 Years, Low Actinide Decontamination

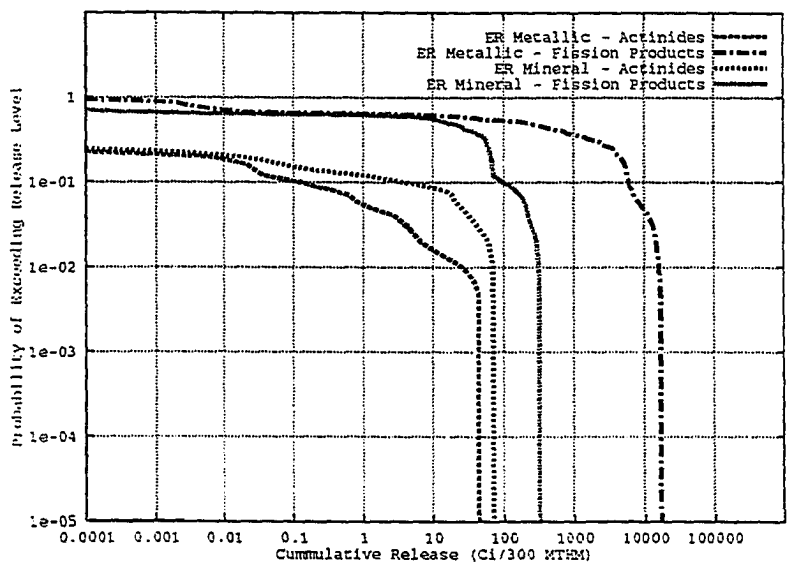

Figure 6.17 Release of Radionuclides From ALMR Wasteforms, MMB Container, Alone, 100,000 Years, Low Actinide Decontamination

products is also reduced by a factor of over five. The maximum possible cumulative release of actinides and fission products for the co-located ALMR waste is $2x10^{2}$ Ci and $2x10^{4}$ Ci, respectively. When the ALMR waste is emplaced alone, the maximum cumulative release of actinides and fission products is reduced to $4x10^{1}$ Ci and $4x10^{3}$ Ci, respectively.

At 100000 years, the release of actinides is reduced by a factor of approximately three while that of the fission products is only slightly reduced (by a factor of 1.3). The maximum possible cumulative release of actinides and fission products for the co-located ALMR waste is $2x10^{2}$ Ci and $2x10^{4}$ Ci, respectively. When the ALMR waste is emplaced alone, the maximum cumulative release of actinides and fission products is reduced to $7x10^{1}$ Ci and $2x10^{4}$ Ci, respectively.

This reduction in the cumulative release when emplacing the ALMR wastes in the repository alone is due to better container performance resulting from lower barrier corrosion rates at the lower repository temperature (see Section 3.7). The results are summarized in Tables 6.9 and 6.10.

Contributions to Total Release: The total release is dominated by the total fission product release, primarily from the ER-metallic wasteform. The release of actinides is similar for each wasteform with the release from the mineral wasteform dominating at both 50000 and 100000 years. This differs from the IMARC results where the release from the ER-metallic wasteform was found to dominate. Figures 6.18 and 6.19 show the contribution of individual radionuclides to the total actinide and fission product release at 50000 years for the metallic and mineral wasteforms, respectively. The total actinide release is dominated by ^{239}Pu and ^{240}Pu. This differs

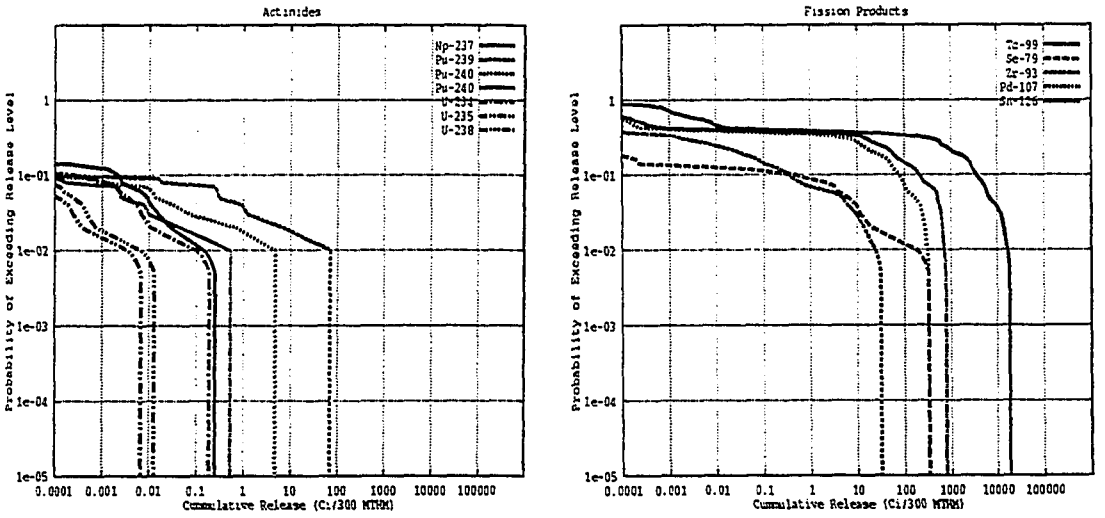

Figure 6.18 Radionuclides That Contribute to the Total Actinide and Fission Product Release From ALMR ER-Metallic Wasteform, MMB Container, Co-Located, 114.0 kW/acre, 50,000 Years, Low Actinide Decontamination

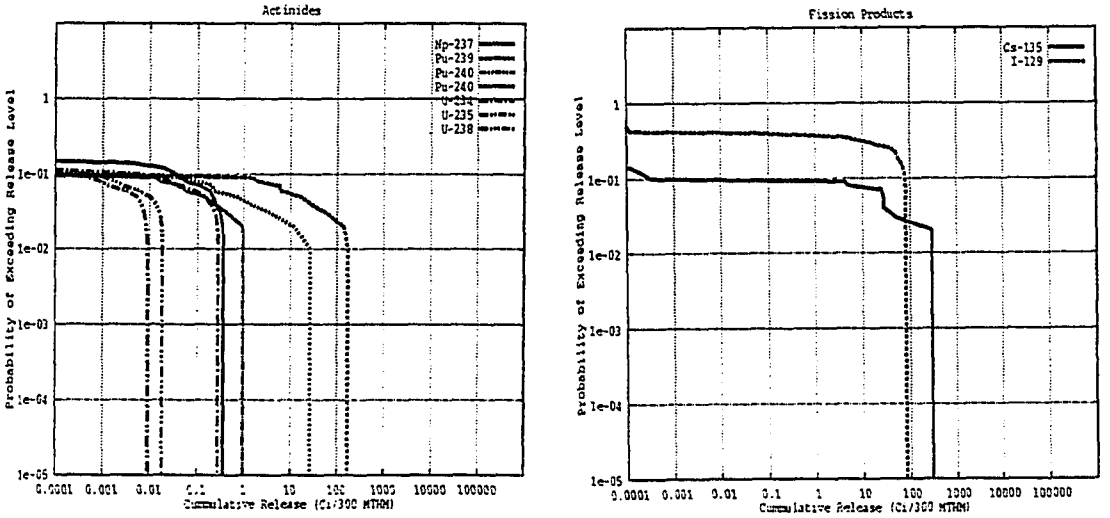

Figure 6.19 Radionuclides That Contribute to the Total Actinide and Fission Product Release From ALMR ER-Mineral Wasteform, MMB Container, Co-Located, 114.0 kW/acre, 50,000 Years, Low Actinide Decontamination

from the LWR SF results as it was observed that ^{237}Np and ^{234}U contributed to the total actinide release. Inclusion of daughter product build-up would not increase the release of these radionuclides to levels comparable with ^{239}Pu and ^{240}Pu. The total fission product release is dominated by ^{99}Tc for the metallic wasteform and both ^{135}Cs and ^{129}I for the mineral wasteform. The release of ^{99}Tc from the metallic wasteform is over two orders of magnitude larger than the release of either ^{129}I or ^{135}Cs from the mineral wasteform. This is similar to the results observed for LWR SF as ^{99}Tc also dominated the fission product release. These trends are identical to those observed with the IMARC PA tool.

Comparison With LWR SF: Comparisons of Figures 6.9 and 6.10 (LWR SF - MMB, 114.0 kW/acre, 50000 and 100000 years) with Figures 6.14 and 6.15 (LMR - MMB, co-located at 114.0 kW/acre, 50000 and 100000 years) shows that the release of actinides is significantly lower for the ALMR wasteforms. The actinide release from the ALMR wasteforms are less than that from the LWR SF - MMB container (114.0 kW/acre) at 50000 and 100000 years after emplacement by well over one order of magnitude. This decrease is slightly lower than that observed from the IMARC PA analyses where a two order of magnitude reduction was observed. Figure 6.20 shows the comparison at 50000 years. At 50000 years, the maximum actinide possible release from LWR SF is $4x10^3$ Ci while from the ALMR wasteforms is $2x10^2$ Ci. At 100000 years, the maximum possible actinide releases are $8x10^3$ Ci for LWR SF and $2x10^2$Ci for the ALMR wasteforms.

A greater reduction in the cumulative actinide release as compared to the SF-MMB container is observed at 50000 and 100000 years after emplacement when the

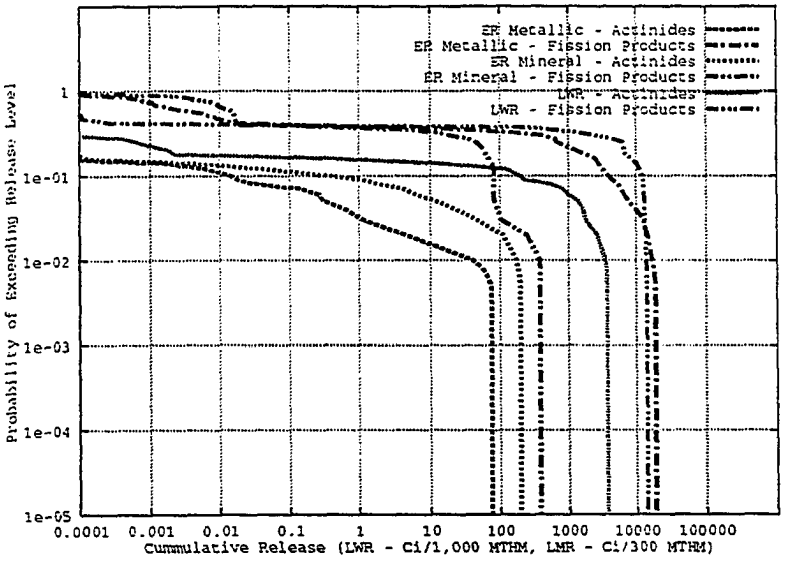

Figure 6.20: Comparison of the Release of Radionuclides From the LWR SF and ALMR Wasteforms, MMB Container, 114.0 kW/acre, 50000 Years.

ALMR waste is buried alone. The maximum possible releases are reduced by the following: LWR - $4x10^3$ Ci vs. ALMR - $4x10^1$ Ci at 50000 years, LWR - $8x10^3$ Ci vs. ALMR - $7x10^1$ Ci at 100000 years.

At 10000 years after emplacement no actinide release is observed for either LWR SF or any of the ALMR wasteforms, co-located or alone.

It can be seen that the release of fission products at 50000 and 100000 years is very similar. The maximum cumulative release of fission products from the co-located ALMR metallic mineral wasteform - MMB container (^{99}Tc) is slightly larger than that of SF - MMB container (^{99}Tc) at 50000 and 100000 years (LWR - $1x10^4$ Ci vs. ALMR - $1x10^4$ Ci at 50000 years, LWR - $1x10^4$ Ci vs. ALMR - $2x10^4$ Ci at 100000 years). Again, Figure 6.20 shows the comparison at 50000 years.

When the ALMR waste is emplaced alone the total fission product release is less than that from the SF-MMB container at 50000 years. At 100000 years. however, the total fission product release from the ALMR wasteform again exceeds that from the SF-MMB wasteform. The maximum possible release of fission products are: LWR - $1x10^4$ Ci vs. ALMR -$4x10^3$ Ci at 50000 years, LWR - $1x10^4$ Ci vs. ALMR -$2x10^4$ Ci at 100000 years).

At 10000 years after emplacement no fission product release is observed for either LWR SF or any of the ALMR wasteforms, co-located or alone

Effect of Pyroprocess Actinide Decontamination Factor: Figure 6.21 shows the effects of the pyroprocess actinide decontamination factor on the cumulative total actinide release from the metallic wasteform at 50000 years. Increasing the actinide decontamination factor by a factor of five results in a reduction in the cumulative

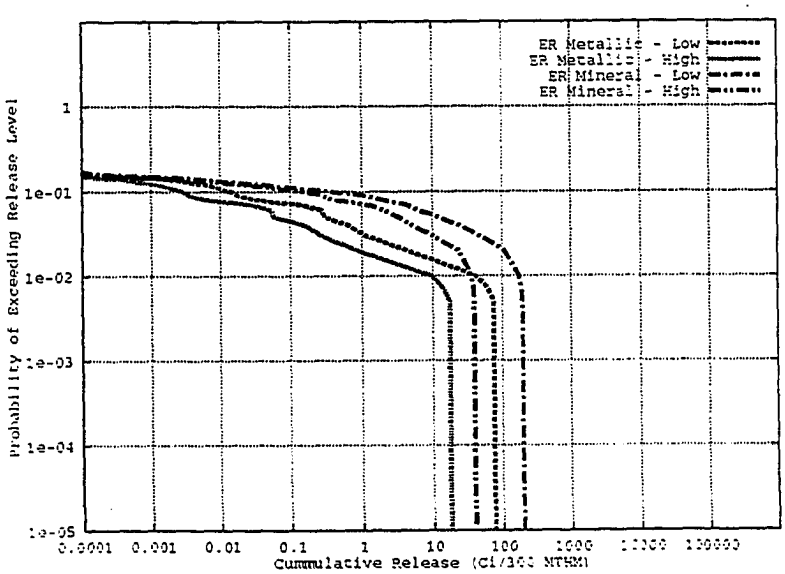

Figure 6.21 Effect of Actinide Decontamination Factor on the Release of Actinides From the ALMR Wasteforms, 50,000 Years

actinide release by approximately an order of magnitude. The smallest release occurs when a high pyroprocess actinide decontamination factor is utilized and the waste is emplaced in the repository alone. The release of fission products is not changed as the actinide decontamination factor does not impact the fission product inventory

6.4.4 RIP Results for the Actinide Recycle Wasteforms

CCDFs for the co-located actinide recycle metallic and mineral wasteforms are provided in Figures 6.22 and 6.23 at 50000 and 100000 years after emplacement, respectively. CCDFs for the actinide recycle wasteforms are provided in Figures 6.24 and 6.25 at 50000 and 100000 years after emplacement for the case when the waste is emplaced in the repository alone. These analyses have also assumed a low pyroprocess decontamination factor of $1x10^{3}$. No releases occur for either of these scenarios at 10000 years. Minor releases were observed for the co-located loading scenario at 10000 years when utilizing IMARC. This difference is again attributed to the RIP assumptions of lower unsaturated zone percolation flux as discussed in Section 6.4.2. For the scenario where the wastes are emplaced alone, the containers have yet to fail. This also was observed with IMARC.

Contributions to Total Release: It can be seen that the cumulative total actinide release is dominated primarily by the ER mineral and metallic wasteforms. The radionuclide that contributes to the total actinide release from each of these wasteforms is ^{239}Pu with minor contributions from ^{240}Pu, ^{242}Pu, ^{234}U, and ^{237}Np. The other wasteform containing actinides is the oxide reduction-mineral waste stream. The initial inventory of this wasteform is based on a 0.01% loss of actinides in the reduction

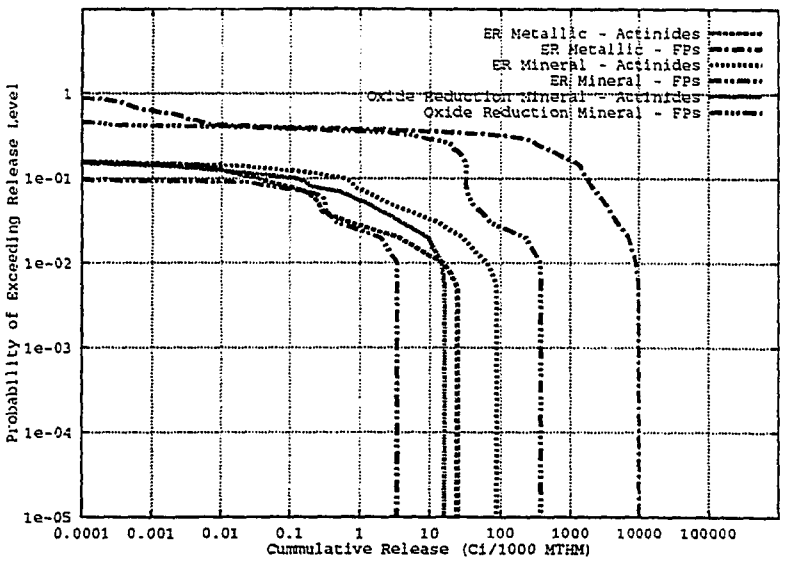

Figure 6.22 Release of Radionuclides From Actinide Recycle Wasteforms, MMB Container, Co-Located, 114.0 kw/acre, 50,000 Years, Low Actinide Decontamination

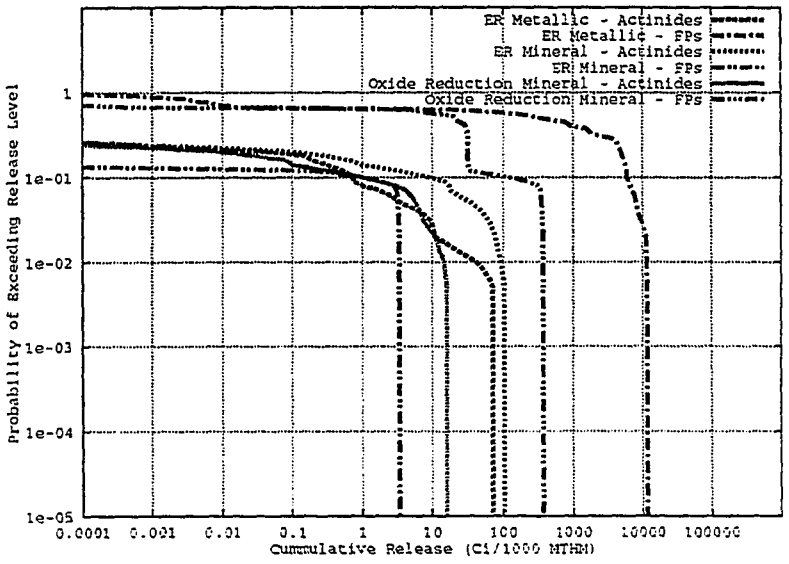

Figure 6.23 Release of Radionuclides From Actinide Recycle Wasteforms, MMB Container, Co-Located, 114.0 kw/acre, 100,000 Years, Low Actinide Decontamination

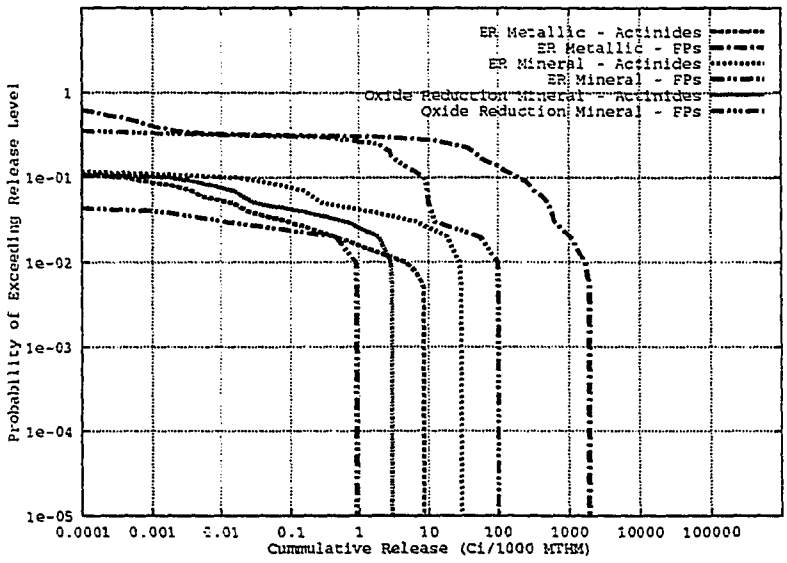

Figure 6.24 Release of Radionuclides From Actinide Recycle Wasteforms, MMB Container, Alone, 50,000 Years, Low Actinide Decontamination

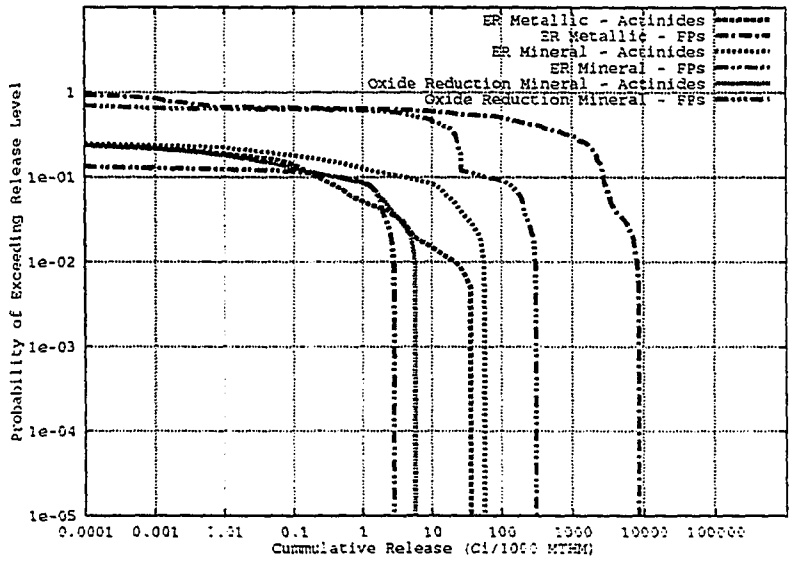

Figure 6.25 Release of Radionuclides From Actinide Recycle Wasteforms, MMB Container, Alone, 100,000 Years, Low Actinide Decontamination

process. This inventory, on a per MTHM basis, is equivalent to the high actinide decontamination ER wasteform inventories. As such, for the low actinide decontamination case, the ER wasteforms dominate the actinide release. The release of actinides from the oxide reduction - mineral wasteform will be comparable (and may exceed) to that from the ER wasteforms if a high actinide decontamination factor is utilized. Again, ^{239}Pu and ^{240}Pu dominate the total actinide release from the oxide reduction - mineral wasteform.

The cumulative total fission product release is dominated by the ER-metallic wasteform. This form contains a large inventory of ^{99}Tc, (see Tables 4.10 and 5.2), which has been observed to be the only contributor to the total fission product release from SF. The release of fission products from the other wasteforms is at least an order of magnitude smaller. The primary fission products released from each wasteform are: Oxide Reduction Mineral - ^{135}Cs, and ER Mineral - ^{135}Cs (to a small extent). Again, similar results were obtained with IMARC.

Comparison with LWR SF: Comparisons of Figures 6.9 and 6.10 (LWR SF - MMB 114.0 kW/acre, 50000 and 100000 years) with Figures 6.22 and 6.23 (LMR - MMB co-located at 114.0 kW/acre, 50000 and 100000 years) show that the release of actinides is significantly lower for the actinide recycle wasteforms The maximum possible cumulative release of total actinides from the co-located actinide recycle, ER wasteforms are lower than that from the SF MMB container by well over an order of magnitude at 50000 and 100000 years (LWR - $4x10^{3}$ Ci vs. Actinide Recycle - $9x10^{1}$ Ci at 50000 years, LWR - $8x10^{3}$ Ci vs. Actinide Recycle $1x10^{2}$ Ci at 100000 years). Figure 6.26 provides the comparison at 50000 years.

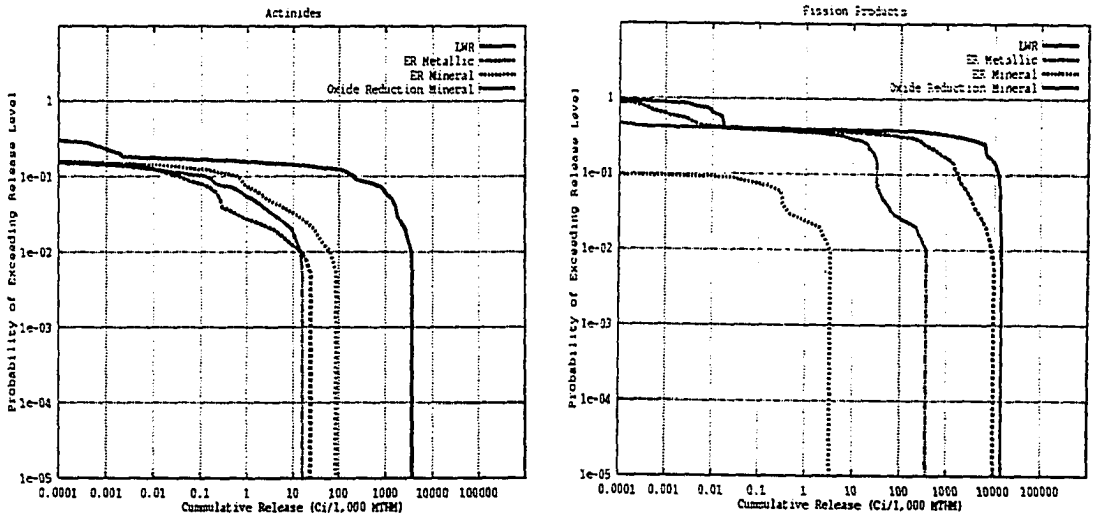

Figure 6.26: Comparison of the Release of Radionuclides From the LWR SF and Actinide Recycle Wasteforms, MMB Container, 114.0 kW/acre, 50000 Years.

A greater reduction in the actinide release is observed at 50000 and 100000 years after emplacement when the actinide recycle wasteforms are buried alone. The maximum possible releases are: LWR - $4x10^3$ Ci vs. Actinide Recycle - $3x10^1$ Ci at 50000 years, LWR - $8x10^3$ Ci vs. $6x10^1$ Ci at 100000 years).

It can be seen that the release of fission products is similar for the co-located ALMR wasteforms (ER-metallic, ^{99}Tc) relative to LWR SF (^{99}Tc) at 50000 and 100000 years (LWR - $1x10^4$ Ci vs. Actinide Recycle - $1x10^4$ Ci at 50000 years, LWR - $1x10^4$ Ci vs. $1x10^4$ Ci at 100000 years). Again, Figure 6.26 provides the comparison at 50000 years.

Significant reductions in the total fission product cumulative release are observed when the actinide recycle waste is emplaced in the repository alone The maximum possible releases are: LWR - $1x10^4$ Ci vs. Actinide Recycle - $2x10^3$ Ci at 50000 years, LWR - $1x10^4$ Ci vs. $8x10^3$ Ci at 100000 years.

Effect of Pyroprocess Actinide Decontamination Factor: Figure 6.27 shows the effects of the pyroprocess actinide decontamination factor on the cumulative total actinide release from the actinide recycle ER wasteforms at 50000 years. Increasing the actinide decontamination factor by an order of magnitude results in a reduction in the cumulative total actinide release by approximately an order of magnitude. It can be seen that the smallest total actinide release occurs when a high pyroprocess actinide decontamination factor is utilized and the waste is emplaced in the repository alone.

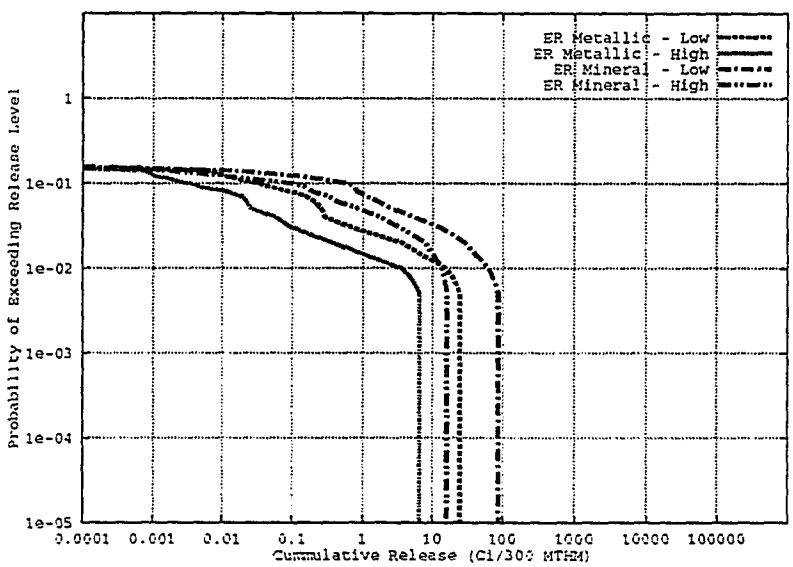

Figure 6.27 Effect of Actinide Decontamination Factor on the Release of Actinides From the Actinide Recycle, ER-Metallic Wasteform, 50,000 Years

The release of fission products is not changed as the actinide decontamination factor does not impact the fission product inventory.

A summary of the comparisons between the ALMR/actinide recycle wasteforms and SF emplaced in MMB containers is provided in Table 6.9 for the actinides and in Table 6.10 for the fission products.

Table 6.9 Maximum Cumulative Total Release of Actinides, from ALMR Wasteforms, (Ci/1000 MTHM equivalent)

Time After Emplacement (Years)	SF-MMB 114.0 kw/acre	ALMR Low/High Decontamination		Actinide Recycle Low/High Decontamination	
		Co-Located	Alone	Co-Located	Alone
10000	0	0 0	0 0	0 0	0 0
50000	$4x10^3$	$2x10^2$ $4x10^1$	$4x10^1$ $4x10^0$	$9x10^1$ $2x10^1$	$3x10^1$ $3x10^0$
100000	$8x10^3$	$2x10^2$ $4x10^1$	$7x10^1$ $7x10^0$	$1x10^2$ $2x10^1$	$6x10^1$ $6x10^0$

Table 6.10 Maximum Cumulative Total Release of Fission Products from ALMR Wasteforms, (Ci/1000 MTHM equivalent)

Time After Emplacement (Years)	SF-MMB 114.0 kw/acre	ALMR		Actinide Recycle	
		Co-Located	Alone	Co-Located	Alone
10000	0	0	0	0	0
50000	$1x10^4$	$2x10^4$	$4x10^3$	$1x10^4$	$2x10^3$
100000	$1x10^4$	$2x10^4$	$2x10^4$	$1x10^4$	$8x10^3$

6.4.5 RIP Results for Weapons Grade Plutonium Disposition Options

RIP PA analyses have been completed for the wasteforms derived from the different options being considered for the disposition of weapons grade plutonium. The options evaluated are spiking (irradiating to low burnups) in both PWRs and ALMRs, irradiating to a burnup level commensurate with spent fuel in both PWRs and ALMRs, continued irradiation followed by recycling in an ALMR, and mixing with DHLW followed by vitrification into borosilicate glass.

Details regarding the irradiation conditions and burnup levels are provided in Section 4.4.5 for the PWR and ALMR disposition options. The radionuclide inventories are provided in Table 4.11 for the PWR options, Table 4.12 for the ALMR options, and Table 4.7 for the DHLW option. The matrix alteration rates for the LWR SF and ALMR wasteforms are identical to those utilized in the previous RIP analyses. The matrix alteration rate for DHLW is described in section 4.3.2. It should be noted that the matrix alteration rate for DHLW has dependencies on both pH and temperature. This differs from DHLW matrix alteration rates used in IMARC where three discrete rates were used, representing low, moderate and high alteration.

The following assumptions were again made regarding emplacement strategies in order to be consistent with the IMARC analyses. The SF discharged from a PWR used to dispose of weapons grade plutonium was emplaced in the repository with commercial SF at an APD of 114.0 kW/acre. The spiked DHLW and the various ALMR plutonium disposition option wasteforms were assumed to be co-located with commercial SF at an APD of 114.0 kW/acre.

Figures 6.28 and 6.29 provide the CCDFs of cumulative total actinide release

for each weapons grade plutonium disposition options at 50000, and 100000 years following emplacement. No release from any wasteform was observed at 10000 years. This differs from the IMARC results where releases from the DHLW and ALMR alternatives demonstrated small releases. As was discussed previously, this is attributed to the lower ground water flux and radionuclide retardation within the saturated zone that was assumed in the RIP model.

At 50000 years (Figure 6.28), the LWR spent fuel option results in the largest releases. This is closely followed by the ALMR options (spiking and spent fuel) and the LWR spiking option. It can be concluded that at 50000 years, the once through options result in essentially identical releases. The DHLW option results in releases smaller than those observed for any of the LWR or ALMR once through options. The ALMR recycle alternative with a low actinide decontamination factor results in a significantly lower release. The high actinide decontamination factor (not shown) leads to a further reduction in the release. Table 6.11 provides the maximum possible total actinide release obtained from each wasteform.

Different trends are observed at 100000 years (Figure 6.29) where the ALMR once through options results in the largest releases. The once through LWR options and the DHLW option result in essentially identical releases that are significantly lower than that from the once through ALMR options. The ALMR recycle option again results in the lowest release. Table 6.11 again provides the maximum possible total actinide release obtained from each wasteform.

The results at 50000 and 100000 differ slightly from those obtained with the IMARC PA tool. In general, the results are identical with the releases from the once

Table 6.11: Maximum Cumulative Total Release of Actinides (Ci/1000 MTHM equivalent) from Weapons Grade Plutonium Disposition Alternatives

Alternative	50000 years	100000 years
LWR Spike	$2x10^3$	$1x10^4$
LWR Spent Fuel	$3x10^3$	$9x10^3$
DHLW	$1x10^3$	$1x10^4$
ALMR Spike	$3x10^3$	$4x10^4$
ALMR Spent Fuel	$3x10^3$	$3x10^4$
ALMR Recycle Low / High Actinide Decont.	$2x10^2$ $4x10^1$	$2x10^2$ $4x10^1$

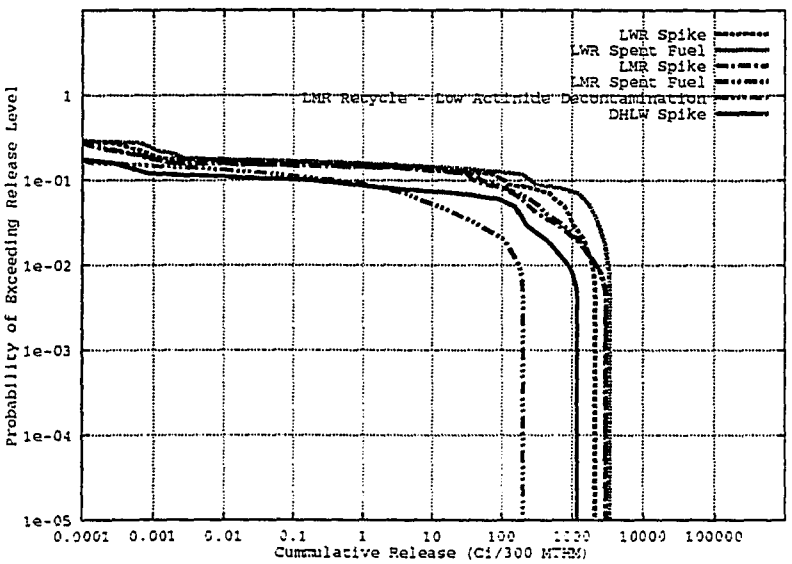

Figure 6.28 Total Actinide Release From Weapons Grade Plutonium Disposition Alternatives, MMB Container, ALMR Wastes Co-Located With SF, 50000 years

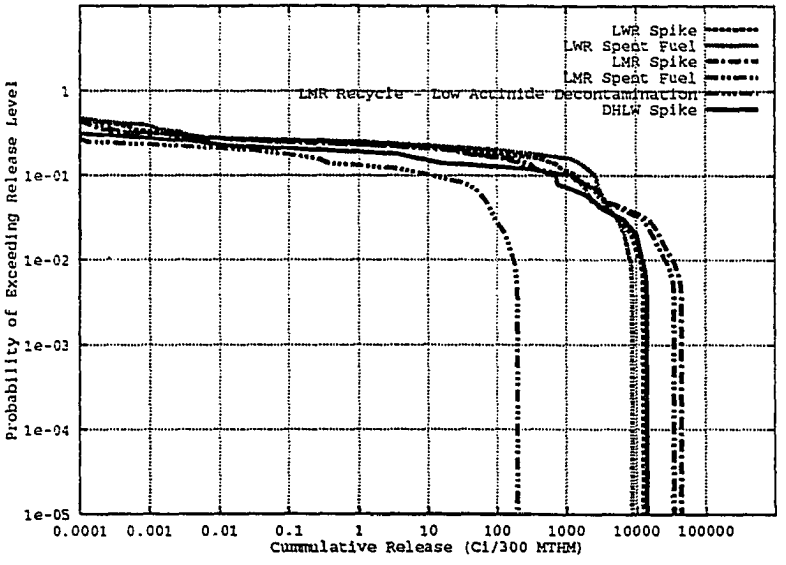

Figure 6.29 **Total Actinide Release From Weapons Grade Plutonium Disposition Alternatives, MMB Container, ALMR Wastes Co-Located With SF, 100000 years**

through cycles being similar and the release from the ALMR recycle option being significantly smaller. The release of actinides from the ALMR wasteform is higher for RIP than for IMARC, compare Figures 5.11 and 5.12 with Figures 6.14 and 6.15, respectively. Since the IMARC analyses indicate that both the LWR and ALMR once through options result in essentially identical releases, the RIP analyses can be expected to result in slightly higher ALMR actinide releases. This is observed at 100000 years.

The difference between IMARC and RIP in the DHLW release is attributed to the implementation of the matrix alteration rate into both models. Recall that IMARC uses three discrete matrix alteration rates and it has been demonstrated, section 5.4.6, that the resulting CCDFs are derived from the high alteration rate/wasteform surface

area branches of the logic tree. RIP, on the other hand, samples from distributions of matrix alteration rate and wasteform surface area. The IMARC high DHLW matrix alteration rate utilized equation 4.9 and was based on a temperature of 80 °C, a pH of 2.0 and a cracking factor of 30, resulting in a matrix alteration rate of 280.6 g/m^2yr. RIP also used equation 4.9, but the pH was derived from a uniform distribution from 6 to 9 and the cracking factor was derived from a uniform distribution from 10 to 30. As such, the high DHLW alteration rate assumed in IMARC cannot be obtained with RIP.

6.4.6 RIP Sensitivity Analysis, ALMR Electrorefiner Mineral Wasteform

Sensitivity analyses were conducted using RIP for the ALMR ER mineral wasteform. The purpose of this analysis is to determine the factors that influence the release of radionuclides from this wasteform and to complement the sensitivity analysis conducted earlier using IMARC, see section 5.4.6. The mineral wasteform was chosen to be studied as it has actinide releases that are comparable to the metallic wasteform, but slightly higher. The results obtained for the metallic wasteform will be similar. As with the IMARC analysis, the scenario where the ALMR wastes are co-located with commercial LWR SF at an APD of 114.0 kW/acre was evaluated. The radionuclide inventory resulting from the low actinide decontamination factor was utilized. It has been shown that a high actinide decontamination factor results in significantly lower releases. The MMB container design was utilized.

The first analysis conducted was to determine the relation between the total actinide release to the accessible environment and the number of realizations sampled in the calculation. The base case of 100 realizations was compared to calculations

utilizing 500 and 1000 realizations. The results are presented in Figure 6.30. It can be seen that increasing the number of realizations does not impact the results to any extent that warrants the use of a higher number of realizations. Also shown are the 5/95% confidence intervals for the 100 realization case. As the number of realizations increase, the confidence interval decreases. The confidence bounds shown are applicable to the all CCDFs presented previously involving the RIP tool. It is not possible to determine confidence intervals with the IMARC tool because of its fault tree approach to PA analysis.

Two sets of sensitivity analyses were conducted regarding repository system performance. The first set evaluated the dependence of the total actinide release to the accessible environment on: the flow mode (matrix or fracture), parameters

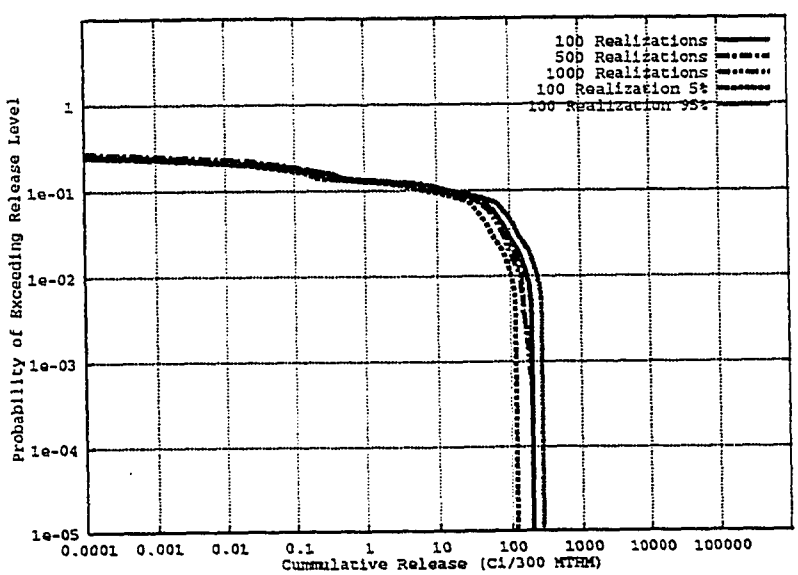

Figure 6.30 Sensitivity Analysis, Total Actinide Release to the Accessible Environment - Number of Realizations, MMB Container, ALMR ER Mineral Wasteform, Co-Located, 114.0 kW/acre, 100000 years

affecting the ground water travel time (saturated zone flux, dry infiltration rate, climactic multiplier, high percolation rate) matrix alteration rate, sorption, and solubility. The second set evaluated the dependence of the total actinide release from the waste package on: matrix alteration rate, dry infiltration rate, effective catchment area, geometric factor for diffusion, and $^{237}Np/^{239}Pu$ solubility. RIP has the ability to analyze these dependencies directly from the output of a given case. It should be noted that none of the other parameters are held constant while the parameter of interest is varied. This analysis was conducted at 100000 years.

The IMARC sensitivity analysis indicated that the release of radionuclides to the accessible environment was strongly dependent on the ground water flow mode. A detailed study of the dependency was conducted using RIP. The identical conclusion was drawn. Several cases were analyzed in addition to the base model (matrix = 80%, fracture = 20%) including: matrix flow only with retardation in all zones, fracture only with no retardation in the saturated zone, and fracture only with retardation only in the saturated zone. The results are provided in Figure 6.31 which provides the cumulative actinide release at 100000 years for the ER-mineral wasteform.

It can be seen that the significant actinide release occur for the base case only for realizations that result in fracture flow with no retardation in the saturated zone. If retardation is allowed in the saturated zone, consistent with the SNL PA [18], the maximum actinide release from a fracture flow mode drops by almost an order of magnitude. In this scenario, all of the plutonium is retarded and the total actinide release is dominated by ^{237}Np and ^{235}U.

Under matrix flow conditions, the cumulative actinide release is reduced

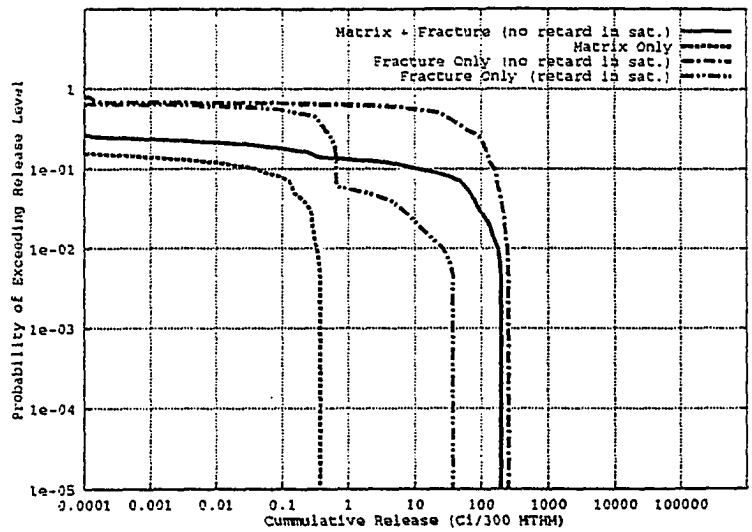

Figure 6.31 Sensitivity Analysis, Total Actinide Release to the Accessible Environment - Flow Mode CCDF, MMB Container, ALMR ER Mineral Wasteform, Co-Located, 114.0 kW/acre, 100000 years

significantly. The probability of any release decreases relative to the base model, but more importantly, the maximum possible cumulative actinide release decreases by over two orders of magnitude. Again, ^{239}Pu is strongly sorbed (within the Topopah Springs Welded unit) and the total release is dominated by ^{237}Np and ^{235}U.

The total fission product release is not dependent on the flow mode. ^{99}Tc dominates the total fission product release and is not retarded. As such, in any flow mode, the release of ^{99}Tc is dependent on the ground water velocity only. In these models, the ground water velocity is independent of the flow mode.

Figure 6.32 further demonstrates the dependence of total actinide release to the environment on the dominating flow mode. The RIP model assumed a uniform distribution between zero and one to determine if fracture or matrix flow was dominating. If this parameter was less than 0.2, fracture flow conditions existed. It

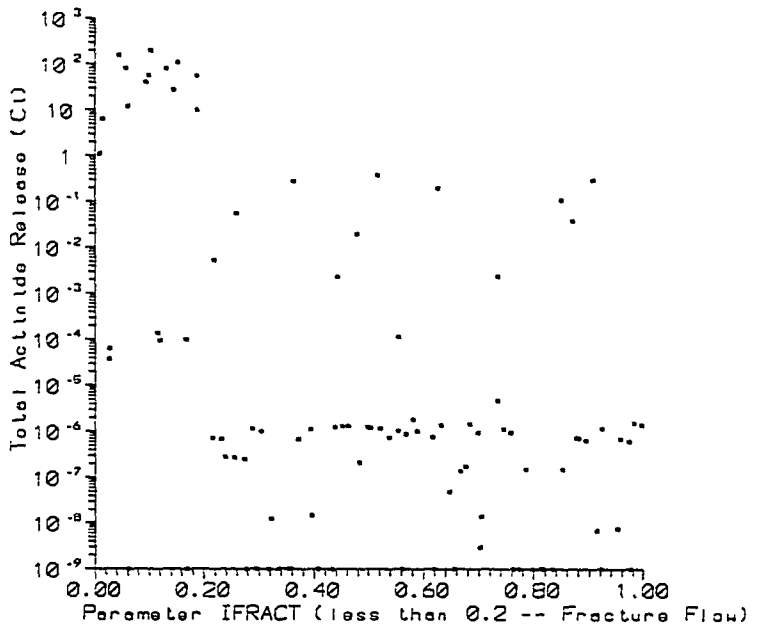

Figure 6.32 Sensitivity Analysis, Total Actinide Release to the Accessible Environment - Flow Mode, MMB Container, ALMR ER Mineral Wasteform, Co-Located, 114.0 kW/acre, 100000 years

can be seen in Figure 6.32 that the total actinide release is largest by several orders of magnitude when fracture flow conditions exist. When matrix flow exists the total actinide release tends to be very small with only a few realizations resulting in larger releases.

The results obtained in the preceding section indicated that the release of actinides from the various pyroprocess fuel cycles is reduced significantly relative to that of directly disposed LWR SF. In light of the above observances, the question exists as to whether this conclusion would hold true in a matrix flow condition.

Figure 6.33 shows the dependence of the cumulative actinide release at 100000 years from LWR SF on the flow mode. Again, the release from the base

model is dominated by those that occur under fracture flow conditions with no retardation in the saturated zone. If matrix flow dominates, the total actinide release decreases significantly, but not to the extent observed for the ALMR ER-mineral wasteform. Plutonium is again effectively sorbed, but the release is still quite large and dominated by ^{237}Np. It should be noted that the inventory of ^{237}Np in LWR SF is significantly larger than in the various pyroprocess wasteforms.

A comparison of the cumulative actinide release at 100000 years from the ALMR ER-mineral and LWR SF wasteforms for a matrix flow mode only model is provided in Figure 6.34. The maximum release from the ALMR wasteform is observed to be over three orders of magnitude lower than that for LWR SF. Similar results were obtained at 50000 years for this wasteform and for the LWR actinide recycle

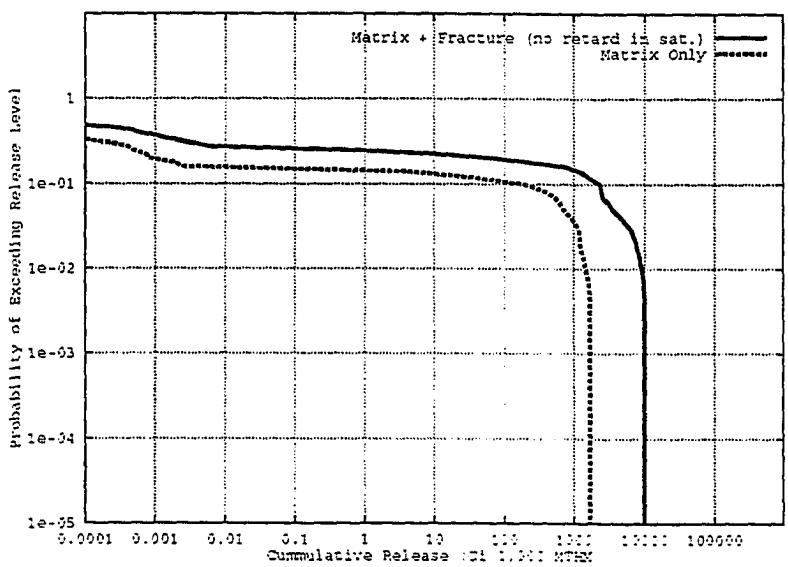

Figure 6.33 Sensitivity Analysis, Total Actinide Release to the Accessible Environment - Flow Mode, MMB Container, LWR SF, 114.0 kW/acre, 100000 years

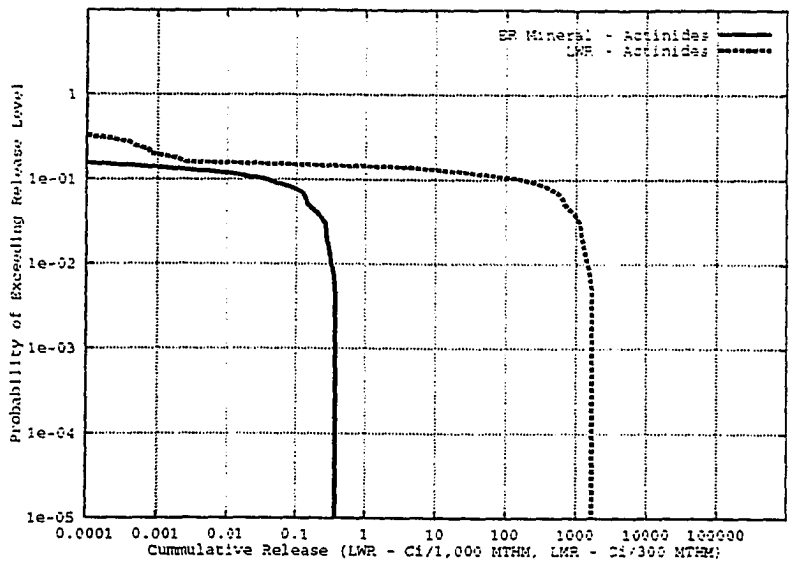

Figure 6.34 Sensitivity Analysis, Total Actinide Release to the Accessible Environment - Comparison of ALMR ER-Mineral and LWR SF Wasteforms -Matrix Flow, MMB Container, Co-Located, 114.0 kW/acre, 100000 years

wasteforms at both 50000 and 100000 years. As was stated previously, these releases are dominated primarily by ^{237}Np (and ^{235}U for the pyroprocess wasteforms) as all plutonium is retarded. The pyroprocess fuel cycle reduces the inventory of ^{237}Np and ^{241}Pu (^{237}Np precursor) to very small levels as compared to LWR SF, see Tables 4.10 and 4.12. It should be noted that an ALMR is ^{239}Pu fueled, so the ALMR wastes have a considerable ^{239}Pu inventory relative to LWR SF. The ^{239}Pu is strongly sorbed under matrix flow conditions. In short, a greater reduction in the total actinide release occurs for pyroprocess wasteforms relative to LWR SF under matrix flow conditions.

The cumulative release of radionuclides to the accessible environment at a given time depends heavily on the ground water travel time between the repository and

the accessible environment regardless of the flow mode. Recall, both IMARC and the RIP model utilized in this study solve the one-dimensional advection/dispersion equation (equation 5.2) for radionuclide transport. In the RIP model, this time is dependent on several stochastic modeling parameters including: The dry infiltration rate, the climactic multiplier, the hydraulic conductivity, the saturated zone velocity, the rock porosity, and time.

The ground water travel time for column one of the RIP conceptual model is shown in Figure 6.35. It should be noted that this column represents the shortest distance between the repository and the saturated zone (and the accessible environment). Hence, it provides the shortest travel time for a given realization. Ground water travel time distributions are shown for the conditions existing at 10000, 50000, and 100000 years following emplacement. It can be seen that as the time increases, the ground water travel time decreases. This is due to the increasing unsaturated zone percolation flux caused by the linear transition to pluvial conditions.

Figure 6.35 demonstrates that for over 40-50% of the realizations, the ground water travel time is greater than 100000 years. The significant releases occur for ground water travel times less than 100000 years. Smaller releases occur for ground water travel times in excess of 100000 years for non-sorbing elements or elements with low realized retardation coefficients. This is due to the spatial concentration gradient term in the advection/dispersion equation. This phenomenon is seen in the total cumulative fission product release at 100000 years (Figures 6.7, 6.10, 6.15, and 6.23) as the spatial concentration gradient of ^{99}Tc is sufficiently large to result in small releases in spite of long travel times. This results in the CCDFs approaching one

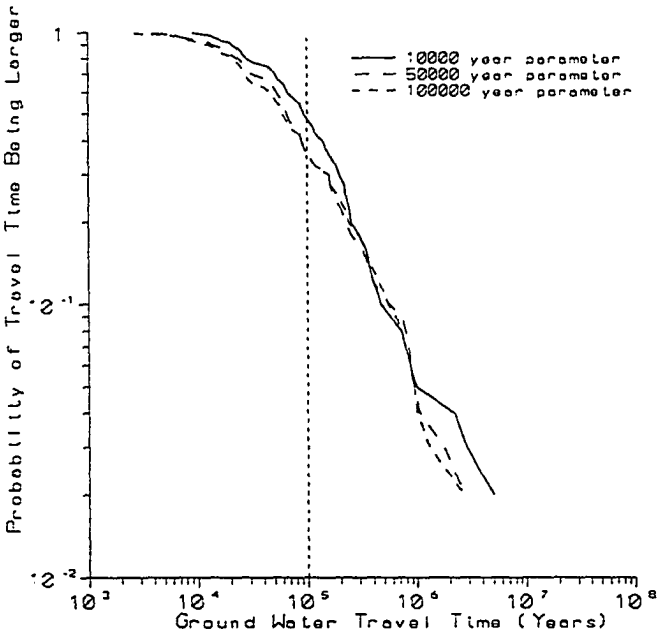

Figure 6.35 Sensitivity Analysis, Distributions of Ground Water Travel Time Between Repository and the Accessible Environment

rather than 50% at low release levels. The CCDFs will never achieve a probability of one as certain realizations result in ground water travel times so large that no releases occur.

If fracture flow conditions exist with no retardation (20% of the realizations in the base model), the cumulative release of actinides will behave in a manner identical to that described above. This is seen in Figure 6.31. If both matrix and fracture flow are assumed to occur in a PA analysis, the large releases associated with fracture flow occur at probability levels that approach 20%. At lower release levels, the probability increases above 20% as matrix flow releases begin to contribute to the CCDF in a manner as discussed above. The CCDF will not approach the high probability levels at low releases seen for the fission products due to retardation.

Figure 6.36 shows the cumulative release of actinides form the ALMR ER-mineral wasteform under matrix flow conditions at 100000 years as a function of the column one ground water time. This plot utilizes the ground water travel time at 100000 years as it is the most rapid and provides a limit to the most flow that can be realized in a 100000 year calculation. The observations discussed above are shown. The significant releases occur only for low travel times (less than 50000 years). Minor releases occur for travel times in excess of 100000 years (but not greater than 200000 years). Recall, these releases are dominated by ^{237}Np and ^{235}U which are not strongly sorbing.

The largest releases were found to occur for realizations resulting in low ground water travel times and low retardation coefficients. Figure 6.37 shows the cumulative

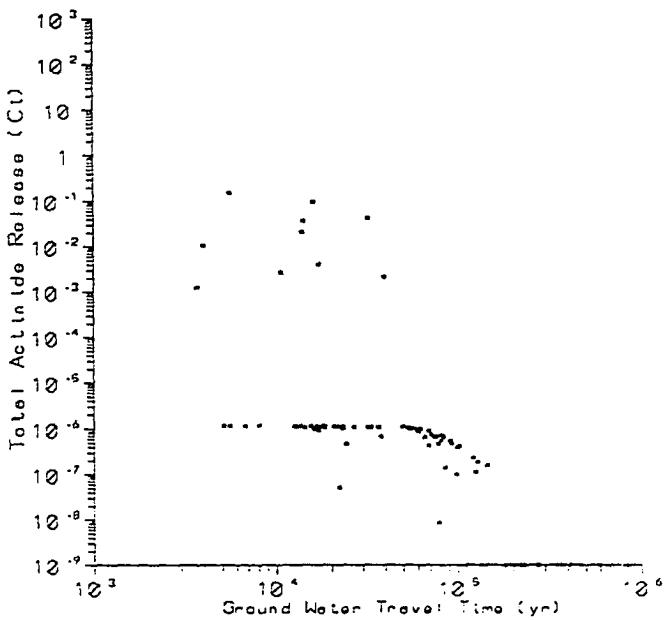

Figure 6.36 Sensitivity Analysis, Total Actinide Release to the Accessible Environment - Column 1 Ground Water Travel Time, ALMR ER-Mineral Wasteform, Co-Located, 114.0 kW/acre, 100000 years

actinide release form the ALMR ER-mineral wasteform at 100000 years as a function of the ^{237}Np distribution coefficient (de-vitrified, vitric, and zeolitic rock). The maximum releases occur for low values of the de-vitrified and zeolitic distribution coefficients. The release is not dependent on the vitric distribution coefficient as it is not strongly sorbing. The maximum cumulative actinide releases occurred for realizations resulting in very low values of the de-vitrified sorption coefficient. De-vitrified rock comprises the majority of the pathway thickness between the repository and the accessible environment. Again, low values of the zeolitic distribution coefficient and low ground water travel times are required in addition to the low de-vitrified distribution coefficient for significant releases.

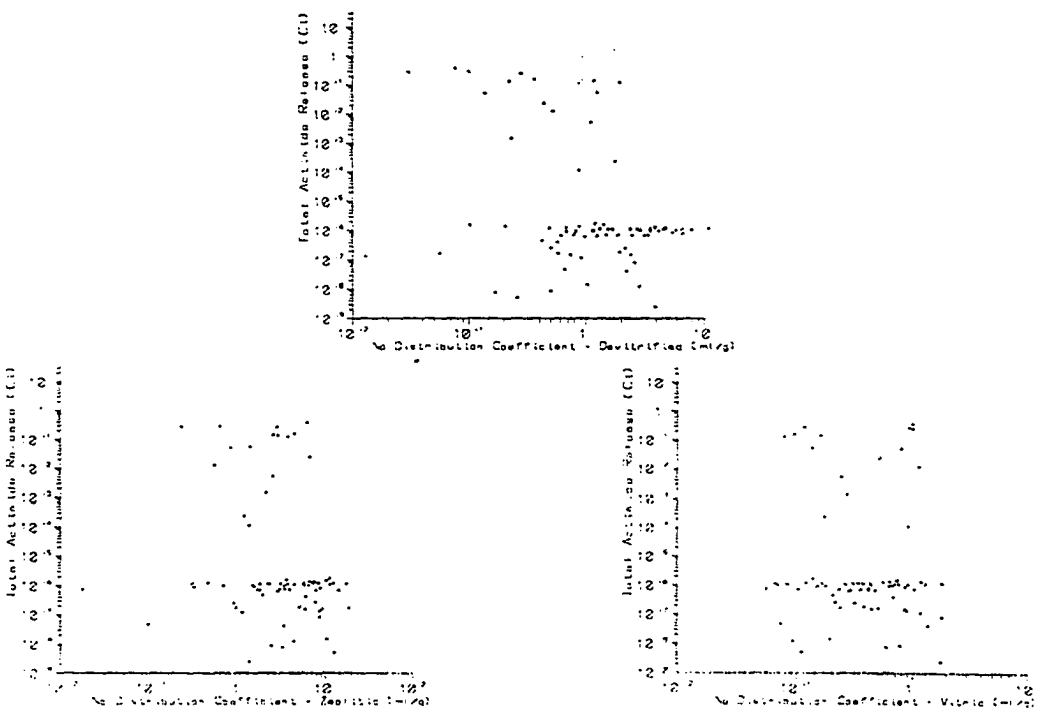

Figure 6.37 Sensitivity Analysis, Total Actinide Release to the Accessible Environment - Np^{237} Distribution Coefficient, ALMR ER-Mineral Wasteform, Co-Located, 114.0 kW/acre, 100000 years

Figure 6.38 shows the effects of climate changed induced lifting of the water table on the cumulative release of actinides from the ALMR ER-mineral wasteform at 100000 years for matrix dominated flow. Variations in the water table height were found to have little effect on the maximum possible actinide release when considering the overall CCDF. Figure 6.39 demonstrates that several of the larger releases occurred for realizations where the water table height increased. This relates back to the issue of low ground water travel time because increasing the water table height lowers the ground water travel time. For fracture flow and/or non-sorbing elements, variations in the water table have no effect on the cumulative release since the maximum amount is released regardless of the water table position.

Figure 6.40 demonstrates that the total actinide release to the accessible environment at 100000 years does not depend on the matrix alteration rate for either matrix or fracture flow. It can be seen that there is a significant amount of scatter in the data, however three trends are observed. A high trend exists for releases at approximately 100 Ci that is for fracture flow realizations. Another trend exists at approximately 10^{-1} Ci that arises from the matrix flow realizations that result in high releases (low ground water travel time and low retardation). A lower trend exists at approximately 10^{-6} Ci resulting from matrix flow with long ground water travel times in conjunction with retardation.

Figure 6.41 demonstrates that the total actinide release to the accessible environment is not dependent on the saturated zone percolation flux. This is expected given the large saturated zone flux relative to that of the unsaturated zone. The travel time through the saturated zone is typically on the order of a few thousand years.

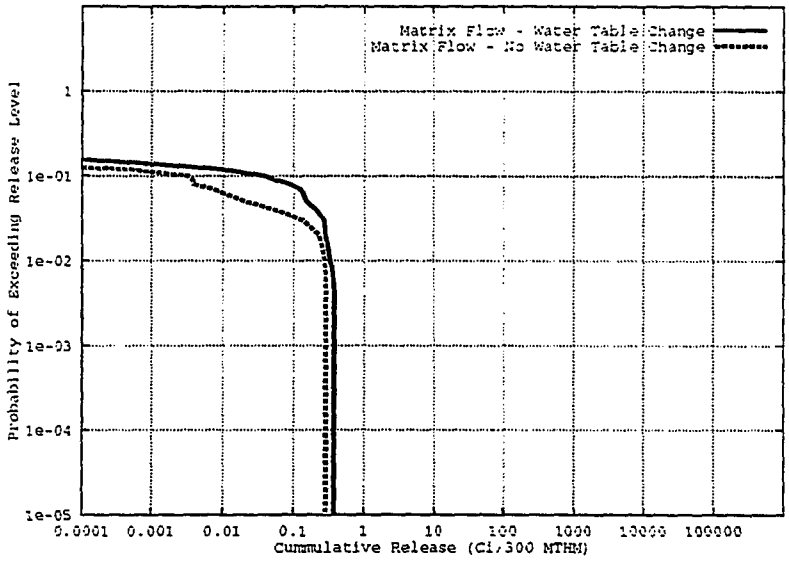

Figure 6.38 Sensitivity Analysis, Total Actinide Release to the Accessible Environment - CCDF Water Table Position, ALMR ER-Mineral Wasteform, Co-Located, 114.0 kW/acre, 100000 years

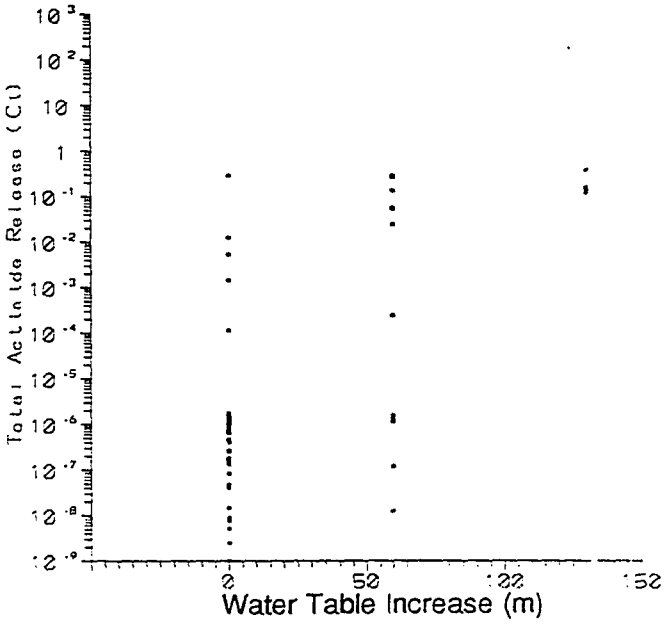

Figure 6.39 Sensitivity Analysis, Total Actinide Release to the Accessible Environment - Water Table Position, ALMR ER-Mineral Wasteform, Co-Located, 114.0 kW/acre, 100000 years

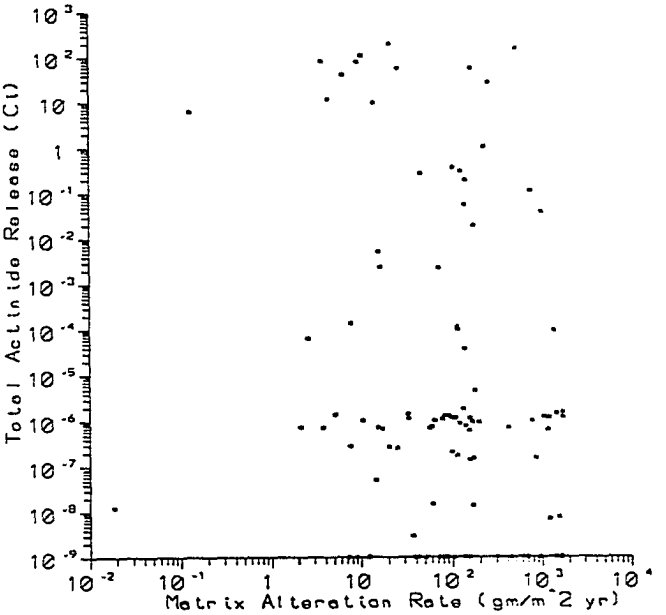

Figure 6.40 Sensitivity Analysis, Total Actinide Release to the Accessible Environment - Matrix Alteration Rate, MMB Container, ALMR ER Mineral Wasteform, Co-Located, 114.0 kW/acre, 100000 years

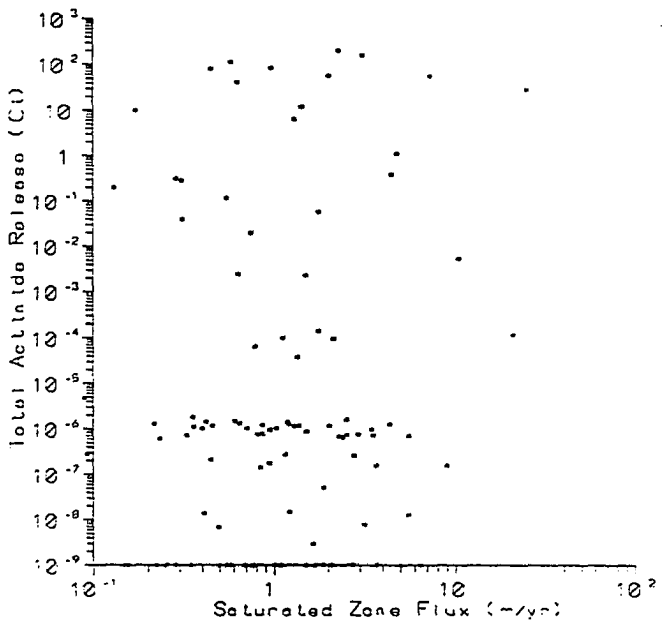

Figure 6.41 Sensitivity Analysis, Total Actinide Release to the Accessible Environment - Saturated Zone Flux, MMB Container, ALMR ER Mineral Wasteform, Co-Located, 114.0 kW/acre, 100000 years

Figure 6.42 shows the cumulative actinide release at 100000 years as a function of the dry infiltration rate for cases of matrix/fracture flow and matrix flow alone. For the matrix/fracture flow case (highest releases), there is no dependence on the dry infiltration rate. For fracture flow with no retardation in the saturated zone, the release is not confined to the very low ground water travel times. Any of the dry infiltration rates sampled, combined with other stochastic parameters (climactic multiplier, rock porosity) can result in ground water velocities of sufficient magnitude to lead to significant releases. This does not hold true for a matrix flow case. Significant releases do not occur for dry infiltration rates less than 10^{-4} m/yr. The higher infiltration rates are required for release due to retardation.

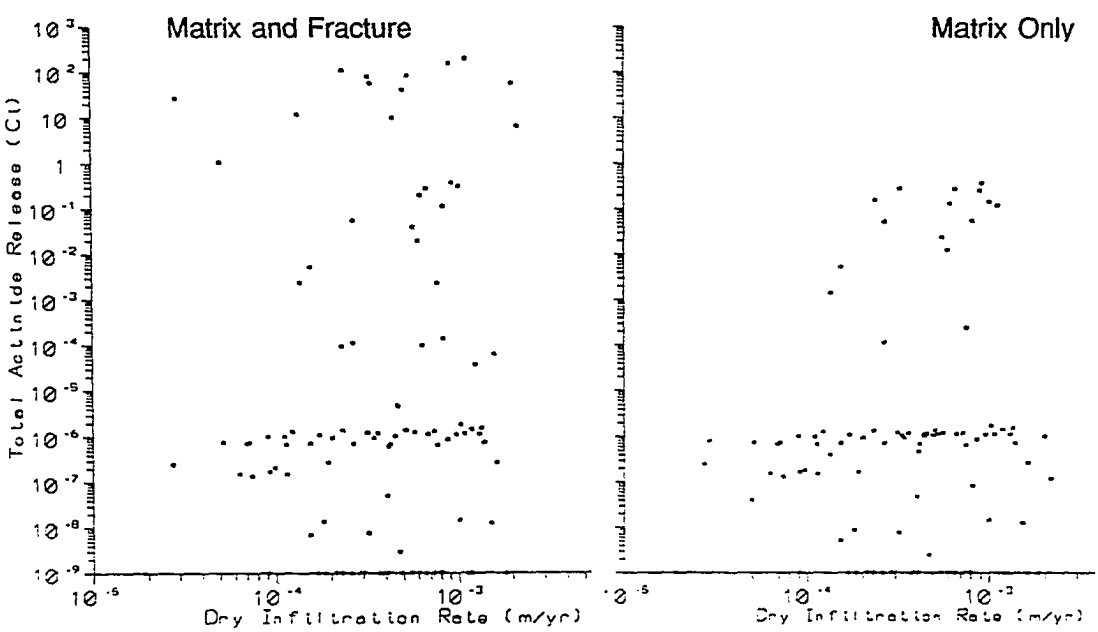

Figure 6.42 Sensitivity Analysis, Total Actinide Release to the Accessible Environment - Dry Infiltration Rate, MMB Container, ALMR ER Mineral Wasteform, Co-Located, 114.0 kW/acre, 100000 years

Figure 6.43 demonstrates that the total actinide release to the accessible environment is not dependent on elemental solubility. The ^{237}Np (matrix) and ^{239}Pu (fracture) solubilities were parameters chosen to investigate. Again, note the three tiered distribution for the case of fracture flow.

The above analysis demonstrated that the total actinide release to the accessible environment depends primarily on the flow mode that is dominating. Attention is now turned to waste package performance. Figure 6.44 shows the dependence of the total actinide release from the waste package at 100000 years on the matrix alteration rate. It can be seen that there is only a slight dependency for matrix alteration rates greater than 1 g/m^2 yr. Below this, the total actinide release begins to decrease rapidly. It is not believed that matrix alteration rates this low can

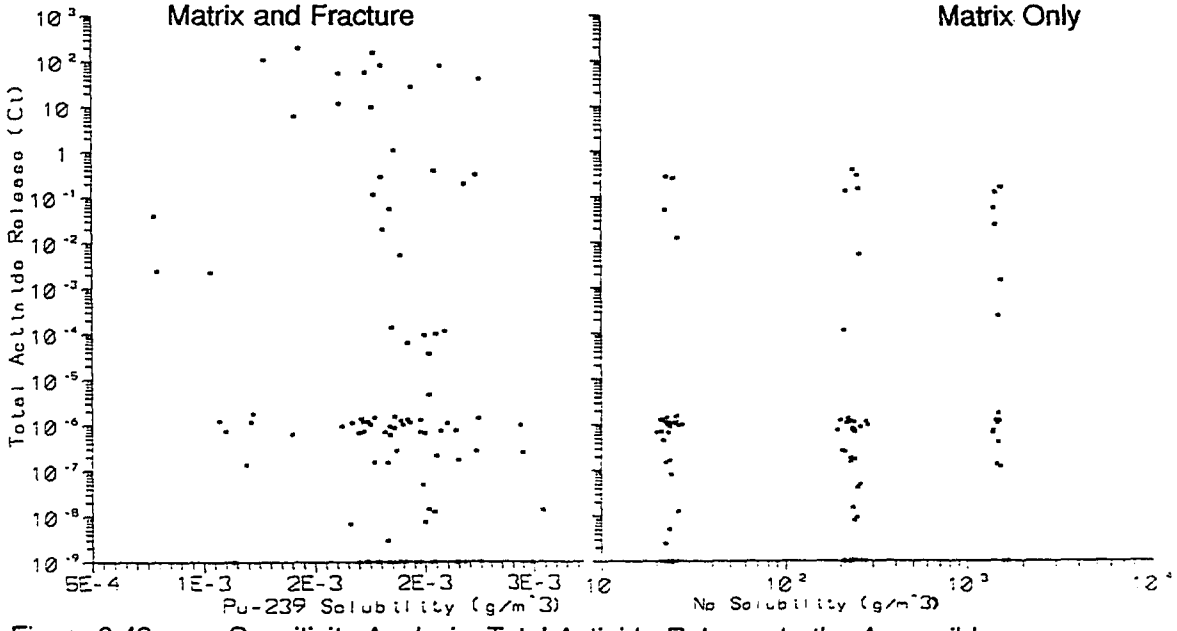

Figure 6.43 Sensitivity Analysis, Total Actinide Release to the Accessible Environment - Np^{237} and Pu^{239} Solubility, MMB Container, ALMR ER Mineral Wasteform, Co-Located, 114.0 kW/acre, 100000 years

be achieved. The nominal matrix alteration rate used in the IMARC analyses (obtained from test measurements) is 182.5 g/m^2 yr. Changes in the matrix alteration rate by an order of magnitude about this value produce no appreciable changes in the total actinide release at 100000 years when utilizing RIP.

Figure 6.45 demonstrates that the dry percolation has no effect on the total actinide release from the waste package at 100000 years. Figures 6.46 and 6.47 demonstrate that neither the effective catchment area nor the geometric factor for diffusion effect the total actinide release from the waste package at 100000 years. Figure 6.48 demonstrates that the solubility of both ^{237}Np and ^{239}Pu do not effect the total actinide release from the waste package at 100000 years.

These sensitivity analyses were repeated at 25000 and 50000 years and identical results were obtained.

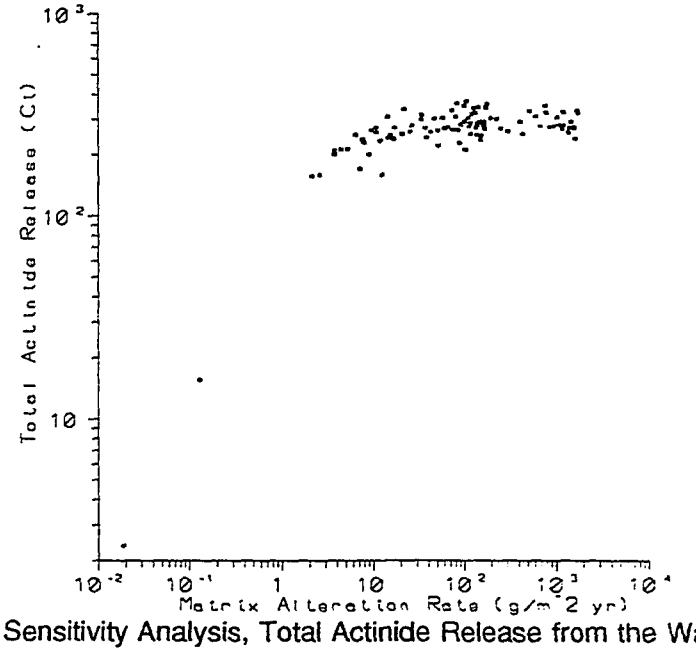

Figure 6.44 Sensitivity Analysis, Total Actinide Release from the Waste Package - Matrix Alteration, MMB Container, ALMR ER Mineral Wasteform, Co-Located, 114.0 kW/acre, 100000 years

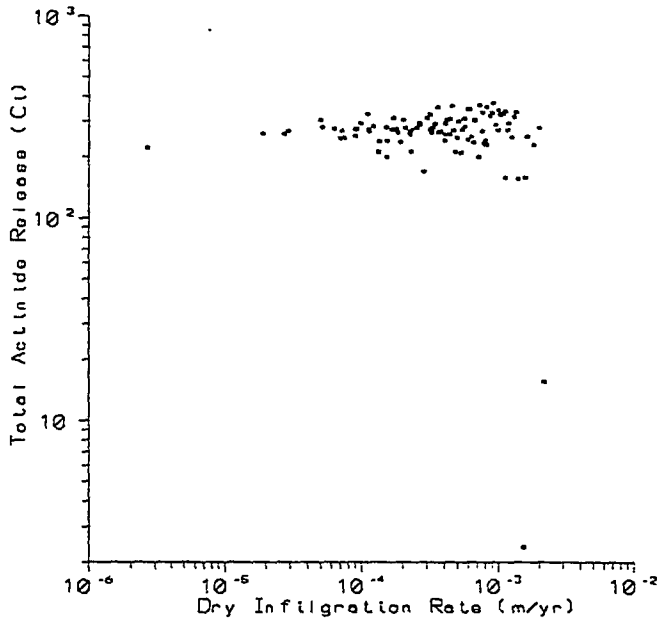

Figure 6.45 Sensitivity Analysis, Total Actinide Release from the Waste Package - Dry Infiltration Rate, MMB Container, ALMR ER Mineral Wasteform, Co-Located, 114.0 kW/acre, 100000 years

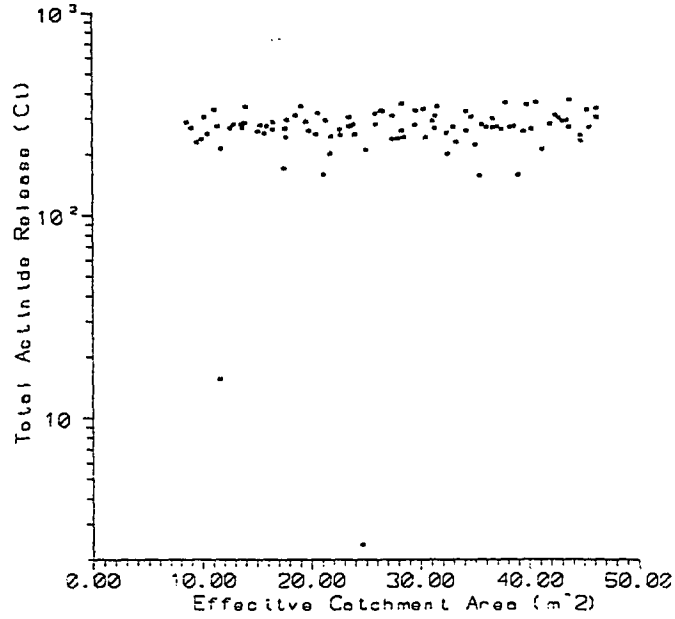

Figure 6.46 Sensitivity Analysis, Total Actinide Release from the Waste Package - Effective Catchment Area, MMB Container, ALMR ER Mineral Wasteform, Co-Located, 114.0 kW/acre, 100000 years

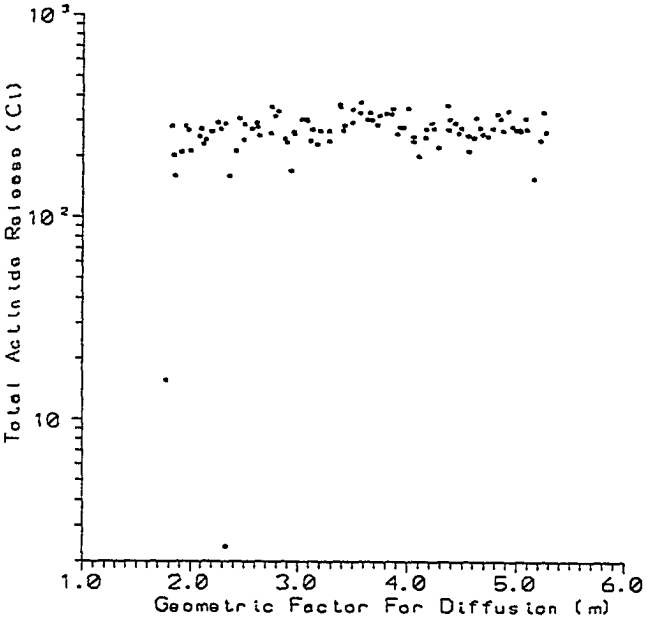

Figure 6.47 Sensitivity Analysis, Total Actinide Release from the Waste Package - Geometric Factor for Diffusion, MMB Container, ALMR ER Mineral Wasteform, Co-Located, 114.0 kW/acre, 100000 years

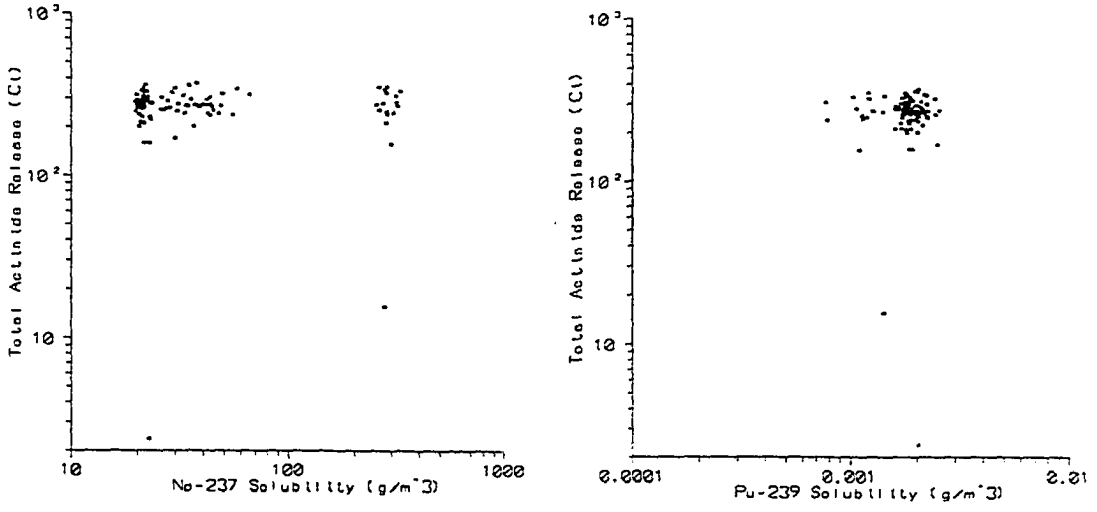

Figure 6.48 Sensitivity Analysis, Total Actinide Release from the Waste Package - Np^{237} and Pu^{239} Solubility, MMB Container, ALMR ER Mineral Wasteform, Co-Located, 114.0 kW/acre, 100000 years

7 CONCLUSION AND FUTURE WORK

7.1 Conclusion

The primary objectives of this research project have been completed. Performance assessment (PA) analyses have been completed for high level nuclear waste forms derived from once through Light Water Reactor (LWR) spent fuel (SF), defense high level waste (DHLW), the closed advanced liquid metal reactor (ALMR) pyroprocess fuel cycle, and the recycling of LWR actinides in the closed ALMR pyroprocess fuel cycle. The IMARC (Integrated Multiple Assumptions and Release Calculations) and RIP (Repository Integration Program) PA tools was utilized.

A model was developed to predict the time dependent failure distribution of the engineered barrier system (EBS). This model utilized the Weibull distribution as the tool to estimate the failure properties of each barrier of the multi-barrier waste containers. The sequential failure of each barrier was included in the model.

The EBS failure model was utilized to predict the time dependent failure distribution of container designs proposed for the isolation of SF and DHLW at Yucca Mountain. It was assumed that a container design similar to that of DHLW will also be used to dispose wastes generated from the ALMR pyroprocess fuel cycle. The near field repository conditions resulting from the emplacement of nuclear waste were accounted for in the estimation of barrier degradation properties. Three emplacement

scenarios were considered for LWR SF with areal power densities (APD) of 28.5, 57.0, and 114.0 kW/acre. These represent cool, moderate, and hot repository thermal loadings. For DHLW and ALMR wastes, two loading scenarios were considered: co-location with LWR SF at an APD of 114.0 kW/acre, and emplacement in the repository alone. The barriers were assumed to fail through both uniform and localized corrosion.

The failure of small single barrier waste containers was found to be dependent on the dry out period only. This container was assumed to be fabricated from corrosion resistant Alloy 825. The Alloy 825 corrosion model did not include any temperature dependency. As such, post dry out repository temperature does not impact container performance. All small single barrier containers used to isolate LWR SF failed within 10,000 years with the 114.0 kW/acre thermal loading resulting in the longest containment.

The failure of large metallic multi-barrier (MMB) containers is dependent on both the dry out period and the post dry out repository temperature. This container was assumed to be fabricated from an outer corrosion allowance carbon steel barrier and an inner corrosion resistant Alloy 825 barrier. The carbon steel corrosion model did include a temperature dependence. All MMB containers used to isolate LWR SF failed within a 50,000 year period with the longest containment resulting from a 114.0 kW/acre thermal loading. The 57.0 kW/acre resulted in the most rapid failure.

An APD of 28.5 kW/acre results in short dry out times and relatively low corrosion rates. A loading of 114.0 kW/acre results in long dry out times, but high relative corrosion rates. When compared to the 28.5 kW/acre loading, the long dry out time overwhelms the slower corrosion rate. A loading of 57.0 kW/acre leads to dry out

times and corrosion rates between the two extremes. The shorter dry out time at 57.0 kW/acre relative to 114.0 kW/acre results in more rapid failure in spite of the reduced corrosion rate. The more rapid corrosion rate at 57.0 kW/acre, relative to 28.5 kW/acre results in more rapid failure in spite of the longer dry out time.

Containers holding either DHLW or ALMR wastes were found to fail at essentially the same rate as the same containers holding LWR SF when these wasteforms are co-located in the repository. When the DHLW or ALMR wastes are emplaced in the repository alone utilizing a MMB container, the containment time increases significantly. All containers fail within a 150,000 year period. This results from the low corrosion rates due to the lower repository temperature.

The results from applying the EBS failure model to the various wasteform/ container designs were used to determine container failure parameters (Weibull parameters) for input into the PA tools.

Source term models were obtained from available sources for LWR SF and DHLW. The source term models developed for the various pyroprocess wasteforms were based on a combination of laboratory measurements and those models presented in the literature. The initial inventory of radionuclides within each wasteform was obtained, and in the case of the pyroprocess wasteforms, adjusted to account for the current processes being developed. Both low and high pyroprocess actinide recovery factors were considered. Empirical relations were developed to model the buildup of ^{237}Np and ^{234}U daughter products during the isolation period. These relations were used in the IMARC analyses, but could not be implemented in RIP.

IMARC and RIP PA analyses were conducted to evaluate the performance at

Yucca Mountain of the SF waste form, the metallic/mineral waste forms from the pyroprocessing of ALMR fuel, and the metallic/mineral waste forms from the pyroprocessing of spent LWR fuels to recycle actinides. Three repository thermal loadings (APDs 28.5, 57.0 and 114.0 kw/acre) were evaluated for SF. Two emplacement scenarios were evaluated when considering the various pyroprocess waste forms. The first case considered the co-location of the pyroprocess waste forms with SF at an APD of 114.0 kw/acre. The second case considered the emplacement of the pyroprocess waste forms in the repository alone. Two waste container designs were considered. These are a small, single metallic barrier, borehole emplaced container (SCP) for LWR SF, and a large metallic multi-barrier, drift emplaced container (MMB) for LWR SF, DHLW, and the ALMR wastes.

The IMARC PA tool was modified to evaluate the waste forms considered in this study. The modifications required were 1) the initial inventory of radionuclides contained in each waste container, 2) the inclusion of a parametric estimate of radionuclide daughter product build-up, and 3) changes to the source term models to reflect the waste form type (alteration rate) and waste package physical characteristics.

A set of RIP models were developed based on existing Yucca Mountain PA analyses for each wasteform/container under consideration. Modifications or enhancements to these models were made to 1) account for higher ground water percolation under pluvial conditions, 2) include a model for fracture dominated flow, 3) adjust the initial inventory of radionuclides contained in each waste container, 4) change the source term models to reflect the waste form type (alteration rate) and waste package physical characteristics.

The results of the PAs for LWR SF are summarized in Table 7.1. The differences between the RIP and IMARC results at 10000 years are attributed to the modeling of unsaturated zone percolation flux. The high unsaturated zone percolation flux used in the IMARC analyses is over ten times greater than the expected unsaturated zone percolation flux utilized in the RIP analyses. This leads to faster travel times between the repository and the accessible environment in certain branches of the IMARC logic tree.

Table 7.1: Summary of IMARC and RIP Results for LWR SF

PA Tool	10000 years	50000 and 100000 years
IMARC	Release of both actinides and fission products from both container designs. APD of 114.0 kW/acre smallest (no release from MMB container). Release from MMB container smaller (or non-existent) relative to SCP container for a given APD.	Cumulative release of actinides and fission products essentially identical regardless of thermal loading for given container design. Release of actinides and fission products slightly smaller for MMB container relative to SCP container.
	Actinide release dominated by ^{237}Np and its daughters, ^{239}Pu, and ^{240}Pu. Fission product release dominated by ^{99}Tc.	
RIP	Fission product release and small actinide release for APD = 28.5 and 57.0 kW/acre for SCP container. Small fission product release and no actinide release for APD = 114.0 kW/acre for SCP container. Small fission product release only for MMB container at APDs of 28.5 and 57.0 kW/acre (no fission product release for APD = 114.0 kW/acre. Release from MMB container smaller (or non-existent) relative to SCP container for a given APD.	Cumulative release of fission products essentially identical regardless of thermal loading for given container design. Actinide release dependent on APD. Release of fission products identical for both container designs. Actinide release essentially identical at APDs of 57.0 and 114.0 kW/acre. For APD = 28.5 kW/acre release from MMB higher.
	Actinide release dominated by ^{239}Pu, ^{237}Np, and ^{234}U for fracture flow and ^{237}Np and ^{234}U for matrix fllow. Fission product release dominated by ^{99}Tc for both flow modes.	

At 50000 and 100000 years, the IMARC results indicate that for a given container design the total actinide release is independent of the APD while the RIP results show that the release is dependent on the APD. This difference is attributed to the temperature dependent Pu solubility limit model utilized in RIP. As the APD, and hence repository temperature increases, the solubility of Pu decreases. This results in a reduction in the amount of plutonium, hence total actinide, released.

The results of the PAs for the ALMR and LWR actinide recycle wasteforms are summarized in Tables 7.2 and 7.3, respectively for the low pyroprocess actinide recovery cases. Both show actinide releases less than those obtained for LWR SF. Emplacing these wastes into the repository alone resulted in lower releases due to longer container lifetime.

Sensitivity analyses were conducted using both IMARC and RIP regarding the performance of the ALMR wasteforms. For the IMARC analyses, the electrorefiner metallic wasteform was considered. For the RIP analyses, the electrorefiner mineral wasteform was considered. The performance of other wasteforms (LWR SF, other pyroprocess wasteforms, and DHLW) are also expected to behave similarly with respect to variations in the parameters evaluated.

Both IMARC and RIP indicate that increasing the pyroprocess actinide recovery factor leads to significant reductions in the total actinide release to the accessible environment. The fission product release is not impacted.

Both tools also indicate that the cumulative release of actinides to the accessible environment is strongly dependent on the ground water flow mode. The maximum releases were found to occur when fracture flow dominates. Under matrix

Table 7.2: Summary of IMARC and RIP Results for the ALMR Wasteforms

PA Tool	10000 years	50000 and 100000 years
IMARC	Small releases when co-located with LWR SF. Probability of any release less than 10^{-2}. Maximum actinide release < 10 Ci/300 MTHM, Maximum fission product release < 100 Ci/300 MTHM. No release from LWR SF - MMB container at 114.0 kW/acre. No release when emplaced alone	Release of actinides significantly lower than that observed for LWR SF when co-located. (maximum possible actinides release lower by over two orders of magnitude). Significant reductions in release when emplaced alone (factor of four at 50000 years and factor of two at 100000 years). Release of fission products essentially identical (slightly lower) than that observed for LWR SF when co-located. Further reduction when emplaced alone.
	Total release dominated by fission product release from electrorefiner metallic wasteform. Fission product release dominated by ^{99}Tc. Actinide release comparable from both electrorefiner metallic and mineral wasteforms. Dominated by ^{239}Pu, and ^{240}Pu.	
RIP	No actinide or fission product release observed.	Release of actinides significantly lower than that observed for LWR SF when co-located. (maximum possible actinides release lower by well over one order of magnitude). Significant reductions in actinide release when emplaced alone (nearly an order of magnitude at 50000 years and factor of three at 100000 years). Release of fission products essentially identical (slightly lower) than that observed for LWR SF when co-located. Further reduction when emplaced alone.
	Total release dominated by fission product release from electrorefiner metallic wasteform. Fission product release dominated by ^{99}Tc. Actinide release comparable from both electrorefiner metallic and mineral wasteforms. Dominated by ^{239}Pu, and ^{240}Pu for fracture flow, ^{237}Np and ^{235}U for matrix flow.	

dominated flow, sorption of the actinides, particularly plutonium, is greatly enhanced. Under matrix flow conditions, ^{237}Np and ^{235}U dominate the release of actinides. A larg reduction in the total actinide release is seen for the pyroprocess wasteforms, relative to that observed for LWR SF, due to the significantly lower ^{237}Np and ^{241}Pu inventories in the waste. The release of fission products (primarily ^{99}Tc) is independent of the flow

Table 7.3: Summary of IMARC and RIP Results for the LWR Actinide Recycle Wasteforms

PA Tool	10000 years	50000 and 100000 years
IMARC	Small releases when co-located with LWR SF. Probability of any release less than 10^{-2}. Maximum actinide release < 10 Ci/300 MTHM, Maximum fission product release < 100 Ci/1000 MTHM. No release from LWR SF - MMB container at 114.0 kW/acre. No release when emplaced alone	Release of actinides significantly lower than that observed for LWR SF when co-located. (maximum possible actinides release lower by over two orders of magnitude). Significant reductions in release when emplaced alone (factor of four at 50000 years and factor of two at 100000 years). Release of fission products essentially identical (slightly lower) than that observed for LWR SF when co-located. Further reduction when emplaced alone.
	Total release dominated by fission product release from electrorefiner metallic wasteform. Fission product release dominated by ^{99}Tc. Actinide release comparable from both electrorefiner metallic and mineral wasteforms. Dominated by ^{239}Pu, and ^{240}Pu. ^{237}Np inventory effectively reduced.	
RIP	No actinide or fission product release observed.	Release of actinides significantly lower than that observed for LWR SF when co-located. (maximum possible actinides release lower by well over one order of magnitude). Significant reductions in actinide release when emplaced alone (nearly an order of magnitude at 50000 years and factor of three at 100000 years). Release of fission products essentially identical (slightly lower) than that observed for LWR SF when co-located. Further reduction when emplaced alone.
	Total release dominated by fission product release from electrorefiner metallic wasteform. Fission product release dominated by ^{99}Tc. Actinide release comparable from both electrorefiner metallic and mineral wasteforms. Dominated by ^{239}Pu, and ^{240}Pu for fracture flow, ^{237}Np and ^{235}U for matrix flow. ^{237}Np inventory effectively reduced, but still dominates under matrix flow.	

mode since they do not strongly sorb to tuff.

The IMARC sensitivity analyses indicate that the cumulative release of actinides to the accessible environment is also strongly dependent on the container failure parameters, the water contact mode, and the matrix alteration rate. Several wasteform

design (effective catchment area, internal free volume, wasteform radius) and repository near field (backfill diffusion coefficient, porosity, and hydraulic saturation) variables were found not to impact wasteform performance.

The RIP sensitivity analysis indicates that the release of actinides to the accessible environment is not dependent on the matrix alteration rate, the saturated zone ground water flow rate, or elemental solubility properties. It was found that the release to the accessible environment is dependent on the ground water travel time (dry infiltration rate, climactic multiplier, and rock porosity) and elemental sorptive properties. For fracture flow, significant actinide releases occur in a 100000 year period only for ground water travel times less than 100000 years. For matrix flow, the significant releases occur in a 100000 year period only for very low ground water travel times and low retardation coefficients, particularly in the de-vitrified rock layers.

The RIP sensitivity analysis indicated that the total actinide release from the waste package is slightly dependent on the matrix alteration rate only at low levels (below those assumed in the IMARC analyses). No other variables were found to impact the release from the waste package.

The overall conclusion drawn from the use of two PA tools is that the total actinide release to the accessible environment is substantially lower for the ALMR and LWR actinide recycle wasteforms relative to LWR SF. It should be noted that in both the IMARC and RIP PA models, the maximum releases occur for fracture dominated flow. As stated before, under matrix dominated flow, sorption of the actinides (particularly plutonium) is greatly enhanced and ^{237}Np tends to dominate the total

actinide release. The release of fission products is independent of the flow mode since they do not strongly sorb to tuff and will dominate the release in a matrix flow situation.

As such, the benefits of incorporating LWR actinides into the closed ALMR fuel cycle are apparent at Yucca Mountain regardless of the flow mode. If fracture flow dominates, the reduction in the plutonium inventory through recycling will lead to reductions in the total actinide release relative to that from LWR SF. If matrix flow dominates, the reduction in the neptunium and plutonium inventory (^{241}Pu especially) through recycling leads to reductions in the total actinide release relative to that from LWR SF. The degree of reduction is largest when matrix flow dominates since the ALMR is fueled with ^{239}Pu and under fracture flow conditions any plutonium that escapes from the closed fuel cycle is released to the accessible environment. Under matrix flow conditions, all plutonium is retarded and the ^{237}Np is reduced significantly due to fissioning in the reactor.

Regardless of the flow mode at Yucca Mountain, the radionuclide release to the accessible environment can be reduced by utilizing an LWR actinide recycle campaign in conjunction with ALMRs. The optimum future scenario involving nuclear reactors is to process all LWR fuel to recover the actinides and then use it to fuel ALMRs. This results in ALMR and actinide recycle wastes being emplaced in the repository alone. Heat generation will be negligible, leading to a low repository temperature and low corrosion rates. In addition, the uncertainty regarding the repository hydrothermal conditions over long time scales and the associated uncertainty in future ground water chemistry, container performance, and waste form dissolution will be reduced

significantly. The development of a pyroprocess with a high actinide recovery factor will lead to a further reduction in the release of actinides to the environment.

IMARC and RIP PA analyses were also conducted to evaluate the behavior of various wasteforms produced by weapons grade plutonium disposition options. The options evaluated included spiking in an LWR or ALMR, irradiating to a burnup level commensurate with spent fuel in an LWR or an ALMR, irradiating in an ALMR and subsequent pyroprocessing in a closed fuel cycle, and mixing with DHLW and vitrification into borosilicate glass. Both IMARC and RIP indicate that the once through spiking and spent fuel options result in large releases to the accessible environment regardless of the reactor design utilized. The IMARC PA analyses indicate that the once through LWR and ALMR options result in essentially identical releases, the DHLW option gives the largest release, and the ALMR closed fuel cycle option gives the lowest release.

The RIP PA analyses indicate that at 50000 years the once through options are comparable, and largest. At 100000 years the ALMR options result in the largest releases. The RIP results indicate that the DHLW release is less than that resulting from IMARC. This is attributed to different implementations of the matrix alteration rate models in each tool. RIP also indicates that the ALMR closed fuel cycle option gives the lowest release.

Based on these analyses, it is concluded that using the weapons grade plutonium in a closed ALMR fuel cycle will lead to significant reductions in the actinide release to the accessible environment. This again assumes that fracture dominated flow conditions exist in the repository environment.

7.2 Future Work

The completion of this project has given rise to several areas where future research endeavors are warranted. These are discussed below.

- Further refine the engineered barrier performance model to include non-sequential, independent failure modes. These could include weld failure, galvanic corrosion, microbiological enhanced corrosion, microstructrural degradation, internal degradation due to nitric acid evolution (primarily from water logged LWR spent fuel rods.
- Application of the engineered barrier system model to other container designs that are proposed.
- Further investigation into fracture dominated flow at Yucca Mountain. The results presented in this project depend strongly upon the flow mode. If fracture flow with little retardation exists, significant releases occur from all wasteforms considered with ^{239}Pu being the dominant actinide released. If matrix flow exists, the release is reduced significantly (especially for the pyroprocess wasteforms), and is dominated by ^{237}Np. Which radionuclide is released to the accessible environment may be a significant factor in the radiation dose that members of the public could receive. In addition, it has been shown that the benefits of the closed pyroprocess fuel cycle are stronger when matrix flow is prevalent.
- Conduct a probability - based radiation dose assessment based on the models detailed in this project. Future licensing criteria may be based on radiation dose. In addition, comparisons of wasteform performance that are based on

radiation dose may reveal additional information that has not been observed. It will be necessary to consider dispersion of the radionuclides within both the geosphere and biosphere.

- A significant amount of uncertainty exists regarding future climactic changes and its effects on ground water percolation at Yucca Mountain. Although the RIP analyses indicate that the cumulative release of actinides over the long-term to the accessible environment does not depend on the ground water flow, the timing of the release will depend heavily on the ground water flow. Further studies are needed to determine the time-history performance of both wasteform release and accessible environment release as a function of ground water flow.
- The source term models for the ALMR wasteforms were based on short duration laboratory tests in water. Further testing is warranted to determine the performance characteristics of these wasteforms in the long-term and under off-normal environmental conditions. The results of these tests can be included in subsequent performance assessment analyses.
- The source term models used for all wasteforms are quite simple with release controlled by either diffusive or advective processes. For most of the actinides the release is solubility limited. Further research is needed to identify whether the release of actinides is solubility limited or if any other transport mechanisms exist.
- Additional research is needed to identify the final chemical species that will exist following wasteform dissolution. For example, certain species may exist,

such as colloids, where mass transport away from the waste package and through the geosphere is enhanced. Other species may form that have rather low solubility concentrations and will precipitate.

- The issue of nuclear criticality has recently been brought up especially in the case of isolating weapons grade plutonium. Both IMARC and RIP can be used to track the migration of radionuclides over time in a probabilistic nature. The results can be used in conjunction with neutronic analyses to determine the probability of a critical situation existing in the long term.

REFERENCES

[1] Y.S. Tang, and J.H. Saling, Radioactive Waste Management, Hemisphere Publishing Company, Washington DC, 1990.

[2] Characteristics of Potential Repository Wastes, Office of Civilian Radioactive Waste Management, U.S. Department of Energy, Washington DC 1992, DOE/RW-0184-R1

[3] 97th United States Congress, Nuclear Waste Policy Act of 1982, Public Law 97-435, 1983.

[4] Environmental Assessment, Deaf Smith County Site, Texas, Volumes 1-3, U.S. Department of Engery, Washington DC, 1986, DOE/RW-0069.

[5] Environmental Assessment, Reference Repository Location, Hanford Site, Washington, Volumes 1-3, U.S. Department of Energy, Washington DC, 1986, DOE/RW-0071.

[6] Environmental Assessment - Yucca Mountain Site, Nevada Research and Development Area, Nevada, Volumes 1-3, U.S. Department of Energy, Washington DC, 1986, DOE/RW-0073.

[7] 100th United States Congress, Nuclear Waste Policy Ammendment Act, Omnibus Budgen Reconciliation Act for Fiscal Year 1988, Public Law 100-203, 1987.

[8] Site Characterization Plan, Yucca Mountain Site, Nevada Research and Development Area, Nevada, Volumes 1-6,U.S. Department of Energy, Washington DC, 1988, DOE/RW-0199.

[9] Code of Federal Regulations, Title 10, Part 60, 1994

[10] Code of Federal Regulations, Title 40, Part 191, 1994

[11] 102nd United States Congress, Energy Policy Act of 1992, Public Law 102-486, 1992.

[12] Demonstration of a Risk-Based Approach to High-Level Radioactive Waste Repository Evaluation, Electric Power Research Institute, 1990, EPRI-NP-7057.

[13] Phase 2: Demonstration of a Risk-Based Approach to High-Level Radioactive Waste Repository Evaluation, Electric Power Research Institute, 1992, EPRI-TR-100384.

[14] Total System Performance Assessment - 1993: An Evaluation of the Potential Yucca Mountain Repository, Prepared for the U.S. Department of Energy By Intera, Inc. March 1994, Document Number B00000000-01717-2200-00099-Rev.01.

[15] RIP Repository Performance Assessment and Strategy Evaluation Model: Theory and Capabilities, Version 3.20, Golder Associates Inc, Redmond WA, 933-1469, May, 1994.

[16] RIP Repository Performance Assessment and Strategy Evaluation Model: User's Guide, Version 3.20, Golder Associates Inc, Redmond WA, 933-1469, May, 1994.

[17] An Initial Total-System Performance Assessment for Yucca Mountain. Sandia National Laboratory, 1992, SAND-91-2795.

[18] Total - System Performance Assessment for Yucca Mountain - SNL Second Iteration (TSPA-1993), Sandia National Laboratory, 1194, SAND-93-2675.

[19] The New Reactors, Nuclear News 35, No. 9, 65, 1992.

[20] F.E. Tippets, S.M. Davies, L.N. Salerno, C.R. Snyder, "Prism: A Passively Safe, Economical, and Testable Advance Power Reactor," Proceedings of the American Power Conference, Volume 48, 1986, p. 694.

[21] R.C. Berglund, P.M. Magee, C.E. Boardman, G.L. Gyorey, "Performance and Safety Design of the Advanced Liquid Metal Reactor," Proceedings of the American Power Conference, Volume 53-1, 1991, p. 440.

[22] Y.I. Chang, "The Integral Fast Reactor," Nuclear Technology, Vol. 88, Nov. 1989, p. 129.

[23] C.E. Till and Y.I. Chang, "The Integral Fast Reactor Concept," Proceedings of the American Power Conference, Volume 53-1, 1991, p. 440.

[24] Y.I. Chang, "Fission Energy: The Integral Fast Reactor," Argonne National Laboratory Report DE90 001760, CONF-8909263-1, 1989.

[25] C.E. Till, Y.I. Chang, M.J. Lineberry, "The Integral Fast Reactor," Argonne National Laboratory Report DE90 005659, CONF-900305-1, 1990.

[26] Y.I. Chang, "A Next - Generation Reactor Concept: The Integral Fast Reactor (IFR)," Proceedings of the Seventh KAIF/KNS Annual Conference, Seoul, South Korea, 1992, CONF-290417.

[27] M.J. Lineberry, D.R. Pedersen, L.C. Walters, "Advances in the Integral Fast Reactor Program," Proceedings of the American Power Conference, Volume 53-1, 1991, p. 434.

[28] Y.I. Chang and C.E. Till, "Economic Prospects of the Integral Fast Reactor (IFR) Fuel Cycle," Proceedings of hte International Conference on Fast Reactors and Related Fuel Cycles, Kyoto, Japan, October 28 - November 1, 1991.

[29] C.E. Till and Y.I. Chang, "Integrating the Fuel Cycle at IFR," Nuclear Engineering International, Nov. 1992, p. 33.

[30] P.H. Royl, J.E. Cahalan, G. Friedel, G. Kussmaul, J. Moreau, M. Perks, R.A. Wigeland, "Performance of Metal and Oxide Fuel Cores During Accidents in Large Liquid-Metal-Cooled Cores," Nuclear Technology, Vol. 97, Feb. 1992, p. 198.

[31] J.P. Ackerman, "Chemical Basis for Pyrochemical Reprocessing Nuclear Fuel," Industry and Chemical Research, Vol 30, No. 1, 1991, p.141.

[32] Z. Tomczuk, J.P. Ackerman, R.D.Wolson, and W.E. Miller, "Uranium Transport to Solid Electrodes in Pyrochemical Reprocessing of Nuclear Fuel," Journal of the Electrochemical Society, Vol 139, No. 12, 1992, p. 3523.

[33] L.S. Chow, J.K. Basco, J.P. Ackeman, T.R. Johnson, Molten Salt/Metal Extraction for Recovery of Transuranic Elements, Argonne National Laboratory, 1992, ANL/CP-75688.

[34] T.R. Johnson, M.A. Lewis, A.E. Newman, J.J. Laidler, "Treatment of High-Level Wastes from the IFR Fuel Cycle," Proceedings of the American Chemical Society Meeting, Washington D.C., August 23-28, 1992.

[35] Unpublished work, T.R. Johnson, Argonne National Laboratory, 1992.

[36] W.H. Hannum, J.E. Battles, T.R. Johnson, C.C. McPheeters, "Actinide Consumption: Nuclear Resource Conservation Without Breeding," Proceedings of the American Power Conference, Volume 53-1, 1991, p. 1208.

[37] Projected Waste Packages Resulting From Alternative Spent Fuel Separation Processes, Electric Power Research Institute, 1991, EPRI-NP-7262.

[38] Unpublished work, C.C. McPheeters and R.D. Pierce, Argonne National Laboratory, 1992.

[39] Personal Communication with J.P. Ackerman, Argonne National Laboratory, June 29, 1994.

[40] The Effects of Transuranic Separation on Waste Disposal, Electric Power Research Institute, 1991, EPRI-NP-7263.

[41] "Status of Electrometallurgical Treatment," Presented by J.P. Ackerman (ANL) to the Technology Integration Working Group in support of the DOE Technology Integration Plan, Feb. 1, 1995.

[42] M. Benedict, T.H. Pigford, H.W. Levi, Nuclear Chemical Engineering, Second Edition, McGraw-Hill Book Company, New Yory, 1981.

[43] T.H. Pigford, Actinide Burning and Waste Disposal, University of California, Berkely, Nuclear Engineering Department, 1990, UCB-NE-4176.

[44] F.Berkhout, A. Diakov, H. Fieveson, M. Miller, F. Von Hippel, "Plutonium: True Separation Anxiety," The Bulletin of the Atomic Scientists, Vol. 48, No. 9, Nov. 1992, p.28.

[45] J.J. Stern, "Weapons Material and the Commercial Fuel Cycle," Transactions of the ANS, Vol 68, 1993, p. 72.

[46] F. Von Hippel, M. Miller, H. Fieveson, A. Diakov, F. Berkhout, "Eliminating Nuclear Warheads," Scientific American, Aug. 1993, p. 44.

[47] K.K.S. Pillay, "Disposition Scentarios and Safeguardability of Fissile Materials Under START," Transactions of the ANS, Vol 69, 1993, p. 99.

[48] G. Grewal, C. Guenther, W. Wood, B. Birnham, "Storage of Weapons Grade Plutonium," Transactions of the ANS, Vol 69, 1993, p. 90.

[49] M.R. Buckner, P.B. Parks, J.G. Angelos, J.M. McKibben, "Ability of SRS to Support Plutonium Disposition Options," Transactions of the ANS, Vol 69, 1993, p. 92.

[50] G.F. Berkhout, "Civil Plutonium in Europe and Japan," Plutonium and Security, The Military Aspects of the Plutonium Economy, F. Barnaby, ed. Macmillan Acedemic and Professional, Ltd. London, 1992.

[51] Pu Disposition Study Requirements Document, Office of Nuclear Energy, U.S. Department of Energy, March 1993.

[52] R.W. Rathburn, J.R. Chandler, "Utilization of Weapons Plutonium in LWR Cores," Transactions of the ANS, Vol 68, 1993, p. 73.

[53] W.W. Crump, E.P. Flynn, R.W. Knapp, "System 80+: The Premeir Plutonium Burner," Transactions of the ANS, Vol 68, 1993, p. 75.

[54] D. Biswas, R. Rathburn, H. Garkisch, "Characteristics of a 100% MOX-Fueled PWR Design for Weapons Plutonium Disposition," Transactions of the ANS, Vol 69, 1993, p. 95.

[55] W.H. Hannum and M.J. Lineberry, "Flexible Plutonium Management With IFR Technology," Transactions of the ANS, Vol 69, 1993, p. 91.

[56] Management and Disposition of Excess Weapons Grade Plutonium: Report of the Panel on Reactor-Related Options, National Academy Press, Washington DC, 1994.

[57] U. Gat, J.R. Engel, H.L. Dodds, "Molten Salt Reactor for Burning Dismantled Fuel," Nuclear Technology, Vol. 100, No. 3, 1992, p. 390.

[58] D. Alberstein, A.M. Baxter, C.J. Hamilton, "The MHTGR - Maximum Plutonium Destruction Without Recycle," Transactions of the ANS, Vol 69, 1993, p. 95.

[59] C.D. Bowman, F.Venneri, "Accelerator Driven Thermal Spectrum System for Weapons Plutonium Destruction," Transactions of the ANS, Vol 69, 1993, p. 102.

[60] J.M. Ryskamp, B.G. Schnitzler, C.D. Fletcher, R.L. Moore, M.J. Gaetta, L.B. Lundberg, S.N. Jahshan, G.S. Chang, "A New Reactor Concept Without Uranium or Thorium for Burning Weapons Grade Plutonium," Transactions of the ANS, Vol 69, 1993, p. 96.

[61] D.A. Brownson, D.J. Hanson, "Evaluation of Weapons Grade Plutonium Disposition Options," Transactions of the ANS, Vol 69, 1993, p. 100.

[62] Waste Package Design Status Report, Fiscal Year 1993, Office of Civilian Radioactive Waste Management, U.S. Department of Energy, Sept. 1993, U.S. DOE Document No. B00000000-570500007-00.

[63] Survey of Degradation Modes of Candidate Materials for High-Level Radioactive-Waste Disposal Containers, Lawrence Livermore National Laboratory, 1988, UCID-21362, Volumes 1-8.

[64] W.M. Nutt, D.W. Vinson, and D.B. Bullen, "A Review of Iron-Base, Corrosion-Allowance Materials for High-Level Waste Disposal Containers: I. Atmospheric Corrosion, II. Aqueous Corrosion," Accepted for publication in Corrosion Reviews, September 21, 1994.

[65] G.E. Gdowski, Survey of Degradation Modes of Four Nickel Chromium Molybdenum Alloys, Lawrence Livermore National Laboratory, March 1991, UCRL-ID-108330.

[66] J.K. McCoy, T.W. Doering, "Prediction of Cladding Life in Waste Package Environments," High Level Radioactive Waste Management, Proceedings of the Fifth International Conference, Las Vegas, Nevada, April 1994, Volume 1, p. 565.

[67] D.B. Bullen, "Containment Barrier System Performance Assessment Modelling," High Level Radioactive Waste Management, Proceedings of the Fourth International Conference, Las Vegas, Nevada, April 1993, Volume 1, p. 470.

[68] Cho-Chi Hu, Failure Rate Evaluation of Multi-Purpose Unit (MPU) Containers in Various Thermal Environments With a Revised Containment Barrier System (CBS) Model, Masters Thesis, Iowa State University, Ames IA, 1993.

[69] D.B. Bullen, "Performance Assessment Modeling of a Multi-Purpose Container," Scientific Basis for Nuclear Waste Management XVII, Materials Research Society, Pittsburgh, Pa. 1993, p. 860.

[70] T.A. Buscheck and J.J. Nitao, "The Analysis of Repository Heat-Driven Hydrothermal Flow At Yucca Mountain," High Level Radioactive Waste Management, Proceedings of the Fourth International Conference, Las Vegas, Nevada, April 1993, Volume 1, p. 847.

[71] T.A. Buscheck, J.J. Nitao, S.F. Saterlie, "Evaluation of Thermo-Hydrological Performance in Support of the Thermal Loading Systems Study," High Level Radioactive Waste Management, Proceedings of the Fifth International Conference, Las Vegas, Nevada, April 1994, Volume 1, p. 592.

[72] Evaluation of Spent Fuel as a Final Waste Form, International Atomic Energy Agency, Technical Report Series No. 320, Vienna, Austria, 1991.

[73] W.M. Nutt, The Velocity Dependent Dissolution of Spent Nuclear Fuel in a Geologic Repository, Masters Thesis, Iowa State University, Ames IA, 1989.

[74] W.J. Gray, H.R. Leidler, S.A. Steward, "Parametric Study of LWR Spent Fuel Dissolution," Journal of Nuclear Materials, Vol. 190, 1992, p. 46.

[75] R.E. Einziger, J.A. Cook, "Behavior of Breached Light Water Reactor Spent Fuel Rods in Air and Inert Atmospherses at 229oC," Nuclear Technology, Vol. 69, April 1985, p. 55.

[76] W.L. Bourcier, "Dissolution of Nuclear Waste Glass as a Function of pH, Time, and Temperature," Materials Research Society Symposium Proceedings, Vol. 212, Materials Research Society, Pittsburgh Pa, 1990, p. 371.

[77] H.H. Uhlig, Corrosion and Corrosion Control, 2nd Edition, John Wiley and Sons, New York, 1971.

[78] A.J. Patterson, Radiolysis Effects on Steel Waste Containers Employed in a Spent Nuclear Fuel Dry Storage Environment, Masters Thesis, Iowa State University, Ames IA, 1994.

[79] A.J. Hallihan, Jr., "A Review of the Weibull Distribution", Journal of Quality Technology, Volume 25, No. 2, April 1993, p. 85.

[80] Zirconium Alloy Fuel Clad Tubing, Engineering Guide, First Edition, Sandvik Special Metals Corporation, Kennewick WA, December 1989.

[81] J.J. Duderstadt, L.J. Hamilton, Nuclear Reactor Analysis, John Wiley and Sons, New York, 1976.

[82] Unpublished work, M.A. Lewis, L.J. Smith, T. Koyama, T.R. Johnson, Argonne National Laboratory, 1992.

[83] RadDecay 4.01, Grove Engineering, Incorporated, Rockville MD, 1991.

[84] Personal Communication with J.P. Ackerman, Argonne National Laboratory, January 13, 1995.

[85] ORIGEN 2.1 Isotope Generation and Depletions Code Matrix Exponential Method, CCC-371, Radiation Shielding Information Center, Oak Ridge National Laboratory, August 1991.

[86] IMARC: Integrated Multiple Assumptions and Release Calculations User's Manual, Developed by Risk Engineering Corporation for Electric Power Research Institute, Palo Alto CA, 1993.

APPENDIX A

FORTRAN SOURCE CODE FOR CONTAINER FAILURE MODEL

```
      program barrier
c
c  This program calculates the cummulative failure
c  distribution of multiple barrier high-level
c  nuclear waste containers.  The program numerically
c  solves the integral equation that describes the failure
c  of multi-barrier high level nuclear waste containers.  The
c  basis of the integral equation is the Weibull distribution.
c
c  The program is written to be general in that it solves the
c  equation for a series of containers in three hydrothermal
c  regimes and four water contact modes.  Corrosion models are
c  input for each water contact mode.
c
*****************************************************************
*    Variable declaration block                                 *
*                                                               *
      integer imin, imax, i, istep, j, jmax, k, m
      real thc, mtc, wsc
      real power, tmax
      real thick1, thick2
      real pwd1, dwd1, kwd1, nwd1
      real pmc1, dmc1, kmc1, nmc1
      real pep1, dep1, kep1, nep1
      real pwd2, dwd2, kwd2, nwd2
      real pmc2, dmc2, kmc2, nmc2
      real pep2, dep2, kep2, nep2
      real dry1ind, dry2ind
      real pcond, pconv, phtp
      real empl, early, tearly
      real dcdalpha, dcdbeta, dcdgamma, dcddelta
      real mccdalpha, mccdbeta, mccdgamma, mccddelta
      real wdcdalpha, wdcdbeta, wdcdgamma, wdcddelta
      real epcdalpha, epcdbeta, epcdgamma, epcddelta
      real dcvalpha, dcvbeta, dcvgamma, dcvdelta
      real mccvalpha, mccvbeta, mccvgamma, mccvdelta
      real wdcvalpha, wdcvbeta, wdcvgamma, wdcvdelta
      real epcvalpha, epcvbeta, epcvgamma, epcvdelta
```

```
      real dhtalpha, dhtbeta, dhtgamma, dhtdelta
      real mchtalpha, mchtbeta, mchtgamma, mchtdelta
      real wdhtalpha, wdhtbeta, wdhtgamma, wdhtdelta
      real ephtalpha, ephtbeta, ephtgamma, ephtdelta
      real th101, th21
      real thwd1, mtwd1, wswd1
      real thmc1, mtmc1, wsmc1
      real thep1, mtep1, wsep1
      real thwd2, mtwd2, wswd2
      real thmc2, mtmc2, wsmc2
      real thep2, mtep2, wsep2
      real time, delt1, delt2, econd, econv, ehtp
      real t1, t2, vara, varb, var1, var2, var3
      real dry10in(5000), dry2in(5000), wdin(5000)
      real epin(5000), mcin(5000), sum
      real dry10o, dry2o, wdo, epo, mco
      real cond, conv, htp, fract
      real gauss(10,2), upper, lower
      real dry10t, dry2t, wdt, ept, mct
      character*12 indata, outdata, water
      character*72 case
*                                                               *
*****************************************************************
*     Declaration of input and output files                     *
*     and opening of said files                                 *

*                                                               *
c     input file containing parameters

      print *, 'Enter the name of the input file for'
      print *, 'this run, plus extension.'
      print *,
      read *, indata
c
c     output file containing all results of calculation
c
      print *, 'Enter the name of the output file for'
      print *, 'this run, plus extension.'
      print *,
      read *, outdata
c
c     output file containing information for each water contact
c     mode.  For graphical purposes
c
      print *,
      print *, 'enter the name of the output file for'
```

```
      print *, 'water contact mode data'
      print *,
      read *, water

      open(010,file=indata,status='old')
      open(011,file=outdata,status='new')
      open(021,file=water,status='new')
*                                                                *
******************************************************************
*   Read in parameters from input file                           *
*   see input file description for description of                *
*   parameters                                                   *
*                                                                *
      read(010,*) case
      read(010,*) power, tmax
      read(010,*) thick1, thick2
      read(010,*) pwd1, dwd1, kwd1, nwd1
      read(010,*) pmc1, dmc1, kmc1, nmc1
      read(010,*) pep1, dep1, kep1, nep1
      read(010,*) pwd2, dwd2, kwd2, nwd2
      read(010,*) pmc2, dmc2, kmc2, nmc2
      read(010,*) pep2, dep2, kep2, nep2
      read(010,*) thc, mtc, wsc
      read(010,*) dry1ind, dry2ind
      read(010,*) pcond, pconv, phtp
      read(010,*) empl, early, tearly
      read(010,*) dcdalpha, dcdbeta, dcdgamma, dcddelta
      read(010,*) mccdalpha, mccdbeta, mccdgamma, mccddelta
      read(010,*) wdcdalpha, wdcdbeta, wdcdgamma, wdcddelta
      read(010,*) epcdalpha, epcdbeta, epcdgamma, epcddelta
      read(010,) dcvalpha, dcvbeta, dcvgamma, dcvdelta
      read(010,*) mccvalpha, mccvbeta, mccvgamma, mccvdelta
      read(010,*) wdcvalpha, wdcvbeta, wdcvgamma, wdcvdelta
      read(010,*) epcvalpha, epcvbeta, epcvgamma, epcvdelta
      read(010,*) dhtalpha, dhtbeta, dhtgamma, dhtdelta
      read(010,*) mchtalpha, mchtbeta, mchtgamma, mchtdelta
      read(010,*) wdhtalpha, wdhtbeta, wdhtgamma, wdhtdelta
      read(010,*) ephtalpha, ephtbeta, ephtgamma, ephtdelta
      read(010,*) delt1, istep, dtdiv
*                                                                *
******************************************************************
*   Set coefficients for 10 point gaussian quadrature            *
*   integration of inner integral. From "Elementary              *
*   Numerical Analysis, An Algorithmic Approach"                 *
*   S.D. Conte, and C. De Boor, McGraw Hill Book                 *
*   Company, New York, 1980, 3rd edition                         *
```

```
*                                                                     *
      gauss(1,1)=-0.148874
      gauss(1,2)=0.29552
      gauss(2,1)=-0.433395
      gauss(2,2)=0.269267
      gauss(3,1)=-0.679410
      gauss(3,2)=0.2190864
      gauss(4,1)=-0.8650634
      gauss(4,2)=0.1494513
      gauss(5,1)=-0.973906
      gauss(5,2)=0.0666713
      gauss(6,1)=-1.*gauss(1,1)
      gauss(6,2)=gauss(1,2)
      gauss(7,1)=-1.*gauss(2,1)
      gauss(7,2)=gauss(2,2)
      gauss(8,1)=-1.*gauss(3,1)
      gauss(8,2)=gauss(3,2)
      gauss(9,1)=-1.*gauss(4,1)
      gauss(9,2)=gauss(4,2)
      gauss(10,1)=-1.*gauss(5,1)
      gauss(10,2)=gauss(5,2)
*                                                                     *
**********************************************************************
*   echo output of input data to master output file                   *
*                                                                     *
      write(011,*) case
      write(011,*) 'repository power (kw/acre)', power
      write(011,*) 'barrier 1 thickness (cm)', thick1
      write(011,*) 'barrier 2 thickness (cm)', thick2
      write(011,*)
      write(011,*) '     barrier 1 corrosion parameters'
      write(011,*)
      write(011,*) 'wet drip: intcpt =', pwd1, 'general rate =', dwd1
      write(011,*) '   pitting coefficients  k =', kwd1, ' n =', nwd1
      write(011,*) 'moist cont.: intcpt =', pmc1, 'general rate =', dmc1
      write(011,*) '   pitting coefficients  k =', kmc1, ' n =', nmc1
      write(011,*) 'episodic.: intcpt =', pep1, 'general rate =', dep1
      write(011,*) '   pitting coefficients  k =', kep1, ' n =', nep1
      write(011,*)
      write(011,*) '     barrier 2 corrosion parameters'
      write(011,*)
      write(011,*) 'wet drip: intcpt =', pwd1, 'general rate =', dwd2
      write(011,*) '   pitting coefficients  k =', kwd2, ' n =', nwd2
      write(011,*) 'moist cont.: intcpt =', pmc2, 'general rate =', dmc2
      write(011,*) '   pitting coefficients  k =', kmc2, ' n =', nmc2
      write(011,*) 'episodic.: intcpt =', pep2, 'general rate =', dep2
```

```
      write(011,*) '   pitting coefficients  k =', kep2, ' n =', nep2
      write(011,*)
      write(011,*) 'third barrier parameters '
      write(011,*) 'threshold = ', thc, '  mean time =', mtc
      write(011,*) 'weibull slope =', wsc
      write(011,*)
*                                                                     *
***********************************************************************
*   call subroutine params to calculate Weibull parameters *
*   based on container dimensions and corrosion models   *
*   Output data to master output file                    *
*                                                                     *
c  Barrier 1
      call params(pwd1,dwd1,kwd1,nwd1,thick1,thwd1,mtwd1,wswd1)
      call params(pmc1,dmc1,kmc1,nmc1,thick1,thmc1,mtmc1,wsmc1)
      call params(pep1,dep1,kep1,nep1,thick1,thep1,mtep1,wsep1)
c
      write(011,*) 'parameters for wet drip, barrier 1'
      write(011,*) 'threshold =', thwd1
      write(011,*) 'mean time =', mtwd1
      write(011,*) 'weibull slope =', wswd1
      write(011,*)
      write(011,*) 'parameters for moist continuous, barrier 1'
      write(011,*) 'threshold =', thmc1
      write(011,*) 'mean time =', mtmc1
      write(011,*) 'weibull slope =', wsmc1
      write(011,*)
      write(011,*) 'parameters for episodic, barrier 1'
      write(011,*) 'threshold =', thep1
      write(011,*) 'mean time =', mtep1
      write(011,*) 'weibull slope =', wsep1
      write(011,*)
c
c   barrier 2
c
      call params(pwd2,dwd2,kwd2,nwd2,thick2,thwd2,mtwd2,wswd2)
      call params(pmc2,dmc2,kmc2,nmc2,thick2,thmc2,mtmc2,wsmc2)
      call params(pep2,dep2,kep2,nep2,thick2,thep2,mtep2,wsep2)
      write(011,*) 'parameters for wet drip, barrier 2'
      write(011,*) 'threshold =', thwd2
      write(011,*) 'mean time =', mtwd2
      write(011,*) 'weibull slope =', wswd2
      write(011,*)
      write(011,*) 'parameters for moist continuous, barrier 2'
      write(011,*) 'threshold =', thmc2
      write(011,*) 'mean time =', mtmc2
```

```
      write(011,*) 'weibull slope =', wsmc2
      write(011,*)
      write(011,*) 'parameters for episodic, barrier 2'
      write(011,*) 'threshold =', thep2
      write(011,*) 'mean time =', mtep2
      write(011,*) 'weibull slope =', wsep2
      write(011,*)
c
c   add dryout times to episodic conditions to account for regions
c   that may have dryout times.

      th101=thep1+dry1ind
      th21=thep1+dry2ind

      write(011,*) 'dryout period 1 =', dry1ind
      write(011,*) 'dryout threshold -- barrier 1 =', th101
      write(011,*) 'dryout period 2 =', dry2ind
      write(011,*) 'dryout threshold -- barrier 1 =', th21
      write(011,*)
c
c     third barrier parameter (typically LWR SF clad) input
c     as actual Weibull parameters
c
*                                                                     *
***********************************************************************
*   Initialize calculation.  Set time step at 0.                      *
*   Determine step size for trapezoidal integration of outer          *
*   Integral.  Set loop counters based on step size                   *
*                                                                     *
      time=0
c
      delt2=delt1/dtdiv
      imin=1
      imax=int(tmax/delt1)
*                                                                     *
***********************************************************************
***********************************************************************
*   begin loop to perform calculations at desired time steps          *
*                                                                     *
      do 100 i=imin,imax+1,istep
        time= float(i-1)*delt1
c  parameter m is variable to determine number of calculations
c  performed.  Output to screen only.
        m=1
***********************************************************************
*   calculate fraction of containers that suffer early                *
```

```
*   failures.  Based on Exponential Distribution.  See          *
*   equation 3.3                                                *
*                                                               *
c   fraction of early failures assumed equal for all three
c   hydrothermal modes
c   conduction hydrothermal mode
       econd=0.0
       if(empl.ne.0.0.or.early.ne.0.0) then
         econd=empl+early*(1-exp(-1.0*time/tearly))
       end if
c   convection hydrothermal mode
         econv=econd
C    heat pipe hydrothermal mode
         ehtp=econd
*                                                               *
*****************************************************************
*****************************************************************
* build loops for integration.  Inner integration performs     *
* gaussian quadrature over t2 to determine failure             *
* distribution of inner barrier given outer barrier failure    *
* at time t1.  Outer loop performs trapezoidal rule over t1    *
* to determine the failure profile at time step under          *
* consideration.  See equation 3.8                             *
*                                                               *
c   set outer loop counter based on current time and outer
c   loop time step.  Then begin loop
       jmax=int(time/delt2)
       do 200 j=1,jmax+1
c  determine dummy time for calculation
         t1=float(j-1)*delt2
         m=m+1

c inner loop over t2 -- do gaussian quadrature on each
c water contact mode -- lower limit is t2=t1+threshold for that water
c contact mode.  Upper limit is based on time at which complete failure
c of inner barrier is guaranteed, see below
c
c   t = tm * {-[ln(1-x)]**(1/b)} + tf
c
c     for x --> 1, -ln(1-x) increases.  i.e for 0.99999999, -ln(1-x) = 18.4
c     thus choose this value or larger.
c
c each calculation calls subroutine varbl to determine the coefficients
c of the equation at the given quadrature time points.  10 point
c gaussian quadrature is then performed.
c
```

```
c  initialize inner loop integrations at 0
        dry10in(j)=0.0
        dry2in(j)=0.0
        wdin(j)=0.0
        epin(j)=0.0
        mcin(j)=0.0

c  long dryout time calculation.  Uses episodic conditions following
c  dryout.
c
        lower=t1+thep2
        upper=t1+thep2+mtep2*25.0**(1/wsep2)
        if (upper.gt.time) upper=time
        do 310 k=1,10
         m=m+1
         t2=lower+0.5*(upper-lower)*(gauss(k,1)+1.0)
         call varbl(time,t1,t2,th101,thep2,thc,mtep1,mtep2,mtc,
     +    wsep1,wsep2,wsc,var1,var2,var3,vara,varb)

         dry10in(j)=dry10in(j)+(wsep1*vara*exp(-1.0*var1)
     2    *wsep2*varb*exp(-1.0*var2)*(1-exp(-1.0*var3)))*gauss(k,2)
  310    continue
        dry10in(j)=dry10in(j)*0.5*(upper-lower)
c
c  short dryout time calculation.  Uses episodic conditions following
c  dryout.
c
        lower=t1+thep2
        upper=t1+thep2+mtep2*25.0**(1/wsep2)
        if (upper.gt.time) upper=time
        if (lower.lt.upper) then
         do 320 k=1,10
          m=m+1
          t2=lower+0.5*(upper-lower)*(gauss(k,1)+1.0)
          call varbl(time,t1,t2,th21,thep2,thc,mtep1,mtep2,mtc,
     +     wsep1,wsep2,wsc,var1,var2,var3,vara,varb)
          dry2in(j)=dry2in(j)+(wsep1*vara*exp(-1.0*var1)
     2     *wsep2*varb*exp(-1.0*var2)*(1-exp(-1.0*var3)))*gauss(k,2)
  320     continue
        else
         dry2in(j)=0.0
        end if
         dry2in(j)=dry2in(j)*0.5*(upper-lower)

c  wet drip water contact mode
c
```

```
      lower=t1+thwd2
      upper=t1+thwd2+mtwd2*25.0**(1/wswd2)
      if (upper.gt.time) upper=time
      if (lower.lt.upper) then
       do 330 k=1,10
        m=m+1
        t2=lower+0.5*(upper-lower)*(gauss(k,1)+1.0)
        call varbl(time,t1,t2,thwd1,thwd2,thc,mtwd1,mtwd2,
     +    mtc,wswd1,wswd2,wsc,var1,var2,var3,vara,varb)
        wdin(j)=wdin(j)+(wswd1*vara*exp(-1.0*var1)
     2    *wswd2*varb*exp(-1.0*var2)*(1-exp(-1.0*var3)))*gauss(k,2)
  330   continue
      else
       wdin(j)=0.0
      end if
c      wdin(j)=wdin(j)*0.5*(upper-lower)
c
c  episodic water contact mode
      lower=t1+thep2
      upper=t1+thep2+mtep2*25.0**(1/wsep2)
      if (upper.gt.time) upper=time
      if (lower.lt.upper) then
       do 340 k=1,10
        m=m+1
        t2=lower+0.5*(upper-lower)*(gauss(k,1)+1.0)
        call varbl(time,t1,t2,thep1,thep2,thc,mtep1,mtep2,
     +    mtc,wsep1,wsep2,wsc,var1,var2,var3,vara,varb)
        epin(j)=epin(j)+(wsep1*vara*exp(-1.0*var1)
     2    *wsep2*varb*exp(-1.0*var2)*(1-exp(-1.0*var3)))*gauss(k,2)
  340   continue
      else
       epin(j)=0.0
      end if
      epin(j)=epin(j)*0.5*(upper-lower)
c
c  moist continuous water contact mode
      lower=t1+thmc2
      upper=t1+thmc2+mtmc2*25.0**(1/wsmc2)
      if (upper.gt.time) upper=time

      if (lower.lt.upper) then
       do 350 k=1,10
        m=m+1
        t2=lower+0.5*(upper-lower)*(gauss(k,1)+1.0)
        call varbl(time,t1,t2,thmc1,thmc2,thc,mtmc1,mtmc2,
     +    mtc,wsmc1,wsmc2,wsc,var1,var2,var3,vara,varb)
```

```
          mcin(j)=mcin(j)+(wsmc1*vara*exp(-1.0*var1)
     2     *wsmc2*varb*exp(-1.0*var2)*(1-exp(-1.0*var3)))*gauss(k,2)
350       continue
        else
          mcin(j)=0.0
        end if
        mcin(j)=mcin(j)*0.5*(upper-lower)

200   continue
*                                                                    *
**********************************************************************
*  Trapezoidal rule on outer integral                                *
*                                                                    *
      call trap(dry10in,delt2,jmax+1,sum)
      dry10o=sum
      call trap(dry2in,delt2,jmax+1,sum)
      dry2o=sum
      call trap(wdin,delt2,jmax+1,sum)
      wdo=sum
      call trap(epin,delt2,jmax+1,sum)
      epo=sum
      call trap(mcin,delt2,jmax+1,sum)
      mco=sum
*                                                                    *
**********************************************************************
*  Calculate fraction of containers failed in each hydrothermal      *
*  Mode                                                              *
*                                                                    *
      cond=econd+(dcddelta*dry10o+dcdalpha*dry2o+
     1   (wdcdalpha+wdcdbeta+wdcdgamma+wdcddelta)*wdo+
     2   (epcdalpha+epcdbeta+epcdgamma+epcddelta+
     3   dcdbeta+dcdgamma)*epo+
     4   (mccdalpha+mccdbeta+mccdgamma+mccddelta)*mco)
     5   *(1.0-empl+early)
      conv=econv+(dcvdelta*dry10o+dcvalpha*dry2o+
     1   (wdcvalpha+wdcvbeta+wdcvgamma+wdcvdelta)*wdo+
     2   (epcvalpha+epcvbeta+epcvgamma+epcvdelta+
     3   dcvbeta+dcvgamma)*epo+
     4   (mccvalpha+mccvbeta+mccvgamma+mccvdelta)*mco)
     5   *(1.0-empl+early)
      htp=ehtp+(dhtdelta*dry10o+dhtalpha*dry2o+
     1   (wdhtalpha+wdhtbeta+wdhtgamma+wdhtdelta)*wdo+
     2   (ephtalpha+ephtbeta+ephtgamma+ephtdelta+
     3   dhtbeta+dhtgamma)*epo+
     5   (mchtalpha+mchtbeta+mchtgamma+mchtdelta)*mco)
     4   *(1.0-empl+early)
```

```
*                                                                      *
************************************************************************
*  Determine fraction of containers failed and output to screen *
*  Output to main data file the time and fraction of containers  *
*  failed in total and in each hydrothermal mode. Output to      *
*  data file the fraction of containers failed in each water     *
*  contact mode.                                                 *
*                                                                      *
      fract=cond*pcond+conv*pconv+htp*phtp
      print *, 'Time = (yrs)', time, 'Fract. failed=', fract
      print *, 'Number of loop iterations =', m
      write(011,11) time, fract, cond, conv, htp
      write(021,12) time, dry10o, dry2o, wdo, mco, epo
*                                                                      *
************************************************************************
*  continue master time step loop                                *
*                                                                      *
 100  continue
*                                                                      *
************************************************************************
************************************************************************
************************************************************************
*  Format statements, close data file, stop and end main         *
*                                                                      *
 11   format(f7.0,2x,f5.3,2x,f5.3,2x,f5.3,2x,f5.3)
 12   format(f7.0,2x,f5.3,2x,f5.3,2x,f5.3,2x,f5.3,2x,f5.3)
      close(010)
      close(011)
      close(021)
      stop
      end
************************************************************************
************************************************************************
************************************************************************
*  Subroutine params. Determines Weibull parameters for each  *
*  barrier given thickness of the barrier and the corrosion      *
*  model.  Utilizes numerical recipe for threshold and mean      *
*  time to failure.  given as                                    *
*                                                                *
*   thresh/mean = time - {corr(time)-thickness}/dcorr(time)      *
*                                                                *
*   From "Elementary Numerical Analysis, An Algorithmic          *
*   Approach" S.D. Conte, and C. De Boor, McGraw Hill Book       *
*   Company, New York, 1980, 3rd edition                         *
*                                                                *
*   iterate until convergence                                    *
```

```
*  Calls functions corr and dcorr                                        *
*                                                                        *
      subroutine params(p,d,k,n,thick,th,mt,ws)
      real p, d, k, n, thick, th, mt, ws
      real x, coe, delt, f0, fn
      real fract, xaxs(19), yaxs(19)
      real sumx, sumy, num, den
      integer i
c
c   start at time = 1 year
c   convergence is 10 years
c
c   threshold time to failure.  time for corrosion of 50%
c   of barrier thickness
c
      x=1.0
      coe=thick/2.
      if (coe.gt.p) then
 10     th=x-corr(p,d,k,n,x,coe)/dcorr(d,k,n,x)
        if(abs(th-x).gt.10.) then
         x=th
         go to 10
        end if
      else
       th=0.0
      end if
c
c   mean time to failure.  time for corrosion of 100%
c   of barrier thickness
c
      x=1.
      coe=thick
 20   mt=x-corr(p,d,k,n,x,coe)/dcorr(d,k,n,x)
      if(abs(mt-x).gt.10) then
       x=mt
       go to 20
      end if
c
c  calculate weibull slope based equation 3.11
c
      delt=(mt-th)/20.0
      fn=thick
      f0=thick/2
      do 100 i=3,19
        time=float(i-1)*delt+th
        fract=(corr(p,d,k,n,time,0.0)-f0)/(fn-f0)
```

```
      xtime=float(i-1)*delt
      xaxs(i-2)=log(xtime)
      temp=log(1.0/(1.0-fract))
      yaxs(i-2)=log(temp)
 100  continue

      sumy=0.0
      sumx=0.0
      do 300 i=1,17

      sumx=sumx+xaxs(i)
      sumy=sumy+yaxs(i)
 300   continue
      sumx=sumx/17.
      sumy=sumy/17.
      num=0.0
      den=0.0
      do 400 i=1,17
      num=(xaxs(i)-sumx)*(yaxs(i)-sumy)+num
      den=den+(xaxs(i)-sumx)**2
 400   continue
      ws=num/den
c
c   return to main and end
      return
      end
*************************************************************************
*************************************************************************
*  function corr.  calculates corrosion of barrier given          *
*  corrosion model.  Subtracts thickness under consideration  *
*  from subroutine params                                         *
*                                                                 *
      function corr(p,d,k,n,x,coe)
      real p, d, n, x, coe, corr, k
      corr=p+d*x+k*x**n-coe
      return
      end
*************************************************************************
*************************************************************************
*  function dcorr.  calculates derivative of corrosion rate of    *
*  barrier given corrosion model.  from subroutine params         *
*                                                                  *
      function dcorr(d,k,n,x)
      real d, n, x, dcorr, k
      dcorr=d+n*k*x**(n-1.)
      return
```

```
      end
**********************************************************************
**********************************************************************
*  soubroutine varbl.  calculates coefficients in sequential      *
*  failure rate equation 3.8                                      *
*                                                                 *
      subroutine varbl(t,tim1,tim2,tf1,tf2,tf3,mt1,mt2,mt3,
     +  ws1,ws2,ws3,v1,v2,v3,va,vb)
       real chk1, chk2, chk3, t, tf1, tf2, tf3
       real mt1, mt2, mt3, ws1, ws2, ws3
       real v1, v2, v3, va, vb
c
c   see equation 3.8 for definition of variables va, vb, v1, v2, v3
c
       v1=0.0
       v2=0.0
       v3=0.0
       va=0.0
       vb=0.0
        chka=(tim1-tf1)
        chk1=(tim1-tf1)/mt1
        chkb=(tim2-tim1-tf2)
        chk2=(tim2-tim1-tf2)/mt2
        chk3=(t-tim2-tf3)/mt3

        if(chka.gt.0.0) va=(chka**(ws1-1.0))/(mt1**ws1)
        if(chk1.gt.0.0) v1=chk1**ws1
        if(chkb.gt.0.0) vb=(chkb**(ws2-1.0))/(mt2**ws2)
        if(chk2.gt.0.0) v2=chk2**ws2
        if(chk3.gt.0.0) v3=chk3**ws3
c
c  if values greater than 35, set to 35 to prevent underflow
c
        if(v1.gt.35.0) v1=35
        if(v2.gt.35.0) v2=35
        if(v3.gt.35.0) v3=35

        return
        end
**********************************************************************
**********************************************************************
*  Subroutine trap.  Performs numerical trapezoidal integration   *
*                                                                 *
*                                                                 *
*   From "Elementary Numerical Analysis, An Algorithmic           *
*   Approach" S.D. Conte, and C. De Boor, McGraw Hill Book        *
```

```
*   Company, New York, 1980, 3rd edition                              *
*                                                                     *
      subroutine trap(array,h,lcount,int)
      real array(5000), int, sum, h
      integer lcount, l

      int=h/2.0*(array(1)+array(lcount))
      sum=0.0
      do 10 l=2,lcount-1
        sum=sum+array(l)
 10    continue
      int=int+h*sum
      return
      end
**********************************************************************
```

DEFINITION OF INPUT PARAMETERS

1. case — case title
2. power, tmax — APD under consideration, maximum time of calculation
3. thick1, thick2 — thickness of outer and inner barrier

the following cards define the corrosion model for each barrier (1,2) in each water contact mode. wd - wet drip, mc - moist continuous ep - episodic. corrosion model is of the following form, fit to data.

corr=p+d*x+k*x**n

4. pwd1, dwd1, kwd1, nwd1
5. pmc1, dmc1, kmc1, nmc1
6. pep1, dep1, kep1, nep1
7. pwd2, dwd2, kwd2, nwd2
8. pmc2, dmc2, kmc2, nmc2
9. pep2, dep2, kep2, nep2

third barrier parameters are input as Weibull parameters. Must be determined in advance

10. thc, mtc, wsc

11. dry1ind, dry2ind — Dry out times
12. pcond, pconv, phtp — Fraction of containers in conduction, convection, and heat pipe hydrothermal modes

13. empl, early, tearly — Fraction of containers failed at emplacement, fraction of containers susceptible for early failure, time constant for early failure

cards 14 through 25 provide the fraction of containers in each water contact mode, in each temperature regime, and in each hydrothermal mode.

water contact modes: d = dry, mc = moist continuous, wd = wet drip, ep = episodic
hydrothermal regimes: cd = conduction, cv = convection, ht = heat pipe
four temperature regimes: alpha, beta, gamma, delta (determined by user)

Within a given hydrothermal regime, the sum through all water contact modes and temperature regimes must equal one minus the fraction of containers failed at emplacement minus the fraction of containers susceptible to early failures..

14. dcdalpha, dcdbeta, dcdgamma, dcddelta
15. mccdalpha, mccdbeta, mccdgamma, mccddelta
16. wdcdalpha, wdcdbeta, wdcdgamma, wdcddelta

17. epcdalpha, epcdbeta, epcdgamma, epcddelta
18. dcvalpha, dcvbeta, dcvgamma, dcvdelta
19. mccvalpha, mccvbeta, mccvgamma, mccvdelta
20. wdcvalpha, wdcvbeta, wdcvgamma, wdcvdelta
21. epcvalpha, epcvbeta, epcvgamma, epcvdelta
22. dhtalpha, dhtbeta, dhtgamma, dhtdelta
23. mchtalpha, mchtbeta, mchtgamma, mchtdelta
24. wdhtalpha, wdhtbeta, wdhtgamma, wdhtdelta
25. ephtalpha, ephtbeta, ephtgamma, ephtdelta

26. delt1, istep, dtdiv — step size, number of time steps for each loop increment (typically set at 1), reduction in step size for calculation of inner integral.

APPENDIX B

IMARC INPUT FILES

This Appendix provides the input files utilized in the IMARC executions. Detailed descriptions of each input file are provide in the IMARC Users Manual [86].

The first set of files is the radionuclide input file. The data required is the radionuclide ID, its half-life, three solubility levels (representing low, moderate and high), the amount (Ci/MTHM), its specific activity (Ci/gm), the EPA limit for that radionuclide (not used) and two sets of retardation parameters for low, moderatel and high cases.

The following changes were required to model the ER-metallic wasteform.

The inventory for the ER-metallic wasteform consisted of the inventory from Reference 37 with the ER-metal wastes, non-fuel hardware wastes, and fuel hardware wastes combined.

Solubility limits for Zr^{93}, Sn^{126}, and Pd^{107} were obtained from the Intera 1993 Total System Performance Analysis [14]. No data existed for Pd so the solubility values for Ni were utilized since these elements are of the same periodicity. In the Intera PA, the solubility is represented by probability distributions. Since IMARC uses three discrete levels, the following method was used.

The low solubility was chosen as the minimum value

The moderate solubility was chosen as the expected value

The high solubility was chosen as the maximum value

Retardation values for Zr^{93}, and Sn^{126} were obtained from Sandia National Laboratory 1993 PA analysis [18]. No data existed for Pd so the retardation values of Np were used as an estimate.. In the Sandia PA, the the sorption coefficeint is represented by probability distributions. Since IMARC utilizes retardation coefficients for two layers of rock, and three discrete levels for each layer, it was necessary to convert the sorption coefficient distributions to discrete levels. This was accomplished in the following manner. The expected values of the sorption coefficient were obtained for devitrified and zeolitic tuffs [18] (devitrified -- Zr = 1050 ml/g Sn = 110 ml/g, zeolitic -- Zr = 550 ml/g, Sn = 200 ml/g) . These values were then multiplied by the density of rock in each layer (layer 1 - zeolitic 1.61 g/cm^3, layer 2 - devitrified 2.30 g/cm^3) [12] to give the moderate values for the retardation coefficient. The low and high retardation values were five times smaller and larger, respectively, than the moderate retardation value, consistant with the approach taken in the IMARC theory [12] for the other radionuclides.

LWR Spent Fuel, Both Container Types

Number of Nuclides, Solubility/Retardation Levels, Probability of Retardation Levels

13 3 0.333 0.334 0.333

Index	Name	Half Life	Solubility Limit (gm/m**3)			Inventory	Activity	EPA	Rho * Kd (Level 1)			Rho * Kd (Level 2)		
		(yrs)	low	moderate	high	(Ci/MTHM)	(Ci/gm)	Limit	low	moderate	high	low	moderate	high
1	C14	5.73e+03	1.00e+00	1.40e+00	1.40e+02	0.00e+00	4.45e+00	1.00e+02	0.0	0.0	0.0	0.0	0.0	0.0
2	Se79	6.50e+04	7.90e+02	7.90e+03	5.50e+05	4.79e-01	6.97e-02	1.00e+02	1.0	4.8	2.4	3.2	16.0	81.0
3	Tc99	2.15e+05	3.50e-02	1.00e+02	9.90e+05	1.51e+01	1.70e-02	1.00e+04	0.0	0.0	0.0	0.1	0.7	3.5
4	I129	1.59e+07	1.00e+00	3.90e+02	1.00e+05	3.72e-02	1.74e-04	1.00e+02	0.0	0.0	0.0	0.0	0.0	0.0
5	Cs135	3.00e+06	1.20e+00	3.90e+02	2.10e+03	5.67e-01	8.82e-04	1.00e+03	2500.0	12500.0	62500.0	133.0	667.0	3300.0
6	Ra226	1.62e+03	1.00e-05	4.00e-04	1.00e-01	2.64e-06	9.88e-01	1.00e+02	8000.0	40000.0	0.0	12000.0	58000.0	0.0
7	U234	2.47e+05	5.00e-01	2.40e+00	5.00e+01	2.72e+00	6.18e-03	1.00e+02	1.7	8.5	42.0	0.8	4.1	20.0
8	U235	7.10e+08	5.00e-01	2.40e+00	5.00e+01	1.68e-02	2.14e-06	1.00e+02	1.7	8.5	42.0	0.8	4.1	20.0
9	U238	4.51e+09	5.00e-01	2.40e+00	5.00e+01	3.14e-01	3.33e-07	1.00e+02	1.7	8.5	42.0	0.8	4.1	20.0
10	Np237	2.14e+06	4.00e-04	3.60e+02	7.20e+02	3.23e+00	7.05e-04	1.00e+02	3.6	18.0	90.0	3.2	16.0	80.0
11	Pu239	2.44e+04	6.00e-05	9.60e-04	4.30e-01	3.75e+02	6.13e-02	1.00e+02	45.0	225.0	1120.0	30.0	150.0	750.0
12	Pu240	6.58e+03	6.00e-05	9.60e-04	4.30e-01	5.75e+02	2.26e-01	1.00e+02	45.0	225.0	1120.0	30.0	150.0	750.0
13	Pu242	3.79e+05	6.00e-05	9.60e-04	4.30e-01	2.18e+00	3.90e-03	1.00e+02	45.0	225.0	1120.0	30.0	150.0	750.0

ALMR Electrorefiner Metallic Wasteform (Low Actinide Decontamination)

Number of Nuclides, Solubility/Retardation Levels, Probability of Retardation Levels

13 3 0.333 0.334 0.333

Index	Name	Half Life	Solubility Limit (gm/m**3)			Inventory	Activity	EPA	Rho * Kd (Level 1)			Rho * Kd (Level 2)		
		(yrs)	low	moderate	high	(Ci/MTHM)	(Ci/gm)	Limit	low	moderate	high	low	moderate	high
1	C14	5.73e+03	1.00e+00	1.40e+00	1.40e+02	0.00e+00	4.45e+00	1.00e+02	0.0	0.0	0.0	0.0	0.0	0.0
2	Se79	6.50e+04	7.90e+02	7.90e+03	5.50e+05	2.38e+00	6.97e-02	1.00e+02	1.0	4.8	2.4	3.2	16.0	81.0
3	Tc99	2.15e+05	3.50e-02	1.00e+02	9.90e+05	8.17e+01	1.70e-02	1.00e+04	0.0	0.0	0.0	0.1	0.7	3.5
4	Zr93	1.53e+06	9.18e-08	7.90e-04	9.10e-03	1.06e+01	2.51e-03	1.00e+02	177.1	885.5	4427.5	483.0	2415.0	12075.0
5	Pd107	6.50e+06	5.90e-02	1.05e+02	5.90e+03	1.26e+00	5.14e-04	1.00e+03	3.6	18.0	90.0	3.2	16.0	80.0
6	Sn126	1.00e+05	1.30e-06	6.50e-03	1.30e-02	9.87e+00	2.84e-02	1.00e+02	64.4	322.0	1610.0	50.6	253.0	1265.0
7	U234	2.47e+05	5.00e-01	2.40e+00	5.00e+01	4.60e-03	6.18e-03	1.00e+02	1.7	8.5	42.0	0.8	4.1	20.0
8	U235	7.10e+08	5.00e-01	2.40e+00	5.00e+01	4.98e-07	2.14e-06	1.00e+02	1.7	8.5	42.0	0.8	4.1	20.0
9	U238	4.51e+09	5.00e-01	2.40e+00	5.00e+01	6.19e-05	3.33e-07	1.00e+02	1.7	8.5	42.0	0.8	4.1	20.0
10	Np237	2.14e+06	4.00e-04	3.60e+02	7.20e+02	2.85e-03	7.05e-04	1.00e+02	3.6	18.0	90.0	3.2	16.0	80.0
11	Pu239	2.44e+04	6.00e-05	9.60e-04	4.30e-01	1.35e+00	6.13e-02	1.00e+02	45.0	225.0	1120.0	30.0	150.0	750.0
12	Pu240	6.58e+03	6.00e-05	9.60e-04	4.30e-01	1.79e+00	2.26e-01	1.00e+02	45.0	225.0	1120.0	30.0	150.0	750.0
13	Pu242	3.79e+05	6.00e-05	9.60e-04	4.30e-01	3.42e-03	3.90e-03	1.00e+02	45.0	225.0	1120.0	30.0	150.0	750.0

ALMR Electrorefiner Mineral Wasteform (Low Actinide Decontamination)

Number of Nuclides, Solubility/Retardation Levels, Probability of Retardation Levels

13	3	0.333	0.334	0.333										
Index	Name	Half Life	Solubility Limit (gm/m**3)			Inventory	Activity	EPA	Rho * Kd (Level 1)			Rho * Kd (Level 2)		
		(yrs)	low	moderate	high	(Ci/MTHM)	(Ci/gm)	Limit	low	moderate	high	low	moderate	high
1	C14	5.73e+03	1.00e+00	1.40e+00	1.40e+02	0.00e+00	4.45e+00	1.00e+02	0.0	0.0	0.0	0.0	0.0	0.0
2	Se79	6.50e+04	7.90e-02	7.90e+03	5.50e+05	0.00e+00	6.97e-02	1.00e+02	1.0	4.8	2.4	3.2	16.0	81.0
3	Tc99	2.15e+05	3.50e-02	1.00e+02	9.90e+05	0.00e+00	1.70e-02	1.00e+04	0.0	0.0	0.0	0.1	0.7	3.5
4	I129	1.59e+07	1.00e+00	3.90e+02	1.00e+05	2.75e-01	1.74e-04	1.00e+02	0.0	0.0	0.0	0.0	0.0	0.0
5	Cs135	3.00e+06	1.20e+00	3.90e+02	2.10e+03	9.99e-01	8.82e-04	1.00e+03	2500.0	12500.0	62500.0	133.0	667.0	3300.0
6	Ra226	1.62e+03	1.00e-05	4.00e-04	1.00e-01	0.00e+00	9.88e-01	1.00e+02	8000.0	40000.0	0.0	12000.0	58000.0	0.0
7	U234	2.47e+05	5.00e-01	2.40e+00	5.00e+01	4.60e-03	6.18e-03	1.00e+02	1.7	8.5	42.0	0.8	4.1	20.0
8	U235	7.10e+08	5.00e-01	2.40e+00	5.00e+01	4.98e-07	2.14e-06	1.00e+02	1.7	8.5	42.0	0.8	4.1	20.0
9	U238	4.51e+09	5.00e-01	2.40e+00	5.00e+01	6.19e-05	3.33e-07	1.00e+02	1.7	8.5	42.0	0.8	4.1	20.0
10	Np237	2.14e+06	4.00e-04	3.60e+02	7.20e+02	2.85e-03	7.05e-04	1.00e+02	3.6	18.0	90.0	3.2	16.0	80.0
11	Pu239	2.44e+04	6.00e-05	9.60e-04	4.30e-01	1.35e+00	6.13e-02	1.00e+02	45.0	225.0	1120.0	30.0	150.0	750.0
12	Pu240	6.58e+03	6.00e-05	9.60e-04	4.30e-01	1.79e+00	2.26e-01	1.00e+02	45.0	225.0	1120.0	30.0	150.0	750.0
13	Pu242	3.79e+05	6.00e-05	9.60e-04	4.30e-01	3.42e-03	3.90e-03	1.00e+02	45.0	225.0	1120.0	30.0	150.0	750.0

Actinide Recycle Oxide Reduction Wasteform

Number of Nuclides, Solubility/Retardation Levels, Probability of Retardation Levels

13	3	0.333	0.334	0.333										
Index	Name	Half Life	Solubility Limit (gm/m**3)			Inventory	Activity	EPA	Rho * Kd (Level 1)			Rho * Kd (Level 2)		
		(yrs)	low	moderate	high	(Ci/MTHM)	(Ci/gm)	Limit	low	moderate	high	low	moderate	high
1	C14	5.73e+03	1.00e+00	1.40e+00	1.40e+02	0.00e+00	4.45e+00	1.00e+02	0.0	0.0	0.0	0.0	0.0	0.0
2	Se79	6.50e+04	7.90e-02	7.90e+03	5.50e+05	1.00e-08	6.97e-02	1.00e+02	1.0	4.8	2.4	3.2	16.0	81.0
3	Tc99	2.15e+05	3.50e-02	1.00e+02	9.90e+05	1.00e-08	1.70e-02	1.00e+04	0.0	0.0	0.0	0.1	0.7	3.5
4	I129	1.59e+07	1.00e+00	3.90e+02	1.00e+05	3.16e-02	1.74e-04	1.00e+02	0.0	0.0	0.0	0.0	0.0	0.0
5	Cs135	3.00e+06	1.20e+00	3.90e+02	2.10e+03	3.42e-01	8.82e-04	1.00e+03	2500.0	12500.0	62500.0	133.0	667.0	3300.0
6	Ra226	1.62e+03	1.00e-05	4.00e-04	1.00e-01	1.00e-08	9.88e-01	1.00e+02	8000.0	40000.0	0.0	12000.0	58000.0	0.0
7	U234	2.47e+05	5.00e-01	2.40e+00	5.00e+01	1.95e-04	6.18e-03	1.00e+02	1.7	8.5	42.0	0.8	4.1	20.0
8	U235	7.10e+08	5.00e-01	2.40e+00	5.00e+01	1.97e-06	2.14e-06	1.00e+02	1.7	8.5	42.0	0.8	4.1	20.0
9	U238	4.51e+09	5.00e-01	2.40e+00	5.00e+01	3.12e-05	3.33e-07	1.00e+02	1.7	8.5	42.0	0.8	4.1	20.0
10	Np237	2.14e+06	4.00e-04	3.60e+02	7.20e+02	3.77e-04	7.05e-04	1.00e+02	3.6	18.0	90.0	3.2	16.0	80.0
11	Pu239	2.44e+04	6.00e-05	9.60e-04	4.30e-01	3.14e-02	6.13e-02	1.00e+02	45.0	225.0	1120.0	30.0	150.0	750.0
12	Pu240	6.58e+03	6.00e-05	9.60e-04	4.30e-01	5.25e-02	2.26e-01	1.00e+02	45.0	225.0	1120.0	30.0	150.0	750.0
13	Pu242	3.79e+05	6.00e-05	9.60e-04	4.30e-01	1.72e-04	3.90e-03	1.00e+02	45.0	225.0	1120.0	30.0	150.0	750.0

Actinide Recycle Electrorefiner Metallic Wasteform (Low Actinide Decontamination)

Number of Nuclides, Solubility/Retardation Levels, Probability of Retardation Levels

13 3 0.333 0.334 0.333

Index	Name	Half Life	Solubility Limit (gm/m**3)			Inventory	Activity	EPA	Rho * Kd (Level 1)			Rho * Kd (Level 2)		
		(yrs)	low	moderate	high	(Ci/MTHM)	(Ci/gm)	Limit	low	moderate	high	low	moderate	high
1	C14	5.73e+03	1.00e+00	1.40e+00	1.40e+02	0.00e+00	4.45e+00	1.00e+02	0.0	0.0	0.0	0.0	0.0	0.0
2	Se79	6.50e+04	7.90e+02	7.90e+03	5.50e+05	4.09e-01	6.97e-02	1.00e+02	1.0	4.8	2.4	3.2	16.0	81.0
3	Tc99	2.15e+05	3.50e-02	1.00e+02	9.90e+05	1.30e+01	1.70e-02	1.00e+04	0.0	0.0	0.0	0.1	0.7	3.5
4	Zr93	1.53e+06	9.18e-08	7.90e-04	9.10e-03	1.94e+00	2.51e-03	1.00e+02	177.1	885.5	4427.5	483.0	2415.0	12075.0
5	Pd107	6.50e+06	5.90e-02	1.05e+02	5.90e+03	1.12e-01	5.14e-04	1.00e+03	3.6	18.0	90.0	3.2	16.0	80.0
6	Sn126	1.00e+05	1.30e-06	6.50e-03	1.30e-02	7.77e-01	2.84e-02	1.00e+02	64.4	322.0	1610.0	50.6	253.0	1265.0
7	U234	2.47e+05	5.00e-01	2.40e+00	5.00e+01	1.95e-03	6.18e-03	1.00e+02	1.7	8.5	42.0	0.8	4.1	20.0
8	U235	7.10e+08	5.00e-01	2.40e+00	5.00e+01	1.97e-05	2.14e-06	1.00e+02	1.7	8.5	42.0	0.8	4.1	20.0
9	U238	4.51e+09	5.00e-01	2.40e+00	5.00e+01	3.12e-04	3.33e-07	1.00e+02	1.7	8.5	42.0	0.8	4.1	20.0
10	Np237	2.14e+06	4.00e-04	3.60e+02	7.20e+02	3.77e-03	7.05e-04	1.00e+02	3.6	18.0	90.0	3.2	16.0	80.0
11	Pu239	2.44e+04	6.00e-05	9.60e-04	4.30e-01	3.14e-01	6.13e-02	1.00e+02	45.0	225.0	1120.0	30.0	150.0	750.0
12	Pu240	6.58e+03	6.00e-05	9.60e-04	4.30e-01	5.29e-01	2.26e-01	1.00e+02	45.0	225.0	1120.0	30.0	150.0	750.0
13	Pu242	3.79e+05	6.00e-05	9.60e-04	4.30e-01	1.72e-03	3.90e-03	1.00e+02	45.0	225.0	1120.0	30.0	150.0	750.0

Actinide Recycle Electrorefiner Mineral Wasteform (Low Actinide Decontamination)

Number of Nuclides, Solubility/Retardation Levels, Probability of Retardation Levels

13 3 0.333 0.334 0.333

Index	Name	Half Life	Solubility Limit (gm/m**3)			Inventory	Activity	EPA	Rho * Kd (Level 1)			Rho * Kd (Level 2)		
		(yrs)	low	moderate	high	(Ci/MTHM)	(Ci/gm)	Limit	low	moderate	high	low	moderate	high
1	C14	5.73e+03	1.00e+00	1.40e+00	1.40e+02	0.00e+00	4.45e+00	1.00e+02	0.0	0.0	0.0	0.0	0.0	0.0
2	Se79	6.50e+04	7.90e+02	7.90e+03	5.50e+05	1.00e-08	6.97e-02	1.00e+02	1.0	4.8	2.4	3.2	16.0	81.0
3	Tc99	2.15e+05	3.50e-02	1.00e+02	9.90e+05	1.00e-08	1.70e-02	1.00e+04	0.0	0.0	0.0	0.1	0.7	3.5
4	I129	1.59e+07	1.00e+00	3.90e+02	1.00e+05	1.00e-08	1.74e-04	1.00e+02	0.0	0.0	0.0	0.0	0.0	0.0
5	Cs135	3.00e+06	1.20e+00	3.90e+02	2.10e+03	3.43e-03	8.82e-04	1.00e+03	2500.0	12500.0	62500.0	133.0	667.0	3300.0
6	Ra226	1.62e+03	1.00e-05	4.00e-04	1.00e-01	1.00e-08	9.88e-01	1.00e+02	8000.0	40000.0	0.0	12000.0	58000.0	0.0
7	U234	2.47e+05	5.00e-01	2.40e+00	5.00e+01	1.95e-03	6.18e-03	1.00e+02	1.7	8.5	42.0	0.8	4.1	20.0
8	U235	7.10e+08	5.00e-01	2.40e+00	5.00e+01	1.97e-05	2.14e-06	1.00e+02	1.7	8.5	42.0	0.8	4.1	20.0
9	U238	4.51e+09	5.00e-01	2.40e+00	5.00e+01	3.12e-04	3.33e-07	1.00e+02	1.7	8.5	42.0	0.8	4.1	20.0
10	Np237	2.14e+06	4.00e-04	3.60e+02	7.20e+02	3.77e-03	7.05e-04	1.00e+02	3.6	18.0	90.0	3.2	16.0	80.0
11	Pu239	2.44e+04	6.00e-05	9.60e-04	4.30e-01	3.14e-01	6.13e-02	1.00e+02	45.0	225.0	1120.0	30.0	150.0	750.0
12	Pu240	6.58e+03	6.00e-05	9.60e-04	4.30e-01	5.29e-01	2.26e-01	1.00e+02	45.0	225.0	1120.0	30.0	150.0	750.0
13	Pu242	3.79e+05	6.00e-05	9.60e-04	4.30e-01	1.72e-03	3.90e-03	1.00e+02	45.0	225.0	1120.0	30.0	150.0	750.0

Weapons Grade Plutonium Disposition LWR Spike Option

Number of Nuclides, Solubility/Retardation Levels, Probability of Retardation Levels

13 3 0.333 0.334 0.333

Index	Name	Half Life	Solubility Limit (gm/m**3)			Inventory	Activity	EPA	Rho * Kd (Level 1)			Rho * Kd (Level 2)		
		(yrs)	low	moderate	high	(Ci/MTHM)	(Ci/gm)	Limit	low	moderate	high	low	moderate	high
1	C14	5.73e+03	1.00e+00	1.40e+00	1.40e+02	0.00e+00	4.45e+00	1.00e+02	0.0	0.0	0.0	0.0	0.0	0.0
2	Se79	6.50e+04	7.90e+02	7.90e+03	5.50e+05	1.16e-01	6.97e-02	1.00e+02	1.0	4.8	2.4	3.2	16.0	81.0
3	Tc99	2.15e+05	3.50e-02	1.00e+02	9.90e+05	4.26e+00	1.70e-02	1.00e+04	0.0	0.0	0.0	0.1	0.7	3.5
4	I129	1.59e+07	1.00e+00	3.90e+02	1.00e+05	1.41e-02	1.74e-04	1.00e+02	0.0	0.0	0.0	0.0	0.0	0.0
5	Cs135	3.00e+06	1.20e+00	3.90e+02	2.10e+03	1.81e-01	8.82e-04	1.00e+03	2500.0	12500.0	62500.0	133.0	667.0	3300.0
6	Ra226	1.62e+03	1.00e-05	4.00e-04	1.00e-01	1.00e-07	9.88e-01	1.00e+02	8000.0	40000.0	0.0	12000.0	58000.0	0.0
7	U234	2.47e+05	5.00e-01	2.40e+00	5.00e+01	3.26e-01	6.18e-03	1.00e+02	1.7	8.5	42.0	0.8	4.1	20.0
8	U235	7.10e+08	5.00e-01	2.40e+00	5.00e+01	3.49e-03	2.14e-06	1.00e+02	1.7	8.5	42.0	0.8	4.1	20.0
9	U238	4.51e+09	5.00e-01	2.40e+00	5.00e+01	3.24e-01	3.33e-07	1.00e+02	1.7	8.5	42.0	0.8	4.1	20.0
10	Np237	2.14e+06	4.00e-04	3.60e+02	7.20e+02	3.48e+00	7.05e-04	1.00e+02	3.6	18.0	90.0	3.2	16.0	80.0
11	Pu239	2.44e+04	6.00e-05	9.60e-04	4.30e-01	1.17e+03	6.13e-02	1.00e+02	45.0	225.0	1120.0	30.0	150.0	750.0
12	Pu240	6.58e+03	6.00e-05	9.60e-04	4.30e-01	8.88e+02	2.26e-01	1.00e+02	45.0	225.0	1120.0	30.0	150.0	750.0
13	Pu242	3.79e+05	6.00e-05	9.60e-04	4.30e-01	2.36e-01	3.90e-03	1.00e+02	45.0	225.0	1120.0	30.0	150.0	750.0

Weapons Grade Plutonium Disposition LWR Spent Fuel Option

Number of Nuclides, Solubility/Retardation Levels, Probability of Retardation Levels

13 3 0.333 0.334 0.333

Index	Name	Half Life	Solubility Limit (gm/m**3)			Inventory	Activity	EPA	Rho * Kd (Level 1)			Rho * Kd (Level 2)		
		(yrs)	low	moderate	high	(Ci/MTHM)	(Ci/gm)	Limit	low	moderate	high	low	moderate	high
1	C14	5.73e+03	1.00e+00	1.40e+00	1.40e+02	0.00e+00	4.45e+00	1.00e+02	0.0	0.0	0.0	0.0	0.0	0.0
2	Se79	6.50e+04	7.90e+02	7.90e+03	5.50e+05	3.18e-01	6.97e-02	1.00e+02	1.0	4.8	2.4	3.2	16.0	81.0
3	Tc99	2.15e+05	3.50e-02	1.00e+02	9.90e+05	1.20e+01	1.70e-02	1.00e+04	0.0	0.0	0.0	0.1	0.7	3.5
4	I129	1.59e+07	1.00e+00	3.90e+02	1.00e+05	3.86e-02	1.74e-04	1.00e+02	0.0	0.0	0.0	0.0	0.0	0.0
5	Cs135	3.00e+06	1.20e+00	3.90e+02	2.10e+03	4.26e-01	8.82e-04	1.00e+03	2500.0	12500.0	62500.0	133.0	667.0	3300.0
6	Ra226	1.62e+03	1.00e-05	4.00e-04	1.00e-01	1.00e-07	9.88e-01	1.00e+02	8000.0	40000.0	0.0	12000.0	58000.0	0.0
7	U234	2.47e+05	5.00e-01	2.40e+00	5.00e+01	2.82e-01	6.18e-03	1.00e+02	1.7	8.5	42.0	0.8	4.1	20.0
8	U235	7.10e+08	5.00e-01	2.40e+00	5.00e+01	1.74e-03	2.14e-06	1.00e+02	1.7	8.5	42.0	0.8	4.1	20.0
9	U238	4.51e+09	5.00e-01	2.40e+00	5.00e+01	3.20e-01	3.33e-07	1.00e+02	1.7	8.5	42.0	0.8	4.1	20.0
10	Np237	2.14e+06	4.00e-04	3.60e+02	7.20e+02	9.15e+00	7.05e-04	1.00e+02	3.6	18.0	90.0	3.2	16.0	80.0
11	Pu239	2.44e+04	6.00e-05	9.60e-04	4.30e-01	4.21e+02	6.13e-02	1.00e+02	45.0	225.0	1120.0	30.0	150.0	750.0
12	Pu240	6.58e+03	6.00e-05	9.60e-04	4.30e-01	1.09e+03	2.26e-01	1.00e+02	45.0	225.0	1120.0	30.0	150.0	750.0
13	Pu242	3.79e+05	6.00e-05	9.60e-04	4.30e-01	4.41e+00	3.90e-03	1.00e+02	45.0	225.0	1120.0	30.0	150.0	750.0

Weapons Grade Plutonium Disposition LMR Spike Option (ER-Metallic)

Number of Nuclides, Solubility/Retardation Levels, Probability of Retardation Levels

13 3 0.333 0.334 0.333

Index	Name	Half Life	Solubility Limit (gm/m**3)			Inventory	Activity	EPA	Rho * Kd (Level 1)			Rho * Kd (Level 2)		
		(yrs)	low	moderate	high	(Ci/MTHM)	(Ci/gm)	Limit	low	moderate	high	low	moderate	high
1	C14	5.73e+03	1.00e+00	1.40e+00	1.40e+02	0.00e+00	4.45e+00	1.00e+02	0.0	0.0	0.0	0.0	0.0	0.0
2	Se79	6.50e+04	7.90e+02	7.90e+03	5.50e+05	1.00e-08	6.97e-02	1.00e+02	1.0	4.8	2.4	3.2	16.0	81.0
3	Tc99	2.15e+05	3.50e-02	1.00e+02	9.90e+05	1.00e-08	1.70e-02	1.00e+04	0.0	0.0	0.0	0.1	0.7	3.5
4	Zr93	1.53e+06	9.18e-08	7.90e-04	9.10e-03	1.00e-08	2.51e-03	1.00e+02	177.1	885.5	4427.5	483.0	2415.0	12075.0
5	Pd107	6.50e+06	5.90e-02	1.05e+02	5.90e+03	1.00e-08	5.14e-04	1.00e+03	3.6	18.0	90.0	3.2	16.0	80.0
6	Sn126	1.00e+05	1.30e-06	6.50e-03	1.30e-02	1.00e-08	2.84e-02	1.00e+02	64.4	322.0	1610.0	50.6	253.0	1265.0
7	U234	2.47e+05	5.00e-01	2.40e+00	5.00e+01	1.00e-08	6.18e-03	1.00e+02	1.7	8.5	42.0	0.8	4.1	20.0
8	U235	7.10e+08	5.00e-01	2.40e+00	5.00e+01	3.32e-03	2.14e-06	1.00e+02	1.7	8.5	42.0	0.8	4.1	20.0
9	U238	4.51e+09	5.00e-01	2.40e+00	5.00e+01	2.64e-01	3.33e-07	1.00e+02	1.7	8.5	42.0	0.8	4.1	20.0
10	Np237	2.14e+06	4.00e-04	3.60e+02	7.20e+02	3.10e+00	7.05e-04	1.00e+02	3.6	18.0	90.0	3.2	16.0	80.0
11	Pu239	2.44e+04	6.00e-05	9.60e-04	4.30e-01	1.16e+04	6.13e-02	1.00e+02	45.0	225.0	1120.0	30.0	150.0	750.0
12	Pu240	6.58e+03	6.00e-05	9.60e-04	4.30e-01	2.71e+03	2.26e-01	1.00e+02	45.0	225.0	1120.0	30.0	150.0	750.0
13	Pu242	3.79e+05	6.00e-05	9.60e-04	4.30e-01	1.00e-08	3.90e-03	1.00e+02	45.0	225.0	1120.0	30.0	150.0	750.0

Weapons Grade Plutonium Disposition LMR Spent Fuel Option (ER-Metallic)

Number of Nuclides, Solubility/Retardation Levels, Probability of Retardation Levels

13 3 0.333 0.334 0.333

Index	Name	Half Life	Solubility Limit (gm/m**3)			Inventory	Activity	EPA	Rho * Kd (Level 1)			Rho * Kd (Level 2)		
		(yrs)	low	moderate	high	(Ci/MTHM)	(Ci/gm)	Limit	low	moderate	high	low	moderate	high
1	C14	5.73e+03	1.00e+00	1.40e+00	1.40e+02	0.00e+00	4.45e+00	1.00e+02	0.0	0.0	0.0	0.0	0.0	0.0
2	Se79	6.50e+04	7.90e+02	7.90e+03	5.50e+05	1.00e-08	6.97e-02	1.00e+02	1.0	4.8	2.4	3.2	16.0	81.0
3	Tc99	2.15e+05	3.50e-02	1.00e+02	9.90e+05	1.00e-08	1.70e-02	1.00e+04	0.0	0.0	0.0	0.1	0.7	3.5
4	Zr93	1.53e+06	9.18e-08	7.90e-04	9.10e-03	1.00e-08	2.51e-03	1.00e+02	177.1	885.5	4427.5	483.0	2415.0	12075.0
5	Pd107	6.50e+06	5.90e-02	1.05e+02	5.90e+03	1.00e-08	5.14e-04	1.00e+03	3.6	18.0	90.0	3.2	16.0	80.0
6	Sn126	1.00e+05	1.30e-06	6.50e-03	1.30e-02	1.00e-08	2.84e-02	1.00e+02	64.4	322.0	1610.0	50.6	253.0	1265.0
7	U234	2.47e+05	5.00e-01	2.40e+00	5.00e+01	5.26e-01	6.18e-03	1.00e+02	1.7	8.5	42.0	0.8	4.1	20.0
8	U235	7.10e+08	5.00e-01	2.40e+00	5.00e+01	1.72e-03	2.14e-06	1.00e+02	1.7	8.5	42.0	0.8	4.1	20.0
9	U238	4.51e+09	5.00e-01	2.40e+00	5.00e+01	2.69e-01	3.33e-07	1.00e+02	1.7	8.5	42.0	0.8	4.1	20.0
10	Np237	2.14e+06	4.00e-04	3.60e+02	7.20e+02	4.81e+00	7.05e-04	1.00e+02	3.6	18.0	90.0	3.2	16.0	80.0
11	Pu239	2.44e+04	6.00e-05	9.60e-04	4.30e-01	6.06e+03	6.13e-02	1.00e+02	45.0	225.0	1120.0	30.0	150.0	750.0
12	Pu240	6.58e+03	6.00e-05	9.60e-04	4.30e-01	2.83e+03	2.26e-01	1.00e+02	45.0	225.0	1120.0	30.0	150.0	750.0
13	Pu242	3.79e+05	6.00e-05	9.60e-04	4.30e-01	1.99e+01	3.90e-03	1.00e+02	45.0	225.0	1120.0	30.0	150.0	750.0

Weapons Grade Plutonium Disposition DHLW Spike Option

Number of Nuclides, Solubility/Retardation Levels, Probability of Retardation Levels

13 3 0.333 0.334 0.333

Index	Name	Half Life	Solubility Limit (gm/m**3)			Inventory	Activity	EPA	Rho * Kd (Level 1)			Rho * Kd (Level 2)		
		(yrs)	low	moderate	high	(Ci/MTHM)	(Ci/gm)	Limit	low	moderate	high	low	moderate	high
1	C14	5.73e+03	1.00e+00	1.40e+00	1.40e+02	0.00e+00	4.45e+00	1.00e+02	0.0	0.0	0.0	0.0	0.0	0.0
2	Se79	6.50e+04	7.90e+02	7.90e+03	5.50e+05	4.59e-02	6.97e-02	1.00e+02	1.0	4.8	2.4	3.2	16.0	81.0
3	Tc99	2.15e+05	3.50e-02	1.00e+02	9.90e+05	1.65e+00	1.70e-02	1.00e+04	0.0	0.0	0.0	0.1	0.7	3.5
4	I129	1.59e+07	1.00e+00	3.90e+02	1.00e+05	9.50e-07	1.74e-04	1.00e+02	0.0	0.0	0.0	0.0	0.0	0.0
5	Cs135	3.00e+06	1.20e+00	3.90e+02	2.10e+03	5.75e-02	8.82e-04	1.00e+03	2500.0	12500.0	62500.0	133.0	667.0	3300.0
6	Ra226	1.62e+03	1.00e-05	4.00e-04	1.00e-01	4.69e-08	9.88e-01	1.00e+02	8000.0	40000.0	0.0	12000.0	58000.0	0.0
7	U234	2.47e+05	5.00e-01	2.40e+00	5.00e+01	9.70e-02	6.18e-03	1.00e+02	1.7	8.5	42.0	0.8	4.1	20.0
8	U235	7.10e+08	5.00e-01	2.40e+00	5.00e+01	3.97e-05	2.14e-06	1.00e+02	1.7	8.5	42.0	0.8	4.1	20.0
9	U238	4.51e+09	5.00e-01	2.40e+00	5.00e+01	1.89e-03	3.33e-07	1.00e+02	1.7	8.5	42.0	0.8	4.1	20.0
10	Np237	2.14e+06	4.00e-04	3.60e+02	7.20e+02	2.60e-02	7.05e-04	1.00e+02	3.6	18.0	90.0	3.2	16.0	80.0
11	Pu239	2.44e+04	6.00e-05	9.60e-04	4.30e-01	4.42e+02	6.13e-02	1.00e+02	45.0	225.0	1120.0	30.0	150.0	750.0
12	Pu240	6.58e+03	6.00e-05	9.60e-04	4.30e-01	1.67e+00	2.26e-01	1.00e+02	45.0	225.0	1120.0	30.0	150.0	750.0
13	Pu242	3.79e+05	6.00e-05	9.60e-04	4.30e-01	2.51e-03	3.90e-03	1.00e+02	45.0	225.0	1120.0	30.0	150.0	750.0

The next set of files is the container failure parameter input. These files are used in a slightly different manner than described in the IMARC Users Manual [86]. The first nine lines of each file are ignored as the current version of IMARC does not utilize them. Three container designs are input for each file. For example, for the SCP design, container parameters are input for each of the three APDs analyzed. The input for each container is described as the following.

1. dummy variable, container type (called for in IMARC execution)
2. time constant for early failure , dryout time 1, dryout time 2 (not used), fraction of containers failed at emplacement, fraction of early failures.
3. threshold time to failure (2-barrier or three barrier) - four temperature regions
4. threshold time to failure (2-barrier or three barrier) - four temperature regions
5. Wiebull slope (2-barrier or three barrier) - four temperature regions

Note that the container model is set up to handle multiple barrier containers (up to 3). The model used in IMARC to predict multiple container failure is not used. The model described in Chapter 4 is utilized instead. To implement the results obtained in Chapter 4 into IMARC, the first set of Weibull parameters are input and the subsequent barrier parameters are set so that they result in rapid failure (the inner barriers are ignored).

Weibull parameters are input for four discrete temperature regimes. The fraction of containers in each regime is input in the vertical path input file described next. It should be noted that in Chapter 4 that the repository was discretized into six rings for hydrothermal calculations. The results were then combined to develop a four temperature history model. Minor changes were required relative to the results obtained in Chapter 4, however their effects on the container performance are mininal.

SCP Container

```
1 1 0.000 0. 0. 0. 0. 0. 0. 0.
1 2 0.000 0. 0. 0. 0. 0. 0. 0.
1 3 0.000 0. 0. 0. 0. 0. 0. 0.
2 1 0.000 0. 0. 0. 0. 0. 0. 0.
2 2 0.000 0. 0. 0. 0. 0. 0. 0.
2 3 0.000 0. 0. 0. 0. 0. 0. 0.
3 1 1.000 0. 0. 0. 0. 0. 0. 0.
3 2 1.000 0. 0. 0. 0. 0. 0. 0.
3 3 1.000 0. 0. 0. 0. 0. 0. 0.
0 1                                                    APD = 28.5 kW/acre
500. 0. 0. 0.0 0.0
500.  0.0 0.0  500.  0.0 0.0  500.  0.0 0.0  500.  0.0 0.0
2250. 0.0 1.0  2250. 0.0 1.0  2250. 0.0 1.0  2250. 0.0 1.0
2.0   0.0 2.0  2.0   0.0 2.0  2.0   0.0 2.0  2.0   0.0 2.0
0 2                                                    APD = 57.0 kW/acre
500. 0. 0. 0. 0.
1500.  0.0 0.0  1375.  0.0 0.0  1000.  0.0 0.0  500.  0.0 0.0
2250.  0.0 1.0  2000.  0.0 1.0  2000.  0.0 1.0  2250. 0.0 1.0
2.0    0.0 2.0  2.0    0.0 2.0  2.0    0.0 2.0  2.0   0.0 2.0
0 3                                                    APD = 114.0 kW/acre
500. 0. 0. 0. 0.
7250.  0.0 0.0  6500.  0.0 0.0  6000.  0.0 0.0  5500.  0.0 0.0
2000.  1.0 1.0  2250.  1.0 1.0  2225.  1.0 1.0  2100.  1.0 1.0
2.05   2.0 2.0  2.10   2.0 2.0  2.1    2.0 2.0  2.1    2.0 2.0
```

MPC Container

```
1 1 0.000 0. 0. 0. 0. 0. 0. 0.
1 2 0.000 0. 0. 0. 0. 0. 0. 0.
1 3 0.000 0. 0. 0. 0. 0. 0. 0.
2 1 0.000 0. 0. 0. 0. 0. 0. 0.
2 2 0.000 0. 0. 0. 0. 0. 0. 0.
2 3 0.000 0. 0. 0. 0. 0. 0. 0.
3 1 1.000 0. 0. 0. 0. 0. 0. 0.
3 2 1.000 0. 0. 0. 0. 0. 0. 0.
3 3 1.000 0. 0. 0. 0. 0. 0. 0.
0 1                                                    APD = 28.5 kW/acre
500. 0. 0. 0.0 0.0
5000.  0.0 0.0  5500.  0.0 0.0  6000.  0.0 0.0  6000.  0.0 0.0
12000. 0.0 1.0  13000. 0.0 1.0  13750. 0.0 1.0  14000. 0.0 1.0
1.7    0.0 2.0  1.75   0.0 2.0  1.7    0.0 2.0  1.7    0.0 2.0
0 2                                                    APD = 57.0 kW/acre
500. 0. 0. 0. 0.
5000.  0.0 0.0  5000.  0.0 0.0  5000.  0.0 0.0  5000.  0.0 0.0
7500.  0.0 1.0  7500.  0.0 1.0  7500.  0.0 1.0  8000.  0.0 1.0
1.4    0.0 2.0  1.35   0.0 2.0  1.35   0.0 2.0  1.35   0.0 2.0
0 3                                                    APD = 114.0 kW/acre
500. 0. 0. 0. 0.
10000. 0.0 0.0  10000. 0.0 0.0  11500. 0.0 0.0  11500. 0.0 0.0
9000.  1.0 1.0  8500.  1.0 1.0  9250.  1.0 1.0  10000. 1.0 1.0
1.6    2.0 2.0  1.55   2.0 2.0  1.6    2.0 2.0  1.6    2.0 2.0
```

ALMR MMB Container Co-Located With Spent LWR Fuel

```
1 1 0.000 0. 0. 0. 0. 0. 0. 0.
1 2 0.000 0. 0. 0. 0. 0. 0. 0.
1 3 0.000 0. 0. 0. 0. 0. 0. 0.
2 1 0.000 0. 0. 0. 0. 0. 0. 0.
2 2 0.000 0. 0. 0. 0. 0. 0. 0.
2 3 0.000 0. 0. 0. 0. 0. 0. 0.
3 1 1.000 0. 0. 0. 0. 0. 0. 0.
3 2 1.000 0. 0. 0. 0. 0. 0. 0.
3 3 1.000 0. 0. 0. 0. 0. 0. 0.
0 1                                                    APD = 28.5 kW/acre
500. 0. 0. 0.0 0.0
6000.  0.0 0.0  6000.  0.0 0.0  6000.  0.0 0.0  6000.  0.0 0.0
15000. 0.0 1.0  15000. 0.0 1.0  15000. 0.0 1.0  15000. 0.0 1.0
1.65   0.0 2.0  1.65   0.0 2.0  1.65   0.0 2.0  1.65   0.0 2.0
0 2                                                    APD = 57.0 kW/acre
500. 0. 0. 0. 0.
5500.  0.0 0.  5500.  0.0 0. 5500.  0.0 0.  5500.  0.0 0.
10250. 0.0 1.  10250. 0.0 1. 10250. 0.0 1.  10250. 0.0 1.
1.55   0.0 2.  1.55   0.0 2. 1.55   0.0 2.  1.55   0.0 2.
0 3                                                    APD = 114.0 kW/acre
500. 0. 0. 0. 0.
7000. 0.0 0.0  7000. 0.0 0.0  7000. 0.0 0.0  7000. 0.0 0.0
9000. 1.0 1.0  9000. 1.0 1.0  9000. 1.0 1.0  9000. 1.0 1.0
1.60  2.0 2.0  1.60  2.0 2.0  1.60  2.0 2.0  1.60  2.0 2.0
```

ALMR MMB Container Emplaced Alone

```
1 1 0.000 0. 0. 0. 0. 0. 0. 0.
1 2 0.000 0. 0. 0. 0. 0. 0. 0.
1 3 0.000 0. 0. 0. 0. 0. 0. 0.
2 1 0.000 0. 0. 0. 0. 0. 0. 0.
2 2 0.000 0. 0. 0. 0. 0. 0. 0.
2 3 0.000 0. 0. 0. 0. 0. 0. 0.
3 1 1.000 0. 0. 0. 0. 0. 0. 0.
3 2 1.000 0. 0. 0. 0. 0. 0. 0.
3 3 1.000 0. 0. 0. 0. 0. 0. 0.
0 1                                                    This set is actual parameters
500. 0. 0. 0.0 0.0
17000. 0.0 0.0  17000. 0.0 0.0  17000. 0.0 0.0  17000. 0.0 0.0
45000. 0.0 1.0  45000. 0.0 1.0  45000. 0.0 1.0  45000. 0.0 1.0
1.3   0.0 2.0  1.3   0.0 2.0  1.3   0.0 2.0  1.3   0.0 2.0
0 2                                                    for use in sensitivity analysis
500. 0. 0. 0. 0.
17000. 0.0 0.0  17000. 0.0 0.0  17000. 0.0 0.0  17000. 0.0 0.
22500. 0.0 1.0  22500. 0.0 1.0  22500. 0.0 1.0  22500. 0.0 1.
1.3   0.0 2.0  1.3   0.0 2.0  1.3   0.0 2.0  1.3   0.0 2.
0 3                                                    for use in sensitivity analysi
500. 0. 0. 0. 0.
17000. 0.0 0.0  17000. 0.0 0.0  17000. 0.0 0.0  17000. 0.0 0.0
90000. 1.0 1.0  90000. 1.0 1.0  90000. 1.0 1.0  90000. 1.0 1.0
1.3   2.0 2.0  1.3   2.0 2.0  1.3   2.0 2.0  1.3   2.0 2.0
```

ALMR MMB Container Co-Located With LWR Spent Fuel -- Sensitivity

```
1 1 0.000 0. 0. 0. 0. 0. 0. 0.
1 2 0.000 0. 0. 0. 0. 0. 0. 0.
1 3 0.000 0. 0. 0. 0. 0. 0. 0.
2 1 0.000 0. 0. 0. 0. 0. 0. 0.
2 2 0.000 0. 0. 0. 0. 0. 0. 0.
2 3 0.000 0. 0. 0. 0. 0. 0. 0.
3 1 1.000 0. 0. 0. 0. 0. 0. 0.
3 2 1.000 0. 0. 0. 0. 0. 0. 0.
3 3 1.000 0. 0. 0. 0. 0. 0. 0.
0 1                                                    This set is actual parameters
500. 0. 0. 0.0 0.0
7000.  0.0 0.0  7000.  0.0 0.0  7000.  0.0 0.0  7000.  0.0 0.0
4500.  0.0 1.0  4500.  0.0 1.0  4500.  0.0 1.0  4500.  0.0 1.0
1.60   0.0 2.0  1.60   0.0 2.0  1.60   0.0 2.0  1.60   0.0 2.0
0 2                                                    for use in sensitivity analysis
500. 0. 0. 0. 0.
7000.  0.0 0.  7000.  0.0 0. 7000.  0.0 0.  7000.  0.0 0.
18000. 0.0 1.  18000. 0.0 1. 18000. 0.0 1.  18000. 0.0 1.
1.60   0.0 2.  1.60   0.0 2. 1.60   0.0 2.  1.60   0.0 2.
0 3                                                    for use in sensitivity analysis
500. 0. 0. 0. 0.
7000. 0.0 0.0  7000. 0.0 0.0  7000. 0.0 0.0  7000. 0.0 0.0
9000. 1.0 1.0  9000. 1.0 1.0  9000. 1.0 1.0  9000. 1.0 1.0
1.60  2.0 2.0  1.60  2.0 2.0  1.60  2.0 2.0  1.60  2.0 2.0
```

The next set of input files provide the temperature ring discretization utilized in the IMARC executions. Again, these are used in a slightly different manner than described in the IMARC Users MAunal [85]. The purpose of this file is to discretize the containers between heat transfer mechanisms, water contact modes, and temperature histories. Container discretization is allowed for three APD values. Which set of parameters is utilized is input upon execution of IMARC. Three heat transfer modes exist for each APD. Four water contact modes exist for each APD. Four temperature regimes exist for each water contact mode.

The IMARC3 input file determines which heat transfer mechanism is utilized. In this study, only one undefined heat transfer mechanism was utilized. Therefore the only data input is on the first line for each APD. In addition, only the moist continuous and wet drip water contact modes were utilized. As such, data is entered only in the first two water contact locations, with 50% of the containers residing in each water contact mode.

The discretization is accomplished by determining the fraction of containers in each temperature regime that match the associated container failure parameters. As was stated previously, in the Chapter 4 analysis of container performance six temperature regions were modeled. The results were combined to four for input into IMARC.

Water Contact Mode and Temperature Ring Discretization SCP Container
LWR Spent Fuel

1 APD INDEX 1 = 28.5 kW/acre

Moist-Cont				Wet Drip				Episodic				Dry				
Alpha	Beta	Gamma	Delta	Alpha	Beta	Gamma	Delta	Alpha	Beta	Gamma	Delta	Alpha	Beta	Gamma	Delta	
0.125	0.125	0.125	0.125	0.125	0.125	0.125	0.125	0.000	0.000	0.000	0.000	0.000	0.000	0.000	0.000	* this line
0.000	0.020	0.001	0.000	0.000	0.040	0.001	0.000	0.000	0.040	0.003	0.000	0.000	0.040	0.003	0.000	
0.000	0.120	0.050	0.000	0.000	0.130	0.050	0.000	0.000	0.050	0.050	0.000	0.000	0.050	0.050	0.000	

2 APD INDEX 2 = 57 kW/acre

Moist-Cont				Wet Drip				Episodic				Dry				
Alpha	Beta	Gamma	Delta	Alpha	Beta	Gamma	Delta	Alpha	Beta	Gamma	Delta	Alpha	Beta	Gamma	Delta	
0.0835	0.1665	0.0835	0.1665	0.0835	0.1665	0.0835	0.1665	0.000	0.000	0.000	0.000	0.000	0.000	0.000	0.000	* this line
0.010	0.010	0.040	0.000	0.010	0.015	0.030	0.000	0.060	0.015	0.060	0.000	0.320	0.360	0.070	0.000	
0.000	0.025	0.150	0.000	0.005	0.030	0.150	0.000	0.045	0.005	0.200	0.000	0.250	0.040	0.100	0.000	

3 APD INDEX 3 = 114 kW/acre

Moist-Cont				Wet Drip				Episodic				Dry				
Alpha	Beta	Gamma	Delta	Alpha	Beta	Gamma	Delta	Alpha	Beta	Gamma	Delta	Alpha	Beta	Gamma	Delta	
0.1665	0.0835	0.1665	0.0835	0.1665	0.0835	0.1665	0.0835	0.000	0.000	0.000	0.000	0.000	0.000	0.000	0.000	* this line
0.020	0.000	0.020	0.000	0.030	0.000	0.010	0.000	0.100	0.000	0.040	0.010	0.100	0.000	0.040	0.010	
0.010	0.000	0.100	0.000	0.020	0.000	0.100	0.000	0.020	0.000	0.150	0.000	0.020	0.000	0.150	0.000	

Water Contact Mode and Temperature Discretization MMB Container, Spent LWR Fuel

1 APD INDEX 1 = 36 kW/acre

Moist-Cont				Wet Drip				Episodic				Dry				
Alpha	Beta	Gamma	Delta	Alpha	Beta	Gamma	Delta	Alpha	Beta	Gamma	Delta	Alpha	Beta	Gamma	Delta	
0.250	0.0835	0.0835	0.083	0.250	0.0835	0.0835	0.083	0.000	0.000	0.000	0.000	0.000	0.000	0.000	0.000	* this line
0.000	0.020	0.001	0.000	0.000	0.040	0.001	0.000	0.000	0.040	0.003	0.000	0.000	0.040	0.003	0.000	
0.000	0.120	0.050	0.000	0.000	0.130	0.050	0.000	0.000	0.050	0.050	0.000	0.000	0.050	0.050	0.000	

2 APD INDEX 2 = 57 kW/acre

Moist-Cont				Wet Drip				Episodic				Dry				
Alpha	Beta	Gamma	Delta	Alpha	Beta	Gamma	Delta	Alpha	Beta	Gamma	Delta	Alpha	Beta	Gamma	Delta	
0.250	0.0835	0.0835	0.083	0.250	0.0835	0.0835	0.083	0.000	0.000	0.000	0.000	0.000	0.000	0.000	0.000	* this line
0.010	0.010	0.040	0.000	0.010	0.015	0.030	0.000	0.060	0.015	0.060	0.000	0.320	0.360	0.070	0.000	
0.000	0.025	0.150	0.000	0.005	0.030	0.150	0.000	0.045	0.005	0.200	0.000	0.250	0.040	0.100	0.000	

3 APD INDEX 3 = 114 kW/acre

Moist-Cont				Wet Drip				Episodic				Dry				
Alpha	Beta	Gamma	Delta	Alpha	Beta	Gamma	Delta	Alpha	Beta	Gamma	Delta	Alpha	Beta	Gamma	Delta	
0.167	0.1665	0.083	0.0835	0.167	0.1665	0.083	0.0835	0.000	0.000	0.000	0.000	0.000	0.000	0.000	0.000	* this line
0.020	0.000	0.020	0.000	0.030	0.000	0.010	0.000	0.100	0.000	0.040	0.010	0.100	0.000	0.040	0.010	
0.010	0.000	0.100	0.000	0.020	0.000	0.100	0.000	0.020	0.000	0.150	0.000	0.020	0.000	0.150	0.000	

Water Contact Mode and Temperature Discretization, MMB Container, ALMR

1 APD INDEX 1 = 36 kW/acre

Moist-Cont				Wet Drip				Episodic				Dry				
Alpha	Beta	Gamma	Delta	Alpha	Beta	Gamma	Delta	Alpha	Beta	Gamma	Delta	Alpha	Beta	Gamma	Delta	
0.125	0.125	0.125	0.125	0.125	0.125	0.125	0.125	0.000	0.000	0.000	0.000	0.000	0.000	0.000	0.000	* this line
0.000	0.020	0.001	0.000	0.000	0.040	0.001	0.000	0.000	0.040	0.003	0.000	0.000	0.040	0.003	0.000	
0.000	0.120	0.050	0.000	0.000	0.130	0.050	0.000	0.000	0.050	0.050	0.000	0.000	0.050	0.050	0.000	

2 APD INDEX 2 = 57 kW/acre

Moist-Cont				Wet Drip				Episodic				Dry				
Alpha	Beta	Gamma	Delta	Alpha	Beta	Gamma	Delta	Alpha	Beta	Gamma	Delta	Alpha	Beta	Gamma	Delta	
0.125	0.125	0.125	0.125	0.125	0.125	0.125	0.125	0.000	0.000	0.000	0.000	0.000	0.000	0.000	0.000	* this line
0.010	0.010	0.040	0.000	0.010	0.015	0.030	0.000	0.060	0.015	0.060	0.000	0.320	0.360	0.070	0.000	
0.000	0.025	0.150	0.000	0.005	0.030	0.150	0.000	0.045	0.005	0.200	0.000	0.250	0.040	0.100	0.000	

3 APD INDEX 3 = 114 kW/acre

Moist-Cont				Wet Drip				Episodic				Dry				
Alpha	Beta	Gamma	Delta	Alpha	Beta	Gamma	Delta	Alpha	Beta	Gamma	Delta	Alpha	Beta	Gamma	Delta	
0.125	0.125	0.125	0.125	0.125	0.125	0.125	0.125	0.000	0.000	0.000	0.000	0.000	0.000	0.000	0.000	* this line
0.020	0.000	0.020	0.000	0.030	0.000	0.010	0.000	0.100	0.000	0.040	0.010	0.100	0.000	0.040	0.010	
0.010	0.000	0.100	0.000	0.020	0.000	0.100	0.000	0.020	0.000	0.150	0.000	0.020	0.000	0.150	0.000	

Water Contact Mode and Temperature Discretization, MMB Container, ALMR
Water Contact Mode Sensitivity

1 APD INDEX 1 = Moist Continuous

Moist-Cont				Wet Drip				Episodic				Dry				
Alpha	Beta	Gamma	Delta	Alpha	Beta	Gamma	Delta	Alpha	Beta	Gamma	Delta	Alpha	Beta	Gamma	Delta	
0.250	0.250	0.250	0.250	0.000	0.000	0.000	0.000	0.000	0.000	0.000	0.000	0.000	0.000	0.000	0.000	* this line
0.000	0.020	0.001	0.000	0.000	0.040	0.001	0.000	0.000	0.040	0.003	0.000	0.000	0.040	0.003	0.000	
0.000	0.120	0.050	0.000	0.000	0.130	0.050	0.000	0.000	0.050	0.050	0.000	0.000	0.050	0.050	0.000	

2 APD INDEX 2 = Wet Drip

Moist-Cont				Wet Drip				Episodic				Dry				
Alpha	Beta	Gamma	Delta	Alpha	Beta	Gamma	Delta	Alpha	Beta	Gamma	Delta	Alpha	Beta	Gamma	Delta	
0.000	0.000	0.000	0.000	0.250	0.250	0.250	0.250	0.000	0.000	0.000	0.000	0.000	0.000	0.000	0.000	* this line
0.010	0.010	0.040	0.000	0.010	0.015	0.030	0.000	0.060	0.015	0.060	0.000	0.320	0.360	0.070	0.000	
0.000	0.025	0.150	0.000	0.005	0.030	0.150	0.000	0.045	0.005	0.200	0.000	0.250	0.040	0.100	0.000	

3 APD INDEX 3 = 114 kW/acre

Moist-Cont				Wet Drip				Episodic				Dry			
Alpha	Beta	Gamma	Delta	Alpha	Beta	Gamma	Delta	Alpha	Beta	Gamma	Delta	Alpha	Beta	Gamma	Delta
0.125	0.125	0.125	0.125	0.125	0.125	0.125	0.125	0.000	0.000	0.000	0.000	0.000	0.000	0.000	0.000
0.020	0.000	0.020	0.000	0.030	0.000	0.010	0.000	0.100	0.000	0.040	0.010	0.100	0.000	0.040	0.010
0.010	0.000	0.100	0.000	0.020	0.000	0.100	0.000	0.020	0.000	0.150	0.000	0.020	0.000	0.150	0.000

Note: For sensitivity study, APD index was utilized as water contact mode index.

Input files is for IMARC1 execution.

```
INPUT FOR IMARC1 RUN Spent LWR Fuel (Both Container Types) 1/5/95
5                                   ! nlev
3 2 1 4 2                           ! nbranch(nlev)

0 0 0 2  1 1 0.01 0.01              ! node 1 ! ndepend(3) nvar, ncalc(nvar) tol(nvar)
0 0 0 1  1 0.01                     ! node 2
0 0 0 1  1 0.01                     ! node 3
0 0 0 1  1 0.01                     ! node 4
0 0 0 1  1 0.01                     ! node 5

0.05  0.9 0.5  ! FLUXES -- node 1, branch 1
0.90  0.9 1.5  ! FLUXES -- node 1, branch 2
0.05  0.9 5.4  ! FLUXES -- node 1, branch 3

0.45  1       ! LATERAL RE-DISTRIBUTION CODE (none)   - node 2, branch 1
0.55  2       ! LATERAL RE-DISTRIBUTION CODE (moder.) - node 2, branch 1

1.0   1       ! EQUATION FOR FLUX TIME LAG - node 3, branch 1

0.25    0.0       ! DELTA WT GIVEN CLIMATE - node 4[1=2], branch 1
0.25   60.0       ! DELTA WT GIVEN CLIMATE - node 4[1=2], branch 2
0.25  130.0       ! DELTA WT GIVEN CLIMATE - node 4[1=2], branch 3
0.25  230.0       ! DELTA WT GIVEN CLIMATE - node 4[1=2], branch 4

0.8   1       ! FRACTURE-MATRIX COUPLING  --  node 5, branch 1
0.2   2       ! FRACTURE-MATRIX COUPLING  --  node 5, branch 2
```

```
INPUT FOR IMARC1 ALMR AND ACTINIDE RECYCLE 1/5/95
5
3 2 1 4 2

0 0 0 2  1 1 0.01 0.01              ! node 1
0 0 0 1  1 0.01                   ! node 2
0 0 0 1  1 0.01                   ! node 3
0 0 0 1  1 0.01                   ! node 4
0 0 0 1  1 0.01                   ! node 5

0.05  0.9 0.5  ! FLUXES -- node 1, branch 1
0.90  0.9 1.5  ! FLUXES -- node 1, branch 2
0.05  0.9 5.4  ! FLUXES -- node 1, branch 3

0.45  1       ! LATERAL RE-DISTRIBUTION CODE (none)   - node 2, branch 1
0.55  2       ! LATERAL RE-DISTRIBUTION CODE (moder.) - node 2, branch 1

1.0   1       ! EQUATION FOR FLUX TIME LAG - node 3, branch 1

0.25    0.0     ! DELTA WT GIVEN CLIMATE - node 4[1=2], branch 1
0.25   60.0     ! DELTA WT GIVEN CLIMATE - node 4[1=2], branch 2
0.25  130.0     ! DELTA WT GIVEN CLIMATE - node 4[1=2], branch 3
0.25  230.0     ! DELTA WT GIVEN CLIMATE - node 4[1=2], branch 4

0.8   1      ! FRACTURE-MATRIX COUPLING  --  node 5, branch 1
0.2   2      ! FRACTURE-MATRIX COUPLING  --  node 5, branch 2
```

Note: IMARC1 Executed for each wasteform type (Mineral and Metallic) to build nuclid dependent transport files.

```
INPUT FOR DHLW IMARC1 RUN 1/5/95
5
3 2 1 4 2

0 0 0 2  1 1 0.01 0.01              ! node 1
0 0 0 1  1 0.01                   ! node 2
0 0 0 1  1 0.01                   ! node 3
0 0 0 1  1 0.01                   ! node 4
0 0 0 1  1 0.01                   ! node 5

0.05  0.9 0.5  ! FLUXES -- node 1, branch 1
0.90  0.9 1.5  ! FLUXES -- node 1, branch 2
0.05  0.9 5.4  ! FLUXES -- node 1, branch 3

0.45  1       ! LATERAL RE-DISTRIBUTION CODE (none)   - node 2, branch 1
0.55  2       ! LATERAL RE-DISTRIBUTION CODE (moder.) - node 2, branch 1

1.0   1       ! EQUATION FOR FLUX TIME LAG - node 3, branch 1

0.25    0.0     ! DELTA WT GIVEN CLIMATE - node 4[1=2], branch 1
0.25   60.0     ! DELTA WT GIVEN CLIMATE - node 4[1=2], branch 2
0.25  130.0     ! DELTA WT GIVEN CLIMATE - node 4[1=2], branch 3
0.25  230.0     ! DELTA WT GIVEN CLIMATE - node 4[1=2], branch 4

0.8   1       ! FRACTURE-MATRIX COUPLING  --  node 5, branch 1
0.2   2       ! FRACTURE-MATRIX COUPLING  --  node 5, branch 2
Input files for IMARC2 Execution

LWR Spent Fuel SCP Container
```

Input files for IMARC2 Execution

```
INPUT FOR IMARC2 SOURCE TERM CALCULATION LWR SCP 1/5/95
5
3 2 4 3 2

0 0 0 1  1 0.01                    ! node 1
0 0 0 1  1 0.01                    ! node 2
0 0 0 1  1 0.01                    ! node 5
0 0 0 1  1 0.01                    ! node 5
0 0 0 1  1 0.01                    ! node 6

0.34  0.5     ! FLUXES -- node 1, branch 1
0.33  1.5     ! FLUXES -- node 1, branch 2
0.33  5.4     ! FLUXES -- node 1, branch 3

0.50  1       ! LATERAL RE-DISTRIBUTION CODE (none)   -- node 2, branch 1
0.50  2       ! LATERAL RE-DISTRIBUTION CODE (moder.) -- node 2, branch 2

0.25  1.0     ! WATER CONDITION = UNSATURATED  -- node 3, branch 1
0.25  2.0     ! WATER CONDITION = WET DRIP     -- node 3, branch 2
0.25  3.0     ! WATER CONDITION = EPISODIC     -- node 3, branch 3
0.25  4.0     ! WATER CONDITION = SATURATED    -- node 3, branch 4

0.25  0.11    ! REACTION RATE AND SOLUBILITY = LOW      -- node 4, branch 1
0.50  0.55    ! REACTION RATE AND SOLUBILITY = MODERATE -- node 4, branch
2
0.25  2.80    ! REACTION RATE AND SOLUBILITY = HIGH     -- node 4, branch 3

0.00  1.0     ! AIR GAP        -- node 5, branch 1
1.00  2.0     ! NO AIR GAP     -- node 5, branch 2
```

```
INPUT FOR IMARC2 SOURCE TERM CALCULATIONS LWR MMB 1/5/95
5
3 2 4 3 2

0 0 0 1  1 0.01                    ! node 1
0 0 0 1  1 0.01                    ! node 2
0 0 0 1  1 0.01                    ! node 5
0 0 0 1  1 0.01                    ! node 5
0 0 0 1  1 0.01                    ! node 6

0.34  0.5     ! FLUXES -- node 1, branch 1
0.33  1.5     ! FLUXES -- node 1, branch 2
0.33  5.4     ! FLUXES -- node 1, branch 3

0.50  1       ! LATERAL RE-DISTRIBUTION CODE (none)   -- node 2, branch 1
0.50  2       ! LATERAL RE-DISTRIBUTION CODE (moder.) -- node 2, branch 2

0.25  1.0     ! WATER CONDITION = UNSATURATED  -- node 3, branch 1
0.25  2.0     ! WATER CONDITION = WET DRIP     -- node 3, branch 2
0.25  3.0     ! WATER CONDITION = EPISODIC     -- node 3, branch 3
0.25  4.0     ! WATER CONDITION = SATURATED    -- node 3, branch 4

0.25  0.11    ! REACTION RATE AND SOLUBILITY = LOW      -- node 4, branch 1
0.50  0.55    ! REACTION RATE AND SOLUBILITY = MODERATE -- node 4, branch
2
0.25  2.80    ! REACTION RATE AND SOLUBILITY = HIGH     -- node 4, branch 3

0.00  1.0     ! AIR GAP        -- node 5, branch 1
1.00  2.0     ! NO AIR GAP     -- node 5, branch 2
```

```
INPUT FOR IMARC SOURCE TERM CALCULATIONS ALMR METALLIC 1/13/95
5
3 2 4 3 2

0 0 0 1  1 0.01                    ! node 1
0 0 0 1  1 0.01                    ! node 2
0 0 0 1  1 0.01                    ! node 5
0 0 0 1  1 0.01                    ! node 5
0 0 0 1  1 0.01                    ! node 6

0.34  0.5     ! FLUXES -- node 1, branch 1
0.33  1.5     ! FLUXES -- node 1, branch 2
0.33  5.4     ! FLUXES -- node 1, branch 3

0.50  1       ! LATERAL RE-DISTRIBUTION CODE (none)   -- node 2, branch 1
0.50  2       ! LATERAL RE-DISTRIBUTION CODE (moder.) -- node 2, branch 2

0.25  1.0     ! WATER CONDITION = UNSATURATED  -- node 3, branch 1
0.25  2.0     ! WATER CONDITION = WET DRIP     -- node 3, branch 2
0.25  3.0     ! WATER CONDITION = EPISODIC     -- node 3, branch 3
0.25  4.0     ! WATER CONDITION = SATURATED    -- node 3, branch 4

0.25  0.5     ! REACTION RATE AND SOLUBILITY = LOW      -- node 4, branch 1
0.50  5.0     ! REACTION RATE AND SOLUBILITY = MODERATE -- node 4, branch 2
0.25  50.0    ! REACTION RATE AND SOLUBILITY = HIGH     -- node 4, branch 3

0.00  1.0     ! AIR GAP        -- node 5, branch 1
1.00  2.0     ! NO AIR GAP     -- node 5, branch 2
```

NOTES:
Executed for Each metallic wasteform type to obtain proper source term output files.

For sensitivity study of reaction rate, the reaction rate and solubility branch changed for each case. For example, low sensitivity, all assigned a reaction rate of 0.5.

```
INPUT FOR IMARC SOURCE TERM CALCULATIONS ALMR MINERAL 1/13/95
5
3 2 4 3 2

0 0 0 1  1 0.01                    ! node 1
0 0 0 1  1 0.01                    ! node 2
0 0 0 1  1 0.01                    ! node 5
0 0 0 1  1 0.01                    ! node 5
0 0 0 1  1 0.01                    ! node 6

0.34  0.5     ! FLUXES -- node 1, branch 1
0.33  1.5     ! FLUXES -- node 1, branch 2
0.33  5.4     ! FLUXES -- node 1, branch 3

0.50  1       ! LATERAL RE-DISTRIBUTION CODE (none)   -- node 2, branch 1
0.50  2       ! LATERAL RE-DISTRIBUTION CODE (moder.) -- node 2, branch 2

0.25  1.0     ! WATER CONDITION = UNSATURATED  -- node 3, branch 1
0.25  2.0     ! WATER CONDITION = WET DRIP     -- node 3, branch 2
0.25  3.0     ! WATER CONDITION = EPISODIC     -- node 3, branch 3
0.25  4.0     ! WATER CONDITION = SATURATED    -- node 3, branch 4

0.25  18.25   ! REACTION RATE AND SOLUBILITY = LOW      -- node 4, branch 1
0.50  182.5   ! REACTION RATE AND SOLUBILITY = MODERATE -- node 4, br 2
0.25  1825.0  ! REACTION RATE AND SOLUBILITY = HIGH     -- node 4, branch 3

0.00  1.0     ! AIR GAP        -- node 5, branch 1
1.00  2.0     ! NO AIR GAP     -- node 5, branch 2
```

NOTES:
Executed for Each mineral wasteform type to obtain proper source term output files.

```
INPUT FOR IMARC2 DHLW PLUTONIUM DISPOSITION WASTEFORM 1/13/95
5
3 2 4 3 2

0 0 0 1  1 0.01                    ! node 1
0 0 0 1  1 0.01                    ! node 2
0 0 0 1  1 0.01                    ! node 5
0 0 0 1  1 0.01                    ! node 5
0 0 0 1  1 0.01                    ! node 6

0.34  0.5     ! FLUXES -- node 1, branch 1
0.33  1.5     ! FLUXES -- node 1, branch 2
0.33  5.4     ! FLUXES -- node 1, branch 3

0.50  1       ! LATERAL RE-DISTRIBUTION CODE (none)   -- node 2, branch 1
0.50  2       ! LATERAL RE-DISTRIBUTION CODE (moder.) -- node 2, branch 2

0.25  1.0     ! WATER CONDITION = UNSATURATED  -- node 3, branch 1
0.25  2.0     ! WATER CONDITION = WET DRIP     -- node 3, branch 2
0.25  3.0     ! WATER CONDITION = EPISODIC     -- node 3, branch 3
0.25  4.0     ! WATER CONDITION = SATURATED    -- node 3, branch 4

0.33  16.8    ! REACTION RATE AND SOLUBILITY = LOW      -- node 4, branch 1
0.34  40.6    ! REACTION RATE AND SOLUBILITY = MODERATE -- node 4, brnch 2
0.33  280.0   ! REACTION RATE AND SOLUBILITY = HIGH     -- node 4, branch 3

0.00  1.0     ! AIR GAP        -- node 5, branch 1
1.00  2.0     ! NO AIR GAP     -- node 5, branch 2
```

Input Files for IMARC 3 execution

LWR Spent Fuel Wasteforms (only difference is in transport
and source term file definitions)

```
INPUTS FOR IMARC RUNS SCP (MMB) CONTAINER 1/13/95              ! title
fullscp.trn  (scp runs)  fullmmb.trn (mmb runs)                ! transport file
fullscp.src  (scp runs)  fullmmp.src (mmb runs)                ! source term file
15                                                             ! nlev
3 2 4 2 2 3 2 2 2 3 3 2 1 3 1                    ! nbranch(nlev)

 0 0 0 2  1 1 0.01 0.01      !NODE 1        ! ndepend(3)  nvar  ncalc(nvar) tol(nvar)
 0 0 0 1  1 0.01             !NODE 2
 1 0 0 1  1 0.01             !NODE 3  (conditional on node 1)
 0 0 0 1  1 0.01             !NODE 4
 0 0 0 1  1 0.01             !NODE 5
 0 0 0 1  1 0.01             !NODE 6
 0 0 0 1  1 0.01             !NODE 7
 7 0 0 1  1 0.01             !NODE 8  (conditional on node 7)
 0 0 0 1  1 0.01             !NODE 9
 9 0 0 1  1 0.01             !NODE 10 (conditional on node 9)
 0 0 0 1  1 0.01             !NODE 11
 0 0 0 4  1 1 1 1 .01 .01 .01 .01     !NODE 12
 0 0 0 1  1 0.01             !NODE 13
 0 0 0 1  1 0.01             !NODE 14
 0 0 0 1  1 0.01             !NODE 15

0.05    0.9 0.5   ! FLUXES - NODE 1, BRANCH 1              prob  variable(nvar)
0.90    0.9 1.5   ! FLUXES - NODE 1, BRANCH 2              prob  variable(nvar)
0.05    0.9 5.4   ! FLUXES - NODE 1, BRANCH 3              prob  variable(nvar)

0.45    1       ! LATERAL RE-DISTRIBUTION CODE (none)          - NODE  2, BRANCH 1
0.55    2       ! LATERAL RE-DISTRIBUTION CODE (mod.)          - NODE  2, BRANCH
1

1.00     0.0    ! DELTA WT GIVEN CLIMATE-dependent on [1,1]    - NODE  3, BRANCH 1
0.00     60.0   ! DELTA WT GIVEN CLIMATE-dependent on [1,1]    - NODE  3, BRANCH 2
0.00     130.0  ! DELTA WT GIVEN CLIMATE-dependent on [1,1]    - NODE  3, BRANCH 3
0.00     230.0  ! DELTA WT GIVEN CLIMATE-dependent on [1,3]    - NODE  3, BRANCH 4

0.40     0.0    ! DELTA WT GIVEN CLIMATE-dependent on [1,2]    - NODE  3, BRANCH 1
0.60     60.0   ! DELTA WT GIVEN CLIMATE-dependent on [1,2]    - NODE  3, BRANCH 2
0.00     130.0  ! DELTA WT GIVEN CLIMATE-dependent on [1,2]    - NODE  3, BRANCH 3
0.00     230.0  ! DELTA WT GIVEN CLIMATE-dependent on [1,3]    - NODE  3, BRANCH 4

0.00     0.0    ! DELTA WT GIVEN CLIMATE-dependent on [1,2]    - NODE  3, BRANCH 1
0.80     60.0   ! DELTA WT GIVEN CLIMATE-dependent on [1,3]    - NODE  3, BRANCH 2
0.19     130.0  ! DELTA WT GIVEN CLIMATE-dependent on [1,3]    - NODE  3, BRANCH 3
0.01     230.0  ! DELTA WT GIVEN CLIMATE-dependent on [1,3]    - NODE  3, BRANCH 4
```

```
0.80    1        ! STRONG FRACTURE-MATRIX COUPLING          - NODE  4, BRANCH 1
0.20    2        !   WEAK FRACTURE-MATRIX COUPLING          - NODE  4, BRANCH 2

0.50    1000.    ! SATURATED FLOW VELOCITY                  - NODE  5, BRANCH 1
0.50    10000.   ! SATURATED FLOW VELOCITY                  - NODE  5, BRANCH 2

0.33    1        ! MATRIX RETARDATION VALUES LOW            - NODE  6, BRANCH 1
0.34    2        ! MATRIX RETARDATION VALUES MOD            - NODE  6, BRANCH 2
0.33    3        ! MATRIX RETARDATION VALUES HIGH           - NODE  6, BRANCH 3

1.00    1        ! NO VOLCANOES                             - NODE  7, BRANCH 1
0.00    2        ! VOLCANOES                                - NODE  7, BRANCH 2

1.00    0.0      ! DELTA WT GIVEN VOLCANO                   - NODE  8, BRANCH 1
0.00    60.0     ! DELTA WT GIVEN VOLCANO                   - NODE  8, BRANCH 2

1.00    0.0      ! DELTA WT GIVEN VOLCANO                   - NODE  8, BRANCH 1
0.00    60.0     ! DELTA WT GIVEN VOLCANO                     NODE  8, BRANCH 2

1.00    1        ! NO EARTHQUAKES                           - NODE  9, BRANCH 1
0.00    2        ! EARTHQUAKES                              - NODE  9, BRANCH 2

1.00    0.0      ! DELTA WT GIVEN EARTHQUAKES               - NODE 10, BRANCH 1
0.00    60.0     ! DELTA WT GIVEN EARTHQUAKES               - NODE 10, BRANCH 2
0.00    130.0    ! DELTA WT GIVEN EARTHQUAKES               - NODE 10, BRANCH 3

0.931   0.0      ! DELTA WT GIVEN EARTHQUAKES               ` NODE 10, BRANCH 1
0.063   60.0     ! DELTA WT GIVEN EARTHQUAKES               - NODE 10, BRANCH 2
0.006   130.0    ! DELTA WT GIVEN EARTHQUAKES               - NODE 10, BRANCH 3

1.00    1        ! THERMAL PROCESS - CONDUCTION             - NODE 11, BRANCH 1
0.00    2        ! THERMAL PROCESS - HIGH PERM.             - NODE 11, BRANCH 2
0.00    3        ! THERMAL PROCESS - WATER MOBILE IN FRACTURES -
                                                            - NODE 11, BRANCH 3

0.00    0.000 0.000 0.000 0.000  ! NO BOREHOLE FRACTURES   - NODE 12, BRANCH 1
1.00    1.0 1.0 1.0 1.0          ! BOREHOLE FRACTURES      - NODE 12, BRANCH 2

1.0     1        ! CONTAINER (DUMMY NODE)                   - NODE 13, BRANCH 1

0.25    0.11     ! SOLUBILITY LOW                           - NODE 14, BRANCH 1
0.50    0.55     ! SOLUBILITY MODERATE                      - NODE 14, BRANCH 2
0.25    2.80     ! SOLUBILITY HIGH                          - NODE 14, BRANCH 3

1.00    1        ! NO HUMAN INTRUSION                       - NODE 15, BRANCH 1
```

For ALMR and DHLW runs, only parameters changed are the transport and source term file definitions and the solubility assignment.

APPENDIX C

RIP INPUT FILE DESCRIPTION

This is the a description of the RIP input files utlized. This description is taken from an echo of one of the RIP files utilized. The basic model is identical for all wasteforms considered. Different modeling parameters are described for each wasteform.

```
This file is organized as follows:
  *GENERAL INFORMATION*
  *SIMULATION DETAILS*
  *RN TABLE*
  *WASTE PACKAGE DESCRIPTION*
  *NEAR FIELD CONDITIONS*
  *PATHWAY DESCRIPTIONS*
  *RECEPTOR DESCRIPTIONS*
  *DOSE CONVERSION TABLES*
  *DISRUPTIVE EVENTS*
  *STRATEGY*
  *PARAMETER DATABASE*

  *GENERAL INFORMATION*

 The number of defined paths is 48
  The paths are : SAT,BWCOL4,BWCOL5,PPCOL1,PPCOL2,PPCOL3,PPCOL4,PPCOL5
PPCOL6,PPCOL7,PPCOL8,PPCOL9,CHZC1,CHZC2,CHZC3,CHZC4,CHZC5,CHZC6,
CHZC7,CHZC8,CHZC9,CHVC1,CHVC2,CHVC3,CHVC4,CHVC5,CHVC6,CHVC7,
CHVC8,CHVC9,TS3C1,TS3C2,TS3C3,TS3C4,TS3C5,TS3C6,TS3C7,TS3C8,TS3C9,
TS2C1,TS2C2,TS2C3,TS2C4,TS2C5,TS2C6,TS2C7,TS2C8,TS2C9

 The number of defined receptors is 0
  The receptors are :
 The number of defined dose conversion tables is 0
  The dose conversion tables are :
 The number of defined waste packages is dependent on the wasteform under
    consideration.  For LWR SF 6 waste packages are defined.  For DHLW and
    pyroprocess wastes, 1 waste package is defined

  The WPs are  (LWR SF) : RING1,RING2,RING3,RING4,RING5,RING6
  The WPs are  (DHLW and pyroprocess) : RING7

 The Radionuclide Groups are :
  Group  1 AM241
  Group  2 CM244
  Group  3 CS135
  Group  4 I129
```

Group 5 NP237
Group 6 PU238,PU239,PU240,PU241,PU242
Group 7 RA226
Group 8 SE79
Group 9 TC99
Group 10 U234,U235,U238
Group 11 Zr93 (for pyroprocess ER metal only)
Group 12 Sn126 (for pyroprocess ER metal only)
Group 13 Pd107 (for pyroprocess ER metal only)

SIMULATION DETAILS

The number of timesteps used is 10, 50, 100 (depends on time under consideration)
The number of years per timestep is 1000
The total number of realizations is 100
Random results are being generated
Latin-Hypercube sampling is turned on

RN TABLE

RN ID	Decay Rate	Regulatory Limit	Activity	Daughter	
AM241	1.603E-03	1.0E-01	3.82E+04	NP237	
CM244	3.829E-02	2.0E-01	2.36E+04	PU240	
CS135	3.013E-07	1.0E+00	5.52E+00	-	
I129	4.414E-08	1.0E-01	3.62E-01	-	
NP237	3.238E-07	1.0E-01	4.73E+00	-	
PU238	7.897E-03	1.0E-01	3.48E+04	-	
PU239	2.879E-05	1.0E-01	3.65E+03	U235	
PU240	1.060E-04	1.0E-01	5.57E+03	-	
PU241	4.812E-02	2.0E-01	3.47E+05	AM241	
PU242	1.791E-06	1.0E-01	2.12E+01	U238	
RA226	4.331E-04	1.0E-01	2.57E-05	-	
SE79	1.067E-05	1.0E+00	4.68E+00	-	
TC99	3.254E-06	1.0E+01	1.47E+02	-	
U234	2.834E-06	1.0E-01	1.39E+01	-	
U235	9.845E-10	1.0E-01	1.64E-01	-	
U238	1.551E-10	1.0E-01	3.06E+00	U234	
Zr93	4.530E-07	1.0E-01	2.51E-03	-	(for pyroprocess ER metal only)
Sn126	6.938E-06	1.0E-01	2.84E-02	-	(for pyroprocess ER metal only)
Pd106	1.066E-07	1.0E-01	5.14E-04	-	(for pyroprocess ER metal only)

Note: Regulatory limit not used in calculations

WASTE PACKAGE DESCRIPTION

Details of Waste Packages (number of packages dependent on wasteform.
ID : RING1,2,3,4,5,6 (for LWR SF) RING7 (for DHLW and pyroprocess)
Description : WASTE PACKAGE IN RING 1,2,3,4,5,6,7
Numpackages : Depends on MTHM per package and total MTHM considered (1000 MTHM for LWR SF, DHLW and Actinide Recycle, 300 MTHM for pyroprocess wastes.
MTHM per pack : Depends on wasteform and container (see Table 5.2)
MWD per MTHM : 3.64370E+04 (arbitrary -- not used in calculations

Repository Infiltration Rate (m/yr) : VTSW2
Air Alteration Rate (1/yr) : 0.00000E+00
Matrix dissolution Rate (g/m*m/yr) : MALT (depends on wasteform and container)
Surface area of Matrix (m*m/g): ESURF (depends on wasteform and container)
Water volume contacting Matrix (m*m*m): FV (depends on wasteform and container)
Mass of Sorbent (kg): 0.00000E+00
Equilibrium Partition Coefficient for RN all groups, all wasteforms : 0.00000E+00

Effective Catchment Area (m*m): TCATCH (depends on container design)
Geometric factor for diffusion (m): TOMEGA
Fraction of fuel which is wet : 1.00000E+00

Container failure modes for the Waste Package 1,2,3,4,5,6,7

Container failure mode 1
CORROSION FAILURE OF BARRIERS - WEIBULL
Start time for container failure is [dependent on container, wasteform, and location
in repository. Section 3.7 provides information.
Threshold time to failure]
Aging rate of Failure mode: 1.00000E+00
Probability Failure mode is active: 1.00000E+00
Weibull Failure Mode
Alpha : [dependent on container, wasteform, and location
in repository. Section 3.7 provides information.
Weibull Slope]
Beta - Epsilon : [dependent on container, wasteform, and location
in repository. Section 3.7 provides information.
Mean time to failure]

Secondary Barrier failure modes for the Waste Package 1,2,3,4,5,6,7

Cladding failure mode 1
DUMMY SECONDARY BARRIER
Start time for cladding failure is 0.00000E+00
Probability Failure mode is active: 1.00000E+00
Uniform Failure Mode
Duration: 5.00000E+01

Behavior of RNs in Waste Package 1,2,3,4,5,6,7

The number of release paths is 9
Path 1 : TS2C1 Fraction of Balance = 0.1111
Path 2 : TS2C2 Fraction of Balance = 0.1250
Path 3 : TS2C3 Fraction of Balance = 0.1429
Path 4 : TS2C4 Fraction of Balance = 0.1667
Path 5 : TS2C5 Fraction of Balance = 0.2000
Path 6 : TS2C6 Fraction of Balance = 0.2500
Path 7 : TS2C7 Fraction of Balance = 0.3333
Path 8 : TS2C8 Fraction of Balance = 0.5000
Path 9 : TS2C9 Fraction of Balance = 1.0000

RN AM241
Inventory (Ci/container) : [Depends on inventory for wasteform and mass loading See Section 4.4 and Table 5.2]
Free Mass Balance : 0.0000
Gap Mass Balance : 0.0000
This RN is in chemical group 1
This RN is not gaseous
Effective diffusion coefficient (m*m/yr): TEFDIF
Elemental solubility (g/m*m*m): SLAM

RN CM244
Inventory (Ci/container) : [Depends on inventory for wasteform and mass loading See Section 4.4 and Table 5.2]
Free Mass Balance : 0.0000
Gap Mass Balance : 0.0000
This RN is in chemical group 2
This RN is not gaseous
Effective diffusion coefficient (m*m/yr): TEFDIF
Elemental solubility (g/m*m*m): SLCM

RN CS135
Inventory (Ci/container) : [Depends on inventory for wasteform and mass loading See Section 4.4 and Table 5.2]
Free Mass Balance : 0.0000
Gap Mass Balance : 0.0000
This RN is in chemical group 3
This RN is not gaseous
Effective diffusion coefficient (m*m/yr): TEFDIF
Elemental solubility (g/m*m*m): SLCS

RN I129
Inventory (Ci/container) : [Depends on inventory for wasteform and mass loading See Section 4.4 and Table 5.2]
Free Mass Balance : 0.0000
Gap Mass Balance : 0.0000
This RN is in chemical group 4
This RN is not gaseous
Effective diffusion coefficient (m*m/yr): TEFDIF
Elemental solubility (g/m*m*m): SLI

RN NP237
Inventory (Ci/container) : [Depends on inventory for wasteform and mass loading See Section 4.4 and Table 5.2]
Free Mass Balance : 0.0000
Gap Mass Balance : 0.0000
This RN is in chemical group 5
This RN is not gaseous
Effective diffusion coefficient (m*m/yr): TEFDIF
Elemental solubility (g/m*m*m): SLNP

RN PU238
Inventory (Ci/container) : [Depends on inventory for wasteform and mass loading See Section 4.4 and Table 5.2]
Free Mass Balance : 0.0000
Gap Mass Balance : 0.0000
This RN is in chemical group 6
This RN is not gaseous
Effective diffusion coefficient (m*m/yr): TEFDIF
Elemental solubility (g/m*m*m): SLPU

RN PU239
Inventory (Ci/container) : [Depends on inventory for wasteform and mass loading See Section 4.4 and Table 5.2]
Free Mass Balance : 0.0000
Gap Mass Balance : 0.0000
This RN is in chemical group 6
This RN is not gaseous
Effective diffusion coefficient (m*m/yr): TEFDIF
Elemental solubility (g/m*m*m): SLPU

RN PU240
Inventory (Ci/container) : [Depends on inventory for wasteform and mass loading See Section 4.4 and Table 5.2]
Free Mass Balance : 0.0000
Gap Mass Balance : 0.0000
This RN is in chemical group 6
This RN is not gaseous
Effective diffusion coefficient (m*m/yr): TEFDIF
Elemental solubility (g/m*m*m): SLPU

RN PU241
Inventory (Ci/container) : [Depends on inventory for wasteform and mass loading See Section 4.4 and Table 5.2]
Free Mass Balance : 0.0000
Gap Mass Balance : 0.0000
This RN is in chemical group 6
This RN is not gaseous
Effective diffusion coefficient (m*m/yr): TEFDIF
Elemental solubility (g/m*m*m): SLPU

RN PU242
Inventory (Ci/container) : [Depends on inventory for wasteform and mass loading See Section 4.4 and Table 5.2]
Free Mass Balance : 0.0000
Gap Mass Balance : 0.0000
This RN is in chemical group 6
This RN is not gaseous
Effective diffusion coefficient (m*m/yr): TEFDIF
Elemental solubility (g/m*m*m): SLPU

RN RA226
Inventory (Ci/container) : [Depends on inventory for wasteform and mass loading See Section 4.4 and Table 5.2]
Free Mass Balance : 0.0000
Gap Mass Balance : 0.0000
This RN is in chemical group 7
This RN is not gaseous
Effective diffusion coefficient (m*m/yr): TEFDIF
Elemental solubility (g/m*m*m): SLRA

RN SE79
Inventory (Ci/container) : [Depends on inventory for wasteform and mass loading See Section 4.4 and Table 5.2]
Free Mass Balance : 0.0000
Gap Mass Balance : 0.0000
This RN is in chemical group 8
This RN is not gaseous
Effective diffusion coefficient (m*m/yr): TEFDIF
Elemental solubility (g/m*m*m): SLSE

RN TC99
Inventory (Ci/container) : [Depends on inventory for wasteform and mass loading See Section 4.4 and Table 5.2]
Free Mass Balance : 0.0000
Gap Mass Balance : 0.0000
This RN is in chemical group 9
This RN is not gaseous
Effective diffusion coefficient (m*m/yr): TEFDIF
Elemental solubility (g/m*m*m): SLTC

RN U234
Inventory (Ci/container) : [Depends on inventory for wasteform and mass loading See Section 4.4 and Table 5.2]
Free Mass Balance : 0.0000
Gap Mass Balance : 0.0000
This RN is in chemical group 10
This RN is not gaseous
Effective diffusion coefficient (m*m/yr): TEFDIF
Elemental solubility (g/m*m*m): SLU

RN U235
Inventory (Ci/container) : [Depends on inventory for wasteform and mass loading See Section 4.4 and Table 5.2]
Free Mass Balance : 0.0000
Gap Mass Balance : 0.0000
This RN is in chemical group 10
This RN is not gaseous
Effective diffusion coefficient (m*m/yr): TEFDIF
Elemental solubility (g/m*m*m): SLU

RN U238
Inventory (Ci/container) : [Depends on inventory for wasteform and mass loading See Section 4.4 and Table 5.2]
Free Mass Balance : 0.0000
Gap Mass Balance : 0.0000
This RN is in chemical group 10
This RN is not gaseous
Effective diffusion coefficient (m*m/yr): TEFDIF
Elemental solubility (g/m*m*m): SLU

RN ZR93
Inventory (Ci/container) : [Depends on inventory for wasteform and mass loading See Section 4.4 and Table 5.2]
Free Mass Balance : 0.0000
Gap Mass Balance : 0.0000
This RN is in chemical group 11
This RN is not gaseous
Effective diffusion coefficient (m*m/yr): TEFDIF
Elemental solubility (g/m*m*m): SLZR

RN SN126
Inventory (Ci/container) : [Depends on inventory for wasteform and mass loading See Section 4.4 and Table 5.2]
Free Mass Balance : 0.0000
Gap Mass Balance : 0.0000
This RN is in chemical group 12
This RN is not gaseous
Effective diffusion coefficient (m*m/yr): TEFDIF
Elemental solubility (g/m*m*m): SLSN

RN PD107
Inventory (Ci/container) : [Depends on inventory for wasteform and mass loading See Section 4.4 and Table 5.2]
Free Mass Balance : 0.0000
Gap Mass Balance : 0.0000
This RN is in chemical group 12
This RN is not gaseous
Effective diffusion coefficient (m*m/yr): TEFDIF
Elemental solubility (g/m*m*m): SLPD

NEAR-FIELD CONDITIONS

WP groups as defined by the environmental conditions

Group #	TYPE	CONTAC	TEMPV
For LWR Spent Fuel			
1	1	1	1.0000
2	1	2	1.0000
3	2	1	1.0000
4	2	2	1.0000
5	3	1	1.0000
6	3	2	1.0000
7	4	1	1.0000
8	4	2	1.0000
9	5	1	1.0000
10	5	2	1.0000
11	6	1	1.0000
12	6	2	1.0000
For DHLW and pyroprocess wastes			
1	7	1	1.0000
2	7	2	1.0000

CONTAC	% Balance	Description
1	0.500	WET DRIP
2	1.000	MOIST CONT

The repository rewetting temperature is 1.00000E+02 (not used)
Its variability of 0.000 is Uniform
The discretization levels are 1.000

Following shows description of temperature history discretization. Actual values provided in Chapter 3. For LWR SF, six sets of data required for incremental temperature, corresponding to each of the six rings described in the Intera 1993 PA [Reference 14]. For co-located DHLW and ALMR wastes, temperature is for Ring 7 of Intera 1993 PA [14]. For DHLW and ALMR wastes emplaced alone, temperature is ambient.

The temperature time history for the repository is :

Time (yrs)	Temperature
100.0	55.00
316.0	53.00
1000.0	50.00
3160.0	45.00
10000.0	37.00
100000.0	30.00

The variability in the temperature is 1.00000E+00
The variability in the time is 1.00000E+00

The incremental temperature time history for WP RING1 is :

Time (yrs)	Temperature
100.0	125.60
316.0	124.60
1000.0	106.70
3160.0	74.40
10000.0	51.10
100000.0	29.70

The variability in the temperature is 1.00000E+00

The above desrciption is for one waste package ring. Incremental temperatures are input for each ring such that container temperature corresponds to values presented in chapter 3.

PATHWAY DESCRIPTION

The tolerance values for recalculating are :
Fraction of total flow : 0.00000E+00
Mode velocity : 0.00000E+00
Mode porosity : 0.00000E+00
Pathway length : 0.00000E+00
Transition rate : 0.00000E+00

Specified flow balance

Path ID	Total Flow	Discharge (fraction)
SAT	QSAT	AE(1.000)
BWCOL4	QCOL4	SAT(1.000)
BWCOL5	QCOL5	SAT(1.000)
PPCOL1	QCOL1	SAT(1.000)
PPCOL2	QCOL2	SAT(1.000)
PPCOL3	QCOL3	SAT(1.000)
PPCOL4	QCOL4	BWCOL4(FNS613), SAT(1.000)
PPCOL5	QCOL5	BWCOL5(FNS613), SAT(1.000)
PPCOL6	QCOL6	SAT(1.000)
PPCOL7	QCOL79	SAT(1.000)
PPCOL8	QCOL79	SAT(1.000)
PPCOL9	QCOL79	SAT(1.000)
CHZC1	QCOL1	PPCOL1(FNS60), SAT(1.000)
CHZC2	QCOL2	PPCOL2(FNS60), SAT(1.000)
CHZC3	QCOL3	PPCOL3(FNS130), SAT(1.000)
CHZC4	QCOL4	PPCOL4(1.000)
CHZC5	QCOL5	PPCOL5(1.000)
CHZC6	QCOL6	PPCOL6(FNS130), SAT(1.000)
CHZC7	QCOL79	PPCOL7(FNS130), SAT(1.000)
CHZC8	QCOL79	PPCOL8(FNS130), SAT(1.000)
CHZC9	QCOL79	PPCOL9(FNS130), SAT(1.000)
CHVC1	QCOL1	CHZC1(FNS130), SAT(1.000)
CHVC2	QCOL2	CHZC2(FNS130), SAT(1.000)
CHVC3	QCOL3	CHZC3(1.000)
CHVC4	QCOL4	CHZC4(FNS230), SAT(1.000)
CHVC5	QCOL5	CHZC5(FNS230), SAT(1.000)
CHVC6	QCOL6	CHZC6(1.000)
CHVC7	QCOL79	CHZC7(1.000)
CHVC8	QCOL79	CHZC8(1.000)
CHVC9	QCOL79	CHZC9(1.000)
TS3C1	QCOL1	CHVC1(1.000)
TS3C2	QCOL2	CHVC2(1.000)
TS3C3	QCOL3	CHVC3(1.000)
TS3C4	QCOL4	CHVC4(1.000)
TS3C5	QCOL5	CHVC5(1.000)
TS3C6	QCOL6	CHVC6(FNS230), SAT(1.000)
TS3C7	QCOL79	CHVC7(1.000)
TS3C8	QCOL79	CHVC1(1.000)
TS3C9	QCOL79	CHVC9(1.000)
TS2C1	QCOL1	TS3C1(FNS230), SAT(1.000)
TS2C2	QCOL2	TS3C2(FNS230), SAT(1.000)
TS2C3	QCOL3	TS3C3(FNS230), SAT(1.000)
TS2C4	QCOL4	TS3C4(1.000)
TS2C5	QCOL5	TS3C5(1.000)
TS2C6	QCOL6	TS3C6(1.000)
TS2C7	QCOL79	TS3C7(FNS230), SAT(1.000)
TS2C8	QCOL79	TS3C8(FNS230), SAT(1.000)
TS2C9	QCOL79	TS3C9(FNS230), SAT(1.000)

Retardation Values

Pathway SAT

RN group 1 Sorption RAMS Matrix diffusion : 1.00000
RN group 2 Sorption RAMS Matrix diffusion : 1.0000
RN group 3 Sorption RCSSAT Matrix diffusion : 1.0000
RN group 4 Sorption 1.0000 Matrix diffusion : 1.0000
RN group 5 Sorption RNPS Matrix diffusion : 1.0000
RN group 6 Sorption RPUS Matrix diffusion : 1.0000
RN group 7 Sorption RRAS Matrix diffusion : 1.0000
RN group 8 Sorption RUS Matrix diffusion : 1.0000
RN group 9 Sorption 1.0000 Matrix diffusion : 1.0000
RN group 10 Sorption RUS Matrix diffusion : 1.0000

Pathways BWCOL#

RN group 1 Sorption RAMBW Matrix diffusion : 1.0000
RN group 2 Sorption RAMBW Matrix diffusion : 1.0000
RN group 3 Sorption RCSBW Matrix diffusion : 1.0000
RN group 4 Sorption 1.0000 Matrix diffusion : 1.0000
RN group 5 Sorption RNPBW Matrix diffusion : 1.0000
RN group 6 Sorption RPUBW Matrix diffusion : 1.0000
RN group 7 Sorption RRABW Matrix diffusion : 1.0000
RN group 8 Sorption RUBW Matrix diffusion : 1.0000
RN group 9 Sorption 1.0000 Matrix diffusion : 1.0000
RN group 10 Sorption RUBW Matrix diffusion : 1.0000

Pathways PPCOL#

RN group 1 Sorption RAMPPW Matrix diffusion : 1.0000
RN group 2 Sorption RAMPPW Matrix diffusion : 1.0000
RN group 3 Sorption RCSPPW Matrix diffusion : 1.0000
RN group 4 Sorption 1.0000 Matrix diffusion : 1.0000
RN group 5 Sorption RNPPPW Matrix diffusion : 1.0000
RN group 6 Sorption RPUPPW Matrix diffusion : 1.0000
RN group 7 Sorption RRAPPW Matrix diffusion : 1.0000
RN group 8 Sorption RUPPW Matrix diffusion : 1.0000
RN group 9 Sorption 1.0000 Matrix diffusion : 1.0000
RN group 10 Sorption RUPPW Matrix diffusion : 1.0000

Pathways CHZC#

RN group 1 Sorption RAMCHZ Matrix diffusion : 1.0000
RN group 2 Sorption RAMCHZ Matrix diffusion : 1.0000
RN group 3 Sorption RCSCHZ Matrix diffusion : 1.0000
RN group 4 Sorption 1.0000 Matrix diffusion : 1.0000
RN group 5 Sorption RNPCHZ Matrix diffusion : 1.0000
RN group 6 Sorption RPUCHZ Matrix diffusion : 1.0000
RN group 7 Sorption RRACHZ Matrix diffusion : 1.0000
RN group 8 Sorption RUCHZ Matrix diffusion : 1.0000
RN group 9 Sorption 1.0000 Matrix diffusion : 1.0000
RN group 10 Sorption RUCHZ Matrix diffusion : 1.0000

Pathways CHVC#

RN group 1 Sorption RAMCHV Matrix diffusion : 1.0000
RN group 2 Sorption RAMCHV Matrix diffusion : 1.0000
RN group 3 Sorption RCSCHV Matrix diffusion : 1.0000
RN group 4 Sorption 1.0000 Matrix diffusion : 1.0000
RN group 5 Sorption RNPCHV Matrix diffusion : 1.0000
RN group 6 Sorption RPUCHV Matrix diffusion : 1.0000
RN group 7 Sorption RRACHV Matrix diffusion : 1.0000
RN group 8 Sorption RUCHV Matrix diffusion : 1.0000
RN group 9 Sorption 1.0000 Matrix diffusion : 1.0000
RN group 10 Sorption RUCHV Matrix diffusion : 1.0000

TS3C#

RN group 1 Sorption RAMTS3 Matrix diffusion : 1.0000
RN group 2 Sorption RAMTS3 Matrix diffusion : 1.0000
RN group 3 Sorption RCSTS3 Matrix diffusion : 1.0000
RN group 4 Sorption 1.0000 Matrix diffusion : 1.0000
RN group 5 Sorption RNPTS3 Matrix diffusion : 1.0000
RN group 6 Sorption RPUTS3 Matrix diffusion : 1.0000
RN group 7 Sorption RRATS3 Matrix diffusion : 1.0000
RN group 8 Sorption RUTS3 Matrix diffusion : 1.0000
RN group 9 Sorption 1.0000 Matrix diffusion : 1.0000
RN group 10 Sorption RUTS3 Matrix diffusion : 1.0000

TC2C#

RN group 1 Sorption RAMTS2 Matrix diffusion : 1.0000
RN group 2 Sorption RAMTS2 Matrix diffusion : 1.0000
RN group 3 Sorption RCSTS2 Matrix diffusion : 1.0000
RN group 4 Sorption 1.0000 Matrix diffusion : 1.0000
RN group 5 Sorption RNPTS2 Matrix diffusion : 1.0000
RN group 6 Sorption RPUTS2 Matrix diffusion : 1.0000
RN group 7 Sorption RRATS2 Matrix diffusion : 1.0000
RN group 8 Sorption RUTS2 Matrix diffusion : 1.0000
RN group 9 Sorption 1.0000 Matrix diffusion : 1.0000
RN group 10 Sorption RUTS2 Matrix diffusion : 1.0000

Retardation values for Zr, Sn, and Pd for ER metallic set to 1 (no retardation) for all pathways. (Differs from IMARC where sorption allowed)

RN group 11 Sorption 1.0000 Matrix Diffusion: 1.0000 (Zr ER metallic only)
RN group 12 Sorption 1.0000 Matrix Diffusion: 1.0000 (Sn ER metallic only)
RN group 13 Sorption 1.0000 Matrix Diffusion: 1.0000 (Pd ER metallic only)

Details of Path 1
ID : SAT
Description : SATURATED ZONE PATHWAY

ID for dose/conc. conversion table :
Total length of Pathway (m) : LSAT
Total Area of Pathway (m*m) : ASAT
Total Flow through Pathway (m*m*m/yr) :
QSAT

The number of exit paths is 1
Path 1 : AE Fraction of Balance = 1.0000

The number of flow modes is 1

Flow mode #1
Description : FLOW MODE 1

Fraction of balance of remaining total flow :
1.0000
Flow mode velocity : VSAT
Transition rate (m): 1.0000
Dispersivity (m): 0.00000E+00

Details of Path 2
ID : BWCOL4
Description : BULLFROG, COLUMN 4

ID for dose/conc. conversion table :
Total length of Pathway (m) : LBWC4
Total Area of Pathway (m*m) : ACOL4
Total Flow through Pathway (m*m*m/yr) :
QCOL4

The number of exit paths is 1
Path 1 : SAT Fraction of Balance = 1.0000

The number of flow modes is 1

Flow mode #1
Description : FLOW MODE 1

Fraction of balance of remaining total flow :
1.0000
Flow mode velocity : VBW
Transition rate (m): 1.0000
Dispersivity (m): 0.00000E+00

Details of Path 3
ID : BWCOL5
Description : BULLFROG, COLUMN 5

ID for dose/conc. conversion table :
Total length of Pathway (m) : LBWC5
Total Area of Pathway (m*m) : ACOL5
Total Flow through Pathway (m*m*m/yr) :
QCOL5

The number of exit paths is 1

Path 1 : SAT Fraction of Balance = 1.0000

The number of flow modes is 1

Flow mode #1
Description : FLOW MODE 1

Fraction of balance of remaining total flow :
1.0000
Flow mode velocity : VBW
Transition rate (m): 1.0000
Dispersivity (m): 0.00000E+00

Details of Path 4
ID : PPCOL1
Description : PROW PASS COLUMN 1

ID for dose/conc. conversion table :
Total length of Pathway (m) : LPPWC1
Total Area of Pathway (m*m) : ACOL1
Total Flow through Pathway (m*m*m/yr) :
QCOL1

The number of exit paths is 1
Path 1 : SAT Fraction of Balance = 1.0000

The number of flow modes is 1

Flow mode #1
Description : FLOW MODE 1

Fraction of balance of remaining total flow :
1.0000
Flow mode velocity : VPPW
Transition rate (m): 1.0000
Dispersivity (m): 0.00000E+00

Details of Path 5
ID : PPCOL2
Description : PROW PASS COLUMN 2

ID for dose/conc. conversion table :
Total length of Pathway (m) : LPPWC2
Total Area of Pathway (m*m) : ACOL2
Total Flow through Pathway (m*m*m/yr) : QCOL2

The number of exit paths is 1
Path 1 : SAT Fraction of Balance = 1.0000

The number of flow modes is 1

Flow mode #1
Description : FLOW MODE 1

Fraction of balance of remaining total flow : 1.0000
Flow mode velocity : VPPW
Transition rate (m): 1.0000
Dispersivity (m): 0.00000E+00

Details of Path 6
ID : PPCOL3
Description : PROW PASS COLUMN 3

ID for dose/conc. conversion table :
Total length of Pathway (m) : LPPWC3
Total Area of Pathway (m*m) : ACOL3
Total Flow through Pathway (m*m*m/yr) : QCOL3

The number of exit paths is 1
Path 1 : SAT Fraction of Balance = 1.0000

The number of flow modes is 1

Flow mode #1
Description : FLOW MODE 1

Fraction of balance of remaining total flow : 1.0000
Flow mode velocity : VPPW
Transition rate (m): 1.0000
Dispersivity (m): 0.00000E+00

Details of Path 7
ID : PPCOL4
Description : PROW PASS COLUMN 4

ID for dose/conc. conversion table :
Total length of Pathway (m) : LPPWC4
Total Area of Pathway (m*m) : ACOL4
Total Flow through Pathway (m*m*m/yr) : QCOL4

The number of exit paths is 2
Path 1 : BWCOL4 Fraction of Balance = FNS613
Path 2 : SAT Fraction of Balance = 1.0000

The number of flow modes is 1

Flow mode #1
Description : FLOW MODE 1

Fraction of balance of remaining total flow : 1.0000
Flow mode velocity : VPPW
Transition rate (m): 1.0000
Dispersivity (m): 0.00000E+00

Details of Path 8
ID : PPCOL5
Description : PROW PASS COLUMN 5

ID for dose/conc. conversion table :
Total length of Pathway (m) : LPPWC5
Total Area of Pathway (m*m) : ACOL5
Total Flow through Pathway (m*m*m/yr) : QCOL5

The number of exit paths is 2
Path 1 : BWCOL5 Fraction of Balance = FNS613
Path 2 : SAT Fraction of Balance = 1.0000

The number of flow modes is 1

Flow mode #1
Description : FLOW MODE 1

Fraction of balance of remaining total flow : 1.0000
Flow mode velocity : VPPW
Transition rate (m): 1.0000
Dispersivity (m): 0.00000E+00

Details of Path 9
ID : PPCOL6
Description : PROW PASS COLUMN 6

ID for dose/conc. conversion table :
Total length of Pathway (m) : LPPWC6
Total Area of Pathway (m*m) : ACOL6
Total Flow through Pathway (m*m*m/yr) :
QCOL6

The number of exit paths is 1
Path 1 : SAT Fraction of Balance = 1.0000

The number of flow modes is 1

Flow mode #1
Description : FLOW MODE 1

Fraction of balance of remaining total flow :
1.0000
Flow mode velocity : VPPW
Transition rate (m): 1.0000
Dispersivity (m): 0.00000E+00

Details of Path 10
ID : PPCOL7
Description : PROW PASS COLUMN 7

ID for dose/conc. conversion table :
Total length of Pathway (m) : LPPWC7
Total Area of Pathway (m*m) : ACOL79
Total Flow through Pathway (m*m*m/yr) :
QCOL79

The number of exit paths is 1
Path 1 : SAT Fraction of Balance = 1.0000

The number of flow modes is 1

Flow mode #1
Description : FLOW MODE 1

Fraction of balance of remaining total flow :
1.0000
Flow mode velocity : VPPW
Transition rate (m): 1.0000
Dispersivity (m): 0.00000E+00

Details of Path 11
ID : PPCOL8
Description : PROW PASS COLUMN 8

ID for dose/conc. conversion table :
Total length of Pathway (m) : LPPWC8
Total Area of Pathway (m*m) : ACOL79
Total Flow through Pathway (m*m*m/yr) :
QCOL79

The number of exit paths is 1
Path 1 : SAT Fraction of Balance = 1.0000

The number of flow modes is 1

Flow mode #1
Description : FLOW MODE 1

Fraction of balance of remaining total flow :
1.0000
Flow mode velocity : VPPW
Transition rate (m): 1.0000
Dispersivity (m): 0.00000E+00

Details of Path 12
ID : PPCOL9
Description : PROW PASS COLUMN 9

ID for dose/conc. conversion table :
Total length of Pathway (m) : LPPWC9
Total Area of Pathway (m*m) : ACOL79
Total Flow through Pathway (m*m*m/yr) :
QCOL79

The number of exit paths is 1
Path 1 : SAT Fraction of Balance = 1.0000

The number of flow modes is 1

Flow mode #1
Description : FLOW MODE 1

Fraction of balance of remaining total flow :
1.0000
Flow mode velocity : VPPW
Transition rate (m): 1.0000
Dispersivity (m): 0.00000E+00

Details of Path 13
ID : CHZC1
Description : CALICO HILLS ZEOLITIC COLUMN 1
ID for dose/conc. conversion table :
Total length of Pathway (m) : LCHZC1
Total Area of Pathway (m*m) : ACOL1
Total Flow through Pathway (m*m*m/yr) : QCOL1
The number of exit paths is 2
Path 1 : PPCOL1 Fraction of Balance = FNS60
Path 2 : SAT Fraction of Balance = 1.0000

The number of flow modes is 1

Flow mode #1
Description : FLOW MODE 1

Fraction of balance of remaining total flow : 1.0000
Flow mode velocity : VCHN1Z
Transition rate (m): 1.0000
Dispersivity (m): 0.00000E+00

Details of Path 14
ID : CHZC2
Description : CALICO HILLS ZEOLITIC COLUMN 2
ID for dose/conc. conversion table :
Total length of Pathway (m) : LCHZC2
Total Area of Pathway (m*m) : ACOL2
Total Flow through Pathway (m*m*m/yr) : QCOL2

The number of exit paths is 2
Path 1 : PPCOL2 Fraction of Balance = FNS60
Path 2 : SAT Fraction of Balance = 1.0000

The number of flow modes is 1

Flow mode #1
Description : FLOW MODE 1

Fraction of balance of remaining total flow : 1.0000
Flow mode velocity : VCHN1Z
Transition rate (m): 1.0000
Dispersivity (m): 0.00000E+00

Details of Path 15
ID : CHZC3
Description : CALICO HILLS ZEOLITIC COLUMN 3
ID for dose/conc. conversion table :
Total length of Pathway (m) : LCHZC3
Total Area of Pathway (m*m) : ACOL3
Total Flow through Pathway (m*m*m/yr) : QCOL3

The number of exit paths is 2
Path 1 : PPCOL3 Fraction of Balance = FNS130
Path 2 : SAT Fraction of Balance = 1.0000

The number of flow modes is 1

Flow mode #1
Description : FLOW MODE 1

Fraction of balance of remaining total flow : 1.0000
Flow mode velocity : VCHN1Z
Transition rate (m): 1.0000
Dispersivity (m): 0.00000E+00

Details of Path 16
ID : CHZC4
Description : CALICO HILLS ZEOLITIC COLUMN 4
ID for dose/conc. conversion table :
Total length of Pathway (m) : LCHZC4
Total Area of Pathway (m*m) : ACOL4
Total Flow through Pathway (m*m*m/yr) : QCOL4

The number of exit paths is 1
Path 1 : PPCOL4 Fraction of Balance = 1.0000

The number of flow modes is 1

Flow mode #1
Description : FLOW MODE 1

Fraction of balance of remaining total flow : 1.0000
Flow mode velocity : VCHN1Z
Transition rate (m): 1.0000
Dispersivity (m): 0.00000E+00

Details of Path 17
ID : CHZC5
Description : CALICO HILLS ZEOLITIC COLUMN 5
ID for dose/conc. conversion table :
Total length of Pathway (m) : LCHZC5
Total Area of Pathway (m*m) : ACOL5
Total Flow through Pathway (m*m*m/yr) : QCOL5

The number of exit paths is 1
Path 1 : PPCOL5 Fraction of Balance = 1.0000

The number of flow modes is 1

Flow mode #1
Description : FLOW MODE 1

Fraction of balance of remaining total flow : 1.0000
Flow mode velocity : VCHN1Z
Transition rate (m): 1.0000
Dispersivity (m): 0.00000E+00

Details of Path 18
ID : CHZC6
Description : CALICO HILLS ZEOLITIC COLUMN 6
ID for dose/conc. conversion table :
Total length of Pathway (m) : LCHZC6
Total Area of Pathway (m*m) : ACOL6
Total Flow through Pathway (m*m*m/yr) : QCOL6

The number of exit paths is 2
Path 1 : PPCOL6 Fraction of Balance = FNS130
Path 2 : SAT Fraction of Balance = 1.0000

The number of flow modes is 1

Flow mode #1
Description : FLOW MODE 1

Fraction of balance of remaining total flow : 1.0000
Flow mode velocity : VCHN1Z
Transition rate (m): 1.0000
Dispersivity (m): 0.00000E+00

Details of Path 19
ID : CHZC7
Description : CALICO HILLS ZEOLITIC COLUMN 7
ID for dose/conc. conversion table :
Total length of Pathway (m) : LCHZC7
Total Area of Pathway (m*m) : ACOL79
Total Flow through Pathway (m*m*m/yr) : QCOL79

The number of exit paths is 2
Path 1 : PPCOL7 Fraction of Balance = FNS130
Path 2 : SAT Fraction of Balance = 1.0000

The number of flow modes is 1

Flow mode #1
Description : FLOW MODE 1

Fraction of balance of remaining total flow : 1.0000
Flow mode velocity : VCHN1Z
Transition rate (m): 1.0000
Dispersivity (m): 0.00000E+00

Details of Path 20
ID : CHZC8
Description : CALICO HILLS ZEOLITIC COLUMN 8
ID for dose/conc. conversion table :
Total length of Pathway (m) : LCHZC8
Total Area of Pathway (m*m) : ACOL79
Total Flow through Pathway (m*m*m/yr) : QCOL79

The number of exit paths is 2
Path 1 : PPCOL8 Fraction of Balance = FNS130
Path 2 : SAT Fraction of Balance = 1.0000

The number of flow modes is 1

Flow mode #1
Description : FLOW MODE 1

Fraction of balance of remaining total flow : 1.0000
Flow mode velocity : VCHN1Z
Transition rate (m): 1.0000
Dispersivity (m): 0.00000E+00

Details of Path 21
ID : CHZC9
Description : CALICO HILLS ZEOLITIC COLUMN 9
ID for dose/conc. conversion table :
Total length of Pathway (m) : LCHZC9
Total Area of Pathway (m*m) : ACOL79
Total Flow through Pathway (m*m*m/yr) : QCOL79

The number of exit paths is 2
Path 1 : PPCOL9 Fraction of Balance = FNS130
Path 2 : SAT Fraction of Balance = 1.0000

The number of flow modes is 1

Flow mode #1
Description : FLOW MODE 1

Fraction of balance of remaining total flow : 1.0000
Flow mode velocity : VCHN1Z
Transition rate (m): 1.0000
Dispersivity (m): 0.00000E+00

Details of Path 22
ID : CHVC1
Description : CALICO HILLS VITRIC COLUMN 1
ID for dose/conc. conversion table :
Total length of Pathway (m) : LCHVC1
Total Area of Pathway (m*m) : ACOL1
Total Flow through Pathway (m*m*m/yr) : QCOL1

The number of exit paths is 2
Path 1 : CHZC1 Fraction of Balance = FNS130
Path 2 : SAT Fraction of Balance = 1.0000

The number of flow modes is 1

Flow mode #1
Description : FLOW MODE 1

Fraction of balance of remaining total flow : 1.0000
Flow mode velocity : VCHN1V
Transition rate (m): 1.0000
Dispersivity (m): 0.00000E+00

Details of Path 23
ID : CHVC2
Description : CALICO HILLS VITRIC COLUMN 2
ID for dose/conc. conversion table :
Total length of Pathway (m) : LCHVC2
Total Area of Pathway (m*m) : ACOL2
Total Flow through Pathway (m*m*m/yr) : QCOL2

The number of exit paths is 2
Path 1 : CHZC2 Fraction of Balance = FNS130
Path 2 : SAT Fraction of Balance = 1.0000

The number of flow modes is 1

Flow mode #1
Description : FLOW MODE 1

Fraction of balance of remaining total flow : 1.0000
Flow mode velocity : VCHN1V
Transition rate (m): 1.0000
Dispersivity (m): 0.00000E+00

Details of Path 24
ID : CHVC3
Description : CALICO HILLS VITRIC COLUMN 3
ID for dose/conc. conversion table :
Total length of Pathway (m) : LCHVC3
Total Area of Pathway (m*m) : ACOL3
Total Flow through Pathway (m*m*m/yr) : QCOL3

The number of exit paths is 1
Path 1 : CHZC3 Fraction of Balance = 1.0000

The number of flow modes is 1

Flow mode #1
Description : FLOW MODE 1

Fraction of balance of remaining total flow : 1.0000
Flow mode velocity : VCHN1V
Transition rate (m): 1.0000
Dispersivity (m): 0.00000E+00

Details of Path 25
ID : CHVC4
Description : CALICO HILLS VITRIC COLUMN 4
ID for dose/conc. conversion table :
Total length of Pathway (m) : LCHVC4
Total Area of Pathway (m*m) : ACOL4
Total Flow through Pathway (m*m*m/yr) : QCOL4

The number of exit paths is 2
Path 1 : CHZC4 Fraction of Balance = FNS230
Path 2 : SAT Fraction of Balance = 1.0000

The number of flow modes is 1

Flow mode #1
Description : FLOW MODE 1

Fraction of balance of remaining total flow : 1.0000
Flow mode velocity : VCHN1V
Transition rate (m): 1.0000
Dispersivity (m): 0.00000E+00

Details of Path 26
ID : CHVC5
Description : CALICO HILLS VITRIC COLUMN 5
ID for dose/conc. conversion table :
Total length of Pathway (m) : LCHVC5
Total Area of Pathway (m*m) : ACOL5
Total Flow through Pathway (m*m*m/yr) : QCOL5

The number of exit paths is 2
Path 1 : CHZC5 Fraction of Balance = FNS230
Path 2 : SAT Fraction of Balance = 1.0000

The number of flow modes is 1

Flow mode #1
Description : FLOW MODE 1

Fraction of balance of remaining total flow : 1.0000
Flow mode velocity : VCHN1V
Transition rate (m): 1.0000
Dispersivity (m): 0.00000E+00

Details of Path 27
ID : CHVC6
Description : CALICO HILLS VITRIC COL 6

ID for dose/conc. conversion table :
Total length of Pathway (m) : LCHVC6
Total Area of Pathway (m*m) : ACOL6
Total Flow through Pathway (m*m*m/yr) : QCOL6

The number of exit paths is 1
Path 1 : CHZC6 Fraction of Balance = 1.0000

The number of flow modes is 1

Flow mode #1
Description : FLOW MODE 1

Fraction of balance of remaining total flow : 1.0000
Flow mode velocity : VCHN1Z
Transition rate (m): 1.0000
Dispersivity (m): 0.00000E+00

Details of Path 28
ID : CHVC7
Description : CALICO HILLS VITRIC COLUMN 7
ID for dose/conc. conversion table :
Total length of Pathway (m) : LCHVC7
Total Area of Pathway (m*m) : ACOL79
Total Flow through Pathway (m*m*m/yr) : QCOL79

The number of exit paths is 1
Path 1 : CHZC7 Fraction of Balance = 1.0000

The number of flow modes is 1

Flow mode #1
Description : FLOW MODE 1

Fraction of balance of remaining total flow : 1.0000
Flow mode velocity : VCHN1Z
Transition rate (m): 1.0000
Dispersivity (m): 0.00000E+00

Details of Path 29
ID : CHVC8
Description : CALICO HILLS VITRIC COLUMN 8
ID for dose/conc. conversion table :
Total length of Pathway (m) : LCHVC8
Total Area of Pathway (m*m) : ACOL79
Total Flow through Pathway (m*m*m/yr) : QCOL79

The number of exit paths is 1
Path 1 : CHZC8 Fraction of Balance = 1.0000

The number of flow modes is 1

Flow mode #1
Description : FLOW MODE 1

Fraction of balance of remaining total flow : 1.0000
Flow mode velocity : VCHN1V
Transition rate (m): 1.0000
Dispersivity (m): 0.00000E+00

Details of Path 30
ID : CHVC9
Description : CALICO HILLS VITRIC COLUMN 9
ID for dose/conc. conversion table :
Total length of Pathway (m) : LCHVC9
Total Area of Pathway (m*m) : ACOL79
Total Flow through Pathway (m*m*m/yr) : QCOL79

The number of exit paths is 1
Path 1 : CHZC9 Fraction of Balance = 1.0000

The number of flow modes is 1

Flow mode #1
Description : FLOW MODE 1

Fraction of balance of remaining total flow : 1.0000
Flow mode velocity : VCHN1V
Transition rate (m): 1.0000
Dispersivity (m): 0.00000E+00

Details of Path 31
ID : TS3C1
Description : TOPOPAH SPRING 3 COLUMN 1
ID for dose/conc. conversion table :
Total length of Pathway (m) : LTS3
Total Area of Pathway (m*m) : ACOL1
Total Flow through Pathway (m*m*m/yr) : QCOL1

The number of exit paths is 1
Path 1 : CHVC1 Fraction of Balance = 1.0000

The number of flow modes is 1

Flow mode #1
Description : FLOW MODE 1

Fraction of balance of remaining total flow : 1.0000
Flow mode velocity : VTSW3
Transition rate (m): 1.0000
Dispersivity (m): 0.00000E+00

Details of Path 32
ID : TS3C2
Description : TOPOPAH SPRING 3 COLUMN 2
ID for dose/conc. conversion table :
Total length of Pathway (m) : LTS3
Total Area of Pathway (m*m) : ACOL2
Total Flow through Pathway (m*m*m/yr) : QCOL2

The number of exit paths is 1
Path 1 : CHVC2 Fraction of Balance = 1.0000

The number of flow modes is 1

Flow mode #1
Description : FLOW MODE 1

Fraction of balance of remaining total flow : 1.0000
Flow mode velocity : VTSW3
Transition rate (m): 1.0000
Dispersivity (m): 0.00000E+00

Details of Path 33
ID : TS3C3
Description : TOPOPAH SPRING 3 COLUMN 3
ID for dose/conc. conversion table :
Total length of Pathway (m) : LTS3
Total Area of Pathway (m*m) : ACOL3
Total Flow through Pathway (m*m*m/yr) : QCOL3

The number of exit paths is 1
Path 1 : CHVC3 Fraction of Balance = 1.0000

The number of flow modes is 1

Flow mode #1
Description : FLOW MODE 1

Fraction of balance of remaining total flow : 1.0000
Flow mode velocity : VTSW3
Transition rate (m): 1.0000
Dispersivity (m): 0.00000E+00

Details of Path 34
ID : TS3C4
Description : TOPOPAH SPRING 3 COLUMN 4
ID for dose/conc. conversion table :
Total length of Pathway (m) : LTS3
Total Area of Pathway (m*m) : ACOL4
Total Flow through Pathway (m*m*m/yr) : QCOL4

The number of exit paths is 1
Path 1 : CHVC4 Fraction of Balance = 1.0000

The number of flow modes is 1

Flow mode #1
Description : FLOW MODE 1

Fraction of balance of remaining total flow : 1.0000
Flow mode velocity : VTSW3
Transition rate (m): 1.0000
Dispersivity (m): 0.00000E+00

Details of Path 35
ID : TS3C5
Description : TOPOPAH SPRING 3 COLUMN 5
ID for dose/conc. conversion table :
Total length of Pathway (m) : LTS3
Total Area of Pathway (m*m) : ACOL5
Total Flow through Pathway (m*m*m/yr) : QCOL5

The number of exit paths is 1
Path 1 : CHVC5 Fraction of Balance = 1.0000

The number of flow modes is 1

Flow mode #1
Description : FLOW MODE 1

Fraction of balance of remaining total flow : 1.0000
Flow mode velocity : VTSW3
Transition rate (m): 1.0000
Dispersivity (m): 0.00000E+00

Details of Path 36
ID : TS3C6
Description : TOPOPAH SPRING 3 COLUMN 6
ID for dose/conc. conversion table :
Total length of Pathway (m) : LTS3C6
Total Area of Pathway (m*m) : ACOL6
Total Flow through Pathway (m*m*m/yr) ; QCOL6

The number of exit paths is 2
Path 1 : CHVC6 Fraction of Balance = FNS230
Path 2 : SAT Fraction of Balance = 1.0000

The number of flow modes is 1

Flow mode #1
Description : FLOW MODE 1

Fraction of balance of remaining total flow : 1.0000
Flow mode velocity : VTSW3
Transition rate (m): 1.0000
Dispersivity (m): 0.00000E+00

Details of Path 37
ID : TS3C7
Description : TOPOPAH SPRING 3 COLUMN 7
ID for dose/conc. conversion table :
Total length of Pathway (m) : LTS3
Total Area of Pathway (m*m) : ACOL79
Total Flow through Pathway (m*m*m/yr) : QCOL79

The number of exit paths is 1
Path 1 : CHVC7 Fraction of Balance = 1.0000

The number of flow modes is 1

Flow mode #1
Description : FLOW MODE 1

Fraction of balance of remaining total flow : 1.0000
Flow mode velocity : VTSW3
Transition rate (m): 1.0000
Dispersivity (m): 0.00000E+00

Details of Path 38
ID : TS3C8
Description : TOPOPAH SPRING 3 COLUMN 8
ID for dose/conc. conversion table :
Total length of Pathway (m) : LTS3
Total Area of Pathway (m*m) : ACOL79
Total Flow through Pathway (m*m*m/yr) : QCOL79

The number of exit paths is 1
Path 1 : CHVC1 Fraction of Balance = 1.0000

The number of flow modes is 1

Flow mode #1
Description : FLOW MODE 1

Fraction of balance of remaining total flow : 1.0000
Flow mode velocity : VTSW3
Transition rate (m): 1.0000
Dispersivity (m): 0.00000E+00

Details of Path 39
ID : TS3C9
Description : TOPOPAH SPRING 3 COLUMN 9
ID for dose/conc. conversion table :
Total length of Pathway (m) : LTS3
Total Area of Pathway (m*m) : ACOL79
Total Flow through Pathway (m*m*m/yr) : QCOL79

The number of exit paths is 1
Path 1 : CHVC9 Fraction of Balance = 1.0000

The number of flow modes is 1

Flow mode #1
Description : FLOW MODE 1

Fraction of balance of remaining total flow : 1.0000
Flow mode velocity : VTSW3
Transition rate (m): 1.0000
Dispersivity (m): 0.00000E+00

Details of Path 40
ID : TS2C1
Description : TOPOPAH SPRING 2 COLUMN 1
ID for dose/conc. conversion table :
Total length of Pathway (m) : LTS2C1
Total Area of Pathway (m*m) : ACOL1
Total Flow through Pathway (m*m*m/yr) : QCOL1

The number of exit paths is 2
Path 1 : TS3C1 Fraction of Balance = FNS230
Path 2 : SAT Fraction of Balance = 1.0000

The number of flow modes is 1

Flow mode #1
Description : FLOW MODE 1

Fraction of balance of remaining total flow : 1.0000
Flow mode velocity : VTSW3
Transition rate (m): 1.0000
Dispersivity (m): 0.00000E+00

Details of Path 41
ID : TS2C2
Description : TOPOPAH SPRING 2 COLUMN 2
ID for dose/conc. conversion table :
Total length of Pathway (m) : LTS2C2
Total Area of Pathway (m*m) : ACOL2
Total Flow through Pathway (m*m*m/yr) : QCOL2

The number of exit paths is 2
Path 1 : TS3C2 Fraction of Balance = FNS230
Path 2 : SAT Fraction of Balance = 1.0000

The number of flow modes is 1

Flow mode #1
Description : FLOW MODE 1

Fraction of balance of remaining total flow : 1.0000
Flow mode velocity : VTSW2
Transition rate (m): 1.0000
Dispersivity (m): 0.00000E+00

Details of Path 42
ID : TS2C3
Description : TOPOPAH SPRING 2 COLUMN 3
ID for dose/conc. conversion table :
Total length of Pathway (m) : LTS2C3
Total Area of Pathway (m*m) : ACOL3
Total Flow through Pathway (m*m*m/yr) : QCOL3

The number of exit paths is 2
Path 1 : TS3C3 Fraction of Balance = FNS230
Path 2 : SAT Fraction of Balance = 1.0000

The number of flow modes is 1

Flow mode #1
Description : FLOW MODE 1

Fraction of balance of remaining total flow : 1.0000
Flow mode velocity : VTSW2
Transition rate (m): 1.0000
Dispersivity (m): 0.00000E+00

Details of Path 43
ID : TS2C4
Description : TOPOPAH SPRING 2 COLUMN 4
ID for dose/conc. conversion table :
Total length of Pathway (m) : LTS2C4
Total Area of Pathway (m*m) : ACOL4
Total Flow through Pathway (m*m*m/yr) : QCOL4

The number of exit paths is 1
Path 1 : TS3C4 Fraction of Balance = 1.0000

The number of flow modes is 1

Flow mode #1
Description : FLOW MODE 1

Fraction of balance of remaining total flow : 1.0000
Flow mode velocity : VTSW2
Transition rate (m): 1.0000
Dispersivity (m): 0.00000E+00

Details of Path 44
ID : TS2C5
Description : TOPOPAH SPRING 2 COLUMN 5
ID for dose/conc. conversion table :
Total length of Pathway (m) : LTS2C5
Total Area of Pathway (m*m) : ACOL5
Total Flow through Pathway (m*m*m/yr) : QCOL5

The number of exit paths is 1
Path 1 : TS3C5 Fraction of Balance = 1.0000

The number of flow modes is 1

Flow mode #1
Description : FLOW MODE 1

Fraction of balance of remaining total flow : 1.0000
Flow mode velocity : VTSW2
Transition rate (m): 1.0000
Dispersivity (m): 0.00000E+00

Details of Path 45
ID : TS2C6
Description : TOPOPAH SPRING 2 COLUMN 6
ID for dose/conc. conversion table :
Total length of Pathway (m) : LTS2C6
Total Area of Pathway (m*m) : ACOL6
Total Flow through Pathway (m*m*m/yr) : QCOL6

The number of exit paths is 1
Path 1 : TS3C6 Fraction of Balance = 1.0000

The number of flow modes is 1

Flow mode #1
Description : FLOW MODE 1

Fraction of balance of remaining total flow : 1.0000
Flow mode velocity : VTSW2
Transition rate (m): 1.0000
Dispersivity (m): 0.00000E+00

Details of Path 46
ID : TS2C7
Description : TOPOPAH SPRING 2 COLUMN 7
ID for dose/conc. conversion table :
Total length of Pathway (m) : LTS2C7
Total Area of Pathway (m*m) : ACOL79
Total Flow through Pathway (m*m*m/yr) : QCOL79

The number of exit paths is 2
Path 1 : TS3C7 Fraction of Balance = FNS230
Path 2 : SAT Fraction of Balance = 1.0000

The number of flow modes is 1

Flow mode #1
Description : FLOW MODE 1

Fraction of balance of remaining total flow : 1.0000
Flow mode velocity : VTSW2
Transition rate (m): 1.0000
Dispersivity (m): 0.00000E+00

Details of Path 47
ID : TS2C8
Description : TOPOPAH SPRING 2 COLUMN 8
ID for dose/conc. conversion table :
Total length of Pathway (m) : LTS2C8
Total Area of Pathway (m*m) : ACOL79
Total Flow through Pathway (m*m*m/yr) : QCOL79

The number of exit paths is 2

Path 1 : TS3C8 Fraction of Balance = FNS230
Path 2 : SAT Fraction of Balance = 1.0000

The number of flow modes is 1

Flow mode #1
Description : FLOW MODE 1

Fraction of balance of remaining total flow : 1.0000
Flow mode velocity : VTSW2
Transition rate (m): 1.0000
Dispersivity (m): 0.00000E+00

Details of Path 48
ID : TS2C9
Description : TOPOPAH SPRING 2 COLUMN 9
ID for dose/conc. conversion table :
Total length of Pathway (m) : LTS2C9
Total Area of Pathway (m*m) : ACOL79
Total Flow through Pathway (m*m*m/yr) : QCOL79

The number of exit paths is 2
Path 1 : TS3C9 Fraction of Balance = FNS230
Path 2 : SAT Fraction of Balance = 1.0000

The number of flow modes is 1

Flow mode #1
Description : FLOW MODE 1

Fraction of balance of remaining total flow : 1.0000
Flow mode velocity : VTSW2
Transition rate (m): 1.0000
Dispersivity (m): 0.00000E+00

RECEPTOR DESCRIPTIONS
none
DOSE CONVERSION TABLES
none

DISRUPTIVE EVENTS
none

STRATEGY
not used

PARAMETER DATABASE

Parameter No. 1 of 287
Parameter ID : ACOL1
Description : area of column 1

Save Time History : TRUE
The parameter is a constant: 3.98892E+05
The parameter affects the following parameters:
QCOL1,QSAT

Parameter No. 2 of 287
Parameter ID : ACOL2
Description : AREA OF COLUMN 2

Save Time History : TRUE
The parameter is a constant: 4.13673E+05
The parameter affects the following parameters:
QCOL2,QSAT

Parameter No. 3 of 287
Parameter ID : ACOL3
Description : AREA OF COLUMN 3

Save Time History : TRUE
The parameter is a constant: 3.84124E+05
The parameter affects the following parameters:
QCOL3,QSAT

Parameter No. 4 of 287
Parameter ID : ACOL4
Description : AREA OF COLUMN 4

Save Time History : TRUE
The parameter is a constant: 3.17641E+05
The parameter affects the following parameters:
QCOL4,QSAT

Parameter No. 5 of 287
Parameter ID : ACOL5
Description : AREA OF COLUMN 5

Save Time History : TRUE
The parameter is a constant: 3.76737E+05
The parameter affects the following parameters:
QCOL5,QSAT

Parameter No. 6 of 287
Parameter ID : ACOL6
Description : AREA OF COLUMN 6

Save Time History : TRUE
The parameter is a constant: 4.50600E+05
The parameter affects the following parameters:
QCOL6,QSAT

Parameter No. 7 of 287
Parameter ID : ACOL79
Description : AREA OF COLUMN 7-9

Save Time History : TRUE
The parameter is a constant: 5.02316E+05
The parameter affects the following parameters:
QCOL79,QSAT

Parameter No. 8 of 287
Parameter ID : ASAT
Description : AREA OF SATURATED ZONE

Save Time History : TRUE
The Parameter is a function, exp. value =
1600000
Equation : 200*8000

The parameter is a function of the following
parameters:

Parameter No. 9 of 287
Parameter ID : ASURF
Description : surface area of wasteform

Save Time History : TRUE
The parameter is a constant: Depends on
wasteform/container. see Tables 4.1 and 4.2.
For DHLW, it is function that includes the
cracking factor (uniform 10-30)
The parameter affects the following parameters:
ESURF,FV,FVMC

Parameter No. 10 of 287
Parameter ID : CATCH
Description : EFFECTIVE CATCHMENT AREA FOR WET DRIP
Save Time History : TRUE
MMB Container
The parameter is stochastic
The distribution is linear
Sampling bias : No Bias
Uniform : Umin = 8.50000E+00 Umax = 4.65000E+01
SCP Container
The parameter is function
equation: PI*CATRAD**2 with catrad defined uniformly between 0.5 and 1.5 m
The parameter affects the following parameters:
TCATCH

Parameter No. 11 of 287
Parameter ID : DBW
Description : DENSITY BULLFROG

Save Time History : TRUE
The parameter is stochastic
The distribution is linear
Sampling bias : No Bias
Beta : Mean = 2.00000E+00 S.D. = 1.81000E-01 Min = 1.70000E+00 Max = 2.40000E+00
The parameter affects the following parameters:
RAMBW,RAMS,RCSBW,RCSSAT,RNPBW, RNPS,RPUBW,RPUS,RRABW,RRAS,RUBW, RUS,TRAMBW,TRCSBW,TRNPBW,TRPUBW, TRRABW,TRUBW

Parameter No. 12 of 287
Parameter ID : DCHN1V
Description : DENSITY CALICO HILLS VITRIC

Save Time History : TRUE
The parameter is stochastic
The distribution is linear
Sampling bias : No Bias
Beta : Mean = 1.68000E+00 S.D. = 2.20000E-01 Min = 1.30000E+00 Max = 2.10000E+00
The parameter affects the following parameters:

RAMCHV,RCSCHV,RNPCHV,RPUCHV,RRACH V,RUCHV,TRACHV,TRCCHV,TRNCH
TRPCHV,TRRCHV,TRUCHV

Parameter No. 13 of 287
Parameter ID : DCHN1Z
Description : DENSITY CALICO HILLS ZEOLITIC
Save Time History : TRUE
The parameter is stochastic
The distribution is linear
Sampling bias : No Bias
Beta : Mean = 1.68000E+00 S.D. = 2.20000E-01
Min = 1.30000E+00 Max = 2.10000E+00
The parameter affects the following parameters:
RAMCHZ,RCSCHZ,RNPCHZ,RPUCHZ, RRACHZ,RUCHZ,TRACHZ,TRCCHZ,TRNCH TRPCHZ,TRRCHZ,TRUCHZ

Parameter No. 14 of 287
Parameter ID : DPPW
Description : DENSITY PROW PASS

Save Time History : TRUE
The parameter is stochastic
The distribution is linear
Sampling bias : No Bias
Beta : Mean = 2.00000E+00 S.D. = 1.81000E-01
Min = 1.70000E+00 Max = 2.40000E+00
The parameter affects the following parameters:
RAMPPW,RCSPPW,RNPPPW,RPUPPW, RRAPPW,RUPPW,TRAPPW,TRCPPW, TRNPP, TRPPPW,TRRPPW,TRUPPW

Parameter No. 15 of 287
Parameter ID : DRYINF
Description : Dry Infiltration

Save Time History : TRUE
The parameter is stochastic
The distribution is linear
Sampling bias : No Bias
Beta : Mean = 5.00000E-04 S.D. = 4.80000E-04 Min = 0.00000E+00 Max = 1.25000E-02
The parameter affects the following parameters:
DTBL,FNS130,FNS230,FNS60,FNS613,
GWTIM1,GWTIM2,GWTIM3,GWTIM4
GWTIM5,GWTIM6,GWTIM7,GWTIM8,GWTIM9,
GWTM1A,GWTM2A,GWTM3A
GWTM4A,GWTM5A,GWTM6A,GWTM7A,
GWTM8A,GWTM9A,LCHVC1,LCHVC2
LCHVC4,LCHVC5,LCHZC1,LCHZC2,LCHZC3,
LCHZC6,LCHZC7,LCHZC8
LCHZC9,LPPWC3,LPPWC4,LPPWC5,LPPWC6,
LPPWC7,LPPWC8,LPPWC9
LTS2C1,LTS2C2,LTS2C3,LTS2C7,LTS2C8,
LTS2C9,LTS3C6,QCOL1,QCOL2
QCOL3,QCOL4,QCOL5,QCOL6,QCOL79,QSAT,
TUFLUX,UBFLUX,VBW,VCHN1V
VCHN1Z,VPPW,VTSW2,VTSW3

Parameter No. 16 of 287
Parameter ID : DTBL
Description : water table change

Save Time History : TRUE
The Parameter is a function, exp. value = 0
Equation :
if(tuflux<1e-3,0,(if(tuflux>3.4e-3,dtbl2,dtbl1))

The parameter affects the following parameters:

FNS130,FNS230,FNS60,FNS613,GWTIM1,GWT
IM2,GWTIM3,GWTIM4,GWTIM5
GWTIM6,GWTIM7,GWTIM8,GWTIM9,GWTM1A,
GWTM2A,GWTM3A,GWTM4A
GWTM5A,GWTM6A,GWTM7A,GWTM8A,GWTM
9A,LCHVC1,LCHVC2,LCHVC4
LCHVC5,LCHZC1,LCHZC2,LCHZC3,LCHZC6,L
CHZC7,LCHZC8,LCHZC9
LPPWC3,LPPWC4,LPPWC5,LPPWC6,LPPWC7,
LPPWC8,LPPWC9,LTS2C1 LTS2C2,
LTS2C3,LTS2C7,LTS2C8,LTS2C9,LTS3C6

Parameter No. 17 of 287
Parameter ID : DTBL1
Description : water table change moderate flux

Save Time History : TRUE
The parameter is stochastic
The distribution is linear
Sampling bias : No Bias
PDF : Value = 0.00000E+00 Prob = 4.00000E-01
Value = 6.00000E+01 Prob = 6.00000E-01

The parameter affects the following parameters:
DTBL,FNS130,FNS230,FNS60,FNS613,
GWTIM1,GWTIM2,GWTIM3,GWTIM4
GWTIM5,GWTIM6,GWTIM7,GWTIM8,GWTIM9,
GWTM1A,GWTM2A,GWTM3A
GWTM4A,GWTM5A,GWTM6A,GWTM7A,
GWTM8A,GWTM9A,LCHVC1,LCHVC2
LCHVC4,LCHVC5,LCHZC1,LCHZC2,LCHZC3,
LCHZC6,LCHZC7,LCHZC8
LCHZC9,LPPWC3,LPPWC4,LPPWC5,LPPWC6,
LPPWC7,LPPWC8,LPPWC9
LTS2C1,LTS2C2,LTS2C3,LTS2C7,LTS2C8,
LTS2C9,LTS3C6

Parameter No. 18 of 287
Parameter ID : DTBL2
Description : water table change high flux

Save Time History : TRUE
The parameter is stochastic
The distribution is linear
Sampling bias : No Bias
PDF : Value = 6.00000E+01 Prob = 8.00000E-01
Value = 1.30000E+02 Prob = 1.90000E-01
Value = 2.30000E+02 Prob = 1.00000E-02

The parameter affects the following parameters:
DTBL,FNS130,FNS230,FNS60,FNS613,
GWTIM1,GWTIM2,GWTIM3,GWTIM4
GWTIM5,GWTIM6,GWTIM7,GWTIM8,GWTIM9,
GWTM1A,GWTM2A,GWTM3A,GWTM4A,
GWTM5A,GWTM6A,GWTM7A,GWTM8A,
GWTM9A,LCHVC1,LCHVC2, LCHVC4,LCHVC5,
LCHZC1,LCHZC2,LCHZC3,LCHZC6,LCHZC7,
LCHZC8,LCHZC9,LPPWC3,LPPWC4,LPPWC5,
LPPWC6,LPPWC7,LPPWC8,LPPWC9
LTS2C1,LTS2C2,LTS2C3,LTS2C7,LTS2C8,
LTS2C9,LTS3C6

Parameter No. 19 of 287
Parameter ID : DTSW2
Description : DENSITY TOPOPAH SPRING 2

Save Time History : TRUE
The parameter is stochastic
The distribution is linear
Sampling bias : No Bias
Beta : Mean = 2.24000E+00 S.D. = 9.20000E-02 Min = 2.00000E+00 Max = 2.40000E+00
The parameter affects the following parameters:

RAMTS2,RCSTS2,RNPTS2,RPUTS2,RRATS2, RUTS2,TRATS2,TRCTS2,TRNTS TRPTS2,TRRTS2,TRUTS2

Parameter No. 20 of 287
Parameter ID : DTSW3
Description : DENSITY TOPOPAH SPRING 3

Save Time History : TRUE
The parameter is stochastic
The distribution is linear
Sampling bias : No Bias
Beta : Mean = 2.15000E+00 S.D. = 1.91000E-01
Min = 1.70000E+00 Max = 2.50000E+00
The parameter affects the following parameters:

RAMTS3,RCSTS3,RNPTS3,RPUTS3,RRATS3, RUTS3,TRATS3,TRCTS3,TRNTS TRPTS3,TRRTS3,TRUTS3

Parameter No. 22 of 287
Parameter ID : EFFDIF
Description : EFFECTIVE DIFFUSION COEFFICIENT, TUFF GRAVEL
Save Time History : TRUE
The Parameter is a function, exp. value = 0.9758
Equation : -5.9135E-5+7.9154E-4*STSW2+2.103041*STSW 2**2
The parameter affects the following parameters:
TEFDIF

Parameter No. 23 of 287
Parameter ID : EQRAD
Description : equivalent radius of waste package as sphere
Save Time History : TRUE
The Parameter is a function, exp. value = 1.402839
Equation : (3*vol/(4*pi))**0.333
The parameter affects the following parameters:
OMEGA,TOMEGA
The parameter is a function of the following parameters:
LENG,PI,R0,VOL

Parameter No. 24 of 287
Parameter ID : ESURF
Description : effective surface area of wasteform (m*m/g)
Save Time History : TRUE
The Parameter is a function, exp. value = 0.00005359
Equation : asurf/mass

Parameter No. 25 of 287
Parameter ID : FGEOMD
Description : FACTOR IN GEOMETRIC FACTOR FOR DIFFUSION
Save Time History : TRUE
The Parameter is a function, exp. value = 1
Equation : IF(STSW2>0.08,1,0) INTERA 1993 PA [14]
The parameter affects the following parameters:
OMEGA,TOMEGA
The parameter is a function of the following parameters:
STSW2

Parameter No. 26 of 287
Parameter ID : FM
Description : FLUX MULTIPLIER TO ACCOUNT FOR CLIMACTIC CHANGE
Save Time History : TRUE
The parameter is stochastic
The distribution is linear
Sampling bias : No Bias
Triang : Mn= 1.00000E+00 Ml= 2.00000E+01 Mx= 4.00000E+01
The parameter affects the following parameters:
DTBL,FNS130,FNS230,FNS60,FNS613, GWTIM1,GWTIM2,GWTIM3,GWTIM4 GWTIM5,GWTIM6,GWTIM7,GWTIM8,GWTIM9, GWTM1A,GWTM2A,GWTM3A,GWTM4A, GWTM5A,GWTM6A,GWTM7A,GWTM8A ,GWTM9A,LCHVC1,LCHVC2,LCHVC4,LCHVC5, LCHZC1,LCHZC2,LCHZC3,LCHZC6,LCHZC7, LCHZC8,LCHZC9,LPPWC3,LPPWC4,LPPWC5, LPPWC6,LPPWC7,LPPWC8,LPPWC9 LTS2C1,LTS2C2,LTS2C3,LTS2C7,LTS2C8, LTS2C9,LTS3C6,QCOL1,QCOL2,QCOL3, QCOL4,QCOL5,QCOL6,QCOL79,QSAT, TSFLUX,TUFLUX,UBFLUX,VBW,VCHN1V, VCHN1Z,VPPW,VSAT,VTSW2,VTSW3

Parameter No. 27 of 287
Parameter ID : FNS130
Description : fraction of mass not to saturated zone path, wat tbl 130
Save Time History : TRUE
The Parameter is a function, exp. value = 1.
Equation : if(dtbl==130,0.000001,0.999999)

The parameter is a function of the following parameters:
DRYINF,DTBL,DTBL1,DTBL2,FM,HFXSW, HPERC,HPERC1,KSM,TIME,TUFLUX, UBFLUX

Parameter No. 28 of 287
Parameter ID : FNS230
Description : fraction of mass not to saturated zone path, wat tbl 230
Save Time History : TRUE
The Parameter is a function, exp. value = 1.
Equation : if(dtbl==230,0.000001,0.999999)

The parameter is a function of the following parameters:
DRYINF,DTBL,DTBL1,DTBL2,FM,HFXSW, HPERC,HPERC1,KSM,TIME,TUFLUX, UBFLUX

Parameter No. 29 of 287
Parameter ID : FNS60
Description : fraction of mass not to saturated zone path, wat tbl 60
Save Time History : TRUE
The Parameter is a function, exp. value = 1.
Equation : if(dtbl==60,0.000001,0.999999)

The parameter is a function of the following parameters:
DRYINF,DTBL,DTBL1,DTBL2,FM,HFXSW, HPERC,HPERC1,KSM,TIME,TUFLUX UBFLUX

Parameter No. 30 of 287
Parameter ID : FNS613
Description : fraction of mass not to sat zone path, wat tbl 60 or 130
Save Time History : TRUE
The Parameter is a function, exp. value = 1.
Equation :
if(dtbl==60,0.000001,if(dtbl==130,0.000001,0.999999))
The parameter is a function of the following parameters:
DRYINF,DTBL,DTBL1,DTBL2,FM,HFXSW, HPERC,HPERC1,KSM,TIME,TUFLUX, UBFLUX

Parameter No. 31 of 287
Parameter ID : FV
Description : Volume of Water Contacting matrix (for concentration calc)
Save Time History : TRUE
The Parameter is a function, exp. value = 0.522
Equation : if(contac==1,fvwd,fvmc)

The parameter is a function of the following parameters:
ASURF,CONTAC,FVMC,FVWD,TWAT

Parameter No. 32 of 287
Parameter ID : FVMC
Description : Free Volume Moist Continuous

Save Time History : TRUE
The Parameter is a function, exp. value = 0.522
Equation : twat*asurf

The parameter affects the following parameters:
FV
The parameter is a function of the following parameters:
ASURF,TWAT

Parameter No. 33 of 287
Parameter ID : FVWD
Description : Free Volume Wet Drip

Save Time History : TRUE
The parameter is a constant: 1.22 for SCP-LWR, 5.5 MMB-LWR (Table 4.1)
2.142
DHLW/ALMR - MMB (Table 4.2)
The parameter affects the following parameters:
FV

Parameter No. 34 of 287
Parameter ID : GWTIM1
Description : Groundwater Travel Time Column 1
Save Time History : TRUE
The Parameter is a function, exp. value = 87637.7
Equation : gwtm1a+lts3/vtsw3+lts2c1/vtsw2

The parameter is a function of the following parameters:
DRYINF,DTBL,DTBL1,DTBL2,FM,GWTM1A, HFXSW,HPERC,HPERC1,KSM,LCHVC1, LCHZC1,LPPWC1,LSAT,LTS2C1,LTS3,PCHN1V PCHN1Z,PPPW,PSAT,PTSW2,PTSW3,SBFLUX SCHN1V,SCHN1Z,SPPW,STSW2,STSW3,TIME TSFLUX,TUFLUX,UBFLUX,VCHN1V,VCHN1Z, VPPW,VSAT,VTSW2,VTSW3,TSFLUX,TUFLUX, UBFLUX,VCHN1V,VCHN1Z,VPPW,VSAT, VTSW2,VTSW3

Parameter No. 35 of 287
Parameter ID : GWTIM2
Description : Ground water travel time column 2

Save Time History : TRUE
The Parameter is a function, exp. value = 92495.73
Equation : gwtm2a+lts3/vtsw3+lts2c2/vtsw2

The parameter is a function of the following parameters:
DRYINF,DTBL,DTBL1,DTBL2,FM,GWTM2A, HFXSW,HPERC,HPERC1,KSMLCHVC2, LCHZC2,LPPWC2,LSAT,LTS2C2,LTS3,PCHN1V PCHN1Z,PPPW,PSAT,PTSW2,PTSW3,SBFLUX SCHN1V,SCHN1Z,SPPW,STSW2,STSW3,TIME TSFLUX,TUFLUX,UBFLUX,VCHN1V,VCHN1Z,V PPW,VSAT,VTSW2,VTSW3,TSFLUX,TUFLUX, UBFLUX,VCHN1V,VCHN1Z,VPPW,VSAT, VTSW2,VTSW3

Parameter No. 36 of 287
Parameter ID : GWTIM3
Description : Ground water travel time column 3

Save Time History : TRUE
The Parameter is a function, exp. value = 109496.3
Equation : gwtm3a+lts3/vtsw3+lts2c3/vtsw2

The parameter is a function of the following parameters:
DRYINF,DTBL,DTBL1,DTBL2,FM,GWTM3A, HFXSW,HPERC,HPERC1,KSM,LCHVC3, LCHZC3,LPPWC3,LSAT,LTS2C3,LTS3,PCHN1V PCHN1Z,PPPW,PSAT,PTSW2,PTSW3,SBFLUX SCHN1V,SCHN1Z,SPPW,STSW2,STSW3,TIME TSFLUX,TUFLUX,UBFLUX,VCHN1V,VCHN1Z, VPPW,VSAT,VTSW2,VTSW3,TSFLUX,TUFLUX, UBFLUX,VCHN1V,VCHN1Z,VPPW,VSAT, VTSW2,VTSW3

Parameter No. 37 of 287
Parameter ID : GWTIM4
Description : Ground water travel time column 4

Save Time History : TRUE
The Parameter is a function, exp. value = 122529.6
Equation : gwtm4a+lts3/vtsw3+lts2c4/vtsw2

The parameter is a function of the following parameters:
DRYINF,DTBL,DTBL1,DTBL2,FM,GWTM4A, HFXSW,HPERC,HPERC1,KSM,LCHVC4, LCHZC4,LPPWC4,LSAT,LTS2C4,LTS3,PCHN1V PCHN1Z,PPPW,PSAT,PTSW2,PTSW3,SBFLUX SCHN1V,SCHN1Z,SPPW,STSW2,STSW3,TIME TSFLUX,TUFLUX,UBFLUX,VCHN1V,VCHN1Z, VPPW,VSAT,VTSW2,VTSW3,TSFLUX,TUFLUX, UBFLUX,VCHN1V,VCHN1Z,VPPW,VSAT, VTSW2,VTSW3

Parameter No. 38 of 287
Parameter ID : GWTIM5
Description : Ground water travel time column 5

Save Time History : TRUE
The Parameter is a function, exp. value = 117967.8
Equation : gwtm5a+lts3/vtsw3+lts2c5/vtsw2

The parameter is a function of the following parameters:
DRYINF,DTBL,DTBL1,DTBL2,FM,GWTM5A, HFXSW,HPERC,HPERC1,KSM,LCHVC5, LCHZC5,LPPWC5,LSAT,LTS2C5,LTS3,PCHN1V PCHN1Z,PPPW,PSAT,PTSW2,PTSW3,SBFLUX SCHN1V,SCHN1Z,SPPW,STSW2,STSW3,TIME TSFLUX,TUFLUX,UBFLUX,VCHN1V,VCHN1Z,V PPW,VSAT,VTSW2,VTSW3,TSFLUX,TUFLUX, UBFLUX,VCHN1V,VCHN1Z,VPPW,VSAT, VTSW2,VTSW3

Parameter No. 39 of 287
Parameter ID : GWTIM6
Description : ground water travel time column 6

Save Time History : TRUE
The Parameter is a function, exp. value = 125823.9
Equation : gwtm6a+lts3/vtsw3+lts2c6/vtsw2

The parameter is a function of the following parameters:
DRYINF,DTBL,DTBL1,DTBL2,FM,GWTM5A, HFXSW,HPERC,HPERC1,KSM,LCHVC6, LCHZC6,LPPWC6,LSAT,LTS2C6,LTS3,PCHN1V PCHN1Z,PPPW,PSAT,PTSW2,PTSW3,SBFLUX SCHN1V,SCHN1Z,SPPW,STSW2,STSW3,TIME TSFLUX,TUFLUX,UBFLUX,VCHN1V,VCHN1Z,V PPW,VSAT,VTSW2,VTSW3,TSFLUX,TUFLUX, UBFLUX,VCHN1V,VCHN1Z,VPPW,VSAT, VTSW2,VTSW3

Parameter No. 40 of 287
Parameter ID : GWTIM7
Description : ground water travel time column 7

Save Time History : TRUE
The Parameter is a function, exp. value = 110055.5
Equation : gwtm7a+lts3/vtsw3+lts2c7/vtsw2

The parameter is a function of the following parameters:
DRYINF,DTBL,DTBL1,DTBL2,FM,GWTM5A, HFXSW,HPERC,HPERC1,KSM,LCHVC7, LCHZC7,LPPWC7,LSAT,LTS2C7,LTS3,PCHN1V PCHN1Z,PPPW,PSAT,PTSW2,PTSW3,SBFLUX SCHN1V,SCHN1Z,SPPW,STSW2,STSW3,TIME TSFLUX,TUFLUX,UBFLUX,VCHN1V,VCHN1Z,V PPW,VSAT,VTSW2,VTSW3,TSFLUX,TUFLUX, UBFLUX,VCHN1V,VCHN1Z,VPPW,VSAT, VTSW2,VTSW3

Parameter No. 41 of 287
Parameter ID : GWTIM8
Description : ground water travel time column 8

Save Time History : TRUE
The Parameter is a function, exp. value = 103059.5
Equation : gwtm8a+lts3/vtsw3+lts2c8/vtsw2

The parameter is a function of the following parameters:
DRYINF,DTBL,DTBL1,DTBL2,FM,GWTM5A, HFXSW,HPERC,HPERC1,KSM,LCHVC8, LCHZC8,LPPWC8,LSAT,LTS2C8,LTS3,PCHN1V PCHN1Z,PPPW,PSAT,PTSW2,PTSW3,SBFLUX SCHN1V,SCHN1Z,SPPW,STSW2,STSW3,TIME TSFLUX,TUFLUX,UBFLUX,VCHN1V,VCHN1Z,V PPW,VSAT,VTSW2,VTSW3,TSFLUX,TUFLUX, UBFLUX,VCHN1V,VCHN1Z,VPPW,VSAT, VTSW2,VTSW3

Parameter No. 42 of 287
Parameter ID : GWTIM9
Description : ground water travel time column 9

Save Time History : TRUE
The Parameter is a function, exp. value = 96097.03
Equation : gwtm9a+lts3/vtsw3+lts2c9/vtsw2

The parameter is a function of the following parameters:
DRYINF,DTBL,DTBL1,DTBL2,FM,GWTM5A, HFXSW,HPERC,HPERC1,KSM,LCHVC9, LCHZC9,LPPWC9,LSAT,LTS2C9,LTS3,PCHN1V PCHN1Z,PPPW,PSAT,PTSW2,PTSW3,SBFLUX SCHN1V,SCHN1Z,SPPW,STSW2,STSW3,TIME TSFLUX,TUFLUX,UBFLUX,VCHN1V,VCHN1Z,V PPW,VSAT,VTSW2,VTSW3,TSFLUX,TUFLUX, UBFLUX,VCHN1V,VCHN1Z,VPPW,VSAT, VTSW2,VTSW3

Parameter No. 43 of 287
Parameter ID : GWTM1A
Description : Groundwater Travel Time Column 1 (all except ts2 ts3)
Save Time History : TRUE
The Parameter is a function, exp. value = 66637.88
Equation : lsat/vsat+lppwc1/vppw+lchzc1/vchn1z+lchvc1/vchn1v
The parameter affects the following parameters:
GWTIM1
The parameter is a function of the following parameters:
DRYINF,DTBL,DTBL1,DTBL2,FM,HFXSW, HPERC,HPERC1,KSM,LCHVC1,LCHZC1, LPPWC1,LSAT,PCHN1V,PCHN1Z,PPPW,PSAT, SBFLUX,SCHN1V,SCHN1Z,SPPW,TIME, TSFLUX,TUFLUX,UBFLUX,VCHN1V,VCHN1Z, VPPW,VSAT

Parameter No. 44 of 287
Parameter ID : GWTM2A
Description : Groundwater Travel Time Column 2 (all except ts2 ts3)
Save Time History : TRUE
The Parameter is a function, exp. value = 71196.27
Equation :
lsat/vsat+lppwc2/vppw+lchzc2/vchn1z+lchvc2/vchn1v
The parameter affects the following parameters:
GWTIM2
The parameter is a function of the following parameters:
DRYINF,DTBL,DTBL1,DTBL2,FM,HFXSW, HPERC,HPERC1,KSM,LCHVC2,LCHZC2, LPPWC2,LSAT,PCHN1V,PCHN1Z,PPPW,PSAT, SBFLUX,SCHN1V,SCHN1Z,SPPW,TIME, TSFLUX,TUFLUX,UBFLUX,VCHN1V,VCHN1Z, VPPW,VSAT

Parameter No. 45 of 287
Parameter ID : GWTM3A
Description : Groundwater Travel Time Column 3 (all except ts2 ts3)
Save Time History : TRUE
The Parameter is a function, exp. value = 91792.47
Equation :
lsat/vsat+lppwc3/vppw+lchzc3/vchn1z+lchvc3/vchn1v
The parameter affects the following parameters:
GWTIM3
The parameter is a function of the following parameters:
DRYINF,DTBL,DTBL1,DTBL2,FM,HFXSW, HPERC,HPERC1,KSM,LCHVC3,LCHZC3, LPPWC3,LSAT,PCHN1V,PCHN1Z,PPPW,PSAT, SBFLUX,SCHN1V,SCHN1Z,SPPW,TIME, TSFLUX,TUFLUX,UBFLUX,VCHN1V,VCHN1Z, VPPW,VSAT

Parameter No. 46 of 287
Parameter ID : GWTM4A
Description : Groundwater Travel Time Column 4 (all except ts2 ts3)
Save Time History : TRUE
The Parameter is a function, exp. value = 109919.7
Equation :
lsat/vsat+lppwc4/vppw+lchzc4/vchn1z+lchvc4/vchn1v
The parameter affects the following parameters:
GWTIM4
The parameter is a function of the following parameters:
DRYINF,DTBL,DTBL1,DTBL2,FM,HFXSW, HPERC,HPERC1,KSM,LCHVC4,LCHZC4, LPPWC4,LSAT,PCHN1V,PCHN1Z,PPPW,PSAT, SBFLUX,SCHN1V,SCHN1Z,SPPW,TIME, TSFLUX,TUFLUX,UBFLUX,VCHN1V,VCHN1Z, VPPW,VSAT

Parameter No. 47 of 287
Parameter ID : GWTM5A
Description : Groundwater Travel Time Column 5 (all except ts2 ts3)
Save Time History : TRUE
The Parameter is a function, exp. value = 109852.5
Equation :
lsat/vsat+lppwc5/vppw+lchzc5/vchn1z+lchvc5/vchn1v
The parameter affects the following parameters:
GWTIM5
The parameter is a function of the following parameters:
DRYINF,DTBL,DTBL1,DTBL2,FM,HFXSW, HPERC,HPERC1,KSM,LCHVC5,LCHZC5, LPPWC5,LSAT,PCHN1V,PCHN1Z,PPPW,PSAT, SBFLUX,SCHN1V,SCHN1Z,SPPW,TIME, TSFLUX,TUFLUX,UBFLUX,VCHN1V,VCHN1Z, VPPW,VSAT

Parameter No. 48 of 287
Parameter ID : GWTM6A
Description : Groundwater Travel Time Column 6 (all except ts2 ts3)
Save Time History : TRUE
The Parameter is a function, exp. value = 114262.8
Equation :
lsat/vsat+lppwc6/vppw+lchzc6/vchn1z+lchvc6/vchn1v
The parameter affects the following parameters:
GWTIM6
The parameter is a function of the following parameters:
DRYINF,DTBL,DTBL1,DTBL2,FM,HFXSW, HPERC,HPERC1,KSM,LCHVC6,LCHZC6, LPPWC6,LSAT,PCHN1V,PCHN1Z,PPPW,PSAT, SBFLUX,SCHN1V,SCHN1Z,SPPW,TIME, TSFLUX,TUFLUX,UBFLUX,VCHN1V,VCHN1Z, VPPW,VSAT

Parameter No. 49 of 287
Parameter ID : GWTM7A
Description : Groundwater Travel Time Column 7 (all except ts2 ts3)
Save Time History : TRUE
The Parameter is a function, exp. value = 93700.15
Equation :
lsat/vsat+lppwc7/vppw+lchzc7/vchn1z+lchvc7/vchn1v
The parameter affects the following parameters:
GWTIM7
The parameter is a function of the following parameters:
DRYINF,DTBL,DTBL1,DTBL2,FM,HFXSW,
HPERC,HPERC1,KSM,LCHVC7,LCHZC7,
LPPWC7,LSAT,PCHN1V,PCHN1Z,PPPW,PSAT,
SBFLUX,SCHN1V,SCHN1Z,SPPW,TIME,
TSFLUX,TUFLUX,UBFLUX,VCHN1V,VCHN1Z,
VPPW,VSAT

Parameter No. 50 of 287
Parameter ID : GWTM8A
Description : Groundwater Travel Time Column 8 (all except ts2 ts3)
Save Time History : TRUE
The Parameter is a function, exp. value = 88352.11
Equation :
lsat/vsat+lppwc8/vppw+lchzc8/vchn1z+lchvc8/vchn1v
The parameter affects the following parameters:
GWTIM8
The parameter is a function of the following parameters:
DRYINF,DTBL,DTBL1,DTBL2,FM,HFXSW,
HPERC,HPERC1,KSM,LCHVC8,LCHZC8,
LPPWC8,LSAT,PCHN1V,PCHN1Z,PPPW,PSAT,
SBFLUX,SCHN1V,SCHN1Z,SPPW,TIME,
TSFLUX,TUFLUX,UBFLUX,VCHN1V,VCHN1Z,
VPPW,VSAT

Parameter No. 51 of 287
Parameter ID : GWTM9A
Description : Groundwater Travel Time Column 9 (all except ts2 ts3)
Save Time History : TRUE
The Parameter is a function, exp. value = 83037.67
Equation :
lsat/vsat+lppwc9/vppw+lchzc9/vchn1z+lchvc9/vchn1v
The parameter affects the following parameters:
GWTIM9
The parameter is a function of the following parameters:
DRYINF,DTBL,DTBL1,DTBL2,FM,HFXSW,
HPERC,HPERC1,KSM,LCHVC9,LCHZC9,
LPPWC9,LSAT,PCHN1V,PCHN1Z,PPPW,PSAT,
SBFLUX,SCHN1V,SCHN1Z,SPPW,TIME,
TSFLUX,TUFLUX,UBFLUX,VCHN1V,VCHN1Z,
VPPW,VSAT

Parameter No. 52 of 287
Parameter ID : HFXSW
Description : Switch to determine high percolation flux
Save Time History : TRUE
The parameter is stochastic
The distribution is linear
Sampling bias : No Bias
Uniform : Umin = 0.00000E+00 Umax = 1.00000E+00
The parameter affects the following parameters:
DTBL,FNS130,FNS230,FNS60,FNS613,
GWTIM1,GWTIM2,GWTIM3,GWTIM4
GWTIM5,GWTIM6,GWTIM7,GWTIM8,GWTIM9,
GWTM1A,GWTM2A,GWTM3A
GWTM4A,GWTM5A,GWTM6A,GWTM7A,
GWTM8A,GWTM9A,HPERC,LCHVC1,
LCHVCC,LCHVC4,LCHVC5,LCHZC1,LCHZC2,
LCHZC3,LCHZC6,LCHZC7,LCHZC8
LCHZC9,LPPWC3,LPPWC4,LPPWC5,LPPWC6,
LPPWC7,LPPWC8,LPPWC9
LTS2C1,LTS2C2,LTS2C3,LTS2C7,LTS2C8,
LTS2C9,LTS3C6,QCOL1,QCOL2
QCOL3,QCOL4,QCOL5,QCOL6,QCOL79,QSAT,
TUFLUX,VBW,VCHN1V,VCHN1Z
VPPW,VTSW2,VTSW3

Parameter No. 53 of 287
Parameter ID : HPERC
Description : Flux if infiltration exceeds ksm

Save Time History : TRUE
The Parameter is a function, exp. value = 0.002465
Equation : if(hfxsw<=0.5,ksm,hperc1)

The parameter affects the following parameters:
DTBL,FNS130,FNS230,FNS60,FNS613,
GWTIM1,GWTIM2,GWTIM3,GWTIM4
GWTIM5,GWTIM6,GWTIM7,GWTIM8,GWTIM9,
GWTM1A,GWTM2A,GWTM3A
GWTM4A,GWTM5A,GWTM6A,GWTM7A,
GWTM8A,GWTM9A,LCHVC1,LCHVC2
LCHVC4,LCHVC5,LCHZC1,LCHZC2,LCHZC3,L
CHZC6,LCHZC7,LCHZC8
LCHZC9,LPPWC3,LPPWC4,LPPWC5,LPPWC6,
LPPWC7,LPPWC8,LPPWC9
LTS2C1,LTS2C2,LTS2C3,LTS2C7,LTS2C8,
LTS2C9,LTS3C6,QCOL1,QCOL2
QCOL3,QCOL4,QCOL5,QCOL6,QCOL79,QSAT,
TUFLUX,VBW,VCHN1V,VCHN1Z
VPPW,VTSW2,VTSW3
The parameter is a function of the following parameters:
HFXSW,HPERC1,KSM

Parameter No. 54 of 287
Parameter ID : HPERC1
Description : Flux if infiltration exceeds ksm (half the time)
Save Time History : TRUE
The parameter is stochastic
The distribution is linear
Sampling bias : No Bias
Gamma : Mean = 2.46500E-03 S.D. = 2.46500E-03
The parameter affects the following parameters:
DTBL,FNS130,FNS230,FNS60,FNS613,
GWTIM1,GWTIM2,GWTIM3,GWTIM4
GWTIM5,GWTIM6,GWTIM7,GWTIM8,GWTIM9,
GWTM1A,GWTM2A,GWTM3
GWTM4A,GWTM5A,GWTM6A,GWTM7A,
GWTM8A,GWTM9A,HPERC,LCHVC1,
LCHVC,LCHVC4,LCHVC5,LCHZC1,LCHZC2,
LCHZC3,LCHZC6,LCHZC7,LCHZC8
LCHZC9,LPPWC3,LPPWC4,LPPWC5,LPPWC6,
LPPWC7,LPPWC8,LPPWC9
LTS2C1,LTS2C2,LTS2C3,LTS2C7,LTS2C8,
LTS2C9,LTS3C6,QCOL1,QCOL2
QCOL3,QCOL4,QCOL5,QCOL6,QCOL79,QSAT,
TUFLUX,VBW,VCHN1V,VCHN1Z
VPPW,VTSW2,VTSW3

Parameter No. 55 of 287
Parameter ID : IFRACT
Description : Check for Fracture flow

Save Time History : TRUE
The parameter is stochastic
The distribution is linear
Sampling bias : No Bias
Uniform : Umin = 0.00000E+00 Umax = 1.00000E+00
The parameter affects the following parameters:
RAMBW,RAMCHV,RAMCHZ,RAMPPW,
RAMTS2,RAMTS3,RCSBW,RCSCHV,RCSCHZ
RCSPPW,RCSTS2,RCSTS3,RNPBW,RNPCHV,
RNPCHZ,RNPPPW,RNPTS2,RNPTS
RPUBW,RPUCHV,RPUCHZ,RPUPPW,RPUTS2,
RPUTS3,RRABW,RRACHV,RRACHZ
RRAPPW,RRATS2,RRATS3,RUBW,RUCHV,
RUCHZ,RUPPW,RUTS2,RUTS3
RRAPPW,RRATS2,RRATS3,RUBW,RUCHV,
RUCHZ,RUPPW,RUTS2,RUTS3

Parameter No. 56 of 287
Parameter ID : KAMD
Description : DISTRIBUTION COEFFICIENT Am, DEVITRIFIED
Save Time History : TRUE
The parameter is stochastic
The distribution is linear
Sampling bias : No Bias
Uniform : Umin = 1.00000E+02 Umax = 2.00000E+03
The parameter affects the following parameters:
RAMBW,RAMPPW,RAMS,RAMTS2,RAMTS3,
TRAMBW,TRAPPW,TRATS2,TRATS3
RAMBW,RAMPPW,RAMS,RAMTS2,RAMTS3,T
RAMBW,TRAPPW,TRATS2,TRATS3

Parameter No. 57 of 287
Parameter ID : KAMV
Description : DISTRIBUTION COEFFICIENT Am, VITRIC
Save Time History : TRUE
The parameter is stochastic
The distribution is linear
Sampling bias : No Bias
Beta : Mean = 3.80000E+02 S.D. = 7.60000E+01 Min = 1.00000E+02 Max = 1.00000E+03
The parameter affects the following parameters:
RAMCHV,TRACHV

Parameter No. 58 of 287
Parameter ID : KAMZ
Description : DISTRIBUTION COEFFICIENT Am, ZEOLITIC
Save Time History : TRUE
The parameter is stochastic
The distribution is linear
Sampling bias : No Bias
Uniform : Umin = 1.00000E+02 Umax = 1.00000E+03
The parameter affects the following parameters:
RAMCHZ,TRACHZ

Parameter No. 59 of 287
Parameter ID : KCSD
Description : DISTRIBUTION COEFFICIENT Cs, DEVITRIFIED
Save Time History : TRUE
The parameter is stochastic
The distribution is linear
Sampling bias : No Bias
Uniform : Umin = 1.00000E+02 Umax = 2.00000E+02
The parameter affects the following parameters:

RCSBW,RCSPPW,RCSSAT,RCSTS2,RCSTS3, TRCPPW,TRCSBW,TRCTS2,TRCTS
RCSBW,RCSPPW,RCSSAT,RCSTS2,RCSTS3, TRCPPW,TRCSBW,TRCTS2,TRCTS

Parameter No. 60 of 287
Parameter ID : KCSV
Description : DISTRIBUTION COEFFICIENT Cs, VITRIC
Save Time History : TRUE
The parameter is stochastic
The distribution is linear
Sampling bias : No Bias
Uniform : Umin = 1.00000E+02 Umax = 2.00000E+02
The parameter affects the following parameters:
RCSCHV,TRCCHV

Parameter No. 61 of 287
Parameter ID : KCSZ
Description : DISTRIBUTION COEFFICIENT Cs, ZEOLITIC
Save Time History : TRUE
The parameter is stochastic
The distribution is linear
Sampling bias : No Bias
Uniform : Umin = 5.00000E+02 Umax = 3.00000E+03
The parameter affects the following parameters:
RCSCHZ,TRCCHZ

Parameter No. 62 of 287
Parameter ID : KNPD
Description : DISTRIBUTION COEFFICIENT Np, DEVITRIFIED
Save Time History : TRUE
The parameter is stochastic
The distribution is linear
Sampling bias : No Bias
Gamma : Mean = 2.00000E+00 S.D. = 2.00000E+00
The parameter affects the following parameters:
RNPBW,RNPPPW,RNPS,RNPTS2,RNPTS3, TRNPBW,TRNPPW,TRNTS2,TRNTS3
RNPBW,RNPPPW,RNPS,RNPTS2,RNPTS3, TRNPBW,TRNPPW,TRNTS2,TRNTS3

Parameter No. 63 of 287
Parameter ID : KNPV
Description : DISTRIBUTION COEFFICIENT Np, VITRIC
Save Time History : TRUE
The parameter is stochastic
The distribution is linear
Sampling bias : No Bias
Beta : Mean = 5.00000E-01 S.D. = 4.80300E-01 Min = 0.00000E+00 Max = 1.25000E+01
The parameter affects the following parameters:
RNPCHV,TRNCHV

Parameter No. 64 of 287
Parameter ID : KNPZ
Description : DISTRIBUTION COEFFICIENT Np, ZEOLITIC
Save Time History : TRUE
The parameter is stochastic
The distribution is linear
Sampling bias : No Bias
Beta : Mean = 4.00000E+00 S.D. = 3.84300E+00 Min = 0.00000E+00 Max = 1.00000E+02
The parameter affects the following parameters:
RNPCHZ,TRNCHZ

Parameter No. 65 of 287
Parameter ID : KPUD
Description : DISTRIBUTION COEFFICIENT Pu, DEVITRIFIED
Save Time History : TRUE
The parameter is stochastic
The distribution is linear
Sampling bias : No Bias
Beta : Mean = 1.00000E+02 S.D. = 2.50000E+01 Min = 5.00000E+01 Max = 2.00000E+02
The parameter affects the following parameters:
RPUBW,RPUPPW,RPUS,RPUTS2,RPUTS3, TRPPPW,TRPTS2,TRPTS3,TRPUBW
RPUBW,RPUPPW,RPUS,RPUTS2,RPUTS3, TRPPPW,TRPTS2,TRPTS3,TRPUBW

Parameter No. 66 of 287
Parameter ID : KPUV
Description : DISTRIBUTION COEFFICIENT Pu, VITRIC
Save Time History : TRUE
The parameter is stochastic
The distribution is linear
Sampling bias : No Bias
Beta : Mean = 1.00000E+02 S.D. = 2.50000E+01 Min = 5.00000E+01 Max = 2.00000E+02
The parameter affects the following parameters:
RPUCHV,TRPCHV

Parameter No. 67 of 287
Parameter ID : KPUZ
Description : DISTRIBUTION COEFFICIENT Pu, ZEOLITIC
Save Time History : TRUE
The parameter is stochastic
The distribution is linear
Sampling bias : No Bias
Beta : Mean = 4.00000E+01 S.D. = 6.00000E+00 Min = 3.00000E+01 Max = 7.00000E+01
The parameter affects the following parameters:
RPUCHZ,TRPCHZ

Parameter No. 68 of 287
Parameter ID : KRAD
Description : DISTRIBUTION COEFFICIENT Ra, DEVITRIFIED
Save Time History : TRUE
The parameter is stochastic
The distribution is linear
Sampling bias : No Bias
Uniform : Umin = 1.00000E+02 Umax = 5.00000E+02
The parameter affects the following parameters:
RRABW,RRAPPW,RRAS,RRATS2,RRATS3, TRRABW,TRRPPW,TRRTS2,TRRTS3
RRABW,RRAPPW,RRAS,RRATS2,RRATS3, TRRABW,TRRPPW,TRRTS2,TRRTS3

Parameter No. 69 of 287
Parameter ID : KRAV
Description : DISTRIBUTION COEFFICIENT Ra, VITRIC
Save Time History : TRUE
The parameter is stochastic
The distribution is linear
Sampling bias : No Bias
Uniform : Umin = 1.00000E+02 Umax = 5.00000E+02
The parameter affects the following parameters:
RRACHV,TRRCHV

Parameter No. 70 of 287
Parameter ID : KRAZ
Description : DISTRIBUTION COEFFICIENT Ra, ZEOLITIC
Save Time History : TRUE
The parameter is stochastic
The distribution is linear
Sampling bias : No Bias
Uniform : Umin = 1.00000E+03 Umax = 5.00000E+03
The parameter affects the following parameters:
RRACHZ,TRRCHZ

Parameter No. 71 of 287
Parameter ID : KSM
Description : Hydraulic Conductivity, TSW2

Save Time History : TRUE
The parameter is stochastic
The distribution is linear
Sampling bias : No Bias
CDF : Value = 0.00000E+00 Prob = 0.00000E+00
Value = 1.00000E-03 Prob = 6.00000E-01
Value = 2.00000E-03 Prob = 8.00000E-01
Value = 4.00000E-03 Prob = 8.50000E-01
Value = 6.00000E-03 Prob = 9.15000E-01
Value = 1.00000E-02 Prob = 9.60000E-01
Value = 1.20000E-02 Prob = 9.70000E-01
Value = 1.40000E-02 Prob = 9.75000E-01
Value = 2.00000E-02 Prob = 9.90000E-01
Value = 1.00000E-01 Prob = 1.00000E+00

The parameter affects the following parameters:
DTBL,FNS130,FNS230,FNS60,FNS613,
GWTIM1,GWTIM2,GWTIM3,GWTIM4
GWTIM5,GWTIM6,GWTIM7,GWTIM8,GWTIM9,
GWTM1A,GWTM2A,GWTM3A
GWTM4A,GWTM5A,GWTM6A,GWTM7A,
GWTM8A,GWTM9A,HPERC,LCHVC1,
LCHVC,LCHVC4,LCHVC5,LCHZC1,LCHZC2,
LCHZC3,LCHZC6,LCHZC7,LCHZC8
LCHZC9,LPPWC3,LPPWC4,LPPWC5,LPPWC6,
LPPWC7,LPPWC8,LPPWC9
LTS2C1,LTS2C2,LTS2C3,LTS2C7,LTS2C8,LTS
2C9,LTS3C6,QCOL1,QCOL2
QCOL3,QCOL4,QCOL5,QCOL6,QCOL79,QSAT,
TUFLUX,VBW,VCHN1V,VCHN1Z
VPPW,VTSW2,VTSW3

Parameter No. 72 of 287
Parameter ID : KUD
Description : DISTRIBUTION COEFFICIENT U, DEVITRIFIED
Save Time History : TRUE
The parameter is stochastic
The distribution is linear
Sampling bias : No Bias
Uniform : Umin = 0.00000E+00 Umax = 5.00000E+00
The parameter affects the following parameters:

RUBW,RUPPW,RUS,RUTS2,RUTS3,TRUBW,
TRUPPW,TRUTS2,TRUTS3

Parameter No. 73 of 287
Parameter ID : KUV
Description : DISTRIBUTION COEFFICIENT U, VITRIC
Save Time History : TRUE
The parameter is stochastic
The distribution is linear
Sampling bias : No Bias
Uniform : Umin = 0.00000E+00 Umax = 4.00000E+00
The parameter affects the following parameters:
RUCHV,TRUCHV

Parameter No. 74 of 287
Parameter ID : KUZ
Description : DISTRIBUTION COEFFICIENT U, ZEOLITIC
Save Time History : TRUE
The parameter is stochastic
The distribution is linear
Sampling bias : No Bias
Uniform : Umin = 5.00000E+00 Umax = 2.00000E+01
The parameter affects the following parameters:
RUCHZ,TRUCHZ

Parameter No. 75 of 287
Parameter ID : LBWC4
Description : length of bullfrog column 4

Save Time History : TRUE
The parameter is a constant: 4.00000E+00

Parameter No. 76 of 287
Parameter ID : LBWC5
Description : Length of Bullfrog Column 5

Save Time History : TRUE
The parameter is a constant: 3.60000E+01

Parameter No. 77 of 287
Parameter ID : LCHVC1
Description : length of chv-c1 pathway, depends on w tbl 130
Save Time History : TRUE
The Parameter is a function, exp. value = 34
Equation : if(dtbl==130,1,34)

The parameter affects the following parameters:
GWTIM1,GWTM1A
The parameter is a function of the following parameters:
DRYINF,DTBL,DTBL1,DTBL2,FM,HFXSW,
HPERC,HPERC1,KSM,TIME,TUFLUX,
UBFLUX

Parameter No. 78 of 287
Parameter ID : LCHVC2
Description : length of chv-c2 pathway, depends on w tbl 130
Save Time History : TRUE
The Parameter is a function, exp. value = 32
Equation : if(dtbl==130,4,32)

The parameter affects the following parameters:
GWTIM2,GWTM2A
The parameter is a function of the following parameters:
DRYINF,DTBL,DTBL1,DTBL2,FM,HFXSW,
HPERC,HPERC1,KSM,TIME,TUFLUX
UBFLUX

Parameter No. 79 of 287
Parameter ID : LCHVC3
Description : length of chv-c3
Save Time History : TRUE
The parameter is a constant: 3.50000E+01
The parameter affects the following parameters:
GWTIM3,GWTM3A

Parameter No. 80 of 287
Parameter ID : LCHVC4
Description : length of chv-c4 pathway, depends on w tbl 230
Save Time History : TRUE
The Parameter is a function, exp. value = 40
Equation : if(dtbl==230,5,40)

The parameter affects the following parameters:
GWTIM4,GWTM4A
The parameter is a function of the following parameters:
DRYINF,DTBL,DTBL1,DTBL2,FM,HFXSW,
HPERC,HPERC1,KSM,TIME,TUFLU
UBFLUX

Parameter No. 81 of 287
Parameter ID : LCHVC5
Description : length of chv-c5 pathway, depends on w tbl 230
Save Time History : TRUE
The Parameter is a function, exp. value = 38
Equation : if(dtbl==230,36,38)

The parameter affects the following parameters:
GWTIM5,GWTM5A
The parameter is a function of the following parameters:
DRYINF,DTBL,DTBL1,DTBL2,FM,HFXSW,
HPERC,HPERC1,KSM,TIME,TUFLUX,UBFLUX

Parameter No. 82 of 287
Parameter ID : LCHVC6
Description : length of chv-c6

Save Time History : TRUE
The parameter is a constant: 3.20000E+01
The parameter affects the following parameters:
GWTIM6,GWTM6A

Parameter No. 83 of 287
Parameter ID : LCHVC7
Description : length of chv-c7

Save Time History : TRUE
The parameter is a constant: 3.00000E+01
The parameter affects the following parameters:
GWTIM7,GWTM7A

Parameter No. 84 of 287
Parameter ID : LCHVC8
Description : length of chv-c8

Save Time History : TRUE
The parameter is a constant: 3.10000E+01
The parameter affects the following parameters:
GWTIM8,GWTM8A

Parameter No. 85 of 287
Parameter ID : LCHVC9
Description : length of chv-c9

Save Time History : TRUE
The parameter is a constant: 3.30000E+01
The parameter affects the following parameters:
GWTIM9,GWTM9A

Parameter No. 86 of 287
Parameter ID : LCHZC1
Description : length of chn1z-c1 pathway, depends on w tbl 60
Save Time History : TRUE
The Parameter is a function, exp. value = 69
Equation : if(dtbl==60,37,69)

The parameter affects the following parameters:
GWTIM1,GWTM1A
The parameter is a function of the following parameters:
DRYINF,DTBL,DTBL1,DTBL2,FM,HFXSW, HPERC,HPERC1,KSM,TIME,TUFLUX,UBFLUX

Parameter No. 87 of 287
Parameter ID : LCHZC2
Description : length of chn1z-c2 pathway, depends on w tbl 60
Save Time History : TRUE
The Parameter is a function, exp. value = 77
Equation : if(dtbl==60,42,77)

The parameter affects the following parameters:
GWTIM2,GWTM2A
The parameter is a function of the following parameters:
DRYINF,DTBL,DTBL1,DTBL2,FM,HFXSW, HPERC,HPERC1,KSM,TIME,TUFLU,UBFLUX

Parameter No. 88 of 287
Parameter ID : LCHZC3
Description : length of chz-c3 pathway, depends on w tbl 130
Save Time History : TRUE
The Parameter is a function, exp. value = 74
Equation : if(dtbl==130,17,74)

The parameter affects the following parameters:
GWTIM3,GWTM3A
The parameter is a function of the following parameters:
DRYINF,DTBL,DTBL1,DTBL2,FM,HFXSW, HPERC,HPERC1,KSM,TIME,TUFLUX,UBFLUX

Parameter No. 89 of 287
Parameter ID : LCHZC4
Description : length of chz-c4

Save Time History : TRUE
The parameter is a constant: 6.20000E+01
The parameter affects the following parameters:
GWTIM4,GWTM4A

Parameter No. 90 of 287
Parameter ID : LCHZC5
Description : length of chz-c5

Save Time History : TRUE
The parameter is a constant: 6.20000E+01
The parameter affects the following parameters:
GWTIM5,GWTM5A

Parameter No. 91 of 287
Parameter ID : LCHZC6
Description : length of chz-c6 pathway, depends on w tbl 130
Save Time History : TRUE
The Parameter is a function, exp. value = 75
Equation : if(dtbl==130,64,75)

The parameter affects the following parameters:
GWTIM6,GWTM6A
The parameter is a function of the following parameters:
DRYINF,DTBL,DTBL1,DTBL2,FM,HFXSW, HPERC,HPERC1,KSM,TIME,TUFLUX,UBFLUX

Parameter No. 92 of 287
Parameter ID : LCHZC7
Description : length of chz-c7 pathway, depends on w tbl 130
Save Time History : TRUE
The Parameter is a function, exp. value = 78
Equation : if(dtbl==130,19,78)

The parameter affects the following parameters:
GWTIM7,GWTM7A
The parameter is a function of the following parameters:
DRYINF,DTBL,DTBL1,DTBL2,FM,HFXSW, HPERC,HPERC1,KSM,TIME,TUFLUX,UBFLUX

Parameter No. 93 of 287
Parameter ID : LCHZC8
Description : length of chz-c8 pathway, depends on w tbl 130
Save Time History : TRUE
The Parameter is a function, exp. value = 69
Equation : if(dtbl==130,13,69)

The parameter affects the following parameters:
GWTIM8,GWTM8A
The parameter is a function of the following parameters:
DRYINF,DTBL,DTBL1,DTBL2,FM,HFXSW, HPERC,HPERC1,KSM,TIME,TUFLUX,UBFLUX

Parameter No. 94 of 287
Parameter ID : LCHZC9
Description : length of chz-c9 pathway, depends on w tbl 130
Save Time History : TRUE
The Parameter is a function, exp. value = 60
Equation : if(dtbl==130,7,60)

The parameter affects the following parameters:
GWTIM9,GWTM9A
The parameter is a function of the following parameters:
DRYINF,DTBL,DTBL1,DTBL2,FM,HFXSW,
HPERC,HPERC1,KSM,TIME,TUFLUX,UBFLUX

Parameter No. 95 of 287
Parameter ID : LENG
Description : Length of Wastepackage

Save Time History : TRUE
The parameter is a constant: 4.60000E+00
The parameter affects the following parameters:
EQRAD,OMEGA,TOMEGA,VOL

Parameter No. 96 of 287
Parameter ID : LPPWC1
Description : length of ppw-c1

Save Time History : TRUE
The parameter is a constant: 2.80000E+01
The parameter affects the following parameters:
GWTIM1,GWTM1A

Parameter No. 97 of 287
Parameter ID : LPPWC2
Description : length of ppw-c2

Save Time History : TRUE
The parameter is a constant: 2.50000E+01
The parameter affects the following parameters:
GWTIM2,GWTM2A

Parameter No. 98 of 287
Parameter ID : LPPWC3
Description : length of ppw-c3 pathway, depends on w tbl 60
Save Time History : TRUE
The Parameter is a function, exp. value = 73
Equation : if(dtbl==60,13,73)
The parameter affects the following parameters:
GWTIM3,GWTM3A
The parameter is a function of the following parameters:
DRYINF,DTBL,DTBL1,DTBL2,FM,HFXSW,
HPERC,HPERC1,KSM,TIME,TUFLUX,UBFLUX

Parameter No. 99 of 287
Parameter ID : LPPWC4
Description : length of ppw-c4 pathway, depends on w tbl 60 and 130
Save Time History : TRUE
The Parameter is a function, exp. value = 130
Equation : if(dtbl==60,73,(if(dtbl==130,3,130))

The parameter affects the following parameters:
GWTIM4,GWTM4A
The parameter is a function of the following parameters:
DRYINF,DTBL,DTBL1,DTBL2,FM,HFXSW,
HPERC,HPERC1,KSM,TIME,TUFLUX,UBFLUX

Parameter No. 100 of 287
Parameter ID : LPPWC5
Description : length of ppw-c5 pathway, depends on w tbl 60 and 130
Save Time History : TRUE
The Parameter is a function, exp. value = 130
Equation : if(dtbl==60,106,(if(dtbl==130,36,130))

The parameter affects the following parameters:
GWTIM5,GWTM5A
The parameter is a function of the following parameters:
DRYINF,DTBL,DTBL1,DTBL2,FM,HFXSW,
HPERC,HPERC1,KSM,TIME,TUFLUX,UBFLUX

Parameter No. 101 of 287
Parameter ID : LPPWC6
Description : length of ppw-c6 pathway, depends on w tbl 60
Save Time History : TRUE
The Parameter is a function, exp. value = 119
Equation : if(dtbl==60,59,119)

The parameter affects the following parameters:
GWTIM6,GWTM6A
The parameter is a function of the following parameters:
DRYINF,DTBL,DTBL1,DTBL2,FM,HFXSW,
HPERC,HPERC1,KSM,TIME,TUFLUX,UBFLUX

Parameter No. 102 of 287
Parameter ID : LPPWC7
Description : length of ppw-c7 pathway, depends on w tbl 60
Save Time History : TRUE
The Parameter is a function, exp. value = 71
Equation : if(dtbl==60,11,71)

The parameter affects the following parameters:
GWTIM7,GWTM7A
The parameter is a function of the following parameters:
DRYINF,DTBL,DTBL1,DTBL2,FM,HFXSW,
HPERC,HPERC1,KSM,TIME,TUFLUX,UBFLUX

Parameter No. 103 of 287
Parameter ID : LPPWC8
Description : length of ppw-c8 pathway, depends on w tbl 60
Save Time History : TRUE
The Parameter is a function, exp. value = 74
Equation : if(dtbl==60,14,74)

The parameter affects the following parameters:
GWTIM8,GWTM8A
The parameter is a function of the following parameters:
DRYINF,DTBL,DTBL1,DTBL2,FM,HFXSW,
HPERC,HPERC1,KSM,TIME,TUFLUX,UBFLUX

Parameter No. 104 of 287
Parameter ID : LPPWC9
Description : length of ppw-c9 pathway, depends on w tbl 60
Save Time History : TRUE
The Parameter is a function, exp. value = 77
Equation : if(dtbl==60,17,77)

The parameter affects the following parameters:
GWTIM9,GWTM9A
The parameter is a function of the following parameters:
DRYINF,DTBL,DTBL1,DTBL2,FM,HFXSW,
HPERC,HPERC1,KSM,TIME,TUFLUX,UBFLUX

Parameter No. 105 of 287
Parameter ID : LSAT
Description : length of saturated zone

Save Time History : TRUE
The parameter is a constant: 5.00000E+03
The parameter affects the following parameters:

GWTIM1,GWTIM2,GWTIM3,GWTIM4,GWTIM5,
GWTIM6,GWTIM7,GWTIM8
GWTIM9,GWTM1A,GWTM2A,GWTM3A,
GWTM4A,GWTM5A,GWTM6A,GWTM7A
GWTM8A,GWTM9A

Parameter No. 106 of 287
Parameter ID : LTS2C1
Description : length of ts2-c1 pathway, depends on w tbl 230
Save Time History : TRUE
The Parameter is a function, exp. value = 131
Equation : if(dtbl==230,42,131)

The parameter affects the following parameters:
GWTIM1
The parameter is a function of the following parameters:
DRYINF,DTBL,DTBL1,DTBL2,FM,HFXSW,
HPERC,HPERC1,KSM,TIME,TUFLUX,UBFLUX

Parameter No. 107 of 287
Parameter ID : LTS2C2
Description : length of ts2-c2 pathway, depends on w tbl 230
Save Time History : TRUE
The Parameter is a function, exp. value = 133
Equation : if(dtbl==230,57,133)

The parameter affects the following parameters:
GWTIM2
The parameter is a function of the following parameters:
DRYINF,DTBL,DTBL1,DTBL2,FM,HFXSW,
HPERC,HPERC1,KSM,TIME,TUFLUX,UBFLUX

Parameter No. 108 of 287
Parameter ID : LTS2C3
Description : length of ts2-c3 pathway, depends on w tbl 230
Save Time History : TRUE
The Parameter is a function, exp. value = 109
Equation : if(dtbl==230,71,109)

The parameter affects the following parameters:
GWTIM3
The parameter is a function of the following parameters:
DRYINF,DTBL,DTBL1,DTBL2,FM,HFXSW,
HPERC,HPERC1,KSM,TIME,TUFLUX,UBFLUX

Parameter No. 109 of 287
Parameter ID : LTS2C4
Description : length of ts2-c4 pathway

Save Time History : TRUE
The parameter is a constant: 7.50000E+01
The parameter affects the following parameters:
GWTIM4

Parameter No. 110 of 287
Parameter ID : LTS2C5
Description : length of ts2-c5 pathway

Save Time History : TRUE
The parameter is a constant: 4.50000E+01
The parameter affects the following parameters:
GWTIM5

Parameter No. 111 of 287
Parameter ID : LTS2C6
Description : length of ts2-c6 pathway

Save Time History : TRUE
The parameter is a constant: 6.80000E+01
The parameter affects the following parameters:
GWTIM6

Parameter No. 112 of 287
Parameter ID : LTS2C7
Description : length of ts2-c7 pathway, depends on w tbl 230
Save Time History : TRUE
The Parameter is a function, exp. value = 100
Equation : if(dtbl==230,59,100)

The parameter affects the following parameters:
GWTIM7
The parameter is a function of the following parameters:
DRYINF,DTBL,DTBL1,DTBL2,FM,HFXSW,
HPERC,HPERC1,KSM,TIME,TUFLUX,UBFLUX

Parameter No. 113 of 287
Parameter ID : LTS2C8
Description : length of ts2-c8 pathway, depends on w tbl 230
Save Time History : TRUE
The Parameter is a function, exp. value = 89
Equation : if(dtbl==230,43,89)
The parameter affects the following parameters:
GWTIM8
The parameter is a function of the following parameters:
DRYINF,DTBL,DTBL1,DTBL2,FM,HFXSW,
HPERC,HPERC1,KSM,TIME,TUFLUX,UBFLUX

Parameter No. 114 of 287
Parameter ID : LTS2C9
Description : length of ts2-c9 pathway, depends on w tbl 230
Save Time History : TRUE
The Parameter is a function, exp. value = 78
Equation : if(dtbl==230,28,78)

The parameter affects the following parameters:
GWTIM9
The parameter is a function of the following parameters:
DRYINF,DTBL,DTBL1,DTBL2,FM,HFXSW,
HPERC,HPERC1,KSM,TIME,TUFLUX,UBFLUX

Parameter No. 115 of 287
Parameter ID : LTS3
Description : length of topopah spring 3 pathway (all except column 6)
Save Time History : TRUE
The parameter is a constant: 1.00000E+01
The parameter affects the following parameters:

GWTIM1,GWTIM2,GWTIM3,GWTIM4,GWTIM5,
GWTIM6,GWTIM7,GWTIM8,GWTIM9

Parameter No. 116 of 287
Parameter ID : LTS3C6
Description : length of ts3-c6 pathway, depends on w tbl 230
Save Time History : TRUE
The Parameter is a function, exp. value = 10
Equation : if(dtbl==230,6,10)

The parameter is a function of the following parameters:
DRYINF,DTBL,DTBL1,DTBL2,FM,HFXSW,
HPERC,HPERC1,KSM,TIME,TUFLUX,UBFLUX

Parameter No. 117 of 287
Parameter ID : MALT
Description : MATRIX ALTERATION RATE

Save Time History : TRUE

See Chapter 4 for LWR SF and DHLW functions. This parameter is a sthochastic for pyroprocess wasteforms from values given in Chapter 5. Cumulative probability density function utilized. 0.0 -- 0.0, 0.25 -- low, 0.75 -- moderate, 1.00 -- high

Parameter No. 118 of 287
Parameter ID : MASS
Description : Mass of Matrix for fractional alteration calculation
Save Time History : TRUE
The parameter is a constant: 9.74000E+06 for LWR MMB [14] 2.10000E+06 for LWR SCP [14] 6.40000E+06 for ER-Metallic [37] 1.72500E+06 for ER-Mineral [37] 1.47000E+06 for DHLW [1]
The parameter affects the following parameters:
ESURF

Parameter No. 119 of 287
Parameter ID : MEANC
Description : MEAN CARBONATE CONCENTRATION only for LWR SF

Save Time History : TRUE
The parameter is stochastic
The distribution is linear
Sampling bias : No Bias
Uniform : Umin = 2.00000E-03 Umax = 2.00000E-02
The parameter affects the following parameters:
MALT

Parameter No. 120 of 287
Parameter ID : MEANPH only for LWR SF
Description : pH OF NEAR FIELD GROUND WATER
Save Time History : TRUE
The parameter is stochastic
The distribution is linear
Sampling bias : No Bias
Uniform : Umin = 6.00000E+00 Umax = 9.00000E+00
The parameter affects the following parameters:
MALT,SLAM,SLNP,SLPU,SLU

Parameter No. 121 of 287
Parameter ID : OMEGA
Description : GEOMETRIC FACTOR FOR DIFFUSION
Save Time History : TRUE
The Parameter is a function, exp. value = 3.52572
Equation : 4*PI*WPOR*FGEOMD*eqrad

The parameter affects the following parameters:
TOMEGA
The parameter is a function of the following parameters:
EQRAD,FGEOMD,LENG,PI,R0,STSW2,VOL, WPOR

Parameter No. 122 of 287
Parameter ID : PBW
Description : POROSITY OF BULLFROG

Save Time History : TRUE
The parameter is stochastic
The distribution is linear
Sampling bias : No Bias
Beta : Mean = 2.40000E-01 S.D. = 4.80000E-02 Min = 0.00000E+00 Max = 1.00000E+00
The parameter affects the following parameters:
RAMBW,RAMS,RCSBW,RCSSAT,RNPBW, RNPS,RPUBW,RPUS,RRABW,RRA RUBW,RUS,TRAMBW,TRCSBW,TRNPBW, TRPUBW,TRRABW,TRUBW,VBW

Parameter No. 123 of 287
Parameter ID : PCHN1V
Description : POROSITY OF CALICO HILLS VITRIC
Save Time History : TRUE
The parameter is stochastic
The distribution is linear
Sampling bias : No Bias
Beta : Mean = 2.10000E-01 S.D. = 4.20000E-02 Min = 0.00000E+00 Max = 1.00000E+00
The parameter affects the following parameters:

GWTIM1,GWTIM2,GWTIM3,GWTIM4,GWTIM5, GWTIM6,GWTIM7,GWTIM8
GWTIM9,GWTM1A,GWTM2A,GWTM3A, GWTM4A,GWTM5A,GWTM6A,GWTM7A GWTM8A,GWTM9A,RAMCHV,RCSCHV, RNPCHV,RPUCHV,RRACHV,RUCHV,TRACH TRCCHV,TRNCHV,TRPCHV,TRRCHV,TRUCHV VCHN1V

Parameter No. 124 of 287
Parameter ID : PCHN1Z
Description : POROSITY OF CALICO HILLS ZEOLITIC
Save Time History : TRUE
The parameter is stochastic
The distribution is linear
Sampling bias : No Bias
Beta : Mean = 4.10000E-01 S.D. = 8.20000E-02 Min = 0.00000E+00 Max = 1.00000E+00
The parameter affects the following parameters:

GWTIM1,GWTIM2,GWTIM3,GWTIM4,GWTIM5,
GWTIM6,GWTIM7,GWTIM8
GWTIM9,GWTM1A,GWTM2A,GWTM3A,
GWTM4A,GWTM5A,GWTM6A,GWTM7A
GWTM8A,GWTM9A,RAMCHZ,RCSCHZ,
RNPCHZ,RPUCHZ,RRACHZ,RUCHZ,TRACH
TRCCHZ,TRNCHZ,TRPCHZ,TRRCHZ,TRUCHZ,
VCHN1Z

Parameter No. 125 of 287
Parameter ID : PI
Description : The value of PI
Save Time History : TRUE
The parameter is a constant: 3.14159E+00
The parameter affects the following parameters:
EQRAD,OMEGA,TOMEGA,VOL

Parameter No. 126 of 287
Parameter ID : PPPW
Description : POROSITY OF PROW PASS

Save Time History : TRUE
The parameter is stochastic
The distribution is linear
Sampling bias : No Bias
Beta : Mean = 2.40000E-01 S.D. = 4.80000E-02 Min = 0.00000E+00 Max = 1.00000E+00
The parameter affects the following parameters:

GWTIM1,GWTIM2,GWTIM3,GWTIM4,GWTIM5,
GWTIM6,GWTIM7,GWTIM8
GWTIM9,GWTM1A,GWTM2A,GWTM3A,
GWTM4A,GWTM5A,GWTM6A,GWTM7A
GWTM8A,GWTM9A,RAMPPW,RCSPPW,
RNPPPW,RPUPPW,RRAPPW,RUPPW,
TRAPPW,TRCPPW,TRNPPW,TRPPPW,
TRRPPW,TRUPPW,VPPW

Parameter No. 127 of 287
Parameter ID : PSAT
Description : POROSITY OF SATURATED ZONE
Save Time History : TRUE
The parameter is a constant: 2.00000E-02
The parameter affects the following parameters:

GWTIM1,GWTIM2,GWTIM3,GWTIM4,GWTIM5,
GWTIM6,GWTIM7,GWTIM8
GWTIM9,GWTM1A,GWTM2A,GWTM3A,
GWTM4A,GWTM5A,GWTM6A,GWTM7A
GWTM8A,GWTM9A,VSAT

Parameter No. 128 of 287
Parameter ID : PTSW2
Description : POROSITY OF TOPOPAH SPRING 2
Save Time History : TRUE
The parameter is stochastic
The distribution is linear
Sampling bias : No Bias
Beta : Mean = 1.10000E-01 S.D. = 2.20000E-02 Min = 4.40000E-02 Max = 1.97000E-01
The parameter affects the following parameters:

GWTIM1,GWTIM2,GWTIM3,GWTIM4,GWTIM5,
GWTIM6,GWTIM7,GWTIM8
GWTIM9,RAMTS2,RCSTS2,RNPTS2,RPUTS2,
RRATS2,RUTS2,TRATS2,TRCTS
TRNTS2,TRPTS2,TRRTS2,TRUTS2,VTSW2

Parameter No. 129 of 287
Parameter ID : PTSW3
Description : POROSITY OF TOPOPAH SPRING 3
Save Time History : TRUE
The parameter is stochastic
The distribution is linear
Sampling bias : No Bias
Beta : Mean = 9.00000E-02 S.D. = 1.80000E-02 Min = 3.70000E-02 Max = 1.61000E-01
The parameter affects the following parameters:

GWTIM1,GWTIM2,GWTIM3,GWTIM4,GWTIM5,
GWTIM6,GWTIM7,GWTIM8
GWTIM9,RAMTS3,RCSTS3,RNPTS3,RPUTS3,
RRATS3,RUTS3,TRATS3,TRCTS
TRNTS3,TRPTS3,TRRTS3,TRUTS3,VTSW3

Parameter No. 130 of 287
Parameter ID : QCOL1
Description : VOLUMETRIC FLOW RATE, COLUMN 1
Save Time History : TRUE
The Parameter is a function, exp. value = 199.446
Equation : TUFLUX*ACOL1

The parameter affects the following parameters:
QSAT
The parameter is a function of the following parameters:

ACOL1,DRYINF,FM,HFXSW,HPERC,HPERC1, KSM,TIME,TUFLUX,UBFLUX
ACOL1,DRYINF,FM,HFXSW,HPERC,HPERC1, KSM,TIME,TUFLUX,UBFLUX

Parameter No. 131 of 287
Parameter ID : QCOL2
Description : VOLUMETRIC FLOW RATE, COLUMN 2
Save Time History : TRUE
The Parameter is a function, exp. value = 206.8365
Equation : TUFLUX*ACOL2

The parameter affects the following parameters:
QSAT
The parameter is a function of the following parameters:

ACOL2,DRYINF,FM,HFXSW,HPERC,HPERC1 ,KSM,TIME,TUFLUX,UBFLUX

Parameter No. 132 of 287
Parameter ID : QCOL3
Description : VOLUMETRIC FLOW RATE, COLUMN 3
Save Time History : TRUE
The Parameter is a function, exp. value = 192.062
Equation : TUFLUX*ACOL3

The parameter affects the following parameters:
QSAT
The parameter is a function of the following parameters:

ACOL3,DRYINF,FM,HFXSW,HPERC,HPERC1, KSM,TIME,TUFLUX,UBFLUX

Parameter No. 133 of 287
Parameter ID : QCOL4
Description : VOLUMETRIC FLOW RATE, COLUMN 4
Save Time History : TRUE
The Parameter is a function, exp. value = 158.8205
Equation : TUFLUX*ACOL4

The parameter affects the following parameters:
QSAT
The parameter is a function of the following parameters:

ACOL4,DRYINF,FM,HFXSW,HPERC,HPERC1 ,KSM,TIME,TUFLUX,UBFLUX

Parameter No. 134 of 287
Parameter ID : QCOL5
Description : VOLUMETRIC FLOW RATE, COLUMN 5
Save Time History : TRUE
The Parameter is a function, exp. value = 188.3685
Equation : TUFLUX*ACOL5

The parameter affects the following parameters:
QSAT
The parameter is a function of the following parameters:

ACOL5,DRYINF,FM,HFXSW,HPERC,HPERC1, KSM,TIME,TUFLUX,UBFLUX

Parameter No. 135 of 287
Parameter ID : QCOL6
Description : VOLUMETRIC FLOW RATE, COLUMN 6
Save Time History : TRUE
The Parameter is a function, exp. value = 225.3
Equation : TUFLUX*ACOL6

The parameter affects the following parameters:
QSAT
The parameter is a function of the following parameters:

ACOL6,DRYINF,FM,HFXSW,HPERC,HPERC1, KSM,TIME,TUFLUX,UBFLUX

Parameter No. 136 of 287
Parameter ID : QCOL79
Description : VOLUMETRIC FLOW RATE, COLUMNS 7-9
Save Time History : TRUE
The Parameter is a function, exp. value = 251.158
Equation : TUFLUX*ACOL79

The parameter affects the following parameters:
QSAT
The parameter is a function of the following parameters:
ACOL79,DRYINF,FM,HFXSW,HPERC,HPERC1, KSM,TIME,TUFLUX,UBFLUX

Parameter No. 137 of 287
Parameter ID : QSAT
Description : VOLUMETRIC FLOW RATE, SATURATED ZONE
Save Time History : TRUE
The Parameter is a function, exp. value = 1924.308
Equation : QCOL1+QCOL2+QCOL3+QCOL4+QCOL5+QCOL6+3*QCOL79
The parameter is a function of the following parameters:
ACOL1,ACOL2,ACOL3,ACOL4,ACOL5,ACOL6, ACOL79,DRYINF,FM,HFXSW HPERC,HPERC1,KSM,QCOL1,QCOL2,QCOL3, QCOL4,QCOL5,QCOL6,QCOL79 TIME,TUFLUX,UBFLUX

Parameter No. 138 of 287
Parameter ID : R0
Description : radius of waste package

Save Time History : TRUE
The parameter is a constant: 8.95000E-01 MMB, 3.30000E-01 for SCP
The parameter affects the following parameters:
EQRAD,OMEGA,TOMEGA,VOL

Parameter No. 139 of 287
Parameter ID : RAMBW
Description : RETARDATION OF Am, BULLFROG
Save Time History : TRUE
The Parameter is a function, exp. value = 8751
Equation : if(ifract<=0.2,1,trambw)

The parameter is a function of the following parameters:
DBW,IFRACT,KAMD,PBW,TRAMBW

Parameter No. 140 of 287
Parameter ID : RAMCHV
Description : RETARDATION OF Am, CALICO HILLS VITRIC
Save Time History : TRUE
The Parameter is a function, exp. value = 3041
Equation : if(ifract<=0.2,1,trachv)

The parameter is a function of the following parameters:
DCHN1V,IFRACT,KAMV,PCHN1V,TRACHV

Parameter No. 141 of 287
Parameter ID : RAMCHZ
Description : RETARDATION OF Am, CALICO HILLS ZEOLITIC
Save Time History : TRUE
The Parameter is a function, exp. value = 2254.658
Equation : if(ifract<=0.2,1,trachz)

The parameter is a function of the following parameters:
DCHN1Z,IFRACT,KAMZ,PCHN1Z,TRACHZ

Parameter No. 142 of 287
Parameter ID : RAMPPW
Description : RETARDATION OF Am, PROW PASS
Save Time History : TRUE
The Parameter is a function, exp. value = 8751
Equation : if(ifract<=0.2,1,trappw)

The parameter is a function of the following parameters:
DPPW,IFRACT,KAMD,PPPW,TRAPPW

Parameter No. 143 of 287
Parameter ID : RAMS
Description : RETARDATION OF Am, Saturated

Save Time History : TRUE
The Parameter is a function, exp. value = 8751
Equation : 1+DBW/PBW*KAMD

The parameter is a function of the following parameters:
DBW,KAMD,PBW

Parameter No. 144 of 287
Parameter ID : RAMTS2
Description : RETARDATION OF Am, TOPOPAH SPRING 2
Save Time History : TRUE
The Parameter is a function, exp. value = 21382.82
Equation : if(ifract<=0.2,1,trats2)

The parameter is a function of the following parameters:
DTSW2,IFRACT,KAMD,PTSW2,TRATS2

Parameter No. 145 of 287
Parameter ID : RAMTS3
Description : RETARDATION OF Am, TOPOPAH SPRING 3
Save Time History : TRUE
The Parameter is a function, exp. value = 25084.33
Equation : if(ifract<=0.2,1,trats3)

The parameter is a function of the following parameters:
DTSW3,IFRACT,KAMD,PTSW3,TRATS3

Parameter No. 146 of 287
Parameter ID : RCSBW
Description : RETARDATION OF Cs, BULLFROG
Save Time History : TRUE
The Parameter is a function, exp. value = 1251
Equation : if(ifract<=0.2,1,trcsbw)

The parameter is a function of the following parameters:
DBW,IFRACT,KCSD,PBW,TRCSBW

Parameter No. 147 of 287
Parameter ID : RCSCHV
Description : RETARDATION OF Cs, CALICO HILLS VITRIC
Save Time History : TRUE
The Parameter is a function, exp. value = 1201
Equation : if(ifract<=0.2,1,trcchv)

The parameter is a function of the following parameters:
DCHN1V,IFRACT,KCSV,PCHN1V,TRCCHV

Parameter No. 148 of 287
Parameter ID : RCSCHZ
Description : RETARDATION OF Cs, CALICO HILLS ZEOLITIC
Save Time History : TRUE
The Parameter is a function, exp. value = 7171.731
Equation : if(ifract<=0.2,1,trcchz)

The parameter is a function of the following parameters:
DCHN1Z,IFRACT,KCSZ,PCHN1Z,TRCCHZ

Parameter No. 149 of 287
Parameter ID : RCSPPW
Description : RETARDATION OF Cs, PROW PASS
Save Time History : TRUE
The Parameter is a function, exp. value = 1251
Equation : if(ifract<=0.2,1,trcppw)

The parameter is a function of the following parameters:
DPPW,IFRACT,KCSD,PPPW,TRCPPW

Parameter No. 150 of 287
Parameter ID : RCSSAT
Description : RETARDATION OF Cs, Saturated

Save Time History : TRUE
The Parameter is a function, exp. value = 1251
Equation : 1+dbw*kcsd/pbw

The parameter is a function of the following parameters:
DBW,KCSD,PBW

Parameter No. 151 of 287
Parameter ID : RCSTS2
Description : RETARDATION OF Cs, TOPOPAH SPRING 2
Save Time History : TRUE
The Parameter is a function, exp. value = 3055.545
Equation : if(ifract<=0.2,1,trcts2)

The parameter is a function of the following parameters:
DTSW2,IFRACT,KCSD,PTSW2,TRCTS2

Parameter No. 152 of 287
Parameter ID : RCSTS3
Description : RETARDATION OF Cs, TOPOPAH SPRING 3
Save Time History : TRUE
The Parameter is a function, exp. value = 3584.333
Equation : if(ifract<=0.2,1,trcts3)

The parameter is a function of the following parameters:
DTSW3,IFRACT,KCSD,PTSW3,TRCTS3

Parameter No. 153 of 287
Parameter ID : RNPBW
Description : RETARDATION OF Np, BULLFROG
Save Time History : TRUE
The Parameter is a function, exp. value = 17.66667
Equation : if(ifract<=0.2,1,trnpbw)

The parameter is a function of the following parameters:
DBW,IFRACT,KNPD,PBW,TRNPBW

Parameter No. 154 of 287
Parameter ID : RNPCHV
Description : RETARDATION OF Np, CALICO HILLS VITRIC
Save Time History : TRUE
The Parameter is a function, exp. value = 5
Equation : if(ifract<=0.2,1,trnchv)

The parameter is a function of the following parameters:
DCHN1V,IFRACT,KNPV,PCHN1V,TRNCHV

Parameter No. 155 of 287
Parameter ID : RNPCHZ
Description : RETARDATION OF Np, CALICO HILLS ZEOLITIC
Save Time History : TRUE
The Parameter is a function, exp. value = 17.39024
Equation : if(ifract<=0.2,1,trnchz)

The parameter is a function of the following parameters:
DCHN1Z,IFRACT,KNPZ,PCHN1Z,TRNCHZ

Parameter No. 156 of 287
Parameter ID : RNPPPW
Description : RETARDATION OF Np, PROW PASS
Save Time History : TRUE
The Parameter is a function, exp. value = 17.66667
Equation : if(ifract<=0.2,1,trnppw)

The parameter is a function of the following parameters:
DPPW,IFRACT,KNPD,PPPW,TRNPPW

Parameter No. 157 of 287
Parameter ID : RNPS
Description : RETARDATION OF Np, Saturated

Save Time History : TRUE
The Parameter is a function, exp. value = 17.66667
Equation : 1+DBW/PBW*KNPD

The parameter is a function of the following parameters:
DBW,KNPD,PBW

Parameter No. 158 of 287
Parameter ID : RNPTS2
Description : RETARDATION OF Np, TOPOPAH SPRING 2
Save Time History : TRUE
The Parameter is a function, exp. value = 41.72727
Equation : if(ifract<=0.2,1,trnts2)

The parameter is a function of the following parameters:
DTSW2,IFRACT,KNPD,PTSW2,TRNTS2

Parameter No. 159 of 287
Parameter ID : RNPTS3
Description : RETARDATION OF Np, TOPOPAH SPRING 3
Save Time History : TRUE
The Parameter is a function, exp. value = 48.77778
Equation : if(ifract<=0.2,1,trnts3)

The parameter is a function of the following parameters:
DTSW3,IFRACT,KNPD,PTSW3,TRNTS3

Parameter No. 160 of 287
Parameter ID : RPUBW
Description : RETARDATION OF Pu, BULLFROG
Save Time History : TRUE
The Parameter is a function, exp. value = 834.3334
Equation : if(ifract<=0.2,1,trpubw)

The parameter is a function of the following parameters:
DBW,IFRACT,KPUD,PBW,TRPUBW

Parameter No. 161 of 287
Parameter ID : RPUCHV
Description : RETARDATION OF Pu, CALICO HILLS VITRIC
Save Time History : TRUE
The Parameter is a function, exp. value = 801
Equation : if(ifract<=0.2,1,trpchv)

The parameter is a function of the following parameters:
DCHN1V,IFRACT,KPUV,PCHN1V,TRPCHV

Parameter No. 162 of 287
Parameter ID : RPUCHZ
Description : RETARDATION OF Pu, CALICO HILLS ZEOLITIC
Save Time History : TRUE
The Parameter is a function, exp. value = 164.9024
Equation : if(ifract<=0.2,1,trpchz)

The parameter is a function of the following parameters:
DCHN1Z,IFRACT,KPUZ,PCHN1Z,TRPCHZ

Parameter No. 163 of 287
Parameter ID : RPUPPW
Description : RETARDATION OF Pu, PROW PASS
Save Time History : TRUE
The Parameter is a function, exp. value = 834.3334
Equation : if(ifract<=0.2,1,trpppw)

The parameter is a function of the following parameters:
DPPW,IFRACT,KPUD,PPPW,TRPPPW

Parameter No. 164 of 287
Parameter ID : RPUS
Description : RETARDATION OF Pu, Saturated

Save Time History : TRUE
The Parameter is a function, exp. value = 834.3334
Equation : 1+DBW/PBW*KPUD

The parameter is a function of the following parameters:
DBW,KPUD,PBW

Parameter No. 165 of 287
Parameter ID : RPUTS2
Description : RETARDATION OF Pu, TOPOPAH SPRING 2
Save Time History : TRUE
The Parameter is a function, exp. value = 2037.364
Equation : if(ifract<=0.2,1,trpts2)

The parameter is a function of the following parameters:
DTSW2,IFRACT,KPUD,PTSW2,TRPTS2

Parameter No. 166 of 287
Parameter ID : RPUTS3
Description : RETARDATION OF Pu, TOPOPAH SPRING 3
Save Time History : TRUE
The Parameter is a function, exp. value = 2389.889
Equation : if(ifract<=0.2,1,trpts3)

The parameter is a function of the following parameters:
DTSW3,IFRACT,KPUD,PTSW3,TRPTS3

Parameter No. 167 of 287
Parameter ID : RRABW
Description : RETARDATION OF Ra, BULLFROG
Save Time History : TRUE
The Parameter is a function, exp. value = 2501
Equation : if(ifract<=0.2,1,trrabw)

The parameter is a function of the following parameters:
DBW,IFRACT,KRAD,PBW,TRRABW

Parameter No. 168 of 287
Parameter ID : RRACHV
Description : RETARDATION OF Ra, CALICO HILLS VITRIC
Save Time History : TRUE
The Parameter is a function, exp. value = 2401
Equation : if(ifract<=0.2,1,trrchv)

The parameter is a function of the following parameters:
DCHN1V,IFRACT,KRAV,PCHN1V,TRRCHV

Parameter No. 169 of 287
Parameter ID : RRACHZ
Description : RETARDATION OF Ra, CALICO HILLS ZEOLITIC
Save Time History : TRUE
The Parameter is a function, exp. value = 12293.68
Equation : if(ifract<=0.2,1,trrchz)

The parameter is a function of the following parameters:
DCHN1Z,IFRACT,KRAZ,PCHN1Z,TRRCHZ

Parameter No. 170 of 287
Parameter ID : RRAPPW
Description : RETARDATION OF Ra, PROW PASS
Save Time History : TRUE
The Parameter is a function, exp. value = 2501
Equation : if(ifract<=0.2,1,trrppw)

The parameter is a function of the following parameters:
DPPW,IFRACT,KRAD,PPPW,TRRPPW

Parameter No. 171 of 287
Parameter ID : RRAS
Description : RETARDATION OF Ra, Saturated

Save Time History : TRUE
The Parameter is a function, exp. value = 2501
Equation : 1+DBW/PBW*KRAD

The parameter is a function of the following parameters:
DBW,KRAD,PBW

Parameter No. 172 of 287
Parameter ID : RRATS2
Description : RETARDATION OF Ra, TOPOPAH SPRING 2
Save Time History : TRUE
The Parameter is a function, exp. value = 6110.091
Equation : if(ifract<=0.2,1,trrts2)

The parameter is a function of the following parameters:
DTSW2,IFRACT,KRAD,PTSW2,TRRTS2

Parameter No. 173 of 287
Parameter ID : RRATS3
Description : RETARDATION OF Ra, TOPOPAH SPRING 3
Save Time History : TRUE
The Parameter is a function, exp. value = 7167.667
Equation : if(ifract<=0.2,1,trrts3)

The parameter is a function of the following parameters:
DTSW3,IFRACT,KRAD,PTSW3,TRRTS3

Parameter No. 174 of 287
Parameter ID : RUBW
Description : RETARDATION OF U, BULLFROG
Save Time History : TRUE
The Parameter is a function, exp. value = 21.83333
Equation : if(ifract<=0.2,1,trubw)

The parameter is a function of the following parameters:
DBW,IFRACT,KUD,PBW,TRUBW

Parameter No. 175 of 287
Parameter ID : RUCHV
Description : RETARDATION OF U, CALICO HILLS VITRIC
Save Time History : TRUE
The Parameter is a function, exp. value = 17
Equation : if(ifract<=0.2,1,truchv)

The parameter is a function of the following parameters:
DCHN1V,IFRACT,KUV,PCHN1V,TRUCHV

Parameter No. 176 of 287
Parameter ID : RUCHZ
Description : RETARDATION OF U, CALICO HILLS ZEOLITIC
Save Time History : TRUE
The Parameter is a function, exp. value = 52.21951
Equation : if(ifract<=0.2,1,truchz)

The parameter is a function of the following parameters:
DCHN1Z,IFRACT,KUZ,PCHN1Z,TRUCHZ

Parameter No. 177 of 287
Parameter ID : RUPPW
Description : RETARDATION OF U, PROW PASS
Save Time History : TRUE
The Parameter is a function, exp. value = 21.83333
Equation : if(ifract<=0.2,1,truppw)

The parameter is a function of the following parameters:
DPPW,IFRACT,KUD,PPPW,TRUPPW

Parameter No. 178 of 287
Parameter ID : RUS
Description : RETARDATION OF U, Saturated

Save Time History : TRUE
The Parameter is a function, exp. value = 21.83333
Equation : 1+DBW/PBW*KUD

The parameter is a function of the following parameters:
DBW,KUD,PBW

Parameter No. 179 of 287
Parameter ID : RUTS2
Description : RETARDATION OF U, TOPOPAH SPRING 2
Save Time History : TRUE
The Parameter is a function, exp. value = 51.90909
Equation : if(ifract<=0.2,1,truts2)

The parameter is a function of the following parameters:
DTSW2,IFRACT,KUD,PTSW2,TRUTS2

Parameter No. 180 of 287
Parameter ID : RUTS3
Description : RETARDATION OF U, TOPOPAH SPRING 3
Save Time History : TRUE
The Parameter is a function, exp. value = 60.72222
Equation : if(ifract<=0.2,1,truts3)

The parameter is a function of the following parameters:
DTSW3,IFRACT,KUD,PTSW3,TRUTS3

Parameter No. 181 of 287
Parameter ID : SBFLUX
Description : SATURATED ZONE FLUX

Save Time History : TRUE
The parameter is stochastic
The distribution is logarithmic
Sampling bias : No Bias
Normal : Mean = 1.06960E+00 S.D. = 4.85893E-01
The parameter affects the following parameters:

GWTIM1,GWTIM2,GWTIM3,GWTIM4,GWTIM5,
GWTIM6,GWTIM7,GWTIM8
GWTIM9,GWTM1A,GWTM2A,GWTM3A,
GWTM4A,GWTM5A,GWTM6A,GWTM7A
GWTM8A,GWTM9A,TSFLUX,VSAT

Parameter No. 182 of 287
Parameter ID : SBW
Description : SATURATION OF BULLFROG

Save Time History : TRUE
The parameter is a constant: 9.88000E-01
The parameter affects the following parameters:
VBW

Parameter No. 183 of 287
Parameter ID : SCHN1V
Description : SATURATION OF CALICO HILLS VITRIC
Save Time History : TRUE
The parameter is a constant: 8.00000E-02
The parameter affects the following parameters:

GWTIM1,GWTIM2,GWTIM3,GWTIM4,GWTIM5,
GWTIM6,GWTIM7,GWTIM8
GWTIM9,GWTM1A,GWTM2A,GWTM3A,
GWTM4A,GWTM5A,GWTM6A,GWTM7A
GWTM8A,GWTM9A,VCHN1V

Parameter No. 184 of 287
Parameter ID : SCHN1Z
Description : SATURATION OF CALICO HILLS ZEOLITIC
Save Time History : TRUE
The parameter is a constant: 9.22000E-01
The parameter affects the following parameters:
GWTIM1,GWTIM2,GWTIM3,GWTIM4,GWTIM5,
GWTIM6,GWTIM7,GWTIM8
GWTIM9,GWTM1A,GWTM2A,GWTM3A,
GWTM4A,GWTM5A,GWTM6A,GWTM7A
GWTM8A,GWTM9A,VCHN1V

Parameter No. 185 of 287
Parameter ID : SLAM
Description : SOLUBILITY OF Am
Save Time History : TRUE
The Parameter is a function, exp. value = 0.00029
Equation :
IF(MEANPH<=6.5,SLAM1,(IF(MEANPH>7.75,SLAM3,SLAM2)))
The parameter is a function of the following parameters:
MEANPH,SLAM1,SLAM11,SLAM12,SLAM13,
SLAM2,SLAM21,SLAM22,SLAM23
SLAM3,SLAM31,SLAM32,SLAM33,TEMP

Parameter No. 186 of 287
Parameter ID : SLAM1
Description : SOLUBILITY OF Am, pH<=6.5
Save Time History : TRUE
The Parameter is a function, exp. value = 0.00044
Equation :
IF(TEMP<=42.5,SLAM11,(IF(TEMP>75,SLAM13,SLAM12)))
The parameter affects the following parameters:
SLAM
The parameter is a function of the following parameters:
SLAM11,SLAM12,SLAM13,TEMP

Parameter No. 187 of 287
Parameter ID : SLAM11
Description : SOLUBILITY OF Am, T<=42.5, pH<=6.5
Save Time History : TRUE
The parameter is stochastic
The distribution is logarithmic
Sampling bias : No Bias
Normal : Mean = 4.16464E-04 S.D. = 1.44005E-01
The parameter affects the following parameters:
SLAM,SLAM1

Parameter No. 188 of 287
Parameter ID : SLAM12
Description : SOLUBILITY OF Am, 42.5<T<=75, pH<=6.5
Save Time History : TRUE
The parameter is stochastic
The distribution is logarithmic
Sampling bias : No Bias
Normal : Mean = 5.87608E-01 S.D. = 1.18777E-01
The parameter affects the following parameters:
SLAM,SLAM1

Parameter No. 189 of 287
Parameter ID : SLAM13
Description : SOLUBILITY OF Am, 75<T, pH<=6.5
Save Time History : TRUE
The parameter is stochastic
The distribution is logarithmic
Sampling bias : No Bias
Normal : Mean = 2.89914E-04 S.D. = 3.61574E-01
The parameter affects the following parameters:
SLAM,SLAM1

Parameter No. 190 of 287
Parameter ID : SLAM2
Description : SOLUBILITY OF Am, 6.5<pH<=7.75
Save Time History : TRUE
The Parameter is a function, exp. value = 0.00029
Equation :
IF(TEMP<=42.5,SLAM21,(IF(TEMP>75,SLAM23,SLAM22)))
The parameter affects the following parameters:
SLAM
The parameter is a function of the following parameters:
SLAM21,SLAM22,SLAM23,TEMP

Parameter No. 191 of 287
Parameter ID : SLAM21
Description : SOLUBILITY OF Am, T<=42.5, 6.5<pH<=7.75
Save Time History : TRUE
The parameter is stochastic
The distribution is logarithmic
Sampling bias : No Bias
Normal : Mean = 2.81904E-04 S.D. = 1.03349E-01
The parameter affects the following parameters:
SLAM,SLAM2

Parameter No. 192 of 287
Parameter ID : SLAM22
Description : SOLUBILITY OF Am, 42.5<T<=75, 6.5<pH<=7.75
Save Time History : TRUE
The parameter is stochastic
The distribution is logarithmic
Sampling bias : No Bias
Normal : Mean = 1.76917E-03 S.D. = 3.39172E-01
The parameter affects the following parameters:
SLAM,SLAM2

Parameter No. 193 of 287
Parameter ID : SLAM23
Description : SOLUBILITY OF Am, 75<T, 6.5<pH<=7.75
Save Time History : TRUE
The parameter is stochastic
The distribution is logarithmic
Sampling bias : No Bias
Normal : Mean = 6.58086E-05 S.D. = 2.22075E-01
The parameter affects the following parameters:
SLAM,SLAM2

Parameter No. 194 of 287
Parameter ID : SLAM3
Description : SOLUBILITY OF Am, 7.75<pH

Save Time History : TRUE
The Parameter is a function, exp. value = 0.00058
Equation :
IF(TEMP<=42.5,SLAM31,(IF(TEMP>75,SLAM33, SLAM32)))
The parameter affects the following parameters:
SLAM
The parameter is a function of the following parameters:
SLAM31,SLAM32,SLAM33,TEMP

Parameter No. 195 of 287
Parameter ID : SLAM31
Description : SOLUBILITY OF Am, T<=42.5, 7.75<pH
Save Time History : TRUE
The parameter is stochastic
The distribution is logarithmic
Sampling bias : No Bias
Normal : Mean = 4.54429E-04 S.D. = 3.03377E-01
The parameter affects the following parameters:
SLAM,SLAM3

Parameter No. 196 of 287
Parameter ID : SLAM32
Description : SOLUBILITY OF Am, 42.5<T<=75, 7.75<pH
Save Time History : TRUE
The parameter is stochastic
The distribution is logarithmic
Sampling bias : No Bias
Normal : Mean = 2.05061E-03 S.D. = 3.61574E-01
The parameter affects the following parameters:
SLAM,SLAM3

Parameter No. 197 of 287
Parameter ID : SLAM33
Description : SOLUBILITY OF Am, 75<T, 6.5<pH<=7.75
Save Time History : TRUE
The parameter is stochastic
The distribution is logarithmic
Sampling bias : No Bias
Normal : Mean = 7.07169E-05 S.D. = 2.45794E-01
The parameter affects the following parameters:
SLAM,SLAM3

Parameter No. 198 of 287
Parameter ID : SLCM
Description : SOLUBILITY OF Cm

Save Time History : TRUE
The Parameter is a function, exp. value = 0.00001833
Equation : IF(TEMP<=55,SLCML,SLCMH)

The parameter is a function of the following parameters:
SLCMH,SLCML,TEMP

Parameter No. 199 of 287
Parameter ID : SLCMH
Description : SOLUBILITY OF Cm, T>55

Save Time History : TRUE
The parameter is stochastic
The distribution is logarithmic
Sampling bias : No Bias
Triang : Mn= 1.50000E-10 Ml= 1.50000E-09 Mx= 1.50000E-08
The parameter affects the following parameters:
SLCM

Parameter No. 200 of 287
Parameter ID : SLCML
Description : SOLUBILITY OF Cm, T<=55

Save Time History : TRUE
The parameter is stochastic
The distribution is logarithmic
Sampling bias : No Bias
Triang : Mn= 1.20000E-06 Ml= 1.20000E-05 Mx= 1.20000E-04
The parameter affects the following parameters:
SLCM

Parameter No. 201 of 287
Parameter ID : SLCS
Description : SOLUBILITY OF Cs

Save Time History : TRUE
The parameter is stochastic
The distribution is logarithmic
Sampling bias : No Bias
Triang : Mn= 1.20000E+00 Ml= 3.90000E+02 Mx= 2.10000E+03

Parameter No. 202 of 287
Parameter ID : SLI
Description : SOLUBILITY OF I

Save Time History : TRUE
The parameter is stochastic
The distribution is logarithmic
Sampling bias : No Bias
Triang : Mn= 1.00000E+00 Ml= 3.90000E+02 Mx= 1.00000E+05

Parameter No. 203 of 287
Parameter ID : SLNP
Description : SOLUBILITY OF Np

Save Time History : TRUE
The Parameter is a function, exp. value = 31.
Equation :
IF(MEANPH<=6.5,SLNP1,(IF(MEANPH>7.75,SLNP3,SLNP2)))
The parameter affects the following parameters:
SLU
The parameter is a function of the following parameters:
MEANPH,SLNP1,SLNP11,SLNP12,SLNP13,
SLNP2,SLNP21,SLNP22,SLNP23
SLNP3,SLNP31,SLNP32,SLNP33,TEMP

Parameter No. 204 of 287
Parameter ID : SLNP1
Description : SOLUBILITY OF Np, pH<=6.5

Save Time History : TRUE
The Parameter is a function, exp. value = 1300.
Equation :
IF(TEMP<=42.5,SLNP11,(IF(TEMP>75,SLNP13,SLNP12)))
The parameter affects the following parameters:
SLNP,SLU
The parameter is a function of the following parameters:
SLNP11,SLNP12,SLNP13,TEMP

Parameter No. 205 of 287
Parameter ID : SLNP11
Description : SOLUBILITY OF Np, T<=42.5, pH<=6.5
Save Time History : TRUE
The parameter is stochastic
The distribution is logarithmic
Sampling bias : No Bias
Normal : Mean = 1.29812E+03 S.D. = 2.33682E-02
The parameter affects the following parameters:
SLNP,SLNP1,SLU

Parameter No. 206 of 287
Parameter ID : SLNP12
Description : SOLUBILITY OF Np, 42.5<T<=75, pH<=6.5
Save Time History : TRUE
The parameter is stochastic
The distribution is logarithmic
Sampling bias : No Bias
Normal : Mean = 1.49731E+03 S.D. = 2.60343E-02
The parameter affects the following parameters:
SLNP,SLNP1,SLU

Parameter No. 207 of 287
Parameter ID : SLNP13
Description : SOLUBILITY OF Np, 75<T, pH<=6.5
Save Time History : TRUE
The parameter is stochastic
The distribution is logarithmic
Sampling bias : No Bias
Normal : Mean = 2.79288E+02 S.D. = 3.09816E-02
The parameter affects the following parameters:
SLNP,SLNP1,SLU

Parameter No. 208 of 287
Parameter ID : SLNP2
Description : SOLUBILITY OF Np, 6.5<pH<=7.75
Save Time History : TRUE
The Parameter is a function, exp. value = 31.
Equation :
IF(TEMP<=42.5,SLNP21,(IF(TEMP>75,SLNP23, SLNP22)))
The parameter affects the following parameters:
SLNP,SLU
The parameter is a function of the following parameters:
SLNP21,SLNP22,SLNP23,TEMP

Parameter No. 209 of 287
Parameter ID : SLNP21
Description : SOLUBILITY OF Np, T<=42.5, 6.65<pH<=7.75
Save Time History : TRUE
The parameter is stochastic
The distribution is logarithmic
Sampling bias : No Bias
Normal : Mean = 3.06045E+01 S.D. = 6.95982E-02
The parameter affects the following parameters:
SLNP,SLNP2,SLU

Parameter No. 210 of 287
Parameter ID : SLNP22
Description : SOLUBILITY OF Np, 42.5<T<=75, 6.5<pH<=7.75
Save Time History : TRUE
The parameter is stochastic
The distribution is logarithmic
Sampling bias : No Bias
Normal : Mean = 2.29135E+02 S.D. = 3.76936E-02
The parameter affects the following parameters:
SLNP,SLNP2,SLU

Parameter No. 211 of 287
Parameter ID : SLNP23
Description : SOLUBILITY OF Np, 75<T, 6.5<pH<=7.75
Save Time History : TRUE
The parameter is stochastic
The distribution is logarithmic
Sampling bias : No Bias
Normal : Mean = 3.49251E+01 S.D. = 1.06932E-01
The parameter affects the following parameters:
SLNP,SLNP2,SLU

Parameter No. 212 of 287
Parameter ID : SLNP3
Description : SOLUBILITY OF Np, 7.75<pH

Save Time History : TRUE
The Parameter is a function, exp. value = 10
Equation :
IF(TEMP<=42.5,SLNP31,(IF(TEMP>75,SLNP33, SLNP32)))
The parameter affects the following parameters:
SLNP,SLU
The parameter is a function of the following parameters:
SLNP31,SLNP32,SLNP33,TEMP

Parameter No. 213 of 287
Parameter ID : SLNP31
Description : SOLUBILITY OF Np, T<=42.5, 7.75<pH
Save Time History : TRUE
The parameter is stochastic
The distribution is logarithmic
Sampling bias : No Bias
Normal : Mean = 9.80581E+00 S.D. = 8.60086E-02
The parameter affects the following parameters:
SLNP,SLNP3,SLU

Parameter No. 214 of 287
Parameter ID : SLNP32
Description : SOLUBILITY OF Np, 42.5<T<=75, 7.75<pH
Save Time History : TRUE
The parameter is stochastic
The distribution is logarithmic
Sampling bias : No Bias
Normal : Mean = 2.39171E+01 S.D. = 3.61286E-02
The parameter affects the following parameters:
SLNP,SLNP3,SLU

Parameter No. 215 of 287
Parameter ID : SLNP33
Description : SOLUBILITY OF Np, 75<T, 7.75<pH
Save Time History : TRUE
The parameter is stochastic
The distribution is logarithmic
Sampling bias : No Bias
Normal : Mean = 2.09807E+01 S.D. = 1.86041E-02
The parameter affects the following parameters:
SLNP,SLNP3,SLU

Parameter No. 216 of 287
Parameter ID : SLPU
Description : SOLUBILITY OF Pu

Save Time History : TRUE
The Parameter is a function, exp. value = 0.055
Equation :
IF(MEANPH<=6.5,SLPU1,(IF(MEANPH>7.75,SLPU3,SLPU2)))
The parameter is a function of the following parameters:
MEANPH,SLPU1,SLPU11,SLPU12,SLPU13,
SLPU2,SLPU21,SLPU22,SLPU23
SLPU3,SLPU31,SLPU32,SLPU33,TEMP

Parameter No. 217 of 287
Parameter ID : SLPU1
Description : SOLUBILITY OF Pu, pH<=6.5

Save Time History : TRUE
The Parameter is a function, exp. value = 0.26
Equation :
IF(TEMP<=42.5,SLPU11,(IF(TEMP>75,SLPU13,SLPU12)))
The parameter affects the following parameters:
SLPU
The parameter is a function of the following parameters:
SLPU11,SLPU12,SLPU13,TEMP

Parameter No. 218 of 287
Parameter ID : SLPU11
Description : SOLUBILITY OF Pu, T<=42.5, pH<=6.5
Save Time History : TRUE
The parameter is stochastic
The distribution is logarithmic
Sampling bias : No Bias
Normal : Mean = 2.42670E-01 S.D. = 1.61310E-01
The parameter affects the following parameters:
SLPU,SLPU1

Parameter No. 219 of 287
Parameter ID : SLPU12
Description : SOLUBILITY OF Pu, 42.5<T<=75, pH<=6.5
Save Time History : TRUE
The parameter is stochastic
The distribution is logarithmic
Sampling bias : No Bias
Normal : Mean = 6.03510E-03 S.D. = 1.67313E-01
The parameter affects the following parameters:
SLPU,SLPU1

Parameter No. 220 of 287
Parameter ID : SLPU13
Description : SOLUBILITY OF Pu, 75<T, pH<=6.5
Save Time History : TRUE
The parameter is stochastic
The distribution is logarithmic
Sampling bias : No Bias
Normal : Mean = 1.42302E-03 S.D. = 1.40969E-01
The parameter affects the following parameters:
SLPU,SLPU1

Parameter No. 221 of 287
Parameter ID : SLPU2
Description : SOLUBILITY OF Pu, 6.5<pH<=7.75
Save Time History : TRUE
The Parameter is a function, exp. value = 0.055
Equation :
IF(TEMP<=42.5,SLPU21,(IF(TEMP>75,SLPU23,SLPU22)))
The parameter affects the following parameters:
SLPU
The parameter is a function of the following parameters:
SLPU21,SLPU22,SLPU23,TEMP

Parameter No. 222 of 287
Parameter ID : SLPU21
Description : SOLUBILITY OF Pu, T<=42.5, 6.5<pH<=7.75
Save Time History : TRUE
The parameter is stochastic
The distribution is logarithmic
Sampling bias : No Bias
Normal : Mean = 4.67827E-02 S.D. = 2.47067E-01
The parameter affects the following parameters:
SLPU,SLPU2

Parameter No. 223 of 287
Parameter ID : SLPU22
Description : SOLUBILITY OF Pu, 42.5<T<=75, 6.5<pH<=7.75
Save Time History : TRUE
The parameter is stochastic
The distribution is logarithmic
Sampling bias : No Bias
Normal : Mean = 8.63995E-03 S.D. = 1.05766E-01
The parameter affects the following parameters:
SLPU,SLPU2

Parameter No. 224 of 287
Parameter ID : SLPU23
Description : SOLUBILITY OF Pu, 75<T, 6.5<pH<=7.75
Save Time History : TRUE
The parameter is stochastic
The distribution is logarithmic
Sampling bias : No Bias
Normal : Mean = 2.09054E-03 S.D. = 4.12680E-02
The parameter affects the following parameters:
SLPU,SLPU2

Parameter No. 225 of 287
Parameter ID : SLPU3
Description : SOLUBILITY OF Pu, 7.75<pH

Save Time History : TRUE
The Parameter is a function, exp. value = 0.07
Equation :
IF(TEMP<=42.5,SLPU31,(IF(TEMP>75,SLPU33, SLPU32)))
The parameter affects the following parameters:
SLPU
The parameter is a function of the following parameters:
SLPU31,SLPU32,SLPU33,TEMP

Parameter No. 226 of 287
Parameter ID : SLPU31
Description : SOLUBILITY OF Pu, T<=42.5, 7.75<pH
Save Time History : TRUE
The parameter is stochastic
The distribution is logarithmic
Sampling bias : No Bias
Normal : Mean = 6.75557E-02 S.D. = 1.15791E-01
The parameter affects the following parameters:
SLPU,SLPU3

Parameter No. 227 of 287
Parameter ID : SLPU32
Description : SOLUBILITY OF Pu, 42.5<T<=75, 7.75<pH
Save Time History : TRUE
The parameter is stochastic
The distribution is logarithmic
Sampling bias : No Bias
Normal : Mean = 2.89313E-02 S.D. = 2.99158E-02
The parameter affects the following parameters:
SLPU,SLPU3

Parameter No. 228 of 287
Parameter ID : SLPU33
Description : SOLUBILITY OF Pu, 75<T, 7.75<pH
Save Time History : TRUE
The parameter is stochastic
The distribution is logarithmic
Sampling bias : No Bias
Normal : Mean = 1.79723E-03 S.D. = 2.41089E-02
The parameter affects the following parameters:
SLPU,SLPU3

Parameter No. 229 of 287
Parameter ID : SLRA
Description : SOLUBILITY OF Ra

Save Time History : TRUE
The parameter is stochastic
The distribution is logarithmic
Sampling bias : No Bias
Triang : Mn= 1.00000E-05 Ml= 4.00000E-04 Mx= 1.00000E-01

Parameter No. 230 of 287
Parameter ID : SLSE
Description : SOLUBILITY OF Se

Save Time History : TRUE
The parameter is stochastic
The distribution is logarithmic
Sampling bias : No Bias
Triang : Mn= 7.90000E+02 Ml= 7.90000E+03 Mx= 5.50000E+05

Parameter No. 231 of 287
Parameter ID : SLTC
Description : SOLUBILITY OF Tc

Save Time History : TRUE
The parameter is stochastic
The distribution is logarithmic
Sampling bias : No Bias
Triang : Mn= 2.50000E-02 Ml= 1.00000E+02 Mx= 9.90000E+05

Parameter No. 232 of 287
Parameter ID : SLU
Description : SOLUBILITY OF U

Save Time History : TRUE
The Parameter is a function, exp. value = 31.
Equation : SLNP

The parameter is a function of the following parameters:
MEANPH,SLNP,SLNP1,SLNP11,SLNP12,
SLNP13,SLNP2,SLNP21,SLNP22,SLNP23,
SLNP3,SLNP31,SLNP32,SLNP33,TEMP

Parameter ID: SLZR (only for ER-metallic)
Description: SOLUBILITY OF ZR
Save Time History: TRUE
The parameter is stochastic
The distribution is logarithmic
Sampling bias : No Bias
Uniform : Mn= 9.18E-08 Mx= 9.10000E-03

Parameter ID: SLSN (only for ER-metallic)
Description: SOLUBILITY OF SN
Save Time History: TRUE
The parameter is stochastic
Sampling bias : No Bias
Uniform : Mn= 1.30E-06 Mx= 1.30000E-02

Parameter ID: SLPD (only for ER-metallic)
Description: SOLUBILITY OF PD
Save Time History: TRUE
The parameter is stochastic
The distribution is logarithmic
Sampling bias : No Bias
Beta : Mn= 5.90E-02 Mx= 5.90E-03, Mn = 1.05E+02, Coef Var = 0.25

Parameter No. 233 of 287
Parameter ID : SPPW
Description : SATURATION OF PROW PASS

Save Time History : TRUE
The parameter is a constant: 9.88000E-01
The parameter affects the following parameters:

GWTIM1,GWTIM2,GWTIM3,GWTIM4,GWTIM5,
GWTIM6,GWTIM7,GWTIM8
GWTIM9,GWTM1A,GWTM2A,GWTM3A,
GWTM4A,GWTM5A,GWTM6A,GWTM7A,
GWTM8A,GWTM9A,VPPW

Parameter No. 234 of 287
Parameter ID : STSW2
Description : SATURATION OF TOPOPAH SPRING 2
Save Time History : TRUE
The parameter is a constant: 6.81000E-01
The parameter affects the following parameters:

EFFDIF,FGEOMD,GWTIM1,GWTIM2,GWTIM3,
GWTIM4,GWTIM5,GWTIM6
GWTIM7,GWTIM8,GWTIM9,OMEGA,TEFDIF,T
OMEGA,VTSW2

Parameter No. 235 of 287
Parameter ID : STSW3
Description : SATURATION OF TOPOPAH SPRING 3
Save Time History : TRUE
The parameter is a constant: 7.63000E-01
The parameter affects the following parameters:

GWTIM1,GWTIM2,GWTIM3,GWTIM4,GWTIM5,
GWTIM6,GWTIM7,GWTIM8,GWTIM9,VTSW3

Parameter No. 236 of 287
Parameter ID : TCATCH
Description : EFFECTIVE CATCHMENT AREA, CHECK FOR WET DRIP
Save Time History : TRUE
The Parameter is a function, exp. value = 0
Equation : IF(CONTAC==1,CATCH,0)

The parameter is a function of the following parameters:
CATCH,CONTAC

Parameter No. 237 of 287
Parameter ID : TEFDIF
Description :

Save Time History : TRUE
The Parameter is a function, exp. value = 0
Equation : IF(CONTAC==2,EFFDIF,0)

The parameter is a function of the following parameters:
CONTAC,EFFDIF,STSW2

Parameter No. 238 of 287
Parameter ID : TOMEGA
Description : geometric factor for diffusion -- moist continuous
Save Time History : TRUE
The Parameter is a function, exp. value = 0
Equation : IF(CONTAC==2,OMEGA,0)

The parameter is a function of the following parameters:
CONTAC,EQRAD,FGEOMD,LENG,OMEGA,PI, R0,STSW2,VOL,WPOR

Parameter No. 239 of 287
Parameter ID : TRACHV
Description : RETARDATION OF Am, CALICO HILLS VITRIC
Save Time History : TRUE
The Parameter is a function, exp. value = 3041
Equation : 1+DCHN1V/PCHN1V*KAMV

The parameter affects the following parameters:
RAMCHV
The parameter is a function of the following parameters:
DCHN1V,KAMV,PCHN1V

Parameter No. 240 of 287
Parameter ID : TRACHZ
Description : RETARDATION OF Am, CALICO HILLS ZEOLITIC
Save Time History : TRUE
The Parameter is a function, exp. value = 2254.658
Equation : 1+DCHN1Z/PCHN1Z*KAMZ

The parameter affects the following parameters:
RAMCHZ
The parameter is a function of the following parameters:
DCHN1Z,KAMZ,PCHN1Z

Parameter No. 241 of 287
Parameter ID : TRAMBW
Description : RETARDATION OF Am, BULLFROG
Save Time History : TRUE
The Parameter is a function, exp. value = 8751
Equation : 1+DBW/PBW*KAMD

The parameter affects the following parameters:
RAMBW
The parameter is a function of the following parameters:
DBW,KAMD,PBW

Parameter No. 242 of 287
Parameter ID : TRAPPW
Description : RETARDATION OF Am, PROW PASS
Save Time History : TRUE
The Parameter is a function, exp. value = 8751
Equation : 1+DPPW/PPPW*KAMD
The parameter affects the following parameters:
RAMPPW
The parameter is a function of the following parameters:
DPPW,KAMD,PPPW

Parameter No. 243 of 287
Parameter ID : TRATS2
Description : RETARDATION OF Am, TOPOPAH SPRING 2
Save Time History : TRUE
The Parameter is a function, exp. value = 21382.82
Equation : 1+DTSW2/PTSW2*KAMD
The parameter affects the following parameters:
RAMTS2
The parameter is a function of the following parameters:
DTSW2,KAMD,PTSW2

Parameter No. 244 of 287
Parameter ID : TRATS3
Description : RETARDATION OF Am, TOPOPAH SPRING 3
Save Time History : TRUE
The Parameter is a function, exp. value = 25084.33
Equation : 1+DTSW3/PTSW3*KAMD

The parameter affects the following parameters:
RAMTS3
The parameter is a function of the following parameters:
DTSW3,KAMD,PTSW3

Parameter No. 245 of 287
Parameter ID : TRCCHV
Description : RETARDATION OF Cs, CALICO HILLS VITRIC
Save Time History : TRUE
The Parameter is a function, exp. value = 1201
Equation : 1+DCHN1V/PCHN1V*KCSV

The parameter affects the following parameters:
RCSCHV
The parameter is a function of the following parameters:
DCHN1V,KCSV,PCHN1V

Parameter No. 246 of 287
Parameter ID : TRCCHZ
Description : RETARDATION OF Cs, CALICO HILLS ZEOLITIC
Save Time History : TRUE
The Parameter is a function, exp. value = 7171.731
Equation : 1+DCHN1Z/PCHN1Z*KCSZ

The parameter affects the following parameters:
RCSCHZ
The parameter is a function of the following parameters:
DCHN1Z,KCSZ,PCHN1Z

Parameter No. 247 of 287
Parameter ID : TRCPPW
Description : RETARDATION OF Cs, PROW PASS
Save Time History : TRUE
The Parameter is a function, exp. value = 1251
Equation : 1+DPPW/PPPW*KCSD

The parameter affects the following parameters:
RCSPPW
The parameter is a function of the following parameters:
DPPW,KCSD,PPPW

Parameter No. 248 of 287
Parameter ID : TRCSBW
Description : RETARDATION OF Cs, BULLFROG
Save Time History : TRUE
The Parameter is a function, exp. value = 1251
Equation : 1+dbw*kcsd/pbw
The parameter affects the following parameters:
RCSBW
The parameter is a function of the following parameters:
DBW,KCSD,PBW

Parameter No. 249 of 287
Parameter ID : TRCTS2
Description : RETARDATION OF Cs, TOPOPAH SPRING 2
Save Time History : TRUE
The Parameter is a function, exp. value = 3055.545
Equation : 1+DTSW2/PTSW2*KCSD
The parameter affects the following parameters:
RCSTS2
The parameter is a function of the following parameters:
DTSW2,KCSD,PTSW2

Parameter No. 250 of 287
Parameter ID : TRCTS3
Description : RETARDATION OF Cs, TOPOPAH SPRING 3
Save Time History : TRUE
The Parameter is a function, exp. value = 3584.333
Equation : 1+DTSW3/PTSW3*KCSD

The parameter affects the following parameters:
RCSTS3
The parameter is a function of the following parameters:
DTSW3,KCSD,PTSW3

Parameter No. 251 of 287
Parameter ID : TRNCHV
Description : RETARDATION OF Np, CALICO HILLS VITRIC
Save Time History : TRUE
The Parameter is a function, exp. value = 5
Equation : 1+DCHN1V/PCHN1V*KNPV
The parameter affects the following parameters:
RNPCHV
The parameter is a function of the following parameters:
DCHN1V,KNPV,PCHN1V

Parameter No. 252 of 287
Parameter ID : TRNCHZ
Description : RETARDATION OF Np, CALICO HILLS ZEOLITIC
Save Time History : TRUE
The Parameter is a function, exp. value = 17.39024
Equation : 1+DCHN1Z/pchn1z*KNPZ
The parameter affects the following parameters:
RNPCHZ
The parameter is a function of the following parameters:
DCHN1Z,KNPZ,PCHN1Z

Parameter No. 253 of 287
Parameter ID : TRNPBW
Description : RETARDATION OF Np, BULLFROG
Save Time History : TRUE
The Parameter is a function, exp. value = 17.66667
Equation : 1+DBW/PBW*KNPD
The parameter affects the following parameters:
RNPBW
The parameter is a function of the following parameters:
DBW,KNPD,PBW

Parameter No. 254 of 287
Parameter ID : TRNPPW
Description : RETARDATION OF Np, PROW PASS
Save Time History : TRUE
The Parameter is a function, exp. value = 17.66667
Equation : 1+DPPW/PPPW*KNPD
The parameter affects the following parameters:
RNPPPW
The parameter is a function of the following parameters:
DPPW,KNPD,PPPW

Parameter No. 255 of 287
Parameter ID : TRNTS2
Description : RETARDATION OF Np, TOPOPAH SPRING 2
Save Time History : TRUE
The Parameter is a function, exp. value = 41.72727
Equation : 1+DTSW2/PTSW2*KNPD
The parameter affects the following parameters:
RNPTS2
The parameter is a function of the following parameters:
DTSW2,KNPD,PTSW2

Parameter No. 256 of 287
Parameter ID : TRNTS3
Description : RETARDATION OF Np, TOPOPAH SPRING 3
Save Time History : TRUE
The Parameter is a function, exp. value = 48.77778
Equation : 1+DTSW3/PTSW3*KNPD
The parameter affects the following parameters:
RNPTS3
The parameter is a function of the following parameters:
DTSW3,KNPD,PTSW3

Parameter No. 257 of 287
Parameter ID : TRPCHV
Description : RETARDATION OF Pu, CALICO HILLS VITRIC
Save Time History : TRUE
The Parameter is a function, exp. value = 801
Equation : 1+DCHN1V/PCHN1V*KPUV

The parameter affects the following parameters:
RPUCHV
The parameter is a function of the following parameters:
DCHN1V,KPUV,PCHN1V

Parameter No. 258 of 287
Parameter ID : TRPCHZ
Description : RETARDATION OF Pu, CALICO HILLS ZEOLITIC
Save Time History : TRUE
The Parameter is a function, exp. value = 164.9024
Equation : 1+DCHN1Z/PCHN1Z*KPUZ
The parameter affects the following parameters:
RPUCHZ
The parameter is a function of the following parameters:
DCHN1Z,KPUZ,PCHN1Z

Parameter No. 259 of 287
Parameter ID : TRPPPW
Description : RETARDATION OF Pu, PROW PASS
Save Time History : TRUE
The Parameter is a function, exp. value = 834.3334
Equation : 1+DPPW/PPPW*KPUD
The parameter affects the following parameters:
RPUPPW
The parameter is a function of the following parameters:
DPPW,KPUD,PPPW

Parameter No. 260 of 287
Parameter ID : TRPTS2
Description : RETARDATION OF Pu, TOPOPAH SPRING 2
Save Time History : TRUE
The Parameter is a function, exp. value = 2037.364
Equation : 1+DTSW2/PTSW2*KPUD
The parameter affects the following parameters:
RPUTS2
The parameter is a function of the following parameters:
DTSW2,KPUD,PTSW2

Parameter No. 261 of 287
Parameter ID : TRPTS3
Description : RETARDATION OF Pu, TOPOPAH SPRING 3
Save Time History : TRUE
The Parameter is a function, exp. value = 2389.889
Equation : 1+DTSW3/PTSW3*KPUD
The parameter affects the following parameters:
RPUTS3
The parameter is a function of the following parameters:
DTSW3,KPUD,PTSW3

Parameter No. 262 of 287
Parameter ID : TRPUBW
Description : RETARDATION OF Pu, BULLFROG
Save Time History : TRUE
The Parameter is a function, exp. value = 834.3334
Equation : 1+DBW/PBW*KPUD
The parameter affects the following parameters:
RPUBW
The parameter is a function of the following parameters:
DBW,KPUD,PBW

Parameter No. 263 of 287
Parameter ID : TRRABW
Description : RETARDATION OF Ra, BULLFROG
Save Time History : TRUE
The Parameter is a function, exp. value = 2501
Equation : 1+DBW/PBW*KRAD
The parameter affects the following parameters:
RRABW
The parameter is a function of the following parameters:
DBW,KRAD,PBW

Parameter No. 264 of 287
Parameter ID : TRRCHV
Description : RETARDATION OF Ra, CALICO HILLS VITRIC
Save Time History : TRUE
The Parameter is a function, exp. value = 2401
Equation : 1+DCHN1V/PCHN1V*KRAV

The parameter affects the following parameters:
RRACHV
The parameter is a function of the following parameters:
DCHN1V,KRAV,PCHN1V

Parameter No. 265 of 287
Parameter ID : TRRCHZ
Description : RETARDATION OF Ra, CALICO HILLS ZEOLITIC
Save Time History : TRUE
The Parameter is a function, exp. value = 12293.68
Equation : 1+DCHN1Z/PCHN1Z*KRAZ

The parameter affects the following parameters:
RRACHZ
The parameter is a function of the following parameters:
DCHN1Z,KRAZ,PCHN1Z

Parameter No. 266 of 287
Parameter ID : TRRPPW
Description : RETARDATION OF Ra, PROW PASS
Save Time History : TRUE
The Parameter is a function, exp. value = 2501
Equation : 1+DPPW/PPPW*KRAD
The parameter affects the following parameters:
RRAPPW
The parameter is a function of the following parameters:
DPPW,KRAD,PPPW

Parameter No. 267 of 287
Parameter ID : TRRTS2
Description : RETARDATION OF Ra, TOPOPAH SPRING 2
Save Time History : TRUE
The Parameter is a function, exp. value = 6110.091
Equation : 1+DTSW2/PTSW2*KRAD
The parameter affects the following parameters:
RRATS2
The parameter is a function of the following parameters:
DTSW2,KRAD,PTSW2

Parameter No. 268 of 287
Parameter ID : TRRTS3
Description : RETARDATION OF Ra, TOPOPAH SPRING 3
Save Time History : TRUE
The Parameter is a function, exp. value = 7167.667
Equation : 1+DTSW3/PTSW3*KRAD
The parameter affects the following parameters:
RRATS3
The parameter is a function of the following parameters:
DTSW3,KRAD,PTSW3

Parameter No. 269 of 287
Parameter ID : TRUBW
Description : RETARDATION OF U, BULLFROG
Save Time History : TRUE
The Parameter is a function, exp. value = 21.83333
Equation : 1+DBW/PBW*KUD

The parameter affects the following parameters:
RUBW
The parameter is a function of the following parameters:
DBW,KUD,PBW

Parameter No. 270 of 287
Parameter ID : TRUCHV
Description : RETARDATION OF U, CALICO HILLS VITRIC
Save Time History : TRUE
The Parameter is a function, exp. value = 17
Equation : 1+DCHN1V/PCHN1V*KUV
The parameter affects the following parameters:
RUCHV
The parameter is a function of the following parameters:
DCHN1V,KUV,PCHN1V

Parameter No. 271 of 287
Parameter ID : TRUCHZ
Description : RETARDATION OF U, CALICO HILLS ZEOLITIC
Save Time History : TRUE
The Parameter is a function, exp. value = 52.21951
Equation : 1+DCHN1Z/PCHN1Z*KUZ
The parameter affects the following parameters:
RUCHZ
The parameter is a function of the following parameters:
DCHN1Z,KUZ,PCHN1Z

Parameter No. 272 of 287
Parameter ID : TRUPPW
Description : RETARDATION OF U, PROW PASS
Save Time History : TRUE
The Parameter is a function, exp. value = 21.83333
Equation : 1+DPPW/PPPW*KUD
The parameter affects the following parameters:
RUPPW
The parameter is a function of the following parameters:
DPPW,KUD,PPPW

Parameter No. 273 of 287
Parameter ID : TRUTS2
Description : RETARDATION OF U, TOPOPAH SPRING 2
Save Time History : TRUE
The Parameter is a function, exp. value = 51.90909
Equation : 1+DTSW2/PTSW2*KUD

The parameter affects the following parameters:
RUTS2
The parameter is a function of the following parameters:
DTSW2,KUD,PTSW2

Parameter No. 274 of 287
Parameter ID : TRUTS3
Description : RETARDATION OF U, TOPOPAH SPRING 3
Save Time History : TRUE
The Parameter is a function, exp. value = 60.72222
Equation : 1+DTSW3/PTSW3*KUD

The parameter affects the following parameters:
RUTS3
The parameter is a function of the following parameters:
DTSW3,KUD,PTSW3

Parameter No. 275 of 287
Parameter ID : TSFLUX
Description : SATURATED ZONE FLUX ADJUSTED FOR CLIMACTIC CHANGE
Save Time History : TRUE
The Parameter is a function, exp. value = 2
Equation : SBFLUX*1

The parameter affects the following parameters:

GWTIM1,GWTIM2,GWTIM3,GWTIM4,GWTIM5,
GWTIM6,GWTIM7,GWTIM8
GWTIM9,GWTM1A,GWTM2A,GWTM3A,
GWTM4A,GWTM5A,GWTM6A,GWTM7A
GWTM8A,GWTM9A,VSAT
The parameter is a function of the following parameters:
FM,SBFLUX,TIME

Parameter No. 276 of 287
Parameter ID : TUFLUX
Description : UNSAT ZONE FLUX ADJ FOR CLIMATE and Hydraulic Sat
Save Time History : TRUE
The Parameter is a function, exp. value = 0.0005
Equation : if(ubflux>ksm,hperc,ubflux)

The parameter affects the following parameters:
DTBL,FNS130,FNS230,FNS60,FNS613,
GWTIM1,GWTIM2,GWTIM3,GWTIM4
GWTIM5,GWTIM6,GWTIM7,GWTIM8,GWTIM9,
GWTM1A,GWTM2A,GWTM3A
GWTM4A,GWTM5A,GWTM6A,GWTM7A,
GWTM8A,GWTM9A,LCHVC1,LCHVC2
LCHVC4,LCHVC5,LCHZC1,LCHZC2,LCHZC3,
LCHZC6,LCHZC7,LCHZC8
LCHZC9,LPPWC3,LPPWC4,LPPWC5,LPPWC6,
LPPWC7,LPPWC8,LPPWC9
LTS2C1,LTS2C2,LTS2C3,LTS2C7,LTS2C8,
LTS2C9,LTS3C6,QCOL1,QCOL2
QCOL3,QCOL4,QCOL5,QCOL6,QCOL79,QSAT,
VBW,VCHN1V,VCHN1Z,VPPW
VTSW2,VTSW3
The parameter is a function of the following parameters:
DRYINF,FM,HFXSW,HPERC,HPERC1,KSM,
TIME,UBFLUX

Parameter No. 277 of 287
Parameter ID : TWAT
Description : water thickness for moist continuous diffusion (INTERA)
Save Time History : TRUE
The parameter is a constant: 1.00000E-03
The parameter affects the following parameters:
FV,FVMC

Parameter No. 278 of 287
Parameter ID : UBFLUX
Description : Infiltration Rate - Adjusted Linearly for Climate
Save Time History : TRUE
The Parameter is a function, exp. value = 0.0005
Equation : dryinf*(1+(fm-1)*1e-5*time)
the following parameters:
DTBL,FNS130,FNS230,FNS60,FNS613,
GWTIM1,GWTIM2,GWTIM3,GWTIM4
GWTIM5,GWTIM6,GWTIM7,GWTIM8,GWTIM9,
GWTM1A,GWTM2A,GWTM3A
GWTM4A,GWTM5A,GWTM6A,GWTM7A,
GWTM8A,GWTM9A,LCHVC1,LCHVC2
LCHVC4,LCHVC5,LCHZC1,LCHZC2,LCHZC3,L
CHZC6,LCHZC7,LCHZC8
LCHZC9,LPPWC3,LPPWC4,LPPWC5,LPPWC6,
LPPWC7,LPPWC8,LPPWC9
LTS2C1,LTS2C2,LTS2C3,LTS2C7,LTS2C8,
LTS2C9,LTS3C6,QCOL1,QCOL2
QCOL3,QCOL4,QCOL5,QCOL6,QCOL79,QSAT,
TUFLUX,VBW,VCHN1V,VCHN1Z
VPPW,VTSW2,VTSW3
The parameter is a function of the following parameters:
DRYINF,FM,TIME

Parameter No. 279 of 287
Parameter ID : VBW
Description : Velocity of Groundwater in Bullfrog

Save Time History : TRUE
The Parameter is a function, exp. value = 0.002109
Equation : TUFLUX/(PBW*SBW)

The parameter is a function of the following parameters:
DRYINF,FM,HFXSW,HPERC,HPERC1,KSM,
PBW,SBW,TIME,TUFLUX,UBFLUX

Parameter No. 280 of 287
Parameter ID : VCHN1V
Description : VELOCITY OF GROUNDWATER IN CALICO HILLS VITRIC
Save Time History : TRUE
The Parameter is a function, exp. value = 0.02976
Equation : TUFLUX/(PCHN1V*SCHN1V)

The parameter affects the following parameters:

GWTIM1,GWTIM2,GWTIM3,GWTIM4,GWTIM5,
GWTIM6,GWTIM7,GWTIM8
GWTIM9,GWTM1A,GWTM2A,GWTM3A,
GWTM4A,GWTM5A,GWTM6A,GWTM7A
GWTM8A,GWTM9A
The parameter is a function of the following parameters:
DRYINF,FM,HFXSW,HPERC,HPERC1,KSM,
PCHN1V,SCHN1V,TIME,TUFLUX,UBFLUX

Parameter No. 281 of 287
Parameter ID : VCHN1Z
Description : VELOCITY OF GROUNDWATER IN CALICO HILLS ZEOLITIC
Save Time History : TRUE
The Parameter is a function, exp. value = 0.001323
Equation : TUFLUX/(PCHN1Z*SCHN1Z)
The parameter affects the following parameters:
GWTIM1,GWTIM2,GWTIM3,GWTIM4,GWTIM5,
GWTIM6,GWTIM7,GWTIM8
GWTIM9,GWTM1A,GWTM2A,GWTM3A,
GWTM4A,GWTM5A,GWTM6A,GWTM7A
GWTM8A,GWTM9A
The parameter is a function of the following parameters:
DRYINF,FM,HFXSW,HPERC,HPERC1,KSM,PC
HN1Z,SCHN1Z,TIME,TUFLUX
UBFLUX

Parameter No. 282 of 287
Parameter ID : VOL
Description : volume of waste package

Save Time History : TRUE
The Parameter is a function, exp. value = 11.57587
Equation : pi*r0*r0*leng
The parameter affects the following parameters:
EQRAD,OMEGA,TOMEGA
The parameter is a function of the following parameters:
LENG,PI,R0

Parameter No. 283 of 287
Parameter ID : VPPW
Description : VELOCITY OF GROUNDWATER IN PROW PASS
Save Time History : TRUE
The Parameter is a function, exp. value = 0.002109
Equation : TUFLUX/(PPPW*SPPW)
The parameter affects the following parameters:
GWTIM1,GWTIM2,GWTIM3,GWTIM4,GWTIM5,
GWTIM6,GWTIM7,GWTIM8
GWTIM9,GWTM1A,GWTM2A,GWTM3A,
GWTM4A,GWTM5A,GWTM6A,GWTM7A
GWTM8A,GWTM9A
The parameter is a function of the following parameters:

DRYINF,FM,HFXSW,HPERC,HPERC1,KSM,PP
PW,SPPW,TIME,TUFLUX,UBFLUX

Parameter No. 284 of 287
Parameter ID : VSAT
Description : VELOCITY OF GROUNDWATER IN SATURATED ZONE
Save Time History : TRUE
The Parameter is a function, exp. value = 100
Equation : TSFLUX/PSAT
The parameter affects the following parameters:
GWTIM1,GWTIM2,GWTIM3,GWTIM4,GWTIM5,
GWTIM6,GWTIM7,GWTIM8
GWTIM9,GWTM1A,GWTM2A,GWTM3A,
GWTM4A,GWTM5A,GWTM6A,GWTM7A
GWTM8A,GWTM9A
The parameter is a function of the following parameters:
FM,PSAT,SBFLUX,TIME,TSFLUX

Parameter No. 285 of 287
Parameter ID : VTSW2
Description : VELOCITY OF GROUNDWATER IN TOPOPAH SPRING 2
Save Time History : TRUE
The Parameter is a function, exp. value = 0.006675
Equation : TUFLUX/(PTSW2*STSW2)
The parameter affects the following parameters:

GWTIM1,GWTIM2,GWTIM3,GWTIM4,GWTIM5,
GWTIM6,GWTIM7,GWTIM8,GWTIM9
The parameter is a function of the following parameters:
DRYINF,FM,HFXSW,HPERC,HPERC1,KSM,PT
SW2,STSW2,TIME,TUFLUX,UBFLUX

Parameter No. 286 of 287
Parameter ID : VTSW3
Description : VELOCITY OF GROUNDWATER IN TOPOPAH SPRING 3
Save Time History : TRUE
The Parameter is a function, exp. value = 0.007281
Equation : TUFLUX/(PTSW3*STSW3)

The parameter affects the following parameters:

GWTIM1,GWTIM2,GWTIM3,GWTIM4,GWTIM5,
GWTIM6,GWTIM7,GWTIM8
GWTIM9
The parameter is a function of the following parameters:
DRYINF,FM,HFXSW,HPERC,HPERC1,KSM,
PTSW3,STSW3,TIME,TUFLUX,UBFLUX

Parameter No. 287 of 287
Parameter ID : WPOR
Description : POROSITY OF BACKFILL

Save Time History : TRUE
The parameter is stochastic
The distribution is linear
Sampling bias : No Bias
Uniform : Umin = 1.00000E-01 Umax = 3.00000E-01
The parameter affects the following parameters:
OMEGA,TOMEGA